UNIVERSITY OF BELGRADE

Faculty of Technology and Metallurgy

Mr. Ismail A. Ajaj

SYNTHESIS, STRUCTURE AND PROPERTIES OF 2(6)-HYDROXY-6(2)-OXO-*N*(1),4-DISUBSTITUTED-1,2(1,6)-DIHYDROPYRIDINE-3-CARBONITRILES AND THEIR AZO DERIVATIVES

Doctoral Dissertation

Belgrade, 2015.

Faculty of Technology and Metallurgy
University of Belgrade

INFORMATION ABOUT THE THESIS ADVISOR AND EXAMINATION COMMITTEE

Thesis Advisor: Dr Aleksandar Marinković, assistant professor
Faculty of Technology and Metallurgy, University of Belgrade

Final examination committee:

Dr Aleksandar Marinković, assistant professor, Faculty of Technology and Metallurgy, University of Belgrade

Dr Gordana Uščumlić, full professor, Faculty of Technology and Metallurgy, University of Belgrade

Dr Dušan Mijin, full professor, Faculty of Technology and Metallurgy, University of Belgrade

Dr Miloš Milčić, associate professor, Faculty of Chemistry, University of Belgrade

Date: 2015

Faculty of Technology and Metallurgy
University of Belgrade

Information regarding Ph.D Thesis

Title: Synthesis, structure and properties of 2(6)-hydroxy-6(2)-oxo-*N*(1),4-disubstituted-1,2(1,6)-dihydropyridine-3-carbonitriles and their azo derivatives

Abstract: In this work, a simple and convenient synthesis of tautomeric (6 or 2)-hydroxy-4-methyl-(2 or 6)-oxo-1-(substituted phenyl)-(1,2 or 1,6)-dihydropyridine-3-carbonitriles from ethyl acetoacetate and 2-cyano-*N*-(substituted phenyl)-ethanamides using microwave assisted chemistry is presented. The structure of the obtained product was confirmed by the use of FTIR, NMR, UV and MS techniques. Presence of tautomeric forms, 6-hydroxy-4-methyl-2-oxo-1-(substituted phenyl)-1,2-dihydropyridine-3-carbonitriles and 2-hydroxy-4-methyl-6-oxo-1-(substituted phenyl)-1,6-dihydropyridine-3-carbonitriles, and state of equilibrium in DMSO-d_6 of the obtained product was studied by ^{1}H and ^{13}C NMR spectroscopy, as well as B3LYP/6-311++G(d,p) and GIAO/WP04/aug-cc-pVDZ theoretical calculations.

Tautomeric equilibria of title compounds were quantitatively analyzed by UV/Vis spectroscopy and theoretical approaches. Kamlet-Taft and Catalán correlation analysis were done. The LFER correlation results showed significant influence of the solvent effects on the transmission mode of substituent effects. In order to calculate optimal geometries of investigated compounds, a conformation with minimum energies were determined using semi-empirical PM6 method, as well as B3LYP (DFT) hybride method with 6-311G(d,p) basis set.

The state of the tautomeric equilibria of 6(2)-hydroxy-4-methyl-2(6)-oxo-1-(substituted phenyl)-1,2(1,6)-dihydropyridine-3-carbonitriles were evaluated from UV/Vis and NMR spectral data. Quantum chemical calculations of geometries and electronic energies were

performed by density functional theory (B3LYP). The experimental data were interpreted with the aid of time-dependent density functional (TD-DFT) method. Electron charge density was obtained by the use of Quantum Theory of Atoms in Molecules, *i.e*. Bader's analysis. Linear solvation energy relationships (LSER) rationalized solvent influence on tautomeric equilibrium. Linear free energy relationships (LFERs) was applied to the substituent-induced NMR chemical shifts (*SCS*) with σ using SSP (single substituent parameter), inductive (σ_I) and resonance (σ_R) parameters using DSP (dual substituent parameter), as well as the Yukawa–Tsuno model. Theoretical calculations and obtained correlations gave insight into the influence molecular conformation on the transmission of substituent effects, as well as on different solvent–solute interactions on state of tautomeris equilibria.

Key words: Heterocycles, Microwave assisted synthesis, Tautomerism, Solvent effects, Substituent effects, UV/Vis spectroscopy, NMR spectroscopy, DFT

Scientific field: Organic chemistry

Scientific discipline: Organic chemistry

UDK:

Faculty of Technology and Metallurgy
University of Belgrade

Information regarding Ph.D Thesis

Title: Synthesis, structure and properties of 2(6)-hydroxy-6(2)-oxo-*N*(1),4-disubstituted-1,2(1,6)-dihydropyridine-3-carbonitriles and their azo derivatives

Abstract: In this work, a simple and convenient synthesis of tautomeric (6 or 2)-hydroxy-4-methyl-(2 or 6)-oxo-1-(substituted phenyl)-(1,2 or 1,6)-dihydro- pyridine-3-carbonitriles from ethyl acetoacetate and 2-cyano-*N*-(substituted phenyl)-ethanamides using microwave assisted chemistry is presented. The structure of the obtained product was confirmed by the use of FTIR, NMR, UV and MS techniques. Presence of tautomeric forms, 6-hydroxy-4-methyl-2-oxo-1-(substituted phenyl)-1,2-dihydropyridine-3-carbonitriles and 2-hydroxy-4-methyl -6-oxo-1-(substituted phenyl)-1,6-dihydropyridine-3-carbonitriles, and state of equilibrium in DMSO-d_6 of the obtained product was studied by ^{1}H and ^{13}C NMR spectroscopy, as well as B3LYP/6-311++G(d,p) and GIAO/WP04/aug-cc-pVDZ theoretical calculations.

Tautomeric equilibria of title compounds were quantitatively analyzed by UV/Vis spectroscopy and theoretical approaches. Kamlet-Taft and Catalán correlation analysis were done. The LFER correlation results showed significant influence of the solvent effects on the transmission mode of substituent effects. In order to calculate optimal geometries of investigated compounds, a conformation with minimum energies were determined using semi-empirical PM6 method, as well as B3LYP (DFT) hybride method with 6-311G(d,p) basis set.

The state of the tautomeric equilibria of 6(2)-hydroxy-4-methyl-2(6)-oxo-1-(substituted phenyl)-1,2(1,6)-dihydropyridine-3-carbonitriles were evaluated from UV/Vis and NMR spectral data. Quantum chemical calculations of geometries and electronic energies were

performed by density functional theory (B3LYP). The experimental data were interpreted with the aid of time-dependent density functional (TD-DFT) method. Electron charge density was obtained by the use of Quantum Theory of Atoms in Molecules, *i.e*. Bader's analysis. Linear solvation energy relationships (LSER) rationalized solvent influence on tautomeric equilibrium. Linear free energy relationships (LFERs) was applied to the substituent-induced NMR chemical shifts (*SCS*) with σ using SSP (single substituent parameter), inductive (σ_I) and resonance (σ_R) parameters using DSP (dual substituent parameter), as well as the Yukawa–Tsuno model. Theoretical calculations and obtained correlations gave insight into the influence molecular conformation on the transmission of substituent effects, as well as on different solvent–solute interactions on state of tautomeris equilibria.

Key words: Heterocycles, Microwave assisted synthesis, Tautomerism, Solvent effects, Substituent effects, UV/Vis spectroscopy, NMR spectroscopy, DFT

Scientific field: Organic chemistry

Scientific discipline: Organic chemistry

UDK:

CONTENTS

1 INTRODUCTION

2(1*H*)-Pyridone derivatives constitute a very important class of heterocyclic compounds as they are components of the biologically active compounds and it has been shown that many of them exert pronounced biological effects. Many naturally occurring and synthetic compounds containing 2(1*H*)-pyridone ring have a broad spectrum of biological activity. Some of them are cardiotonic agents for the treatment of heart failure, while other possesses antitumor, antibacterial or some other biological activities. Many 3-cyano-2-pyridones derivatives are used in the manufacturing of dyes and pigments, stabilizers for polymers and varnishes, additives for fuels and lubricants, acid-base indicators and other practically important materials. The coordination chemistry of pyridone compounds has been studied in detail in the recent years, the research in this area ranging from bioorganic to pharmaceutical and material chemistry.

Having in mind the significant role of 2(1*H*)-pyridone derivatives in both organic and bioorganic chemistry, it was of interest to study the structure-activity relationships in this series, employing the principles of linear free energy relationships (LFER) and linear solvatochromic energy relationships (LSER). These are standard methods used for the study of structure-property relationships in the study of ^{13}NMR chemical shifts (SCS). Both these approaches were employed in the present work to examine the substituent effects and the mode of their transmission through the pyridone ring in the investigated class of compounds. For that purpose, a number of substituted pyridones and some azo dyes have been synthesized, many those were new compounds, fully characterized and identified.

LSER and LFER correlations and quantum-chemical calculations of 3-cyano-4-(2-, 3-, and 4-substituted phenyl)-6-phenyl-2(1*H*)-pyridones (**2-PY/2-HP**) and 6(2)-hydroxy-4-methyl-2(6)-oxo-1-(substituted phenyl)-1,2(1,6)-dihydropyridine-3-carbonitriles (**2-PY/6-PY**) were performed**.** The UV/Vis spectroscopic data were analyzed by LSER and LFER models to evaluate the tautomeric equilibria and the intramolecular charge transfer (ICT) in the investigated set of compounds. The most widely used LSER model, applied for the quantification of the effect of solvent dipolarity/polarizability and hydrogen-bonding interactions, introduced by Kamlet-Taft and more elaborated LSER model uses Catalán solvent parameters scale, qualitatively and quantitatively interprets the effect of solvent dipolarity, polarizability and

solvent–solute hydrogen bonding interactions. The resolution of the individual bands in UV-Vis spectra was performed according to chemometric method and applied for the evaluation of the state of tautomeric equilibria in both series. Vibrational, NMR and Bader's analysis confirm that the prepared compounds exists in both tautomeric forms in first series and second, except compounds with *para*-hydroxy, **2-PY** form, and *meta*-trifluoromethyl substituent, **6-PY** form.

Transmission of substituent electronic effect, situated at *N*-phenyl rings in 6(2)-hydroxy-4-methyl-2(6)-oxo-1-(substituted phenyl)-1,2(1,6)-dihydropyridine-3-carbonitriles was analyzed on the basis of substituent induced NMR chemical shifts (SCS) chemical shifts (LFER) using the single substituent parameter (SSP) Hammett equation, dual substituent parameter (extended Hammett) DSP equation and Yukawa-Tsuno equation allowed successful quantification of polar (inductive/filed) and resonance effects contribution in overall substituent effect. Negative ρ values were found for several correlations (reverse substituent effect), localized and delocalized π-units of investigated molecules are polarized under substituent dipole influences individualy or as whole netowrk depending on substituent present. The obtained correlation parameters were compared with the corresponding values for structuralally similar pyrimidine carboxylic acids. Through extensive comparisons and discussions of the obtained results, it was possible to separate and quantify the individual substituent effects, that is inductive/field, resonance and steric effects, and also the solvent effects in the reactivity studies.

An additional analysis of solvent and substituent effects on absorption frequencies, NMR shifts, tautomeric equilibria and conformational changes of the studied compounds necessitated quantum-chemical calculations, *i.e*. geometry optimization and charge density analysis. In order to calculate optimal geometries of investigated compounds, a conformation with minimum energies were determined using B3LYP (DFT) hybride method. Deviation, nonplanarity of investigated compounds are determined by the values of torsional angles between *N*-phenyl and pyridone rings in series 3-cyano-4-(substituted phenyl)-6-phenyl-2(1*H*)-pyridones, as well as *N*-phenyl and pyridone ring in series *N*-(substituted phenyl)-3-cyano-4,6-dimethyl-2-pyridones. Transmission mode of substituent effect are discussed in the light of such calculated optimal molecular geometries.

Considering correlation results and explanations given in this dissertation, it could be concluded that substituent electronic effect transmission through investigated molecules are very complex. However, the analysis of statistical data obtained by the use of LFER equations provide very good opportunities, especially DSP-NLR equation, for explaining non-linear contribution of resonance effect to the overall substituent effect transmission.

2 THEORETICAL PARTS

2.1 Structural characteristics of 2-pyridones

2-Pyridones (Figure 2.1.1) are colorless, crystalline, organic derivatives of pyridine with molecular formula $C_5H_4NH(O)$. 2-Pyridones can not be found in nature, but derivatives are isolated as cofactors in hydrogenase enzyme [1].

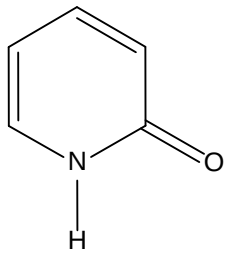

Figure 2.1.1 Structure of 2-pyridones

Other names of 2(1*H*)-pyridinones are: 2-pyridones; 2(1*H*)-pyridones; 1*H*-pyridine-2-ones; 1,2-dihydro-2-oxopyridines; 2-pyridinol; 1*H*-2-pyridones; 2-oxopyridone; 2-hydroxypyridines [2].

2(1*H*)-pyridinones represent nitrogen containing synthetically designed scaffold with a broad spectrum of biological activities. The most prominent feature of 2-pyridones is the amide group; nitrogen with hydrogen bound and a keto group next to it. In peptides, amino acids are linked by this pattern, a feature responsible for some remarkable physical and chemical properties. In this and similar molecules, the hydrogen bound to the nitrogen is suitable for the formation of strong hydrogen bonds to other nitrogen and oxygen containing species [2].

The structure of 2(*H*)-pyridone in the crystalline state that had been determined by measuring the electron densities in two projections. The corresponding bond lengths and angles are signed in the following figure respectively [2].

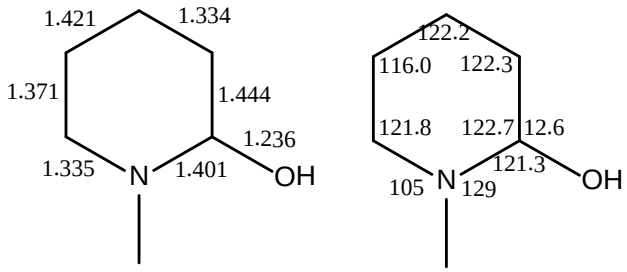

Figure 2.1.2 Bond lengths and angles of crystal 2(1*H*)-pyridones

The pyridinone structure is the stable one, and there is a strong intermolecular hydrogen bond between the nitrogen of one molecule and the oxygen of another which is repeated throughout the structure linking molecules in endless helices. This conclusion is based on the fact that the N-H distance is 1.02 A° (Figure 2.1.2), closely to the normal covalent bond length of 1.00 A°, whereas the observed O-H distance greatly exceeds the normal covalent distance. This obviates the possibility that 2(*H*)-pyridinones exist as a hydrogen-bonded dimmer. The resonance structure of 2(*H*)-pyridinones and their percent contribution as shown below were calculated to give the best correspondence with the observed bond lengths and angles (Figs. 2.1.2 and 2.1.3) [2].

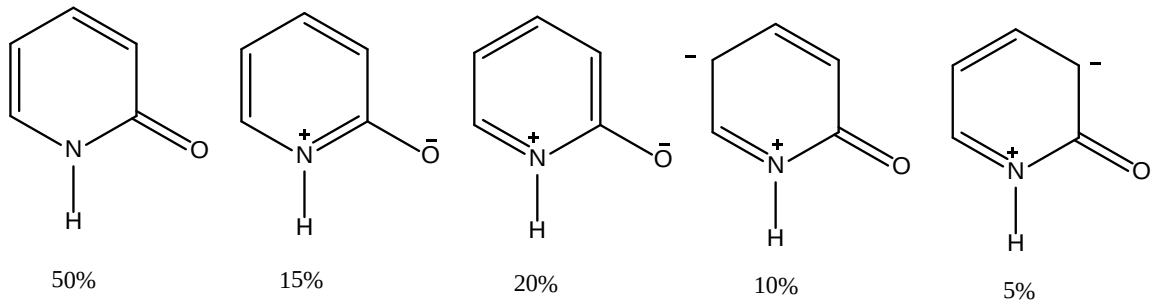

Figure 2.1.3 The resonance structure and percent contribution of 2(1*H*)-pyridones

As expected on the basis of electro negativity trends, the dipolar forms (Figure 2.1.3), with negative charge on oxygen, have much greater significance that those with the negative charge on carbon. These latter forms, however, do account for electrophilic substitutions at position *ortho* and *para* to the C=O group. The large contribution of the dipolar forms with negatives charge on oxygen cause a high polarity on the N——H----O hydrogen bond. 2-Pyridones and 2-hydroxypyridines can form dimers with two hydrogen bonds (Figure 2.1.4) [3].

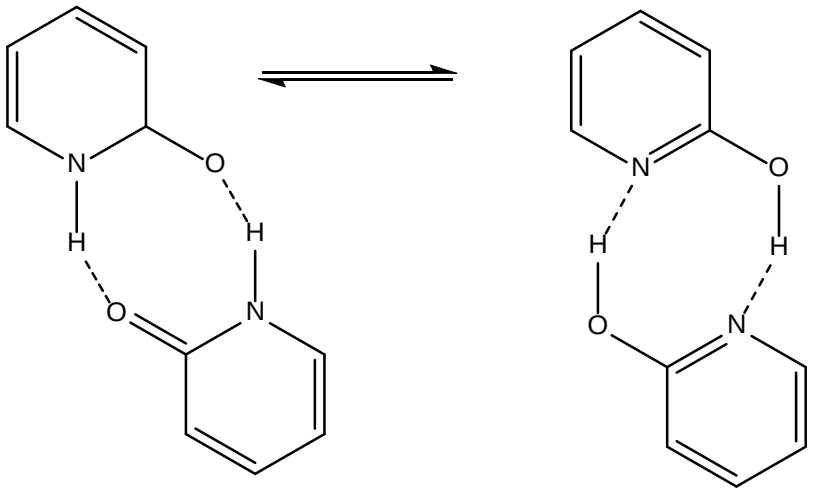

Figure 2.1.4 Hydrogen bonded 2-pyridone/2-hydroxypyridine dimeric structure [3]

2-Pyridones are monomer in the solid state (Figure 2.1.1), howewer, using the hydrogen bonds form chelate structure. Still, some substituted 2-pyridones, such as, for example, 5-methyl-3-carbonitrile-2-pyridone, forms dimer in a solid state. Detection of these structures was performed using crystallographic X-ray method [4,5].

Dimeric form of 2-pyridones is present in solution (Figure 2.1.4). The ratio of dimerization is strongly dependent on the polarity of the solvent. Polar and protic solvents interact with the hydrogen bonds and more monomer is formed. Hydrophobic effects in non-polar solvents lead to a predominance of the dimer. The ratio of the tautomeric forms is also dependent on the solvent. All possible tautomers and dimers can be present and form equilibrium, and the exact measurement of all the equilibrium constants in the system is extremely difficult [3,6,7].

The unique properties of different derivatives of 3-cyano-2(1*H*)-pyridones gives them ability to be used not only in the production of dyes, pigments and additives fin the fuel tank, but also for the synthesis of various derivatives with a wide range of biological activities. Derivatives of 3-cyano-2(1*H*)-pyridones and thiones have found application in the production of dyes, pigments, additives for fuels and lubricants, stabilizers for polymers and coatings, acid-base indicators, etc. However, in recent time, particular attention is focused to the synthesis and testing of 3-cyano-2 (1*H*)-pyridone biological activity. A large number of 3-cyano-2(1*H*)-pyridone derivatives have a cardiotonic activity. Also, the 3-cyano-2(1*H*)-pyridone compounds possess cardiovascular, coronary and vasodilation activity. Milrinone and Amrinone are commercial 3-cyano-2(1*H*)-pyridone drugs. Among other compounds with different biological activities, anti-diabetics, diuretics, anti-oxidants, anti-virus, anti-inflammatory and anti-bacterial medicaments could be mentioned. Derivatives of 3-cyano-2(1*H*)-pyridones are effective sedative and anti-allergic drugs for the treatment of bronchial asthma, dermatitis, and also have been successfully demonstrated in the treatment of hepatitis, and atherosclerosis. Degradable biological products, plant growth regulators, pesticides, herbicides were synthesized on the basis of 3-cyano-pyridin-2(1*H*)-čalkogenona [8]

2.2 Structural characteristics of azo dyes

The azo dyes are by far the most important class, accounting for over 50% of all commercial dyes, and having been studied more than any other class. Azo dyes contain at least one azo 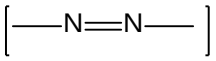 group but can contain two (disazo), three (trisazo), or, more rarely, four (tetrakisazo) or more (polyazo) azo groups. The azo group is attached to two groups, of which at least one, but more usually both, are aromatic.

They exist in the trans form 1 in which the bond angle is ca. 120°, the nitrogen atoms are sp^2 hybridized, and the designation of X and Y groups is consistent with C.I. usage [9].

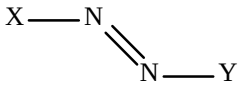

Figure 2.2.1 Structure of azo dyes

In monoazo dyes, the most important type, the A group often contains electron-accepting substituents, and the E group contains electron-donating substituents, particularly hydroxyl and amino groups. If the dyes contain only aromatic groups, such as benzene and naphthalene, they are known as carbocyclic azo dyes. If they contain one or more heterocyclic groups, the dyes are known as heterocyclic azo dyes.

Almost without exception, azo dyes are made by diazotization of a primary aromatic amine followed by coupling of the resultant diazonium salt with an electron-rich nucleophile. The diazotization reaction is carried out by treating the primary aromatic amine with nitrous acid, normally generated in situ with hydrochloric acid and sodium nitrite.

2.3 Conventional method of synthesis

2.3.1 Conventional synthesis of 3-cyano-2-pyridones

2.3.1.1 Synthesis of 3-cyano-2-pyridones from 1,3-diketo derivatives and cyanoacetamide

A series of 3-cyano-4-trifluoromethyl-2-pyridones have been prepared with triflouoromethyldiketones and cyanoacetamide (Figure 2.3.1) [10].

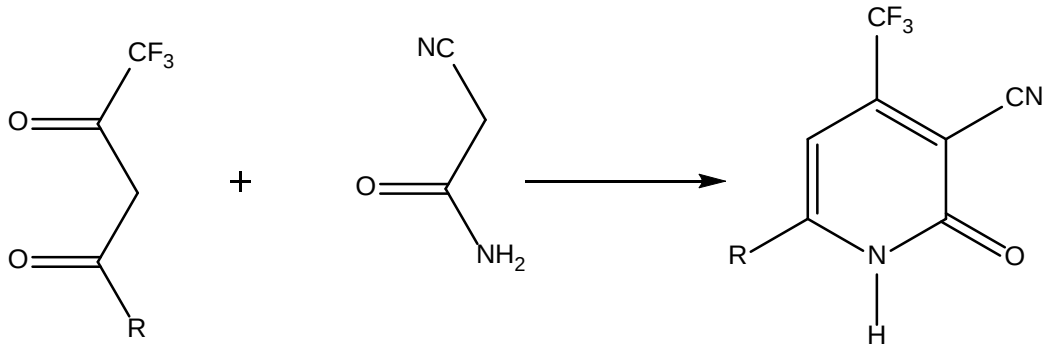

R: CH_3, CF_3, C_6H_5, 2-thienyl

Figure 2.3.1 Synthesis of 3-cyano-4-trifluoromethyl-2-pyridones

5-Substituted-4-methyl-3-cyano-6-hydroxy-2-pyridones were synthesized from the corresponding alkyl ethyl acetoacetate and cyanoacetamide in methanol in the presence of potassium hydroxide at 60 ºC. Cyclization of cyanoacetamide with an alkyl ethyl acetoacetate belongs to a 3-2 type of condensation where the pyridine nucleus is formed (Figure 2.3.2) [11].

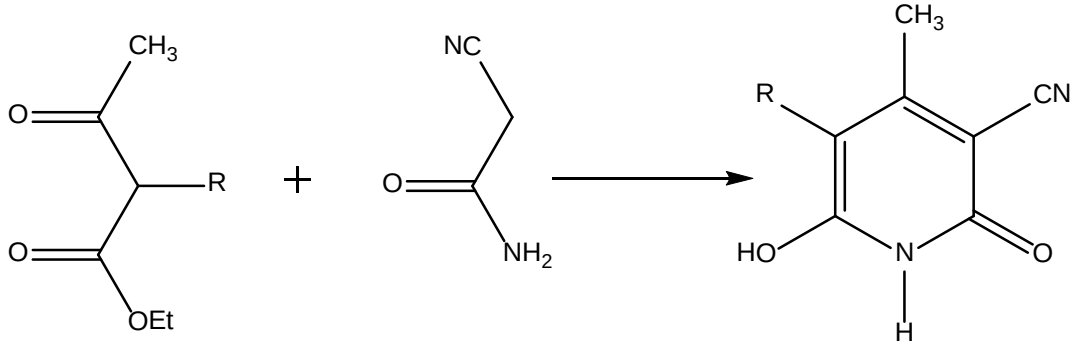

Figure 2.3.2 Synthesis of 5-substituted-4-methyl-3-cyano-6-hydroxy-2-pyridones

The derivatives of 3-cyano-2- pyridones were also obtained from a cyclo-condensation reaction in one step [12], reaction of cyanoacetamide with commercially available diketone, in the

presence of DBU in toluene for 16 h at 90 °C, readily afforded the title compounds (Figure 2.3.3).

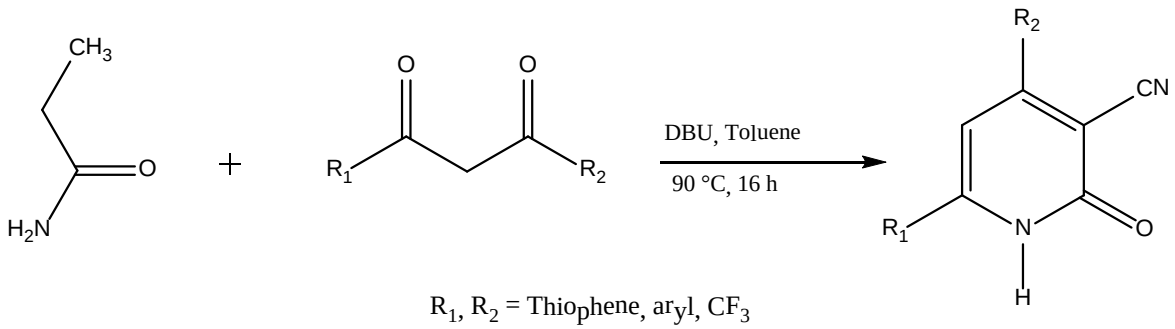

R_1, R_2 = Thiophene, aryl, CF_3

Figure 2.3.3 Synthesis of 3-cyano-2- pyridone derivatives from cyanoacetamide and diketone

Literature survey revealed many reports on synthesis of 3-cyano-2-pyridone by reaction of cyanoacetamide with 1,3-dicarbonyl compounds (Figure 2.3.4) [13-18].

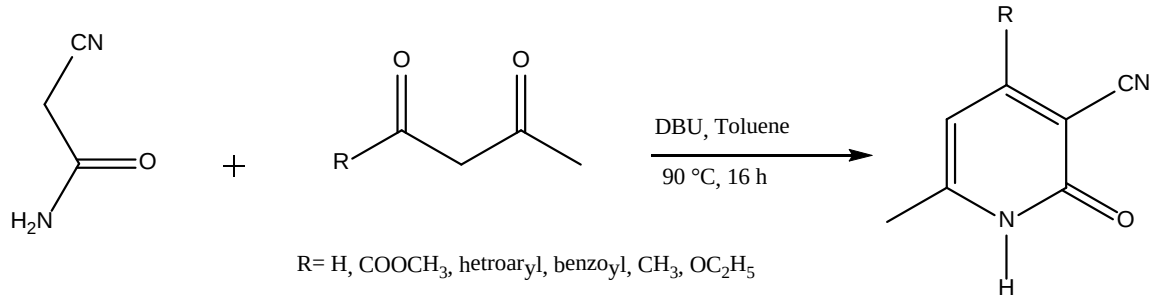

R= H, $COOCH_3$, hetroaryl, benzoyl, CH_3, OC_2H_5

Figure 2.3.4 Synthesis of 3-cyano-2-pyridones by reaction of cyanoacetamide and 1,3-dicarbonyl compounds

3-cyano-2- pyridone derivatives were synthesized by reaction of 1-methoxy-3-phenylhydrazone-2,4-pentanedione and cyanoacetamide in sodium ethoxide (Figure 2.3.5) [19].

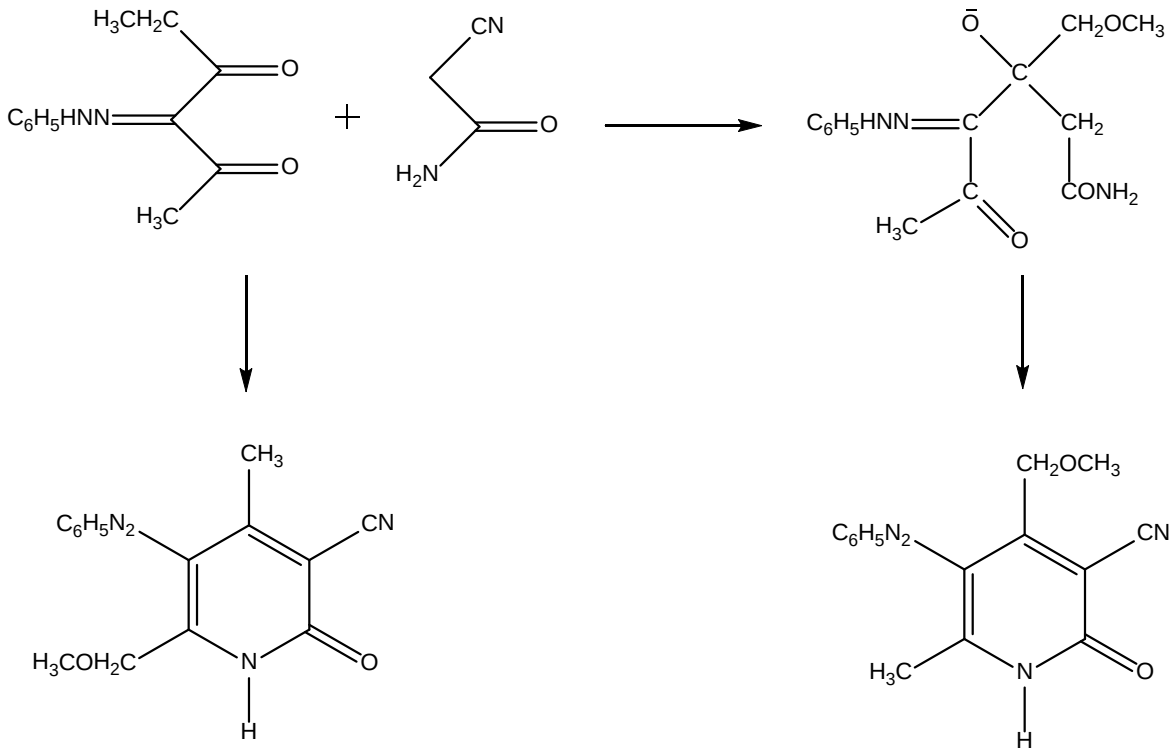

Figure 2.3.5 Synthesis of pyridone derivatives from 1-methoxy-3-phenylhydrazone-2,4-pentanedione and cyanoacetamide

2.3.1.2 Synthesis of 3-cyano-2-pyridones from β-diketo, β-ketoaldehyde and malonaldehyde

Condensation of cyanoacetamide with 1-hydroxymethylene-1-phenyl-2-propanone in piperidine gives 3-cyano-6-methyl-5-phenyl-2-pyridone in low yield (Figure 2.3.6) [20].

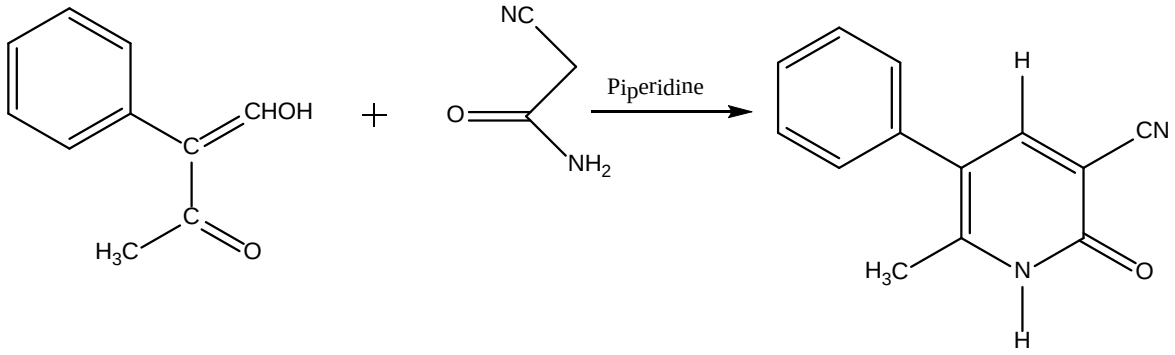

Figure 2.3.6 Synthesis of pyridone derivatives from cyanoacetamide and 1-hydroxymethelen-1-phenyl-2-propanone

Cyanoacetamide condenses with the sodium salt of 1-hydroxymethelen-1-phenyl-2-propanone in piperidine and give 3-cyano-4-methyl-5-phenyl-2-pyridone (Figure 2.3.7) [20].

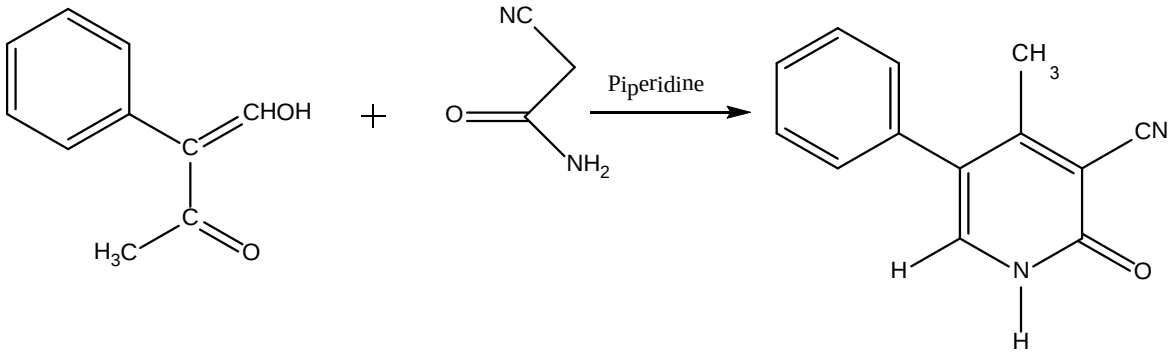

Figure 2.3.7 Synthesis of pyridone derivatives from cyanoacetamide and sodium salt of 1-hydroxymethelen-1-phenyl-2-propanone

The reaction between 2,5-diphenyl-1,3-pentandione and cyanoacetamide in aqueous sodium

carbonate gives 3-cyano-5-phenyl-6-(β-phenylethyl)-2-pyridone (Figure 2.3.8) [21].

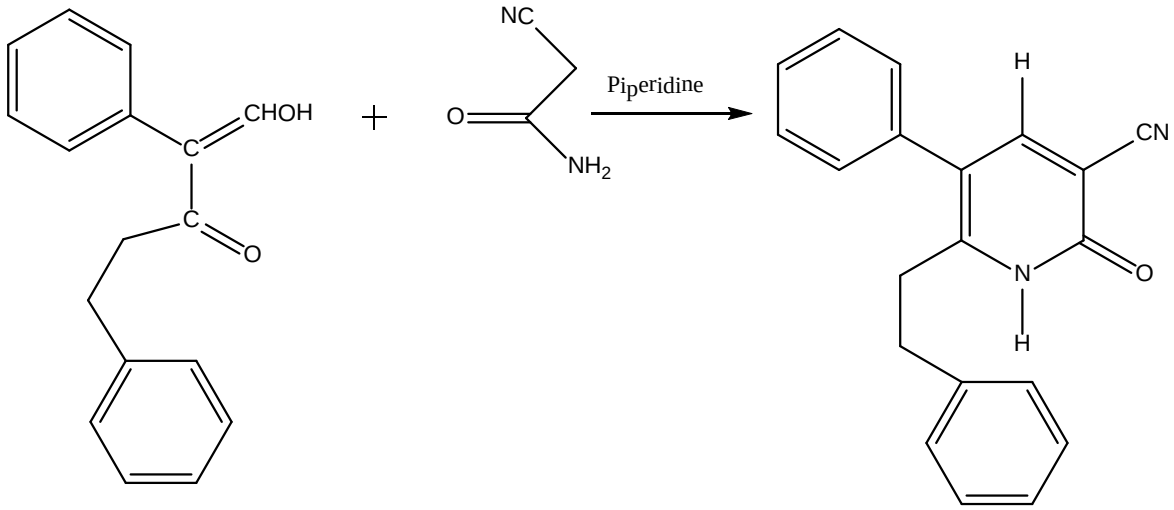

Figure 2.3.8 Synthesis of 3-cyano-5-phenyl-6-(β-phenylethyl)-2-pyridone from2,5-diphenyl-1,3-pentandione and cyanoacetamide

The dicarbonation of acetoacetatealdehyde is alkylated in the γ-position to give salts and copper chelates of β-ketoaldehydes, which are converted by reaction with cyanoacetamide to 3-cyano-2-pyridones (Figure 2.3.9) [22].

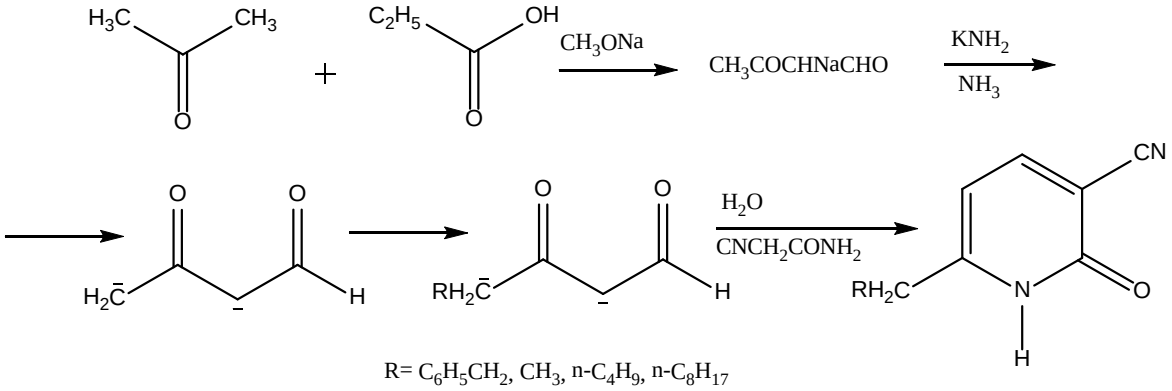

Figure 2.3.9 Synthesis of pyridone derivatives from cyanoacetamide and β-ketoaldehydes

A series of 3-cyano-4-trifluoromethyl-2-pyridones were synthesized by the reaction of trifluromethyldiketones with cyanoacetamide (Figure 2.3.10) [10].

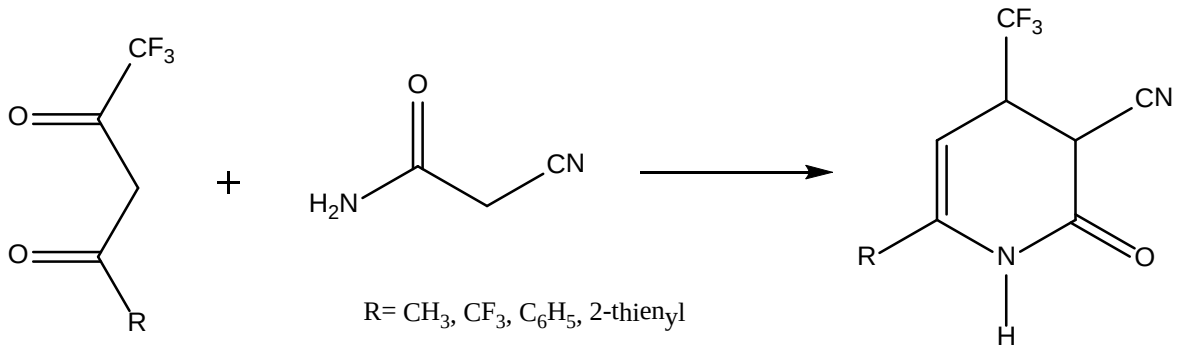

Figure 2.3.10 Synthesis of pyridone derivatives from trifluromethyldiketones and cyanoacetamide

The reaction between 1,1,3,3-tetraethoxypropane (malonaldehyde diethyl acetal) and cyanoacetamide in aqueous triethylamine gives 3-cyano-2-pyridone (Figure 2.3.11) [23].

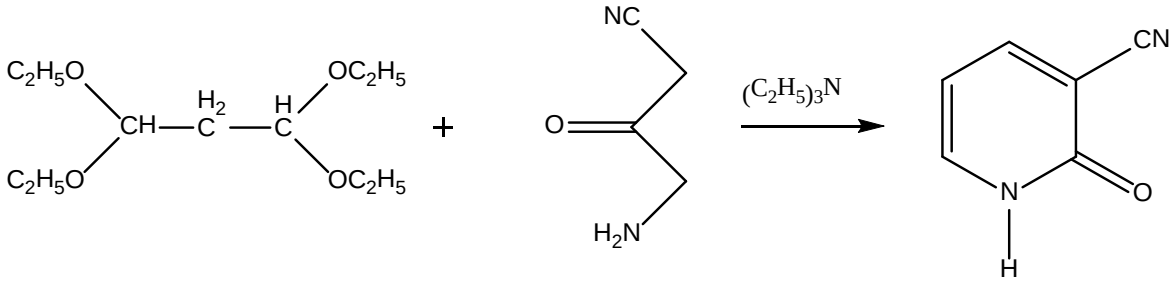

Figure 2.3.11 Synthesis of pyridone derivatives from 1,1,3,3-tetraethoxypropane and cyanoacetamide

2.3.1.3 Reaction of condensation from β-keto acids derivatives

The reaction between ethyl 4,4,4-trifluoroacetoacetate and cyanoacetamide in presence of sodium methoxide gives 3-cyano-6-hydroxy-4-trifluoromethyel-2-pyridone after crystallization from 15% hydrochoric acid. This pyridone appears to tautomerize in the solid state to 5-cyano-6-hydroxy-4-trifluoromethyel-2-pyridone (Figure 2.3.12) [24].

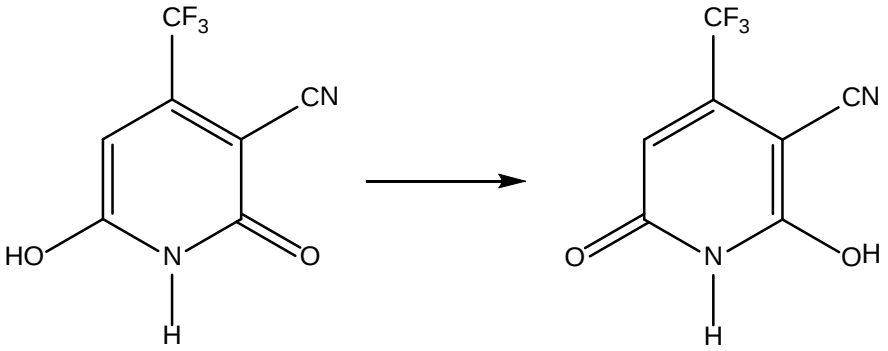

Figure 2.3.12 Synthesis of pyridone derivatives from ethyl 4,4,4-trifluoroacetoacetate and cyanoacetamide

6-amino-5-phenyl-3-cyanopyridin-2-one was synthesized by the reaction of 3-isobutoxy-2-phenylacrylonitrile with cyanoacetamide (Figure 2.3.13) [24].

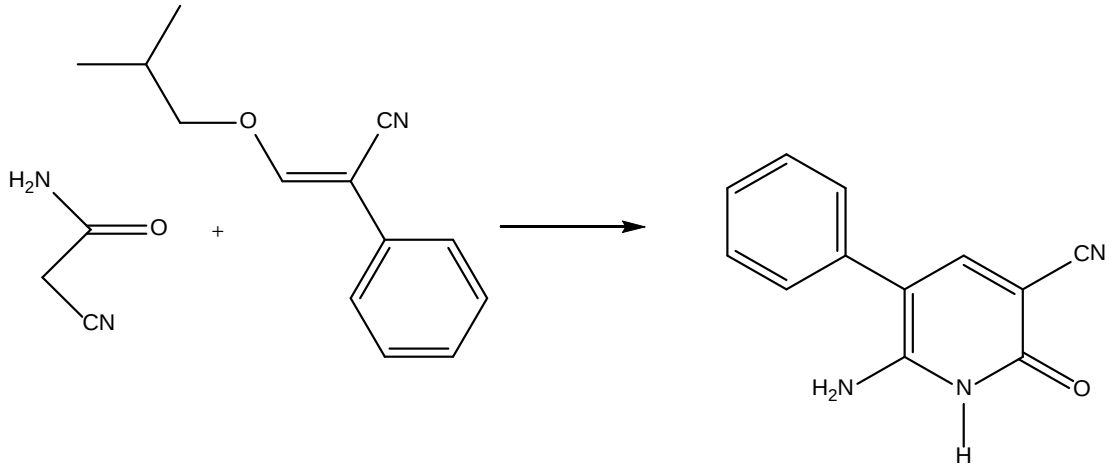

Figure 2.3.13 Synthesis of pyridone derivatives from 3-isobutoxy-2-phenylacrylonitrile and cyanoacetamide

Reaction of ethyl-(2,3,4-trimethoxybenzoyl)-pyruvate with cyanoacetamide in ethanol in presence of piperidine gaves 4-carbehtoxy-6-(2,3,4-trimethoxybenzyl)-3-cyanopyridin-2-one (Figure 2.3.14) [25].

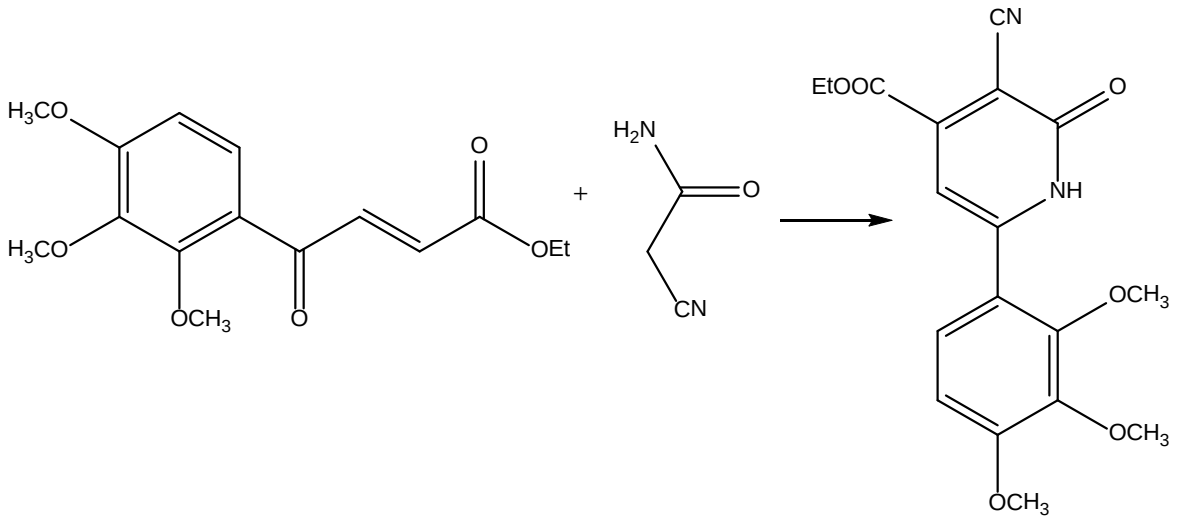

Figure 2.3.14 Synthesis of pyridone derivatives from ethyl-(2,3,4-trimethoxybenzoyl)-pyruvate and cyanoacetamide

2.3.1.4 Reaction of condensation from α,β-unsaturated carbonyl compounds

Condensation of α,β-unsaturated ketones with ethylcyanoacetate in presence of excess ammonium acetate give pyridones via the intermediate (Figure 2.3.15) [26].

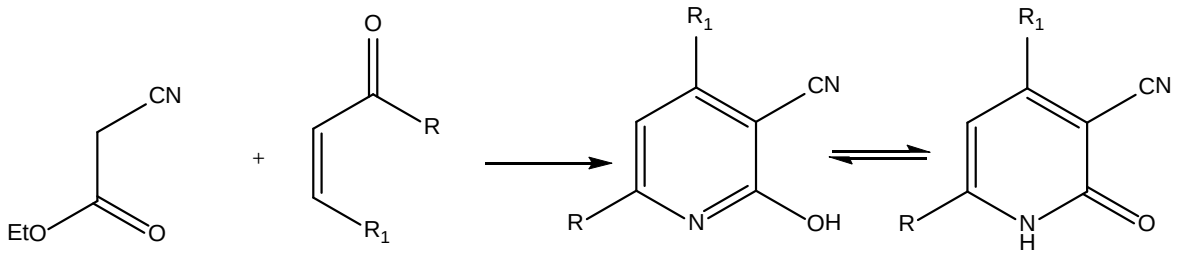

Figure 2.3.15 Synthesis of pyridone derivatives from α,β-unsaturated ketones and ethylcyanoacetate

Chalcones react with ethylcyanoacetate in the presence of ammonium acetate. Reaction products are 3-cyano-4,6-diarylhexahydro-2-pyridones , 3-cyano-4,6-diaryl-2-pyridones and ethyl-2-amino-4,6-diaryl nicotinic acids (Figure 2.3.16) [27].

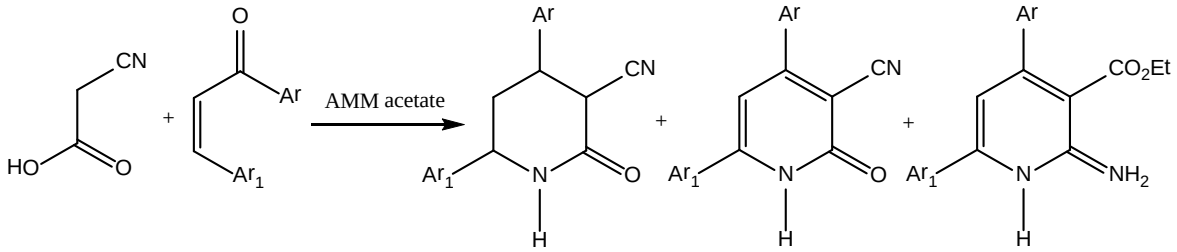

Figure 2.3.16 Synthesis of pyridone derivatives from chalcones and ethylcyanoacetate

Condensation of 2-substituted veratrals with ethyl methyl ketones gives substituted vinyl ketones that react with ethyl cyanoacetate in the presence of ammonium acetate to give 4-aryl-3-cyano-5,6-dimethyl-2-pyridones (Figure 2.3.17) [28].

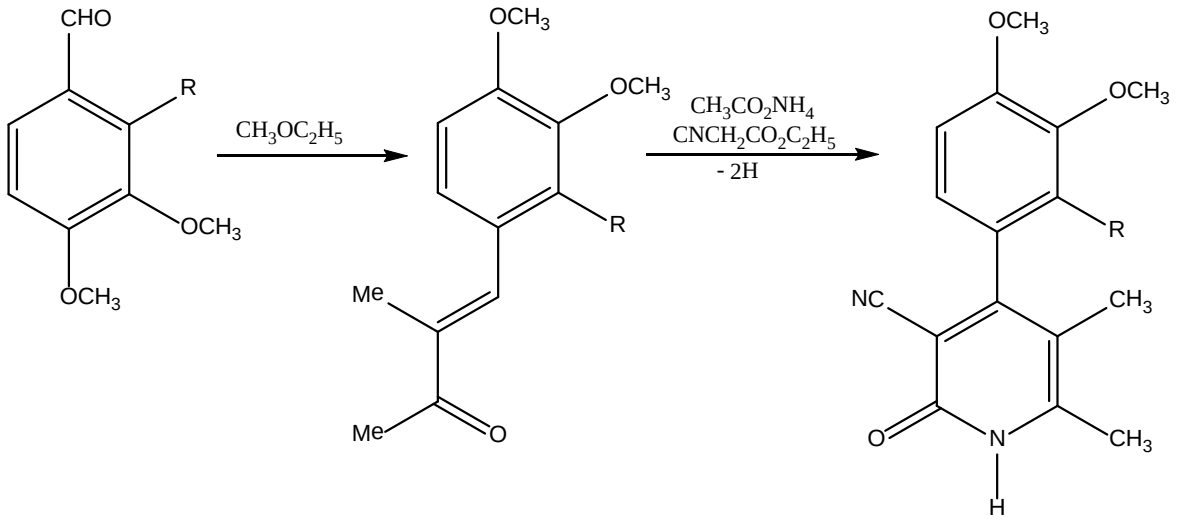

Figure 2.3.17 Synthesis of pyridone derivatives from substituted vinyl ketones and ethyl cyanoacetate

2.3.1.5 Condensation of 2-cyano-3-*(*substituted phenyl)acrylate and acetophenone

One of the ways for synthesis of 2-cyano-3-(substituted phenyl)acrylates is in the absence of a solvent, thereby facilitating the removal of the catalyst and purification of the reaction product. The most likely mechanism of the reaction is shown in Figure 2.3.18. Reactions are carried out in the solid state or in conditions where the temperature of the reaction mixture is above the melting point of the reactants. Knevenagel reaction between the cyanoacetamide and the corresponding aldehydes takes place in a quantitative yield in the conditions of the reaction in the solid state and in the melt. In order to be successfully carried out reaction in the solid state, trimethylamine (catalyst) is necessary, and can be easily removed together with water which separates in the reaction. The catalyst can be avoided if the reactants melt on 150-170 °C, whereby the product crystallized directly upon cooling [29].

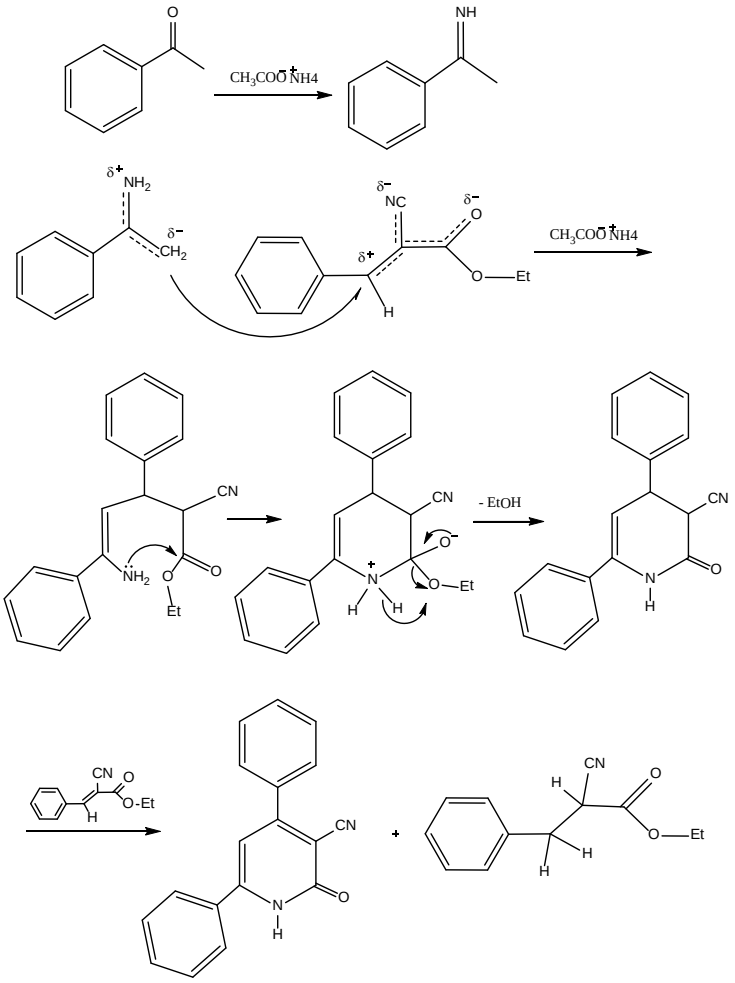

Figure 2.3.18 The mechanism of 3-cyano-4,6-diphenyl-2(1*H*) pyridone synthesis

2.3.1.6 Reaction of condensation from unsaturated acid derivatives

The condensation of diethyl glutaconate and *N*-benzylidenemethylamine or benzylideneaniline (R=CH_3 and C_6H_5 respectivly) in xylene give 1-substituted-3-benzylidene-5-carbethoxy-2-oxo-6-phenylpipeidenes, and form 1-substituted-3-benyzl-5-carboxy-6-phenyl-2-pyridones after heating in methanolic potassium hydroxide (Figure 2.3.19) [30].

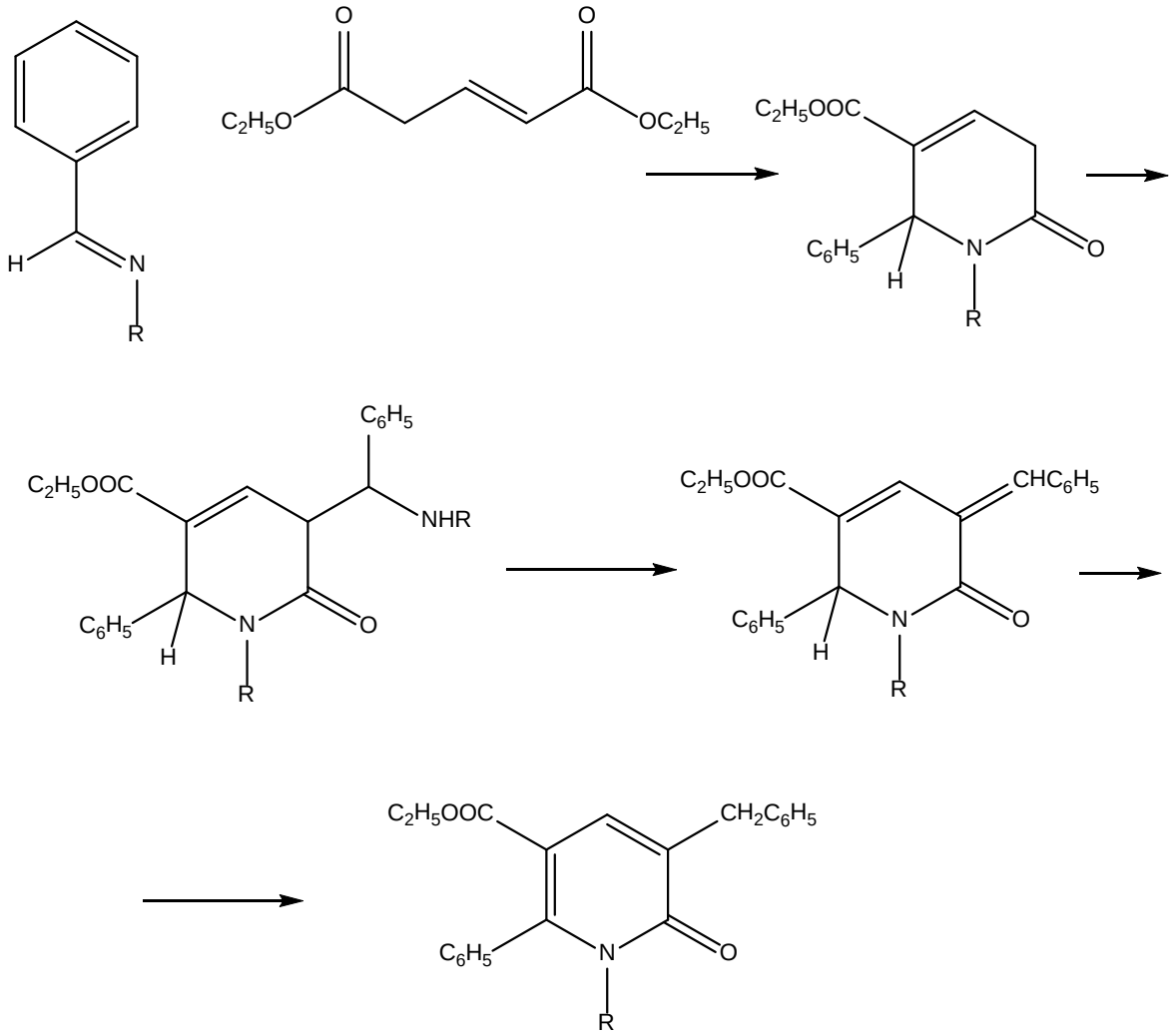

Figure 2.3.19 Synthesis of pyridone derivatives from diethyl glutaconate and *N*-benzyllidenemethylamine or benzylideneaniline

3-Cyano-4-phenyl-2-pyridone were obtained by cyclization reaction of α-cyano-β-methylcinnamide with ethyl formate in the presence of sodium hydride (Figure 2.3.20) [31].

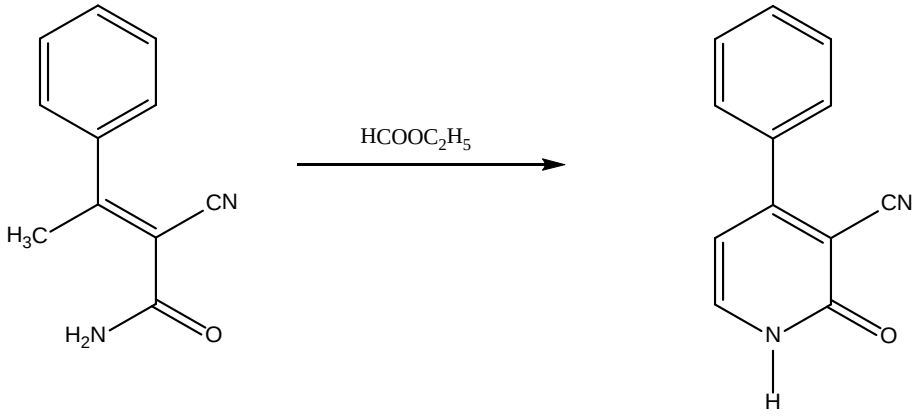

Figure 2.3.20 Synthesis of pyridone derivatives from α-cyano-β-methylcinnamide and ethyl format

Diethyl malonate reacts with ethyl B-aminocrotonate and acetylaceton imine, reaction products are 4-hydroxy-2-pyridon and 4,6-dimethyl-2-pyridone, respectively (Figure 2.3.21) [32].

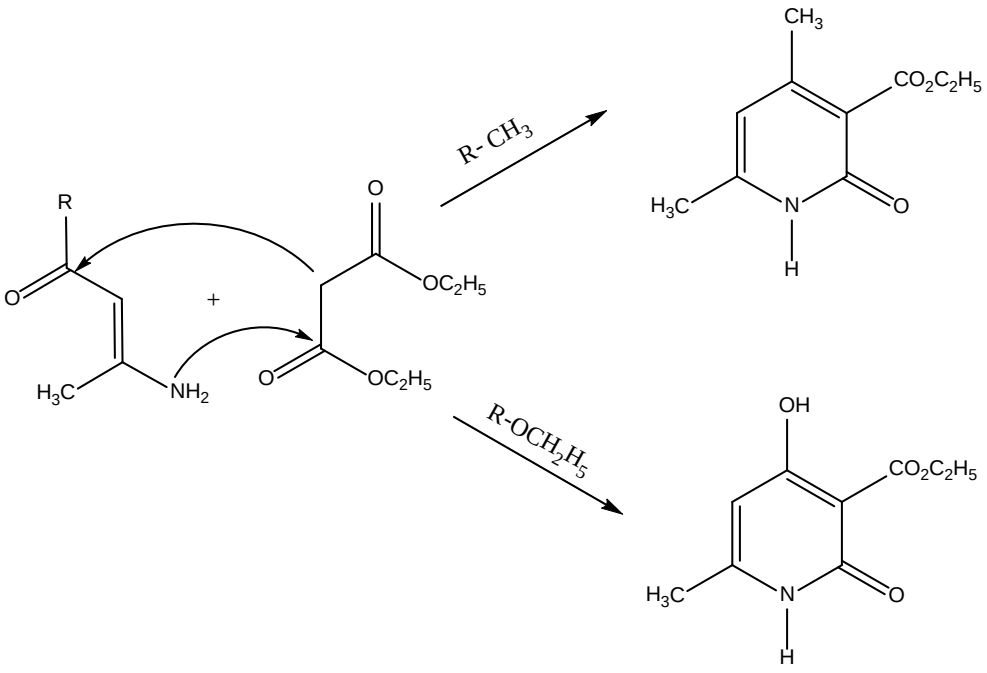

Figure 2.3.21 Synthesis of pyridone derivatives from diethyl malonate, ethyl B-aminocrotonate and acetylaceton imine

4-hydroxy-2-pyridones derivatives were synthesized by condensation of diethylbenzylmalonate with benzyl ether of propiophenone oxime (Figure 2.3.22) [33].

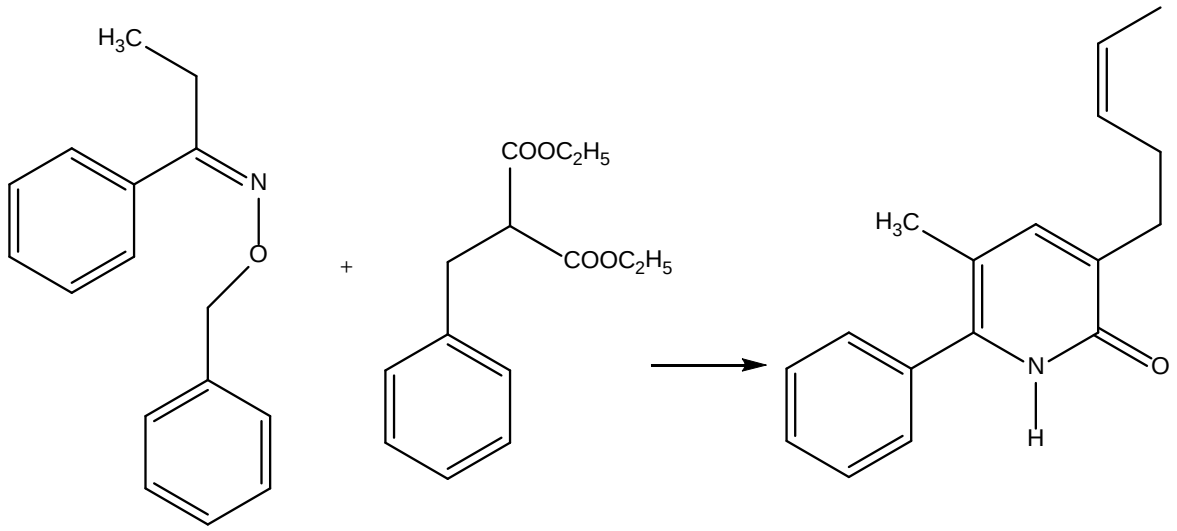

Figure 2.3.22 Synthesis of pyridone derivatives from diethylbenzylmalonate and benzyl ether of propiophenone oxime

3-substituted-4-hydroxy-6-methyl-2(1*H*)-pyridone-5-carbonitriles were synthesized by condensation of substituted diethyl malonate with 3-aminocrotononitrile (Figure 2.3.23) [34].

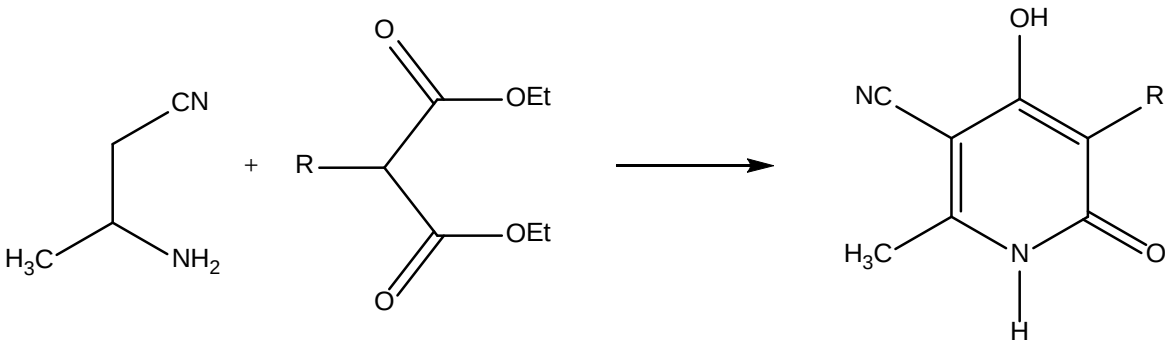

Figure 2.3.23 Synthesis of pyridone derivatives from diethyl malonate and 3-aminocrotononitrile

2.3.1.7 Condesation from β-dimethylaminoketo compounds

Condensation of ketone with dimethylformamide dimethylacetal afforded vinylogous amide, which in turn reacted with cyanoacetamide under basic conditions to generate the 5,6-diaryl-3-cyano-2-pyridones (Figure 2.3.24) [35].

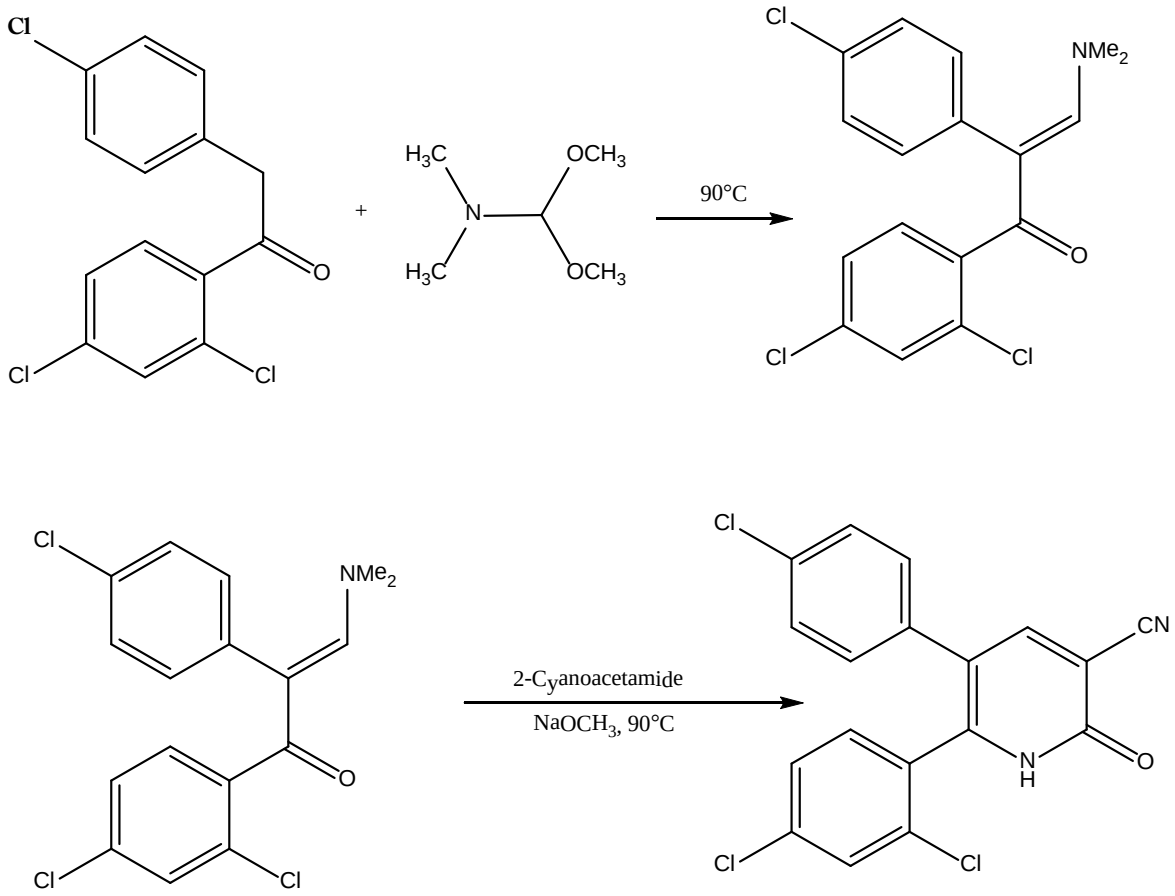

Figure 2.3.24 Synthesis of pyridone derivatives from ketone and dimethylformamide dimethylacetal

It was reported that the conversions of 2-cyano-5-(dimethylamino)-5- phenylpenta-2,4-dienamides into nicotinic acid derivatives by boiling in EtOH/HCl. But, when 2-cyano-5-(dimethylamino)-5-phenylpenta-2,4-dienamides were heated under reflux in AcOH, nicotinic nitrile derivatives were obtained (Figure 2.3.25) [36].

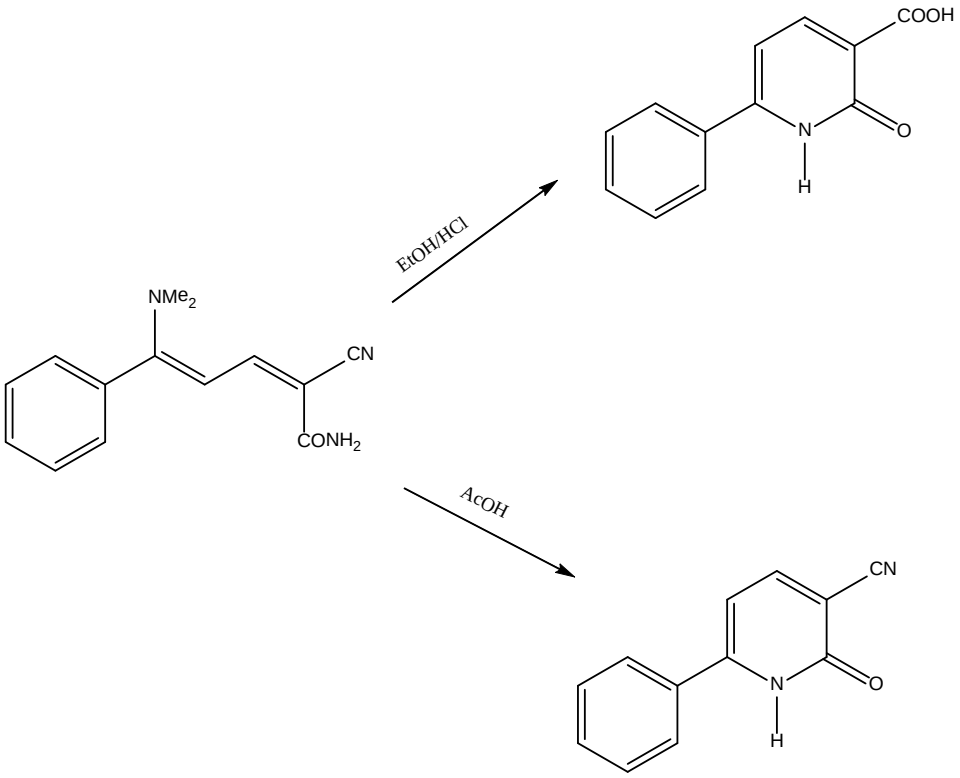

Figure 2.3.25 Synthesis of pyridone derivatives from 2-cyano-5-(dimethylamino)-5-phenylpenta-2,4-dienamides

The reactions between ketones and dimethylformamide-dimethylacetal (DMF-/DMA) gave the corresponding 3-dimethylaminopropen-2-ones, and generally without purification, these were condensed with 2-cyanoacetamide under basic condition to 3-cyano-2-pyridones, reported by Collins et al (Figure 2.3.26) [37].

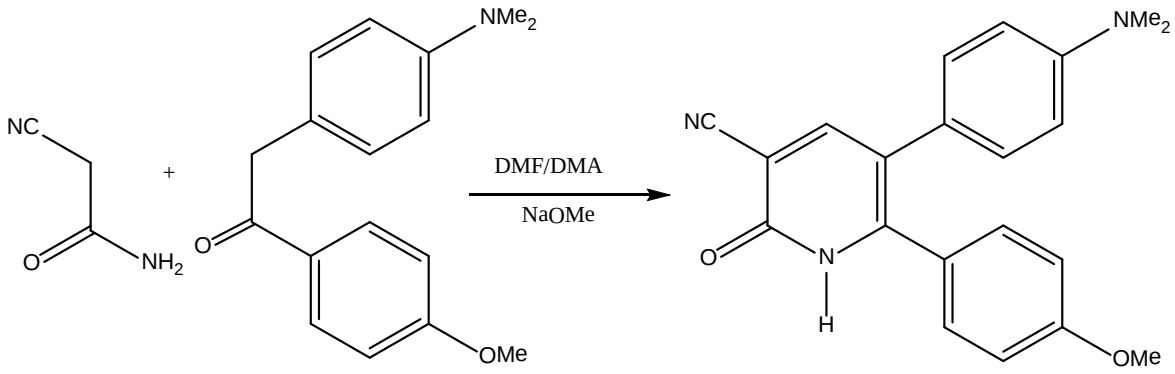

Figure 2.3.26 Synthesis of pyridone derivatives from ketones and dimethylformamide-dimethylacetal

2.3.1.8 Condensation from α,β-unsaturated nitriles

6-Amino-5-phenyl-3-cyanopyridin-2-one was synthesized by the reaction between 3-isobutoxy-2-phenylacrylonitrile and cyanoacetamide (Figure 2.3.27)[24].

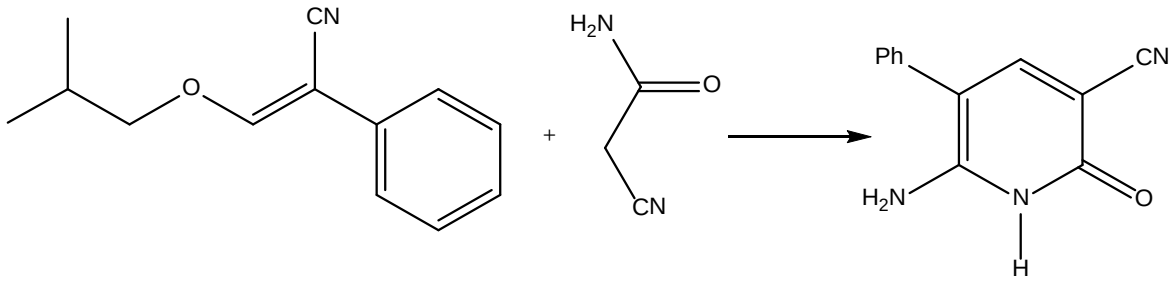

Figure 2.3.27 Synthesis of pyridone derivatives from 3-isobutoxy-2-phenylacrylonitrile and cyanoacetamide

The reactions of the equimolar amount of a-cinnamonitrile and enaminonitrile give pyridone and pyridine derivatives [38]. Formation of pyridone and pyridine derivatives is assumed to proceed via an acyclic intermediate form followed by intramolecular cyclization and spontaneous autooxidation under the reaction conditions in the case of pyridine derivatives and elimination of ethanol for pyridone derivatives (Figure 2.3.28).

The enaminonitrile can be readily synthesized by reaction of 4-cyanopyridine with acetonitrile in the presence of potassium-t-butoxide [39].

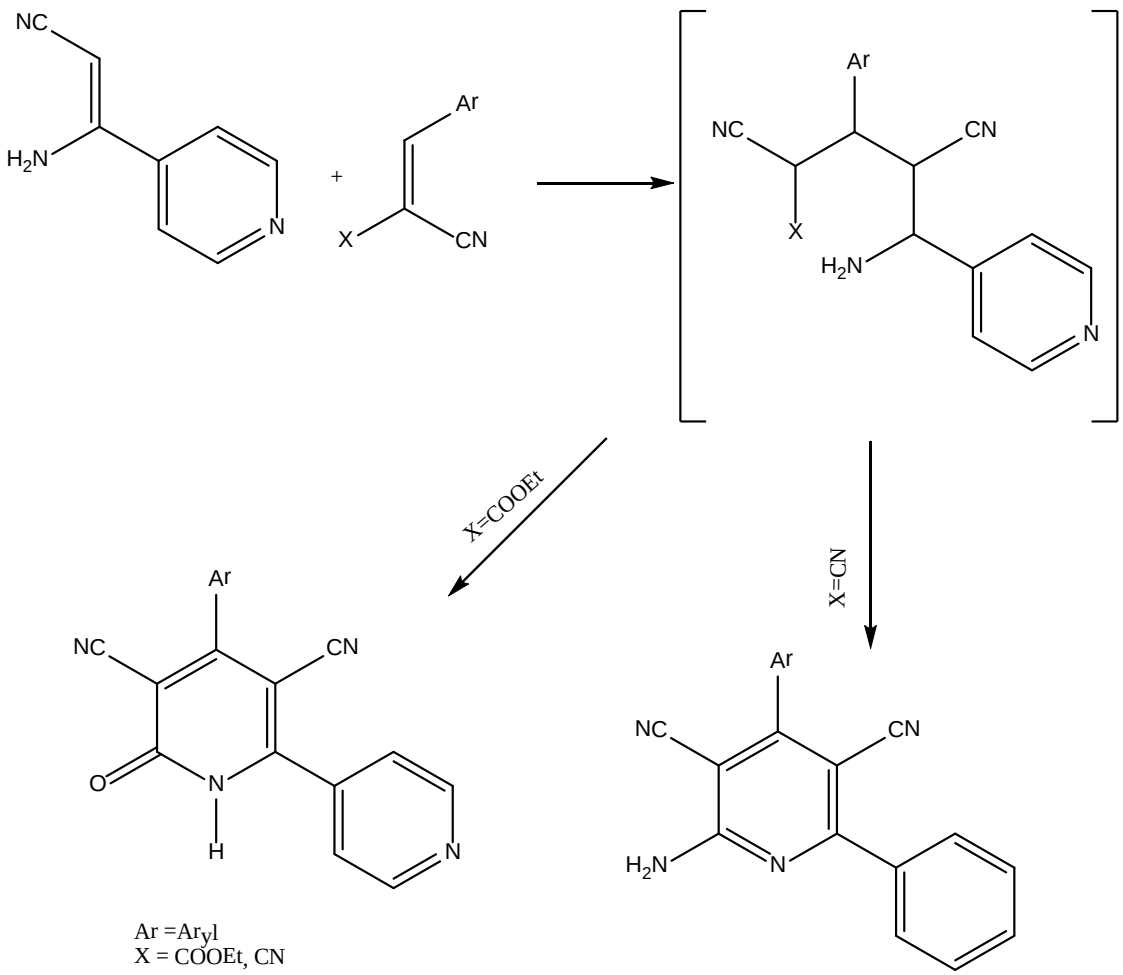

Figure 2.3.28 Synthesis of pyridone derivatives by reaction of 4-cyanopyridine and acetonitrile

2-alkoxy-3-cyanopyridines were achieved by the reaction of malononitrile and chalcones in corresponding sodium alkoxide (Figure 2.3.29) [40-43].

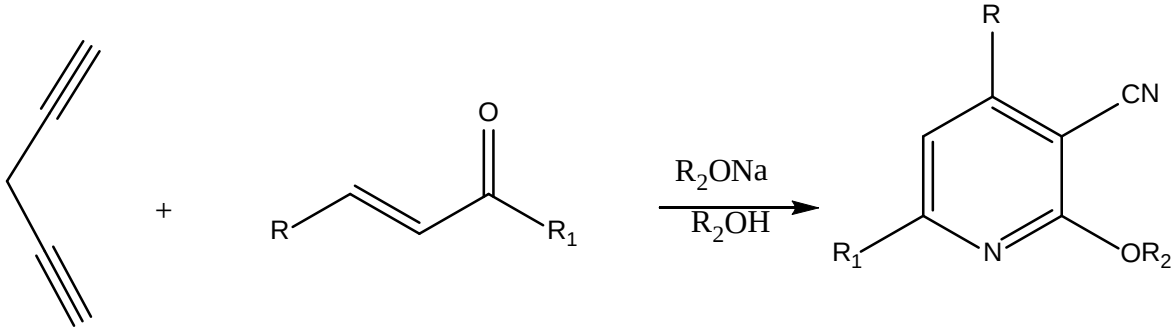

R, R_1 = aryl or hetroaryl

Figure 2.3.29 Synthesis of pyridone derivatives from malononitrile and chalcones in corresponding sodium alkoxide

2.3.1.9 Synthesis from halogen 2-pyridone derivatives

In the reaction of 2,5,6-trichloro-3,4-diphenylpyridine and dimethyl sulfate in water, aqueous sodium hydroxide, product are 3,6-dichloro-4,5-diphenyl-1-methyl-2-pyridone and 5,6-dichloro-3,4-diphenyl-1-methyl-2-pyridone, which hydrogenate to 4,5- and 3,4-diphenyl-1-methyl-2-pyridone, respectively (Figure 2.3.30) [32].

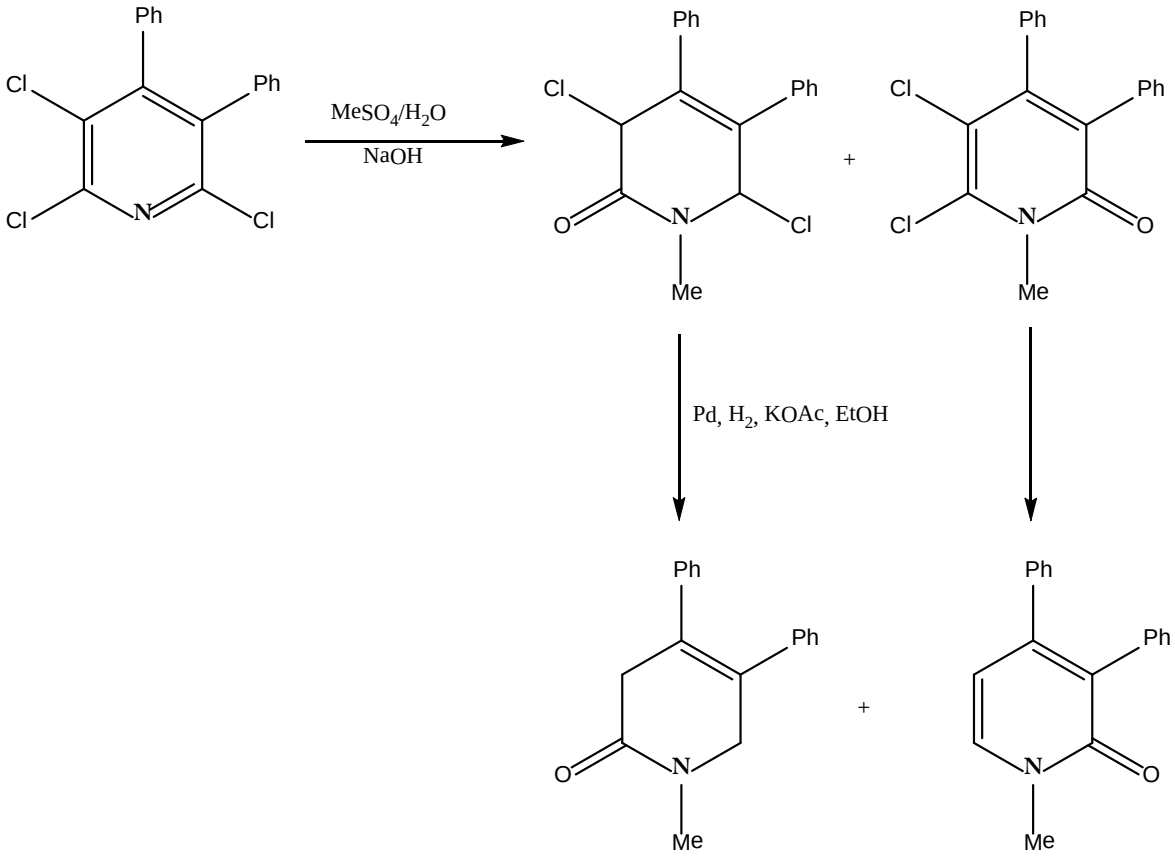

Figure 2.3.30 Synthesis of pyridone derivatives from 2,5,6-trichloro-3,4-diphenylpyridine and dimethyl sulfate

The treatment of 2-, 3-, 4-substituted pyridine-1-oxides and 2-bromopyridine gives 1-(substituted-2-pyridyl)-2-pyridones (Figure 2.3.31)[44].

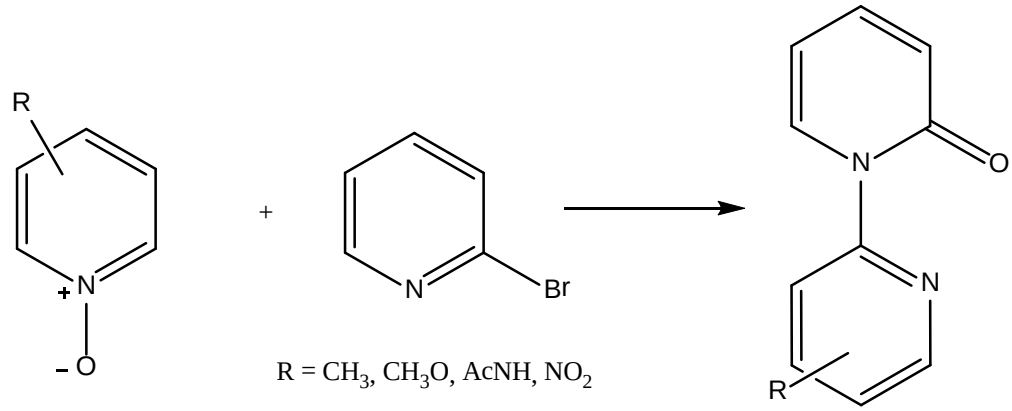

Figure 2.3.31 Synthesis of pyridone derivatives from 2- , 3- ,4-substituted pyridine-1-oxides and 2-bromopyridine

2-(3,5-Dinitro-2-pyridine) pyridinium chloride which can be synthesized by reaction of 3,5-dinitro-2-chloropyridine with pyridine in ether or benzene, is easily hydrolyzed in an alkaline medium to 3,5-dinitro-2-pyridone (Figure 2.3.32) [45].

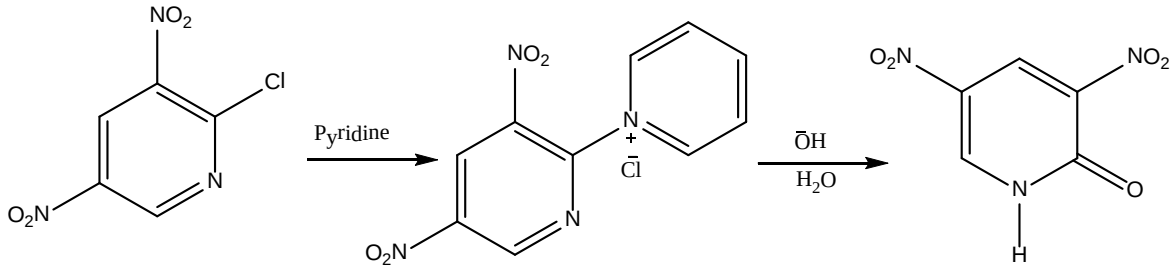

Figure 2.3.32 Synthesis of pyridone derivatives from 2-(3,5-dinitro-2-pyridine) pyridinium chloride alkaline medium

2.3.1.10 Synthesis from other heterocyclic ring

1,2,3,6-Tetra-methyl-4-pyridone was synthesized by reaction of 2,3,6-three-methyl-4-pyrone in aqueous methylamine. The pyridone was converted to the pyrone in dilute sulfuric acid containing mercuric sulfate (Figure 2.3.33) [46].

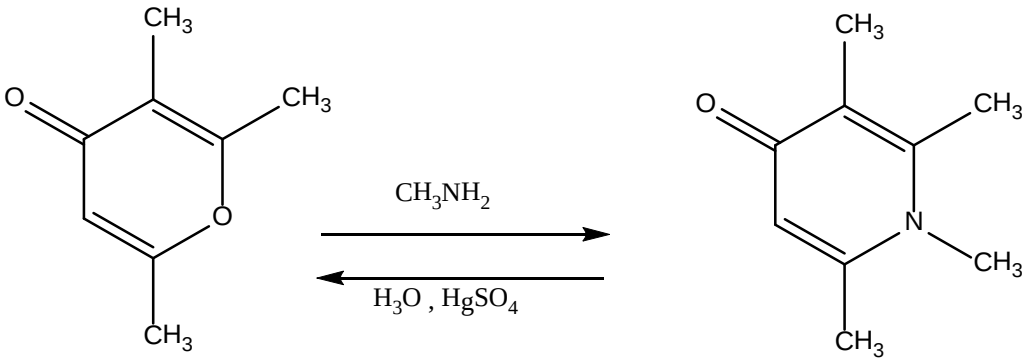

Figure 2.3.33 Synthesis of pyridone derivatives by reaction of 2,3,6-tetra-methyl-4-pyrone in aqueous methylamine

Diels-Alder addition of 3-benzyl-6-methyl-2,5-dihydroxypyrazine to dimethyl acetylenedicarboxylate gives an adduct that decomposes on heating to give equal amounts of these 2-pyridones (Figure 2.3.34) [47].

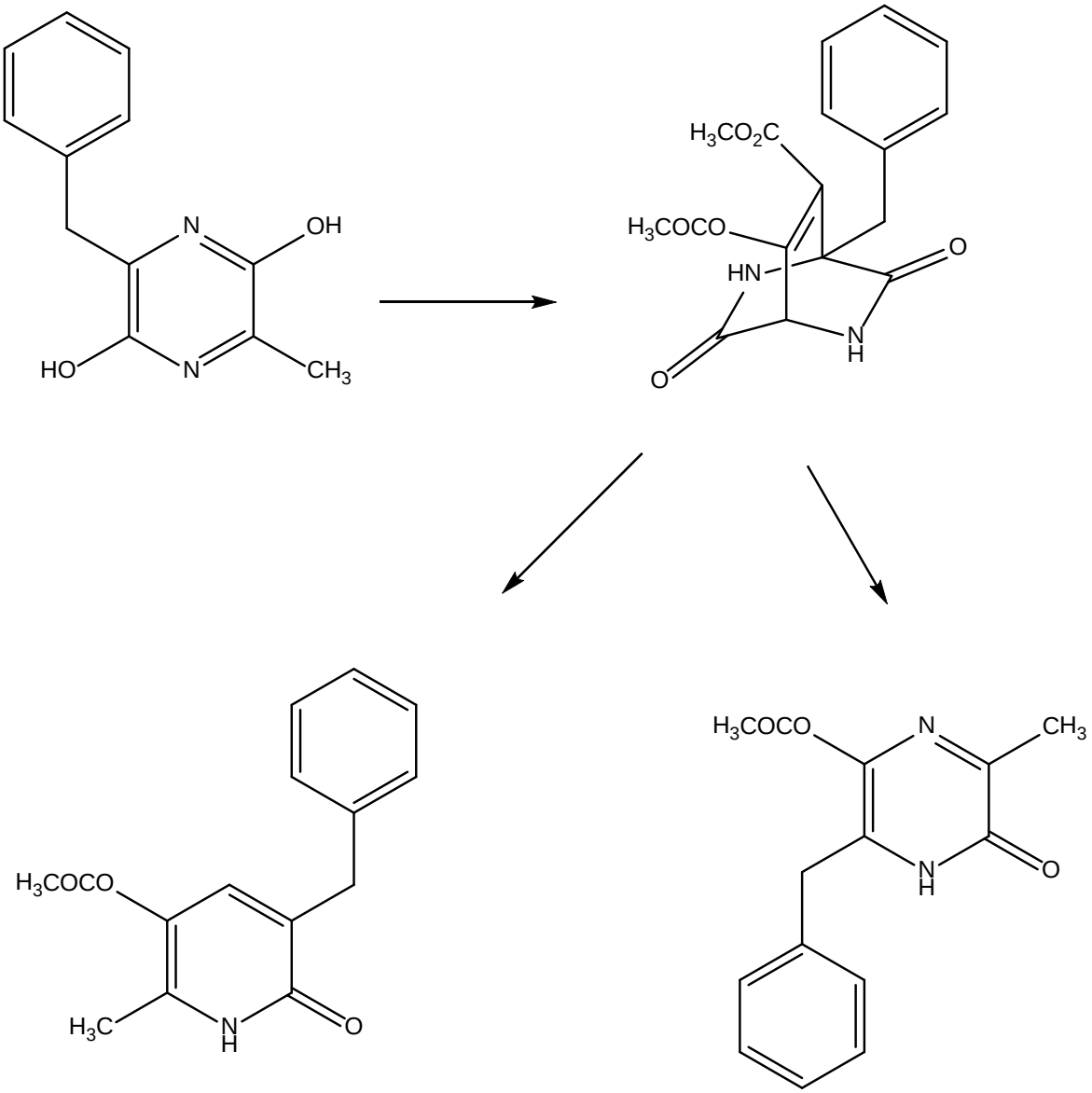

Figure 2.3.34 Synthesis of pyridone derivatives from 3-benzyl-6-methyl-2,5-dihydroxypyrazine

The reaction of benzylmalonic acid and acetophenone-anil in acetic anhydride form 5-benzyl-2-methyl-4,6-dioxo-2,3-diphenylhexahydro-1,3-dione, which rearrange to 3-bezyl-4-hydroxy-1,6-diphenyl-2-pyridone when heated with phosphorus pentoxide (Figure 2.3.35) [33].

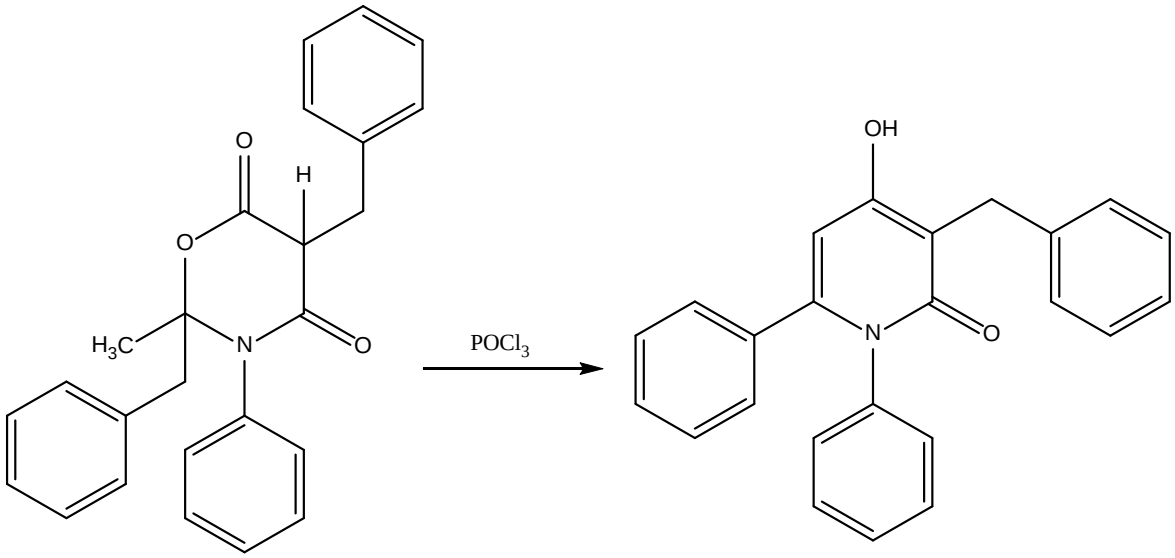

Figure 2.3.35 Synthesis of pyridone derivatives from5-benzyl-2-methyl-4,6-dioxo-2,3-diphenylhexahydro-1,3-dione

3-Hydroxy-2-pyridones were prepared via reaction of pyenylcyclobutenediones and enamines. The reaction took two steps and gaves 1:1 adducts that rearrange with bases to the pyridones (Figure 2.3.36) [48].

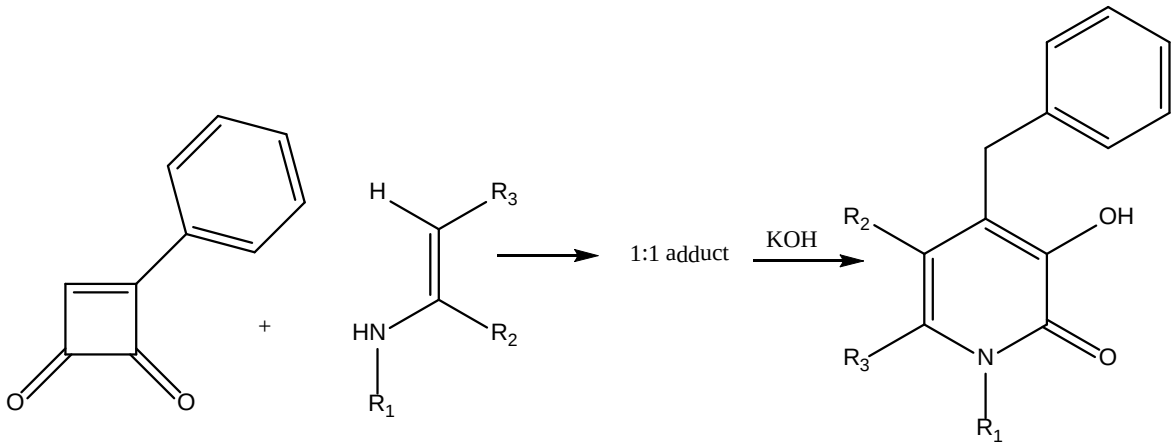

Figure 2.3.36 Synthesis of pyridone derivatives from phenylcyclobutenediones and enamines

2.3.2 Conventional synthesis of azo dyes

2.3.2.1 Diazotization methods

Depending on the basicity and solubility of the amines being diazotized, the following diazotization methods find industrial use:

- Direct diazotization-The primary aromatic amine is dissolved or suspended in aqueous hydrochloric or sulfuric acid, and a concentrated aqueous sodium nitrite solution is added. An excess of 2.5-3 equivalents of acid per equivalent of amine is used. A temperature of 0-5 °C is maintained by adding ice.
- Indirect diazotization-Amines with sulfonic or carboxylic acid groups are often difficult to dissolve in dilute acid. Therefore, the amine is dissolved in water or a weak alkali, and the calculated amount of sodium nitrite solution is added to this amine solution which is stirred into the ice-cooled acid solution already in the vessel. The acid can also be added to the amine–nitrite mixture already at hand.
- Diazotization of weakly basic amines-Weakly basic amines are dissolved in concentrated sulfuric acid and diazotized with nitrosylsulfuric acid, which is easily prepared from solid sodium nitrite and concentrated sulfuric acid.
- Diazotization in organic solvents-The water-insoluble or sparingly soluble amine is dissolved in glacial acetic acid or other organic solvents and, where necessary, diluted with water. After the addition of acid it is diazotized in the usual manner with sodium nitrite solution. Nitrosylsulfuric acid, nitrosyl chloride, alkyl nitrites, or nitrous gases can also be used instead of sodium nitrite. Temperature, pH, and the concentration of the diazotizing solution often have a considerable effect on the progress of diazotization. Physical properties (distribution, particle size) and the addition of emulsifiers and dispersing agents influence the diazotization of slightly soluble amines.

2.3.2.2 Aryl azo pyridone dyes

In the last three or four decades disperse dyes derived from pyridones have gained importance. The azo pyridone dyes are widely used in various fields. They have excellent coloration properties and are suitable for the dyeing of polyester fabrics. Basic features of these dyes are simplicity of their synthesis by diazotation and azo coupling, generally high molar extinction coefficient and medium to high light and wet fastness. The absorption maxima of these dyes show their visible absorption wavelength in the ranging of yellow to orange due to poorly delocalized electrons in pyridone ring, but there are few dyes that have deep color such as red or violet. Pyridone dyes with alkyl and aryl groups in ortho position to azo group show 2-pyridone/2-hydroxypyridine tautomerism and those containing OH and NHR groups conjugated with azo group show azo-hydrazone tautomerism. Determination of azo-hydrazone tautomerism is quite interesting since the tautomers have different physico-chemical properties and most important different coloration. Equilibrium between two tautomers is influenced by the structure of the compounds and the solvent used. The tautomeric behavior is studied using various techniques, including FT-IR, UV-vis and NMR spectroscopy. There are, also, quantum chemical calculations considering azo-hydrazon tautomerism. A great number of pyridone dyes exist in hydrazone form in solid state while in solvents there is a mixture of tautomers. In addition, the X-ray single-crystal diffraction analysis of some commercial pyridone dyes was mentioned and it was established that they all crystallize in the hydrazone form.

Arilazo pyridone colors are synthetic organic colors where the coupling component is usually pyridone derivative, a diazo component can be carbo or heterocyclic compound. The great importance of these dyes and their use in the last few decades is the result of specific properties, such as high excited molar ratio and good resistance to light and wet treatment [49]. It is known for their use of computer technology, LCD screens and graphics inkjet color [50, 51] commonly used arilazo pyridone colors as disperse dyes for coloring and synthetic fibers [52]. The absorption maxima of these dyes are in visibly spectrum in the range between yellow and orange, which is the result of weak electron delocalization in the heterocyclic pyridone ring, but there are also colors that have stronger staining like red and purple [53]. Great use of azo compounds is a result of a relatively simple diazo-coupling reactions as well as a large number of compounds that can be used as diazo and coupling components. The common feature of all the components

for the coupling of the presence of an active hydrogen atom bound to a carbon atom, which is involved in the substitution reaction. Arilazo pyridone color can be obtained in two ways. The first method involves direct coupling of the pyridone, obtained in the reaction of the corresponding diketones, cyanoacetamide or keto ester, and various salts (Figure 2.3.37, reaction time 1), while the second method involves coupling of diazonium salts with diketones or keto ester (Figure 2.3.37, reaction time 2) [54-60].

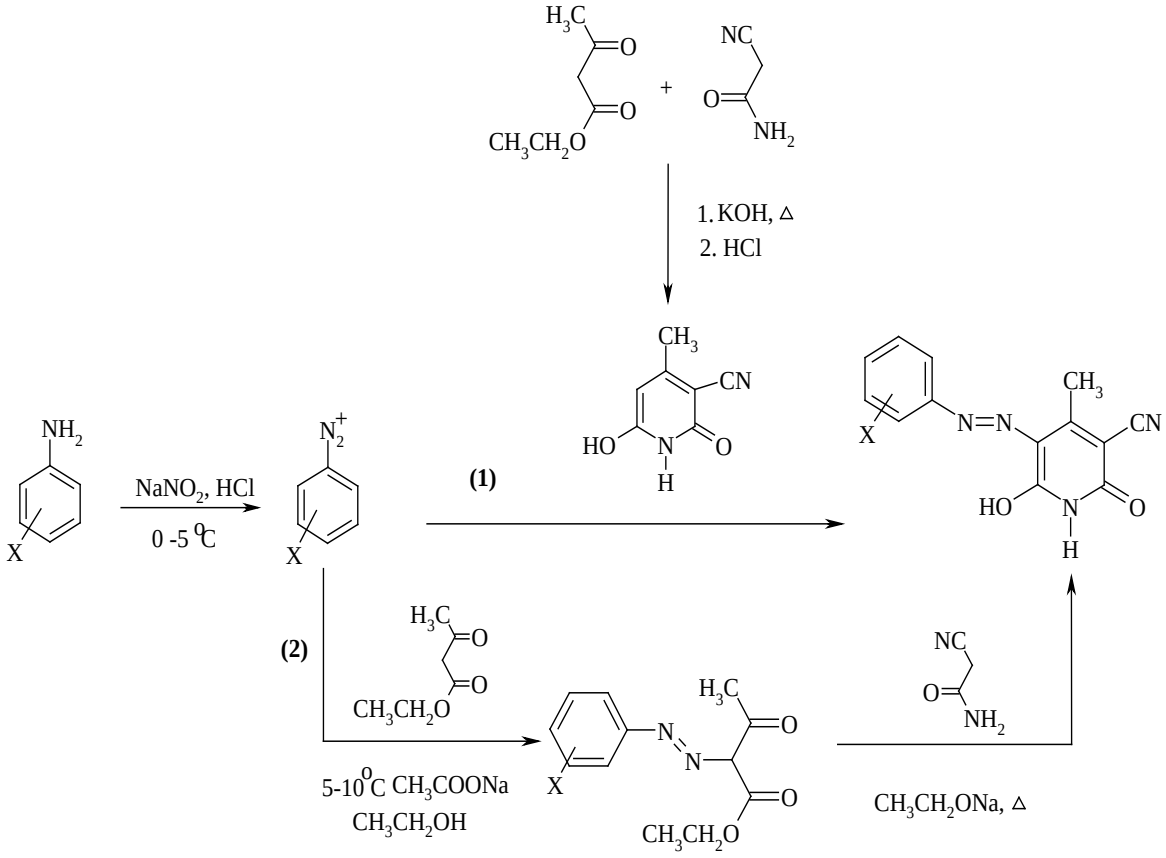

Figure 2.3.37 Synthesis of arylazo pyridone dye

2.3.2.3 Synthesis of azo dyes starting from pyridones

Synthesis of azo dyes from pyridone and their absorption properties in various solvents were widely studied [61].

1-Substituted-3-(p-substituted phenylazo)-2-hydroxy-4-methyl-5-cyano-6-pyridones dyes were prepared by coupling of 1-substituted-2-hydroxy-4-methyl-5-cyano-6-pyridones, which were synthesized via reaction of ethyl acetoacetate and amines in ethanol under reflux, with the diazonium salts (prepared by diazotize p-substituted anilines at 0-5 °C using hydrochloric acid and sodium nitrite) (Figure 2.3.38) [62].

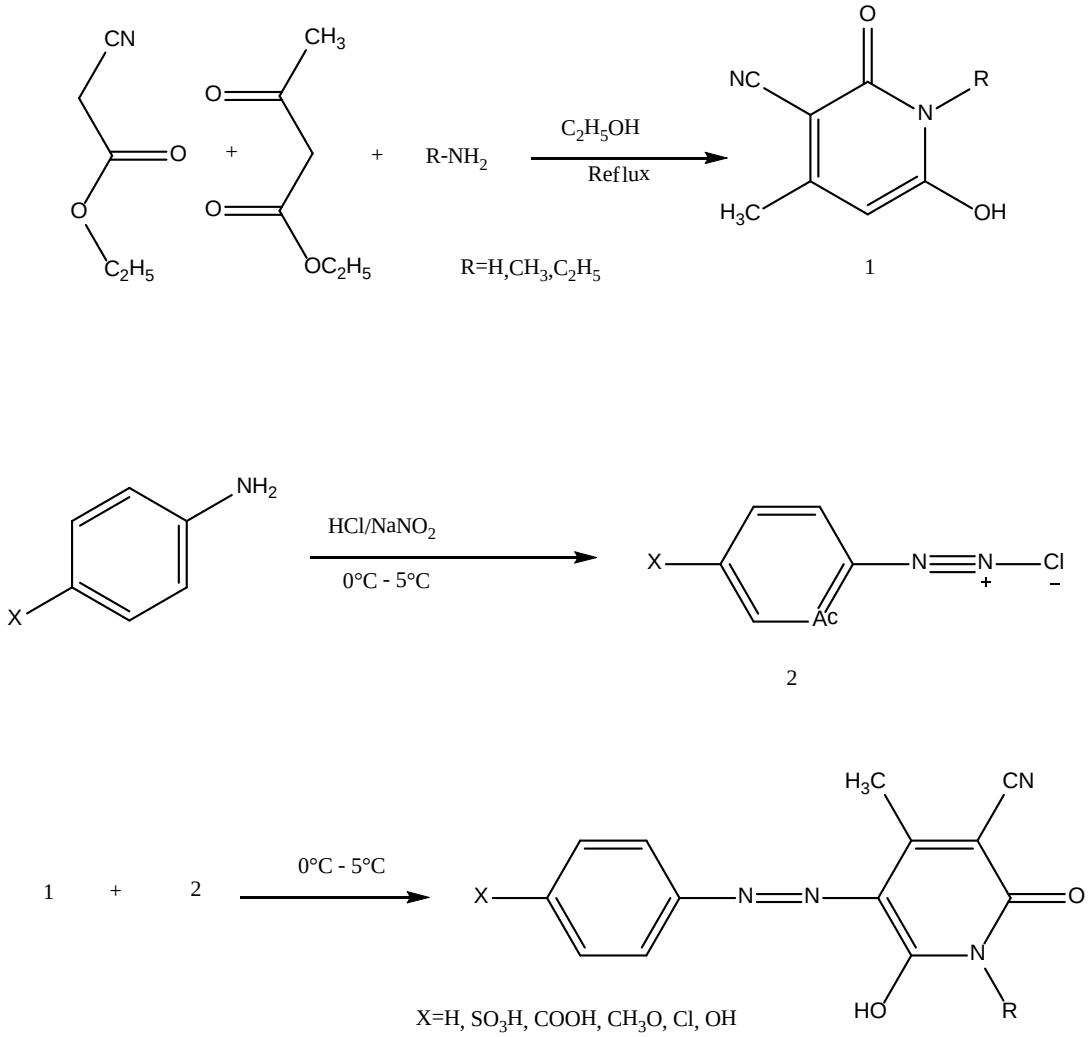

Figure 2.3.38 Synthesis of pyridone derivatives from ethyl acetoacetate amines and diazonium salts

Azo pyridines were synthesized by the diazotization-coupling reaction, as shown in Figure 2.3.38. In this procedure acetylacetone was coupled with diazotised substituted aniline. Reaction intermediate is 3-(substituted-phenylazo)-2,4-pentanedione, which cyclized with cyanoacetamide to an azo-pyridones (Figure 2.3.39) [57].

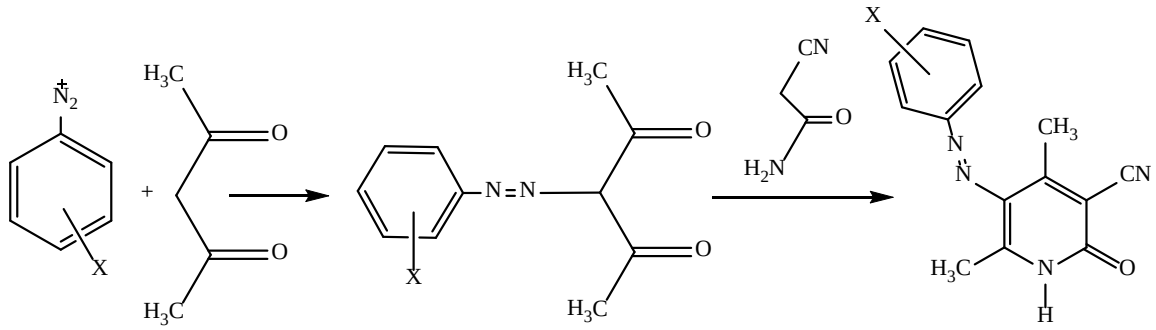

Figure 2.3.39 Synthesis of azo-pyridones derivatives from intermediate (3-(substituted-phenylazo)-2,4-pentanedione)

2.4 Microwave synthesis

2.4.1 Microwave irradiation

Microwave irradiation is electromagnetic irradiation in the frequency range of 0.3 to 300 GHz [63]. All domestic “kitchen” microwave ovens and all dedicated microwave reactors for chemical synthesis operate at a frequency of 2.45 GHz (which corresponds to a wavelength of 12.24 cm) to avoid interference with telecommunication and cellular phone frequencies. The energy of the microwave photon in this frequency region (0.0016 eV) is too low to break chemical bonds and is also lower than the energy of Brownian motion. It is therefore clear that microwaves cannot induce chemical reactions [64-67].

Microwave-enhanced chemistry is based on the efficient heating of materials by “microwave dielectric heating” effects. This phenomenon is dependent on the ability of a specific material (solvent or reagent) to absorb microwave energy and convert it into heat. The electric component [68] of an electromagnetic field causes heating by two main mechanisms: dipolar polarization and ionic conduction. Irradiation of the sample at microwave frequencies results in the dipoles or ions aligning in the applied electric field. As the applied field oscillates, the dipole or ion field attempts to realign itself with the alternating electric field and, in the process, energy is lost in the form of heat through molecular friction and dielectric loss. The amount of heat generated by this process is directly related to the ability of the matrix to align itself with the frequency of the applied field. If the dipole does not have enough time to realign, or reorients too quickly with the applied field, no heating occurs. The allocated frequency of 2.45 GHz used in all commercial systems lies between these two extremes and gives the molecular dipole time to align in the field, but not to follow the alternating field precisely [66,67].

Microwave irradiation has gained popularity in the past decade as a powerful tool for rapid and efficient synthesis of a variety of compounds because of selective absorption of microwave energy by polar molecules [69]. The application of microwave irradiation enhance reaction rate, improve product field in chemical synthesis and provides formation of a variety of carbon-heteroatom bonds.

2.4.1.1 Ecological benefit of microwave synthesis

The term “green chemistry” is defined as invention, design and application of chemical products and processes to reduce or to eliminate the use and generation of hazardous substances. Green chemistry can diminish the need for other approaches to environmental protection. Ideally, the application of green chemistry principles and practice renders regulation, control, clean-up, and remediation unnecessary, and the resultant environmental benefit can be expressed in terms of economic impact [63]. In the past, microwave chemistry was often used only when all other options to perform a particular reaction had failed, or when exceedingly long reaction times or high temperatures were required to complete a reaction. This practice is now slowly changing and, due to the growing availability of microwave reactors in many laboratories, routine synthetic transformations are now also being carried out by microwave heating. Microwave include following advantages, over the conventional heating:

- High efficiency of heating;
- Reduction in unwanted side reaction;
- Improve reproducibility;
- Purity in final product;
- Reduce wastage of heating reaction vessel;
- Environmental heat loss can be avoided;
- Low operating cost;
- Uniform heating occurs throughout the material.

Avoiding organic solvents during the reactions in organic synthesis leads to a clean, efficient and economical technology (green chemistry). There is an increasing interest in the use of environmentally benign reagents and procedures. In other words, the absence of solvents coupled with the high yields and short reaction times often associated with reactions of this type make these procedures very attractive for synthesis. The practical dimension to the microwave heating protocols has been added by accomplishing reactions on solid supports under solvent-free conditions [63]. These solvent-free microwave-assisted reactions provide an opportunity to work with open vessels, thus avoiding the risk of high-pressure development and increasing the potential of such reactions to upscale [70]. The practical feasibility of microwave-assisted

solvent-free synthesis has been demonstrated in various useful transformations [71,72] and in synthesis of heterocyclic systems [73,74].

In many of the published examples, microwave heating has been shown to dramatically reduce reaction times, increase product yields and enhance product purities by reducing unwanted side reactions compared to conventional heating methods. The advantages of this enabling technology have, more recently, also been exploited in the context of multistep total synthesis [75], drug discovery [76], have additionally penetrated related fields such as polymer synthesis [77], nanotechnology [78], material sciences [79], and biochemical processes [80]. The use of microwave irradiation in chemistry has thus become such a popular technique in the scientific community that it might be assumed that, in a few years, most chemists will probably use microwave energy to heat chemical reactions on a laboratory scale. The statement that, in principle, any chemical reaction that requires heat can be performed under microwave conditions has today been generally accepted as a fact by the scientific community [81].

2.4.1.2 Microwave synthesis of organic compounds

The first reports on the use of microwave heating to accelerate organic chemical transformations (MAOS) were published in 1986 [82,83]. In the 1990s, several groups started to experiment with solvent-free microwave chemistry (so-called dry-media reactions), which eliminated the danger of explosions [84,85]. Here, the reagents were pre-adsorbed onto either an essentially microwave-transparent (i.e. silica, alumina or clay) or strongly absorbing (i.e. graphite) inorganic support, that additionally may have been doped with a catalyst or reagent. In order to nonetheless achieve high reaction rates, high-boiling microwave-absorbing solvents have been frequently used in open-vessel microwave synthesis [86]. Because of the recent availability of modern microwave reactors with on-line monitoring of both temperature and pressure, microwave-assisted organic synthesis (MAOS) in dedicated sealed vessels using standard solvents-a technique pioneered by Christopher R. Strauss in the mid-1990s [87] has been celebrating a comeback in recent years. It appears that the combination of rapid heating by microwaves with sealed-vessel (autoclave) technology will most likely be the method of choice for performing MAOS on a laboratory scale in the future.

Reviewing the present literature [69], it appears that most scientists agree that in the majority of cases the reason for the observed rate enhancements is a purely thermal/kinetic effect, i.e., a consequence of the high reaction temperatures that can rapidly be attained when irradiating polar materials in a microwave field.

Since 2001, the number of publications related to MAOS has increased dramatically, to such a level that it might be assumed that, in a few years, most chemists will probably use microwave energy to heat chemical reactions on a laboratory scale [88]. Not only is direct microwave heating able to reduce chemical reaction times significantly, but it is also known to reduce side reactions, increase yields and improve reproducibility. Therefore, many academic and industrial research groups are already using MAOS as a technology for rapid reaction optimization, for the efficient synthesis of new chemical entities or for discovering and probing new chemical reactivity. Microwave have been used to speed up chemical reactions in the laboratories [89] which led scientists to investigate the mechanism of microwave dielectric heating and to identify the advantages of the technique for chemical synthesis [90]. During recent years, microwaves have been extensively used for carrying out chemical reactions and have become a useful non-conventional energy source for performing organic synthesis [82]. This is supported by a great number of publications in recent years, particularly in 2003, related to the application of microwaves as a consequence of a great availability of dedicated and reliable microwave instrumentation [82,91].

The first recorded application of microwave energy in organic synthesis is the aqueous emulsion polymerization of butyl acrylate, acrylic acid and methacrylic acid using pulsed electromagnetic radiation. During the last two decades, the activity in this new technique has experienced exponential growth and has been extensively reviewed [92-95]. Kappe and Dallinger have reported the impact of microwaves on drug discovery [93]. Even microwave-assisted reactions under solvent-free conditions promoted the synthesis of Zincke's salt and its conversion to chiral pyridinium salts in water [94] and microwave- assisted organic transformations using benign reaction media have also been reported [81,95]. Moreover, Varma and co-workers have reported the drug discovery by using aqueous microwave chemistry [94,95].

2.4.2 Microwave synthesis of 3-cyano-2-pyridones

The application of microwave techniques in the synthesis of organic compounds has inevitably led to the microwave synthesis of compounds with the 2-pyridone ring. In the beginning the synthesis was performed using domestic microwave ovens. Due to the problems associated with the use of these ovens in the synthesis (reproducibility, controllability, safety) dedicated microwave reactors were introduced. The basic principles of synthesis of heterocyclic molecules used in conventional synthesis were applied in microwave synthesis [96]. Thus, the pyridone ring can be obtained from fragments containing different numbers of carbon atoms. There are few combinations of fragments: 4-1, 3-2, 1-3-1, 2-2-1, 2-1-2. Condensation of type 4-1 means that the condensation involves two acyclic systems, one has four and the other one carbon atom, while nitrogen can be a part of one of the fragments, or be introduced as a separate fragment. A good example of such combination is a paper by Gorobets et al. [97], in which different carbonyl building blocks were reacted with *N*,*N*-dimethylformamide dimethyl acetal (DMFDMA) to obtain enaminones in high yield (the reaction is carried out in the absence of solvent and at elevated temperature). The obtained enaminones, without purification, react with different methylene nitriles at 100 °C for 5 minutes in the presence of 2-propanol (solvent) and a catalytic amount of piperidine (base). In this way, the authors were able to isolate 18 different 2-pyridones (of 80 possible) with yields varying from 27 to 96%, while some products were obtained in pure form after simple filtration. This synthesis is given in Figure 2.4.1.

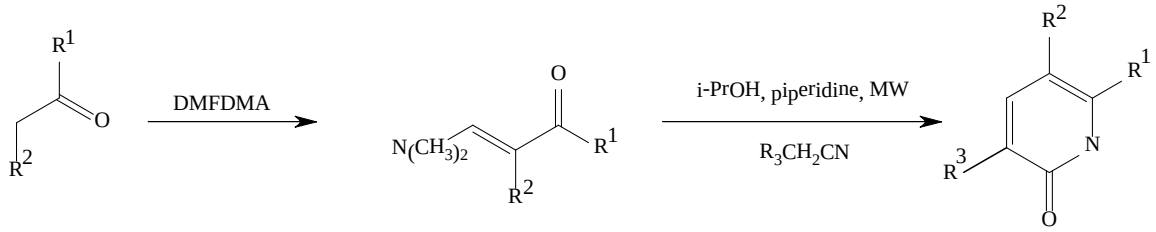

Figure 2.4.1 Microwave synthesis of substituted 2-pyridones from enaminones

An example of 3-2 type condensation of 3-cyano-2-pyridones is shown in Figure 2.4.2 [60].

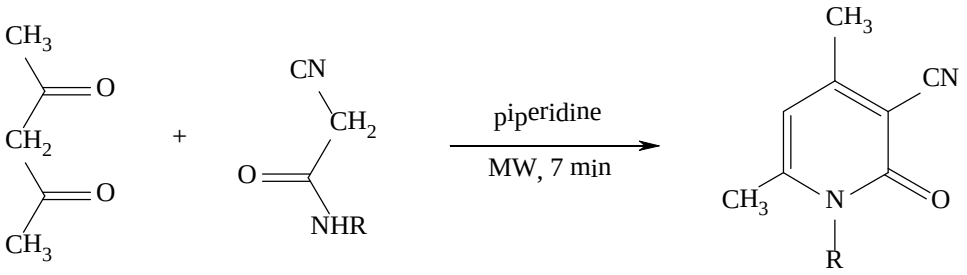

Figure 2.4.2 Synthesis of *N*-substituted 4,6-dimethyl-3-cyano-2-pyridones

N-substituted 4,6-dimethyl-3-cyano-2-pyridones were obtained from acetylacetone and the corresponding *N*-substituted cyanoacetamide using conventional and microwave synthesis in the presence of piperidine as a catalyst. Conventional synthesis was performed by heating the reaction mixture under reflux (solvent mixture water/ethanol). Microwave synthesis was performed using a domestic microwave oven in the absence of solvent. The products were obtained in high yield and in a short reaction time (up to 7 min), while the conventional method of synthesis required up to 4 hours with lower yields (Figure 2.4.3).

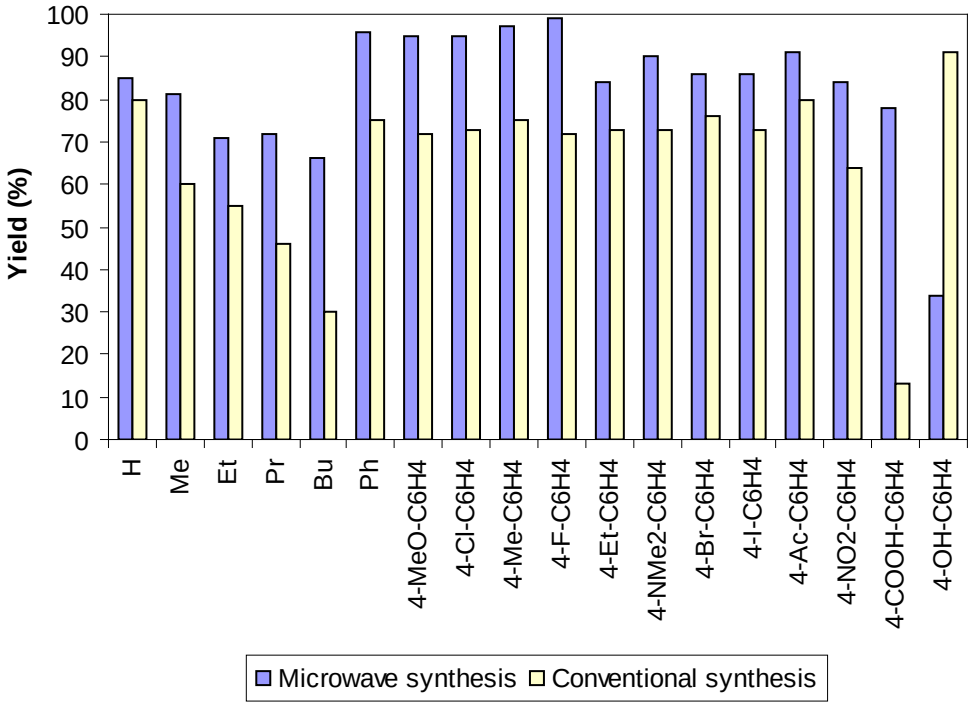

Figure 2.4.3 *N*-Substituted 4,6-dimethyl-3-cyano-2-pyridones yields obtained by microwave and conventional synthesis

6-Hydroxy-3-cyano-4-methyl-2-pyridone was also synthesized using microwave technique (condensation type 3-2). The first microwave synthesis was reported in 1994 in a German patent [98]. In comparison to the conventional synthesis which takes 16.5 h with a yield of 80 %, microwave synthesis is carried out for 5 min with a yield of 96 %. In this synthesis product was obtained starting from cyanoacetamide, ethyl cyanoacetate and ethylamine. This pyridone can also be obtained using conventional synthesis with potassium hydroxide as a catalyst [99,100]. Reaction times were from 1 to 8 h, with yields ranging from 40-60 %. Recently, a synthesis of this pyridone was published, using microwave irradiation in a domestic microwave oven, in the absence of solvent starting from ethyl cyanoacetate and cyanoacetamide, using powered potassium hydroxide as a catalyst (Figure 2.4.4). The obtained yield was 60 %, after only 4 min of irradiation [101].

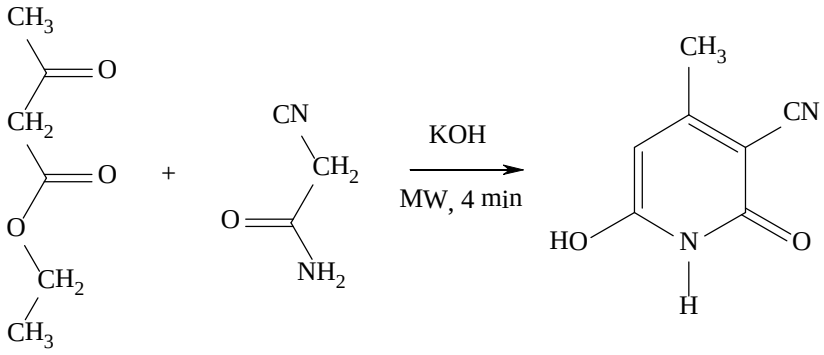

Figure 2.4.4 Synthesis of 4-methyl-6-hydroxy-3-cyano-2-pyridones

Dave et al. reported the microwave synthesis of 4,6-diaryl-3-cyano-2-pyridones starting from cyanoacetamide and 1,3-diarylpropen-1-ones in the presence of powdered potassium hydroxide, with phenyl or substituted phenyl groups in positions 4 and 6 [102]. The authors have reported yields that ranged from 74 to 81 % with high purity of compounds after only 1-2 minutes of irradiation (Figure 2.4.5).

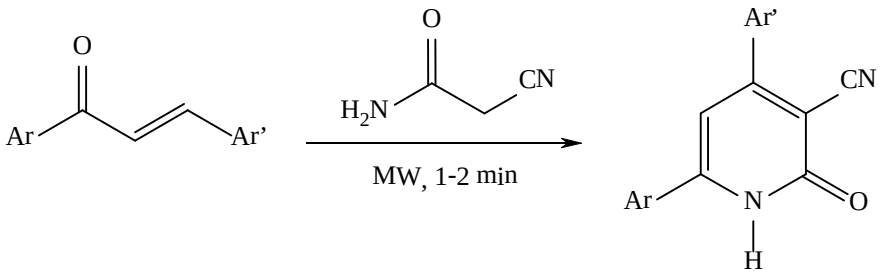

Figure 2.4.5 Synthesis of 4,6-diaryl-3-cyano-2-pyridones

Microwave synthesis of arylazo pyridone dyes [59] is based on the previously described type condensation 3-2. This type of synthesis involves the reaction of phenylazo carbonyl compounds and cyanoacetamide using KOH as base and ethanol as solvents in a dedicated microwave reactor. Synthesis of 5-phenylazo-4,6-dimethyl-3-cyano-2-pyridones and 5-phenylazo-4,6-diphenyl-3-cyano-2-pyridone is shown in Figure 2.4.6. The synthesized derivatives of 4,6-dimethyl-3-cyano-2-pyridone were obtained in nearly quantitative yield, while the derivatives of 4,6-diphenyl-3-cyano-2-pyridones were obtained in a lower yield. Synthesis of 5-phenylazo-4,6-dimethyl-3-cyano-2-pyridone conventional manner [57] also takes place in the presence of a base in ethanol, except that this synthesis occurred during 3 hours with somewhat lower yields (70 – 80 %).

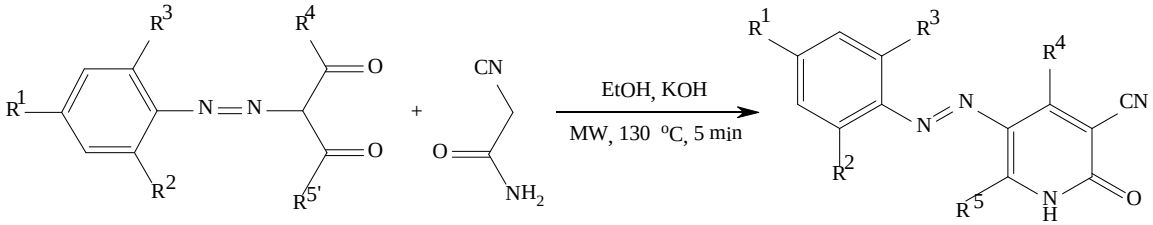

Figure 2.4.6 Microwave synthesis of arylazo 4,6-dimethyl and 4,6-diphenyl-3-cyano-2-pyridone dyes

In a similar way, a synthesis of the 5-phenylazo-2-hydroxy-4-methyl-3-cyano-2-pyridones starting from β-phenylazo keto ester under the same conditions was performed. In addition to these products a derivative of 2-hydroxy-4-phenyl-3-cyano-2-pyridones was obtained. In comparison to derivatives of dialkyl 2-pyridone, lower yields were obtained as a result of lower reactivity of β-keto esters compared to 1,3-diketones [102], but higher than in conventional synthesis (30-60 %) [58].

Synthesis of substituted 3-cyano-2-pyridones at positions 4 and 6 was also carried out using microwave irradiation (1-2-2 type condensation) [103], and under conventional conditions [104] (Figure 2.4.7). By applying microwave irradiation (dedicated microwave reactor) yields of 90-95 % over 5-7 minutes were obtained, while the conventional method of synthesis for 6 hours gave lower yields (67-85 %).

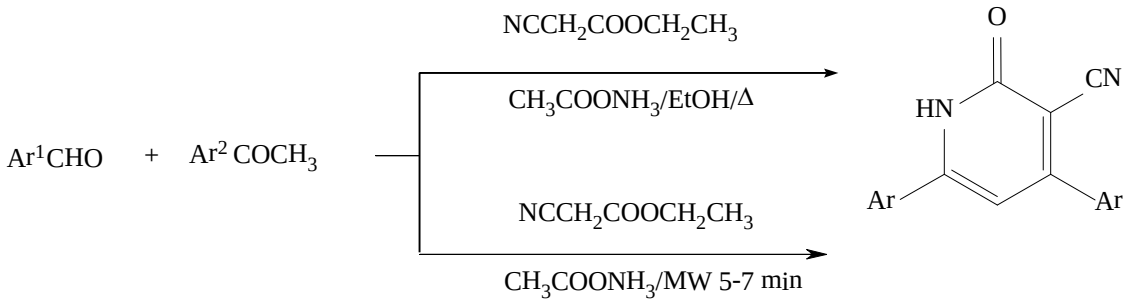

Figure 2.4.7 Conventional and microwave synthesis of substituted 3-cyano-2-pyridones

Another example of microwave synthesis of 2-2-1 condensing type of 2-pyridones is shown in Figure 2.4.8 [105]. The synthesis of 3,5-dicyano-2-pyridone is carried out in aqueous solution starting from aldehydes and malononitrile in the presence of sodium hydroxide as a base. The advantage of this synthesis is short reaction time, efficiency and use of water instead of organic solvents which have a favorable impact on the environment. The method is applicable not only to aromatic aldehydes with electron-donor and electron-acceptor groups, but also to heterocyclic and aliphatic aldehydes.

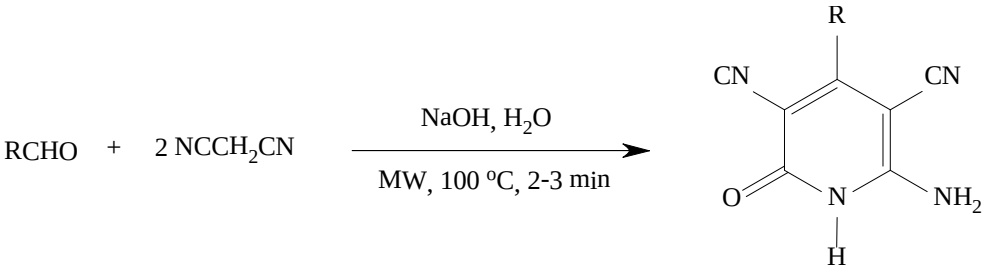

Figure 2.4.8 Synthesis of 4-substituted 6-amino-3,5-dicyano-2-pyridones in aqueous media under microwave irradiation

Syntheses were performed at 100 °C both in the conventional and the microwave method. The reaction time of microwave synthesis was 2-3 minutes while in the conventional synthesis it took 2-3 hours. On the other hand, reaction yields increased from 25-37 % (conventional) to 40-49 % (microwave synthesis).

4-Aryl substituted 5-alkoxycarbonyl-6-methyl-3,4-dihydropyridones were prepared by the reaction of Meldrum's acid, methyl acetoacetate and appropriate benzaldehyde in the presence of ammonium acetate (condensation type 2-2-1) (Figure 2.4.9) [106,107]. Microwave assisted

synthesis, performed in a dedicated microwave reactor, produced pure products in high yield (81-91 %), while the conventional synthesis gave yields lower by 17-28 %.

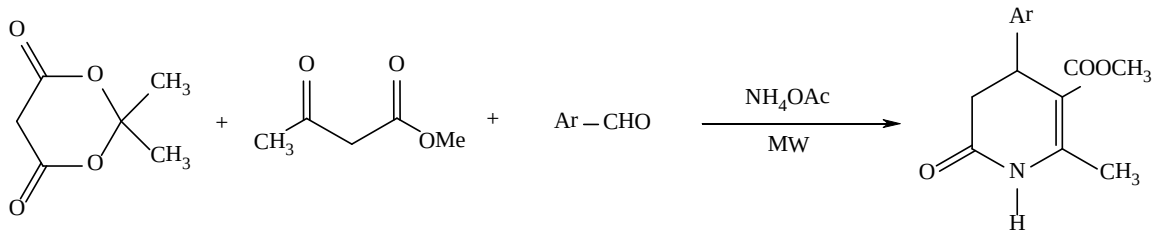

Figure 2.4.9 Synthesis of 4-aryl substituted 5-alkoxycarbonyl-6-methyl-3,4-dihydropyridones

Synthesis of 2-pyridone based bifunctional compounds (1,4-dihydropyridines) by the condensation of dialdehyde, Meldrum's acid, acetoacetic acid and ammonium acetate is another example of 2-2-1 type condensation of pyridones (Figure 2.4.10) [108]. This synthesis was achieved by heating the reaction mixture in a domestic microwave oven for 8 min using small amounts of glycol as an energy transfer reagent (yield 83 %).

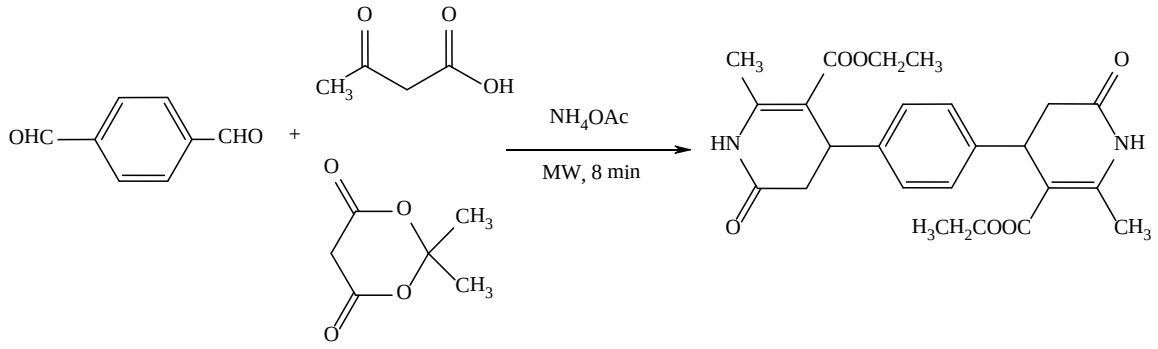

Figure 2.4.10 Synthesis of bifuncional 2-pyridone

2.4.3 Microwave synthesis of azo dyes

Azobenzenes can be also prepared by the reduction of azoxy derivatives. A method recently reported involves the treatment of hydrazine hydrate with azoxyarenes in the presence of aluminium in methanol under reflux or microwave irradiation (Figure 2.4.11). The reaction is very fast, and the azoarenes are obtained in excellent yield [109].

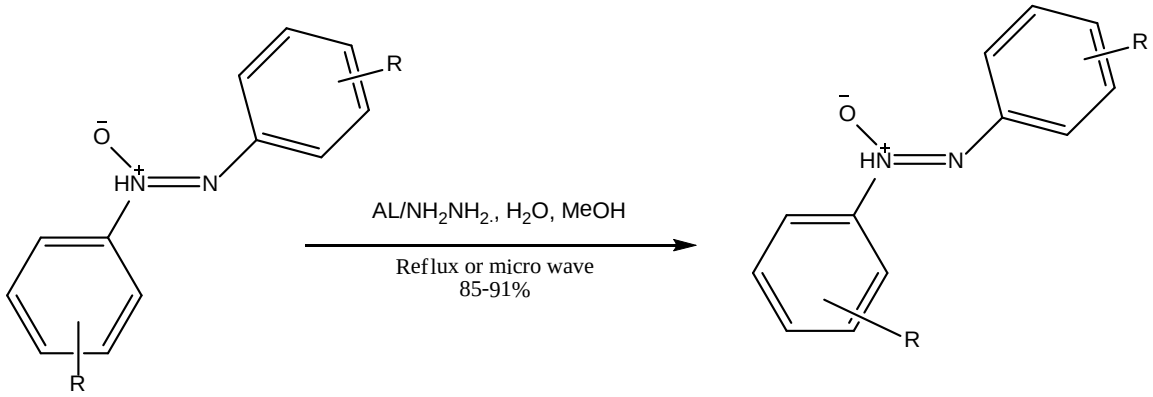

Figure 2.4.11 Synthesis of azobenzene from hydrazine hydrate with azoxyarenes in the presence of aluminium in methanol via microwave irradiation

Aromatic azides when heated in the presence of anilines lead to unsymmetrical azo compounds in low yields. For instance, the decomposition of 4-nitrophenyl azide 140 at 135 ºC in the presence of 4-methylaniline gives the azobenzene in 16 % yield (Figure 2.4.12) [109].

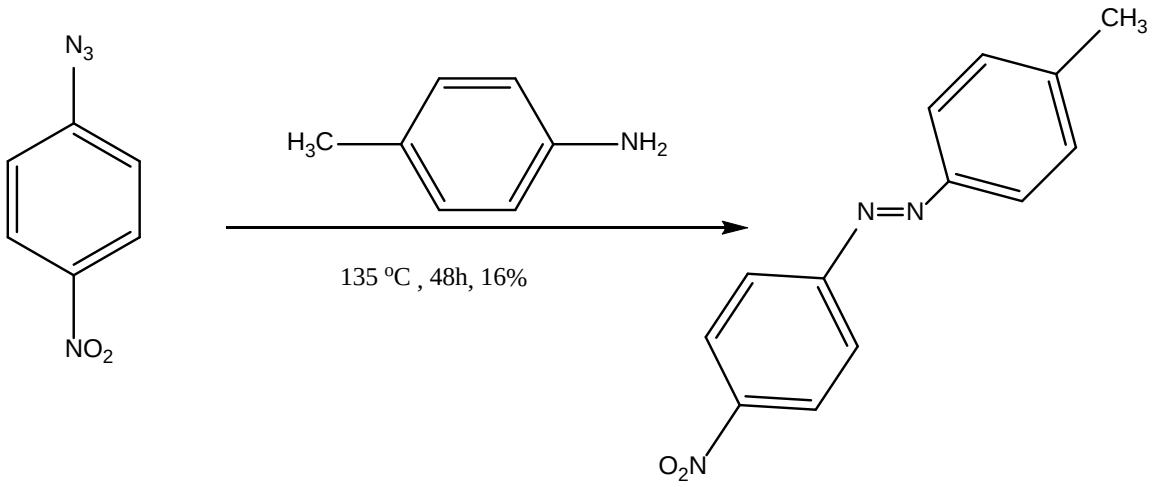

Figure 2.4.12 Synthesis of azo dayes from 4-nitrophenyl azide with 4-methylaniline

2.5 Tautomerism

Tautomerism means, in its most general sense, reversible intramolecular rearrangements in organic molecules, where the electron density changes in individual atoms or atomic groups performed relatively rapidly. In other words, the tautomerism implies the existence of two or more different structural isomers that are in equilibrium and differ among themselves only in the distribution of electron density and the relative position of mobile groups or atoms. They are called tautomers and the process of converting one in other tautomer forms, until the establishment of the steady state is referred to as tautomerism. In most cases, a mobile hydrogen atom, and in this case defined as intramolecular tautomerism prototropy or prototrop tautomerism [110].

2.5.1 Tautomerism in 2-pyridones

The keto/enol tautomeric equilibrium is one of the most important and widespread equilibria in chemical and biological processes. –NH–C(=O)– group makes 2(1*H*)-pyridones susceptible to the PY/HP (lactam/lactim) tautomerism. This type of tautomerism has been the subject of studies in many fields of chemistry and biochemistry. Such studies were used in the explanation of tautomeric equilibria of nucleobases, cytosine [111,112], thymine [113,114], and uracil [60,115,116]; rationalization of structures, properties, and reactivities in heterocyclic chemistry [117], concepts and probes of aromaticity [117], measures of intrinsic stabilities *vs* solvent effects [4], mechanisms of enzymatic catalysis and receptor interactions [117], and possibly even mutations during DNA and RNA replications [117].

One of the model systems of this type of equilibrium in heterocyclic compounds is the pair 2-hydroxypyridine/2-pyridone (2HP/2PY) represented in Figure 2.5.1, where a hydrogen atom is transferred between the N and O sites of the molecule. The 2HP/2PY system is a widely studied model system chosen for its extreme ease of experimental manipulation and the simplification as compared to real nucleobase pairs. For the 2HP/2PY system, the tautomeric equilibrium is slightly shifted to the hydroxy form, the ground state of 2HP being more stable by 3.2 kJ/mol than that of 2PY. For this reason, both tautomers have an appreciable concentration at room temperature. Both of them possess several spectroscopic properties, such as dipole moments, electronic, fluorescence, *etc*. However, tautomeric equilibrium takes place, in nature, in the presence of water molecules. For this

reason, several investigations have been dedicated to the hydrated forms of 2HP/2PY and to the effects of the hydration on the barrier to tautomerization of 2HP/2PY. It has been calculated that in the isolated molecule this barrier is 146-159 kJ/mol and that this value is reduced to about 54-63 kJ/mol in the presence of a single water molecule bridging the N-H and C=O sites of 2PY. The presence of water molecules not only affects the tautomerization barrier but it is also predicted to shift the tautomeric equilibrium from the hydroxy to the keto form (Figure 2.5.1) in a trend that accentuates as the number of water molecules increases.

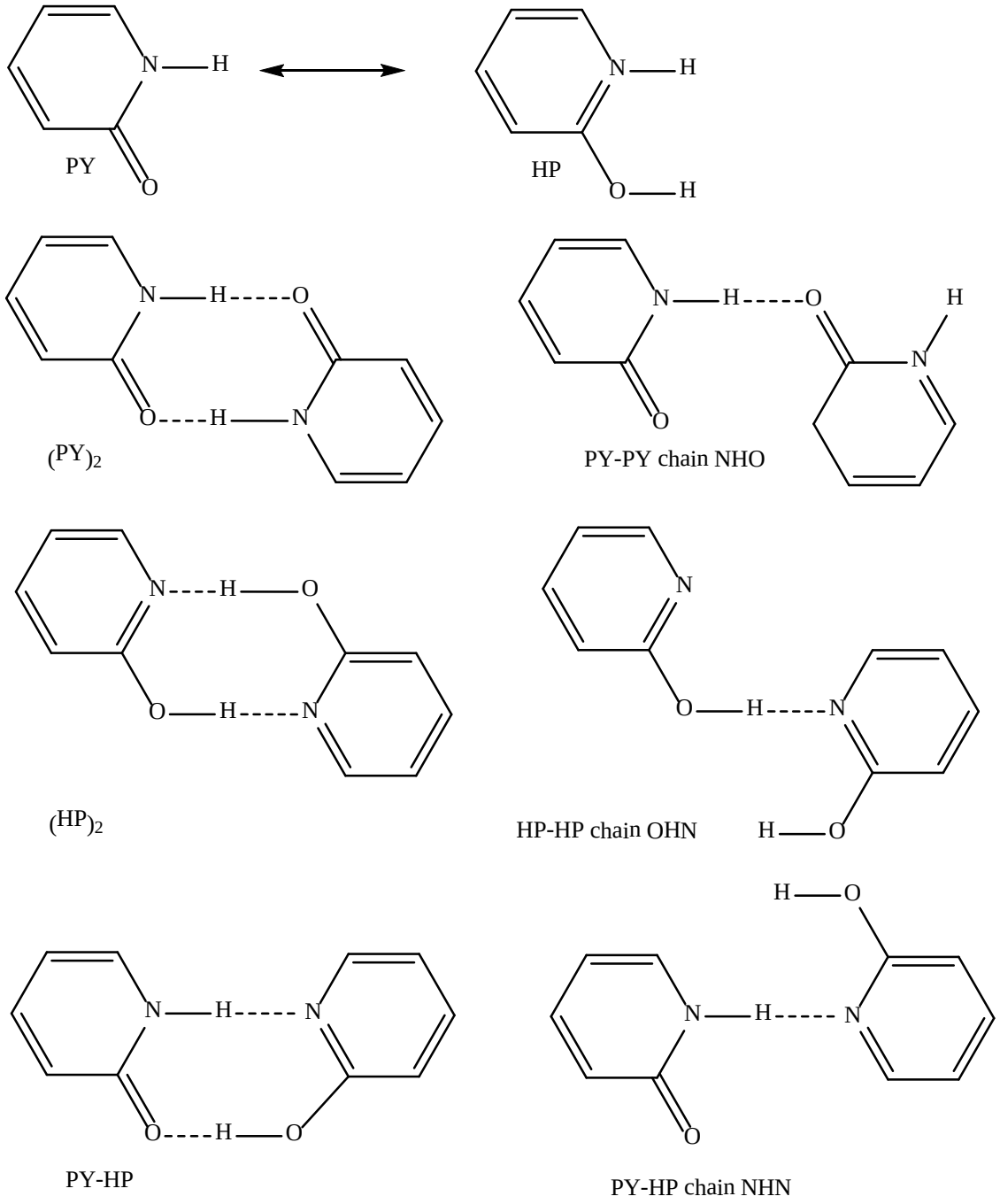

Figure 2.5.1 Tautomeric equilibria in 2PO/2HP, 2PO-H_2O/2HP-H_2O, 2PO-$(H_2O)_2$/2HP-$(H_2O)_2$

Tautomeric equilibrium between PY and HP forms depends on the environment: self-association, solvation, dimerization, ion binding, and substituents present at pyridone nuclei [4]. IR, UV/Vis [4,118], NMR [119], and mass spectrometric studies confirmed that PY predominates in the gas phase under equilibrium conditions [120], and in inert matrices. In nonpolar solvents, both

tautomers exist in comparable amounts; while the tautomeric equilibrium is shifted toward PY form in aqueous solutions, polar solvents, as well as in the crystalline state [121,122]. It is also well known that solvent polarity and hydrogen bonding ability significantly affect the tautomeric equilibrium. Situation in solution is further complicated due to possible self-association where three types of dimmers: PY–PY, HP–HP and mixed PY–HP one can be formed. The presence of dimmers in solution decreases as temperature increases, or it could be dissociated by the addition of solvents with strong HBA/HBD abilities, which break intermolecular hydrogen bonds in dimmers [121-126].

IR, UV, mass spectrometry, photoemission and microwave, have shown that the 2- and 4-hydroxypyridine exist in the gas phase and in an inert atmosphere (N_2 and Ar), in the equilibrium conditions, generally at lactim (hydroxy) form in relation to the situation which exists in solution [121]. 2-Pyridone (PD), converting to 2-hydroxypyridine (HP) through a lactam-lactim isomerization mechanism and can form three different cyclic dimers by hydrogen bond formation: $(PD)_2$, (PD-HP), $(HP)_2$. It was investigated that the complexation chemistry of pyridone in dichloromethane-*d*2 using a combined NMR and Fourier transform infrared (FT-IR) approach. Temperature-dependent ^1H NMR spectra indicate that at low temperatures (<200 K) pyridone in solution predominantly exists as a cyclic $(PD)_2$ dimer, in exchange with PD monomers. At higher temperatures a proton exchange mechanism sets in, leading to a collapse of the doublet of ^{15}N labeled 2-pyridone. Linear FT-IR spectra indicate the existence of several pyridone species, where, however, a straight forward interpretation is hampered by extensive spectral overlap of many vibrational transitions in both the fingerprint and the NH/OH stretching regions. Two-dimensional IR correlation spectroscopy applied on concentration-dependent and temperature-dependent data sets reveals the existence of the $(PD)_2$ cyclic dimer, of PD-CD_2Cl_2 solute-solvent complexes, and of PD-PD chainlike dimers. Regarding the difference in effective time scales of the NMR and FT-IR experiments, milliseconds *vs* (sub)picoseconds, the cyclic dimers (PD-HP) and $(HP)_2$, and the chainlike conformations HP-PD, may function as intermediates in reaction pathways through which the protons exchange between PD units in cyclic $(PD)_2$.

Applying NMR and FT-IR spectroscopy, it is clearly identified the existence of PD-CD_2Cl_2, and cyclic $(PD)_2$ in solution. The NMR results showed that the cyclic dimer $(PD)_2$ is the dominant

species at low temperatures (180 K), which exchanged with PD in monomer form or complexed with the solvent. At low temperature (193 K) the IR spectra supported the NMR conclusions that the solution composition is dominated by cyclic $(PD)_2$. The 2D IR correlation spectra not only showed the existence of PD-CD_2Cl_2 solute-solvent complexes, and of cyclic $(PD)_2$, but also hinted at the presence of chainlike PD-PD as well. At room temperature the presence of the proton exchange between PD units is inferred from the NMR spectra. It suggested that the certain routes for proton transfer observed on the NMR time scale, including (PD-HP) and $(HP)_2$. The fact that these complexes do not significantly show up in the IR spectra indicates that the relative concentration must be minor and their average lifetimes much shorter than milliseconds [124].

In nonpolar solvents, such as chloroform and cyclohexane, there are equilibrium quantity of the tautomeric forms in solution, as opposed to polar solvents, such as water, when a tautomeric equilibrium is shifted completely in favor of the lactam (oxo form), which is also true for the 2 - pyridone in the crystalline state [121]. The values of equilibrium constants in the gas phase are different than in the aqueous phase. The large difference in stability (10^4) of the tautomeric forms in the gas phase and solution, indicating a dominant influence of solvatation to the relative stability of the molecule [121].

Considering the equilibrium tautomer forms in solvents of variable polarity, it was observed that with increasing solvent polarity, equilibrium shifts toward pyridone tautomer. Keto form is more polar than hydroxy, as a result of the contribution of resonance structure in which charge separation occurs. Little effect of solvent on the electronic structure of the ground state of lactim molecules (hydroxy form), a significant effect on the geometry of the molecule, the charge distribution, and vibrational frequencies of lactam (keto form), can be easily understood in terms of a greater contribution to dipolar resonant structures in polar solvents. Construction of hydrogen bonds also play a significant role due to a better stabilization of oxo forms in proton donating solvent, and a better stabilize the hydroxy form by proton-acceptor solvents [121].

Accurately determining of prototropic tautomer equilibrium constant, $K_{T,}$ for 2(4)-hydroxypyridine $\rightleftharpoons$ 2(4)-pyridone is extremely difficult to determine due to molecules association, even in very dilute solutions tautomer in nonpolar solvents as it cyclohexane.

Association of tautomer affects the value of K_T constant which is significantly different compared to the value available for a free molecule [121].

Different models have been developed in order to adequately describe the real situation in the solutions, various forms of solvation hydroxypyridine/pyridone tautomeric pairs with respect to the wells and the possibility of building a hydrogen bond, using multi-parametric regression analysis. *Ab initio* and other calculations methods provide higher stability of 2-hydroxypyridine, in comparison with 2-pyridone in the gas phase. Calculated difference of free energy for lacto/lactam pair in the gas phase at 25 °C is ΔG = 2.9 kJ/mol in favor of the lactam, which is in good agreement with the experimental values [121].

Figure 2.5.2 presents 3-cyano-2(1*H*)-pyridone tautomeric equilibrium of lactam/lactam (2-piridon/2-hidroksipiridin) tautomer, with contribution of dipolar resonance structure of 2-pyridones tautomeric forms [121].

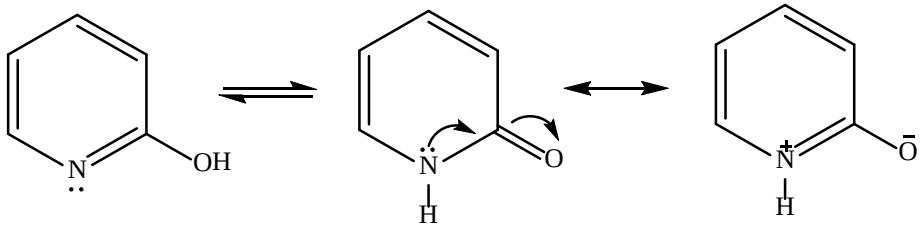

Figure 2.5.2 Lactam/lactam (2-pyridone/2-hydroxypyridine) tautomeric equilibria [127]

Values of the equilibrium constants, K_T=2-pyridone/2-hydroxypyridine tautomer, of 2(1*H*) pyridone at different temperatures are shown in Table 2.5.1.

Table 2.5.1 Tautomeric equilibrium constants K_T in the gas and solution phase at 25...30 °C [121,125]

Solvent	2-Hydroxypyridine	4-Hydroxypyridine
Gas phase	0.4	< 0.1
Cyclohexane	1.7	-
Chloroform	6.0	1.3
Acetonitrile	148	406
Water	910	1900

2.5.2 Tautomerism in azo dyes

In theory, azo dyes can undergo tautomerism: azo/hydrazone for hydroxyazo dyes; azo/imino for aminoazo dyes, and azonium/ammonium for protonated azo dyes [9]. The position of the tautomer is significantly influenced by the polarity of the environments as well as interaction with substrate. Also, it was reported that the position of this equilibrium and, of course, the position of the –OH group significantly affect light fastness properties. Azo-hydrazone tautomerism revealed 1884th year. Since the coupling reaction to form azo obtained, and the reaction of hydrazone form of condensation is assumed to be between these two forms, there is a dynamic equilibrium, that is, tautomerism (Figure 1). This study was followed by extensive studies in the field of azo-hydrazone tautomerism [9,126].

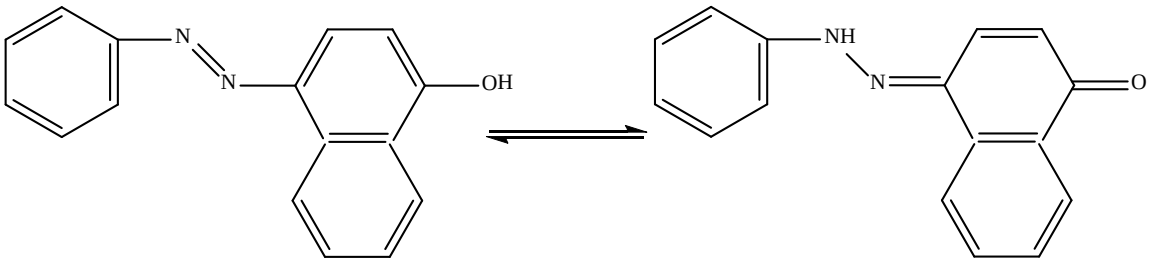

Figure 2.5.3 The tautomeric equilibrium between 4-phenylazonaphthol and 1,4-naphthoquinone phenylhydrazone

The phenomenon of azo-hydrazone tautomerism is very important because tautomer of commercial color have different optical and physical properties (light fastness), toxicological properties, and most importantly, a different coloration. Light fastness is directly related to tautomerism, *i.e.*, the larger the share of the hydrazone form is more stable color [127]. Hydrazone form absorbs light at higher wavelengths and is generally commercially significant [128].

The main structural condition for the existence of azo-hydrazone tautomerism is the presence of labile protons in the molecule that can be exchanged intramolecular. This requirement is reflected in azo dye containing OH and NHR groups were conjugated with the azo group and the tautomerism in solution and in the solid state occured [128]. The phenomenon of azo-hydrazone tautomerism can be viewed as the formation of intramolecular hydrogen bonds [129]. The relative tautomers depends on several factors (such as solvent, temperature, concentration,

aggregation of monomeric molecules, *etc*.), but, in general, depends on the thermodynamic stability of the two tautomers [128,129]. Some azo dyes exist exclusively as the azo tautomers [131], while others are mostly in the hydrazone form [132]. Azo dyes in polar solvents, such as water, are mostly in the hydrazone form, while the proportion of tautomers decreases significantly in organic solvents such as alcohols, dimethylformamide and dimethyl sulfoxide [126].

Tautomers behavior can be examined in solvents with different properties using different methods, including UV-Vis and NMR spectroscopy. These methods are widely used for the qualitative determination of the tautomers relationship, but the quantitative determination has significant limitations. In the case of UV-Vis spectroscopy, equilibrium constants (K_T) can not be obtained directly because the molar ratios of individual excited tautomers could not be calculated due to overlapping peaks. Quantitatively the tautomeric equilibrium can be successfully determined using ^{15}N, ^{14}N and ^{13}C NMR spectra [128].

2.5.2.1 Tautomerism in arylazo pyridone dyes

Previous studies of the structure and properties of azo pyridone dyes show that two types of tautomerism, keto-enol-azo and hydrazine, occurred. The position of tautomer equilibrium is affected by nature of substituents in the pyridone ring and arilazo components, as well as the nature of the solvent (polarity, type of solvent, solute interactions and solvent) [128,130]. Keto occurs in 4,6-disubstituted pyridone azo dye when the substituents are alkyl or aryl groups (Figure 2.5.3). 2-piridon/2-hidroksipiridin study of tautomerism in 5-(3- and 4-substituted arilazo)-4,6-dimethyl-3-cyano-2-pyridones and 5-(3 - and 4-substituted arilazo)-4, 6-diphenyl-3-cyano-2-pyridones have shown that strong electron-donor group and an electron-acceptor moderate groups in protic and aprotic non-polar solvents stabilize the pyridone form. In polar aprotic solvents such as dimethyl sulfoxide and dimethylformamide, the mixture appears in tautomeric forms. Strong electron-acceptor groups favoring the creation of 2-hydroxypyridine form, and a mixture of tautomers in all tested solvents [133,134].

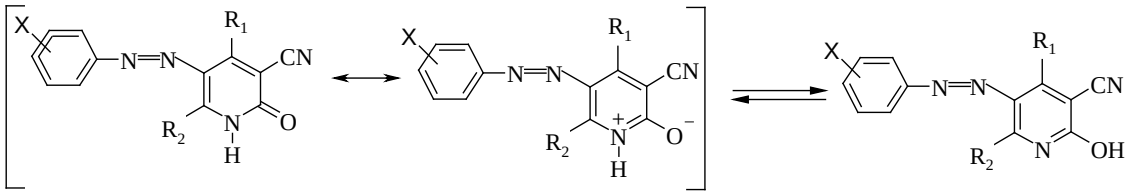

Figure 2.5.4 Keto-enol tautomerism of arylazo pyridone dyes

In the literature there are many works dealing with azo-hydrazone tautomerism arilazo pyridone colors. Cheng et al [135] showed that the pyridone color tints obtained from 1,4-dimethyl-6-hydroxy-3-cyano-2-pyridone moving in a range between yellow and orange (λ_{max} measured in toluene is between 423 and 457 nm). It was found that the colors are in the hydrazone form the basis of IR and UV spectra and confirmed the theoretical fact that the electron-donor groups on the benzene ring show a batochromic shift of the absorption spectra. Home hromofora hydrazone tautomers were the pyridone ring and hydrazone residue, while the phenyl group has a secondary effect. Absorption spectra corresponding to transitions in which the electron density is transferred from the hydrazone group to the carbonyl group pyridone ring (Figure 2.5.5).

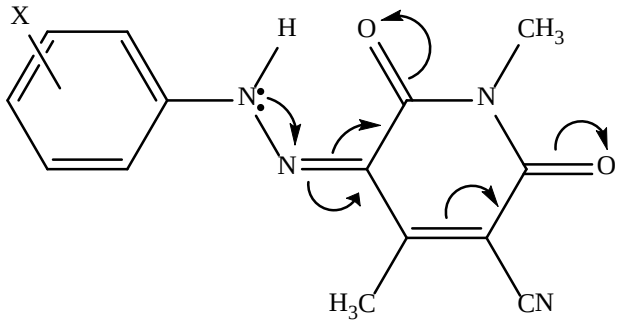

Figure 2.5.5 Transfer of electron density in hydrazone form of arylazo pyridone dye

2.6 Correlation analysis in organic chemistry

Linear free energy relationships (LFERs) give some limited structural information about the activated complex. Transition state structure can be observed by the studies of substituent effects which are used to determine how the free energies of reaction and activation vary as a function of chemical structure [136].

The linear relationships (LFERs) between the free energy of activation or reaction free energy change induced by a substituent and a parameter, describes the electron donating or electron withdrawing characteristics of the substituent. Substituents or solvent changing influence the steric congestion, solvation, leaving group ability, nucleophilicity, acidity or basicity and a variety of other chemical attributes [136].

In molecular orbital theory orbitals are spread out over all atoms in a molecule. Adding or changing of substituents creates new molecular orbitals, i.e. involve the atomic orbitals on the substituents. Even this theory can be used successfully to analyze substituent effects, the concept of delocalized molecular orbitals presents difficulties in visualizing localized changes in a molecule brought about by a substituent change. Therefore, substituent effects are almost always discussed in terms of hybrid valence bond/molecular orbital theory (VBT/MOT), where localized bonding effects and isolated bonds between atoms are considered [136].

Inductive effects

An inductive effect (I) is ability of an atom or group of atoms to withdraw or donate electrons through σ bonds [136] (+I or electron donating, -I or electron withdrawing [137,138]). The classical inductive effect is a polarization through bonds, both of σ- and π-types, becoming progressively attenuated. The other, known as a filed effect, is propagated through space and depends more for its intensity on proximity than on the number of bonds separating source and receptor. Usually, it is difficult to separate these two effect, which may both components of the I [137].

Strongly electronegative atoms or groups are best at drawing electrons to themselves. Conversely, a group can donate electrons via the σ bond framework [139].

Resonance effects

A resonance effect (R) is the ability of an atom or group of atoms to withdraw or donate electrons through π bonds. Many substituents give rise to a perturbation that is greater when they are located *para* than when they are *meta* (the transmission mechanism is of a conjugative nature in which charge is relayed to alternate atoms). '+R effect' results in donation of electrons from substituent to reaction center and '-R effect' in a withdrawal of electrons results [139].

In order to exercise a resonance effect, a substituent must possess a *p*- or π-orbital which is available to conjugate with the π-MOs of the aromatic system. There is no fundamental difference between these two situation, in each case a transfer of charge between two centers by conjugation and the differentiation into +R and –R effects depends of substituent and the reaction centre.

Steric effects

Steric effects can also have a huge influence on the rate of a reaction and conformations. Large atoms or groups influence the manner in which molecules collide, often deflecting the reactants away from the angle or depth of collision necessary for the reaction to occur. For example, the S_N2 reaction becomes slower due to steric effects as the carbon with the leaving group is more highly substituted with alkyl groups. The nucleophile cannot penetrate to the carbon with the leaving group when larger groups are attached [139].

2.6.1 The Hammett equation

The most important and common applied structure reactivity relationship is due to L. P. Hammett. Hammett equation relates rates and the equilibira for many reactions of compounds containing substituted phenyl groups [140]. Work of Hammett [141,142] and Burkhard [143] in early 1930s led to the formulation of the Hammett equation. This relation describes the influence of polar *meta*- or *para*-substituents on the side-chain reactions of benzene derivation and has become known as Hammett equation [144]:

$$\log(k/k_o) = \rho\sigma \tag{2.6.1}$$

$$\log(K/K_o) = \rho\sigma \tag{2.6.2}$$

Where k or K is the rate or equilibrium constant respectively, for a side-chin reaction of a *meta*- or *para*-substituted benzene derivates, and k_0 or K_0 are the rate or equilibrium constants respectively. For unsubstituted "parent" compound, σ is the substituent constant, which depends solely on the nature and position of the substituent X, and ρ is the reaction constant, which depends on the reaction the conditions, such as the reaction medium and temperature, under which it takes place, and also on the nature of the side chain R.

The ionization of benzoic acids in water at 25°C was chosen as the reference system with ρ equal to 1.00. This resulted in electron-withdrawing substituent constants being positive and electron-releasing substituent constants being negative. The validity of equations (2.6.3) and (2.6.4), is restricted to substituents in the *meta*- and *para*-positions of the benzene ring [145,146].

Equilibrium constants and rate constants are related to free energy relationships to free energy differences by the equations [140,147]:

$$\log K = -\Delta G^{\Theta}/2.3RT \tag{2.6.3}$$

where ΔG^{Θ} is the standard free energy change of reaction. For chemical rate processes:

$$\log k = \log(k_B T/h) - \Delta G^{\#}/2.3RT \tag{2.6.4}$$

where $\Delta G^{\#}$ is the standard free energy of activation. (T is the Kelvin scale temperature; R is the gas constant, k_B is the Boltzmann constant, and h is the Plank constant).

$$\log(k/k_o) = \log k - \log k_o = \Delta\Delta G/2.3RT = \rho\sigma \tag{2.6.5}$$

Where the expression ΔΔG is the second difference: the difference between ΔG values for the substituted and unsubstituted reaction.

2.6.1.1 Substituent constant (σ)

Equation by Hammett defines a scale of ability of substituents to influence the acidity of benzoic acid. The substituents are placed *meta* or *para* to the carboxylic group to eliminate any possible steric effects associated with an *ortho* substituent, thus, only field, polarizability, inductive, and resonance effects should be operative [136].

Substituent parameter σ_x is defined for each substituent X in equations 2.6.3 and 2.6.4, while hydrogen is the reference substituent. All acidity equilibrium constants for the substituted benzoic acids are compared to the equilibrium constant for benzoic acid itself. σ_m, σ_p Hammett's substituent are defined by using the dissociation constants of *para*- and *meta*-substituted benzoic acids, which are composite substituent constants as both resonance and inductive/field effects are present. σ^+ are composite substituent constants applied in cases when the reaction site is electron-withdrawing, σ^- are composite substituent constants applied in cases when the reaction site is electron-donating [148]. A different set of σ values is necessary for each different position on the benzoic acid, because the ability of a substituent to influence the acidity of benzoic acid depends upon its position relative to the carboxyl group. When σ is negative, the substituted benzoic acid is less acidic than benzoic acid itself, and when σ is positive, the substituted benzoic acid is more acidic. Electron donating groups have negative σ values and electron withdrawing groups have positive σ values. This trend is exactly as predicted, because electron withdrawing groups should stabilize the negative charge of the carboxylate ion and electron donating groups should destabilize this charge.

2.6.1.2 Application of linear free energy

The practical application of Hammett equation consists in determining the unknown constants, reaction rates and equilibrium. However, in practice, the Hammett equation far more useful for the study of the mechanisms of chemical reactions, that is, the nature of the transition state, and for determining the unknown constants substituents. Many authors have attempted to show that the impact of *meta*- and *para*-substituents in the observed response may confirm or refute the

postulated reaction mechanism [149], significant conclusions can be drawn based on the values of the constants of the reaction ρ, nature of σ values used in the correlation, or on the basis of the linearity or non-linearity of the individual Hammett's dependency.

Not all reactions can be correlated to Hammett's equation, respectively its multi parameter embodiments. There may be several reasons for this change is the most common reaction mechanism, depending on the nature of the substituents. In stepwise reaction, for example, one may make the degree of the reaction rate in the field of electron-acceptor substituents, while others, very varying degrees, may be responsible for the rate of the reaction of the entire process in case of electron-donating substituents.

In the literature, there are a number of papers in which the authors, to study the electronic effects of substituents within a particular series of molecules, correlate ^{1}H NMR, ^{13}C NMR and ^{15}F NMR chemical shifts, and SCS (the difference between the chemical shifts of substituted and unsubstituted compounds) values with a variety of substituents constants [150-152] . Based on these and many other works implies that the choice of the type of substituents of constants that are used in the correlation, the structure of the compound responsible, or the electric requirements of particular substituents, that is, in a way analogous to the different requirements of the reaction in the correlation characteristic parameters (logk/k on or log K/K_o).

The most common cause of a smaller correlation parameters that define the relative importance of correlation are inadequate or inaccurate data, especially if the observed series of frequency or vibration characteristic stretching group sufficiently different. Usually it is the same series of compounds a significantly better correlation between the kinetic parameters of the correlation compared with the absorption peak or absorption frequencies, the same correlation model.

The results achieved in this area of research is another confirmation of the broad range of applications Hammett's equations in elementary, one-parameter and multiparameter form, in order to investigate the electronic structure and reactivity of organic molecules.

2.6.2 The Yukawa-Tsuno and related equations

The concept that substituent electronic effects could be considered to be separable and additive. Substituent effects are result of inductive resonance and steric effects. Inductive and resonance are considered as electronic effects, whereas steric effects largely depend upon the size of the substituent. However, even steric effects are electronic in origin, they are repulsions brought about by atoms approaching within their respective Van der Waals contact distances, where the electron clouds of the groups involved repel each other. However, most researchers separate the sterics and electronics concepts [136].

Yukawa and Tsuno [153] proposed evaluation of -R *para*-substituents in reactions that are more electron demanding than the usual reference reaction. This reaction can be expressed in two equation forms 2.6.6 and 2.6.7 [153,125].

$$\log(k/k_o) = \rho\left[\sigma + r^+\left(\sigma^+ - \sigma\right)\right] \qquad (2.6.6)$$

$$\log(k/k_o) = \rho\left(\sigma + r^+\Delta\sigma_R^+\right) \qquad (2.6.7)$$

Where $\Delta\sigma_R^+$ equals the enhanced resonance effects ($\sigma^+ - \sigma$), r^+ is the extent of the enhanced resonance effects. When r^+ is equal to zero, there is no difference in resonance effects for the new reaction compared to benzoic acid, but when $r^+ > 0$, the new reaction is more sensitive than benzoic acid to resonance effects, and when $r^+ < 0$, the new reaction is less sensitive.

Equations 2.6.8 and 2.6.9 where r^- similarly measure the extent of the enhanced resonance effect and $\Delta\sigma_R^-$ equals ($\sigma^- - \sigma$) are shown below [154]. The equation have been used with σ^n or σ^0 to replace σ, which would appear more rational.

$$\log(k/k_o) = \rho\left[\sigma + r^-\left(\sigma^- - \sigma\right)\right] \qquad (2.6.6)$$

$$\log(k/k_o) = \rho\left(\sigma + r^-\Delta\sigma_R^-\right) \qquad (2.6.7)$$

The Yukawa-Tsuno equation is consider to be a superior treatment to the simple Hammett equation using σ, σ^+ or σ^-.

2.6.3 Correlation analysis of the Carbon-13 nuclear magnetic resonance chemical shifts

Study of the transmission of electronic effects of substituents in organic molecules, exceptionally sensitive to the distribution of electron density at particular carbon atoms, is usually made by the chemical shifts in ^{13}C NMR spectra. Common analysis of ^{13}C substituent chemical shifts (SCS) is based on the principles of linear free energy relationships (LFER) comprising the SSP (Single Substituent Parameter) or DSP (Dual Substituent Parameter) equations in the forms:

$$SCS = \rho\sigma + h \quad (2.6.8)$$

$$SCS = \rho_I\sigma_I + \rho_R\sigma_R + h \quad (2.6.9)$$

Where SCS is the change in chemical shift induced by the substituent, ρ is the proportionality constant reflecting the sensitivity of the ^{13}C NMR chemical shifts to substituent effects, σ is the corresponding substituent constant, and *h* is the intercept.

In the dual-substituent parameter (DSP) equation 2.6.9 SCS are correlated by a linear combination of inductive (σ_I) and depending on the electronic demand of the atom under examination with one of the four different resonance scales (σ_R^o, σ_R^{BA}, σ_R^+ and σ_R^-). Calculated values ρ_I and ρ_R are relative measures of the transmission of inductive and resonance effects through the investigated system.

In some cases the use of single σ scales alone cannot account for long-range effects in all situations where a continuum of resonance response is to be expected. The need of differing σ_R scales can best be accommodated by the use the dual-substituent parameter non-linear resonance (DSP-NLR) method developed by Bromilow et.al [155] which allows the resonance scale to vary with the electron demand of the site. An equation of type 2.6.10 gave an almost perfect correlation of *para*-SCS in 15 *p*-disubstituted benzenes [155] with ε ranging from 0.25 for NMe_2 to -0.72 for NO_2, as well as in eight β-substituted styrenes[56] and 3-phenyl and 3-thienyl-2-cyanoacrylamides [156].

$$SCS = \rho_I\sigma_I + \rho_R\sigma_R^o/(1- \varepsilon\sigma_R^o) + h \quad (2.6.10)$$

Substituent chemical shift data (SCS) relative to the hydrogen substituent were fitted to the nonlinear equation 2.6.10 (DSP-NLR). Starting with ε as zero, the DSP-NLR becomes a DSP

equation, and the data fitting was performed as above to obtain ρ values and the standard deviation.

$$\sigma_R = \sigma_R^o/(1- \varepsilon\sigma_R^o) \quad (2.6.11)$$

The demand parameter (ε) was then incremented in small steps. This modifies the σ_R values which were used to fit the data in the normal way. The changes in (ε) were made until a minimum in the standard deviation of the fit in the experimental data was achieved.

2.7 Correlation of linear solvatation energy relationship (LSER)

2.7.1 Solvatochromism of organic molecules

When the space is filled with a substance omissions beam of electromagnetic rays, can cause leakage or absorption of radiation depending on its frequency, and the structure of the compound. Absorption of electromagnetic radiation energy $\Delta E=hv$, the molecule moves from primary to excited condition manifested by amplification of vibration or rotation of atomic nuclei or exceed the electronic system to a higher energy level. When the system returns to the ground state, it emits energy that is characteristic of a given substance. Ultraviolet absorption spectroscopy studies in the field of electromagnetic radiation of between 200 and 400 nm. Absorption spectra of more atomic molecules are studied from the point of transition of electrons localized in relationships or certain functional groups. The following are possible electric switches to:

- $n \rightarrow \pi^*$, when electrons cross the free electron pair of the less stable anti-bonding π^* orbital;
- $\pi \rightarrow \pi^*$, when electrons bonding π orbital taking the less stable anti-bonding π^* orbital;
- $\sigma \rightarrow \sigma^*$, when electrons bonding σ orbital crossing in less stable anti-bonding σ^* orbital.

Energy absorption in the ultraviolet and visible region determined by the presence of the chromophore group or chromophore - portion of the molecule which occurs in some of the crossing points as described in the absorption of radiation. Any chromophore has a characteristic value that corresponds to the wavelength of the maximum absorption and is determined by the structure of the molecule. The rest of the molecule does not absorb the radiation, but can influence the position of the absorption maximum. Electron-donating groups cause shift of absorption maxima to longer wavelengths (bathochromic effect) and electron-acceptor groups to smaller wavelengths (hypsochromic effect).

It is generally known that the location, shape, and intensity of absorption bands in the UV/Vis spectra depend on the solvent containing the solute, and the rate of chemical reactions and chemical equilibrium position so that a careful selection of the solvent for the reaction or absorption under certain conditions in fact, part of his skill [121,157-164]. Moving and changes the intensity of the absorption band is the result of intermolecular interactions between the solute and the solvent, which may be of type: ion-dipole, dipole-dipole, dipole-induced dipole,

hydrogen bonds, etc. The influence of solvents on the UV/Vis spectrum is referred to solvatochromism. Solvatochromic effects can be:

- **hypsochromic**, blue shift, which means a shift of the absorption maximum to lower wavelengths with increasing solvent polarity (negative solvatochromism);
- **bathochromic**, red shift, which means a shift of the absorption maximum to longer wavelengths with increasing solvent polarity (positive solvatochromism).

2.7.2 Solvatochromic compounds

Solvent effects on the UV/Vis spectrum depends primarily on the type of chromophore and the nature of electronic transitions ($\sigma\rightarrow\sigma^*$, $n\rightarrow\sigma^*$, $\pi\rightarrow\pi^*$, $n\rightarrow\pi^*$) and charge-transfer (CT). Electronic transitions from special interest are $\pi\rightarrow\pi^*$, $n\rightarrow\pi^*$ and CT. Compounds which contain π-electrons, can be classified into three different groups according to the idealized structure: aromatic compounds, polyenes (or Poliina) and polymethine [162,163].

In contrast to the aromatic compounds or polyene structure, the conjugated polymethine represent a series of molecules that are characterized by a straight length of the same connection, and changes the charge metinskog along the chain. They show the common structural properties:

... (N + 3) ... π n = 1, 3, 5, 7, ...

X-(CR) n-X' R = H or the substituents

X, X '= the atoms (N, O, P, S), or atomic group at the chain ends

X = X' polymethine dyes (X = X' = N: cyanine, X = X '= A. oksonoli)

X ≠ X' meropolimetinske paint (X = N and X = O: merocyanine).

Particularly interesting color meropolimetinske (especially merocyanine), whose electronic structure is located between the polyene and polymethine, depending on the nature of X and X', and the polarity of the solvent [164]. These are systems in which the electron-donor group, A, is connected to the electron-acceptor group, and is, through a system of conjugated bonds. Their π-electronic structure can be explained by means of two resonant structure H-R-A D^+-R-A^-. The electronic switch is followed by intramolecular charge transfer between the donor and acceptor groups so that the dipole moment (μ_s) are significantly different from the dipole of the molecules in the ground state (μ_g).

Moving the $\pi \rightarrow \pi^*$ absorption bands of the different colors in the betainic solvent is applied to define the empirical parameter of solvent polarity, ET (30). It can also be used for UV/Vis spectroscopic determination of the share of water or other polar solvent in binary solvent mixtures of different polarity. Solvatochromism application in analytical chemistry are detailed in the literature [165].

2.7.3 Kamlet-Taft and Catalán treatment

Since that solvents may have a strong influence on reaction rates and equilibria, selection of a suitable solvent can be one of the most important features for the success of the planned reaction. The influence of solvents on the rates of chemical reactions was first noted by Berthelot and Pean de Saint-Gilles in 1862 in connection with their studies on esterification of acetic acid and ethanol [166]. Menschutkin in 1890 concluded that a reaction cannot be separated from the medium in which it is performed [167] and discovered that, in reactions between liquids, one of the reaction partners may constitute an unfavourable solvent. Menschutkin related the influence of solvents primarily to their chemical, not their physical properties.

The influence of solvents on chemical equilibria was discovered in 1896, simultaneously with the discovery of keto-enol tautomerism in 1,3-dicarbonyl compounds and the nitro-isonitro tautomerism of primary and secondary nitro compounds [168]. The first one, Stobbe, reviewed these results [169] and divided the solvents into two groups according to their ability to isomerize tautomeric compounds. His classification reflects the modern division into protic and aprotic solvents. The effect of solvent on constitutional and tautomeric isomerization equilibria was later studied in detail by Dimroth [170] and Meyer [171]. Chemists have classified solvents according to [172]:

- Structure, comprising: *protic solvents*: solvents that contain relatively mobile protons, such as those bonded to oxygen, nitrogen, or sulfur (attached to an electronegative atom); and *aprotic solvents*, in which all hydrogen's are bonded to carbon.
- Dielectric constant, comprising; *polar solvents*, those that have high dielectric constants (high polarizability); and *non-polar solvents*, are compounds that have low dielectric constants (low polarizability), these solvents are not miscible with water.

Influences of the solvent on the reactivity of organic compounds and their absorption spectra are more complex and often more specific when compared with the effects of substituents. Property solvent polarity makes it possible to observe these effects only qualitatively. However, the inability to solvent effects and quantify, through physical constants, prompted the introduction of empirical scale. The empirical effects of the scale of the solvent are based on the reactions of reference, which are sensitive to the solvents. They express the empirical measure of solvent polarity, i.e., the empirical measure of its solvation power in a given model reaction. Empirical parameters polarity of which is determined on the basis of a reaction are not universal, and can be applied to other systems.

If the effects of the solvent to separate the different types of interactions between the molecules of the solute and solvent, the obtained parameters may explain their size. In order to address two or more aspects of solvation, resorted to multiparametre approach (Equation 2.6.12).

$$A = A_0 + B\,B + C\,C + D\,D + ... \qquad (2.6.12)$$

Size A is a physical-chemical properties, which depends on the solvent: the logarithm of the rate constant or equilibrium position or absorption maximum in the UV/Vis, IR, NMR and ESR spectra. A_0 is the extrapolated value of the properties in the vapor phase, or an inert solvent. B, C, D, ... are independent, but complementary solvent parameters that describe the different types of interactions between the molecules of the solvent and the solute. The coefficients b , c , d , ... a sensitivity of the described properties of the different types of interactions between the molecules of the solvent and the solute, shall be determined by multiple linear regression.

Multi-parameter model to predict the value of dependent variable based on the values of independent variables and can be applied only to the set of data obtained for a large number of well-chosen solvent. Its validity is examined by appropriate statistical methods. However, the separation of solvent effects on different types of interaction is purely formal, and sometimes it is not theoretically significant, since their actions can not always be separated.

In general, the effects of the solvent, can be subdivided in two different types of contributions: **The specific interactions**, which are described by Drago et al [173] as the localized interaction of the donor-acceptor-type, which include the specific orbits, and are quantified via the AN-

Gutman and DN scale [174] and dear EB and CB scale [175] or interpreted as acid-base interactions involving hydrogen bonding and quantified over Koppel-Palm's B (MeOD) [176], Arnett's DH $_r$ [177], Maria-Gal's DH (BF_3) [178] scale and Kamlet-Taft's [180,181] α and β and Catalán's SA and SB scale [182].

The non-specific interaction, caused by the dielectric action of the solvent as a continuum, and that are modeled Kirkwood [183] and Onsager [184], and are quantified by Kosower [185], Brooker [186], Dong-Winnick [187], Kamlet Taft [188], Drag [189] and Catalán scale [182].

The *solvatochromic comparison method* is used to evaluate a β-scale of solvent hydrogen-bond acceptor (HBA) basicities, and an α-scale of solvent hydrogen-bond donor (HBD) acidities, and π*-scale of solvent dipolarity/polar using UV/Vis spectral data of solvatochromic compounds [190].

Kamlet and Taft have shown that β, α and π* may be applied in the correlation analysis by multiple regression of reaction rates and equilibria, and of spectroscopic data; equation 2.6.13 applies:

$$\nu = \nu_0 + s\pi^* + a\alpha + b\beta \tag{2.6.13}$$

where ν_0, a, b and s are (solvent-independent) coefficients characteristic of the process and indicative of the sensitivity to the accompanying solvent properties.

Kamlet and Taft's solvatochromic parameters have been used in one-, two-, and three-parameter correlations involving different combination of these parameters which are called linear salvation energy relationships (LSER's) [121].

More elaborated LSER model uses Catalán solvent parameters scale [191], i.e., Eq. (2.6.14) which qualitatively and quantitatively interprets the effect of solvent dipolarity, polarizability, and solvent–solute hydrogen bonding interactions:

$$\nu = \nu_0 + aSA + bSb + cSP + dSdP \tag{2.6.14}$$

where SA, SB, SP, and SdP characterize solvent acidity, basicity, polarizability, and dipolarity, respectively. The regression coefficients a–d describe the sensitivity of the absorption maxima to different types of the solvent–solute interactions.

*2.8 **Teorija funkcionala gustine (Density Functional Theory (DFT))***

Teorija funkcionala gustine (DFT) je prvi put pomenuta u dve publikacije Hoenberga, Kona i Šama (sredinom 60-tih godina XX veka[1,2]. Od tog vremena, DFT metoda je postala najuspešnija metoda za računanje elektronske strukture materije. Danas se DFT metoda uspešno primenjuje za proučavanje atoma, molekula, čvrstih tela, tečnosti, kompleksnih materijala, međumolekulskih interakcija, pobuđenih i prelaznih stanja, mehanizama hemijskih reakcija, NMR spektara, itd.

U svojoj originalnoj formulaciji DFT metoda se zasniva na činjenici da se poznavanjem elektronske gustine osnovnog stanja sistema, mogu veoma precizno, odrediti različite osobine molekula, kao što su: geometrija, električne i magnetne osobine, jonizaciona energija, vibracione frekvencije itd.

Glavni cilj svih kvantno-hemjskih pristupa je rešenje nerelativističke, vremenski nezavisne Šredingerove jednačine:

$$\hat{\mathrm{H}}\Psi(r_1, \dots, r_N) = E\Psi(r_1, \dots, r_N)$$

gde je višeelektronska talasna funkcija ($\Psi(r_1,\dots,r_\mathrm{N})$) funkcija od 3N promenjivih (N – ukupan broj elektrona u sistemu). Kada bi mogli da eksplicitno rešimo Šredingerovu jednačinu mogli bi i da predvidimo ponašanje bilo kog elektronskog sistema. Ipak, zbog postojanja velikog broja stepena slobode, ovo je nemoguće. DFT metoda opisuje sistem elektrona koji međusobno interaguju preko njihove gustine a ne preko višeelektronske talasne funkcije. To znači, da za sistem od N elektrona, koji se ponašaju u skladu sa Paulijevim principom i međusobno odbijaju elektrostatičkim interakcijama, osnovna promenjiva sistema (elektronska gustina) zavisi samo od tri prostorne coordinate x, y i z.

DFT metoda se zasniva na dve teoreme Hoenberga i Kona[1] kao i na setu jednačina koje su izveli Kon i Šam[2]. Prva Hoenberg-Konova teorema glasi:

„Energija osnovnog stanja iz Šredingerove jednačine je jedinstveni funkcional elektronske gustine“

Po ovoj teoremi elektronska gustina određuje sve osobine osnovnog stanja sistema, odnosno rešavanjem Šredingerove jednačine se dobija energija osnovnog stanja sistema. Ova teorema ne objašnjava prirodu funkcionala pomoću kojeg se može odrediti energija osnovnog stanja, tako da druga Hoenberg-Konova teorema glasi:

„Elektronska gustina koja minimizuje energiju ukupnog funkcionala je prava elektronska gustina koja odgovara potpunom rešenju Šredingerove jednačine“

Ovim se dokazuje postojanje varijacionog principa u DFT metodama. Ipak, varijacioni princip je ograničen samo na molekule u osnovnom stanju i ne može se primeniti na pobuđena stanja.

Ove dve teoreme su osnova DFT metode, ali one ne pružaju nikakve informacije o načinu na koji se mogu izvoditi proračuni. Kon i Šam su pokazali da se proble pronalaženja prave elektronske gustine može rešiti uvođenjem seta jednoelektronskih jednačina[2]. Elektronska gustina ima isti izraz kao da je izvedena iz Slejterove determinante:

$$\rho(\boldsymbol{r}) = \sum_i |\Psi_i(\boldsymbol{r})|^2$$

U ovom izrazu, Ψ_i predstavlja popunjene atomske/molekulske orbitale, nazvane Kon-Šamove orbitale. Kon i Šam predlažu da se tačna kinetička energija elektrona neinteragujućeg sistema računa pomoću iste elektronske gustine kao kao i realnog, interagujućeg, sistema, pri čemu se elektroni koji ne interaguju kreću u polju efektivnog potencija ostalih elektrona. Ukupna elektronska energija se može podeliti na “poznate” i “nepoznate” termove:

$$E[\boldsymbol{r}] = T_s[\boldsymbol{r}] + E_{ext}[\boldsymbol{r}] + E_{Coul}[\boldsymbol{r}] + E_{XC}[\boldsymbol{r}]$$

“Poznati” termovi su: kinetička energija elektrona T_s, elektron-jezgro privlačenje E_ext, elektron-elektron odbijanje E_Coul, i “nepoznati” term izmene-korelacije (exchange-correlation) $\mathrm{E_{XC}}$. Jedini izraz za koji se eksplicitna forma funkcionala ne može napisati je E_XC. Minimizacijom funkcionala energije se dobijaju Kon-Šamove jednačine:

$$\left[-\frac{\hbar^2}{2m}\nabla^2 + V_{eff}(\boldsymbol{r})\right]\Psi_i(\boldsymbol{r}) = \varepsilon_i\Psi_i(\boldsymbol{r})$$

$$V_{eff}(\boldsymbol{r}) = V_{ext}(\boldsymbol{r}) + V_H(\boldsymbol{r}) + V_{XC}(\boldsymbol{r})$$

$$n(\boldsymbol{r}) = \sum_i |\Psi_i(\boldsymbol{r})|^2$$

$$V_{xc} = \frac{\delta E_{xc}}{\delta\rho(\boldsymbol{r})}$$

Kon-Šamove jednačine se mogu rešavati samo iterativnim tehnikama pomoću metode samosaglasnog polja jer efektivni potencijal V_eff zavisi od $n(\mathbf{r})$, odnosno od $\Psi(\mathbf{r})$, koje su rešenje jednačina. Iz izračunatih energija i funkcija moguće je dobiti ostale karakteristike osnovnog

stanja kao što su: ukupna energija osnovnog stanja, gustina naelektrisanja, vibracione osobine molekula itd.

Potencijal izmene-korelacije (V_{xc}) opisuje efekte Paulijeve izmene i Kulonovih interakcija ne samo kao čisto elektrostatičko odbijanje između elektrona, već uzima u obzir i njihovu kvantnu prirodu. Ovaj term je definisan kao funkcional izvoda energije izmene-korelacije (E_{xc}) u odnosu na elektronsku gustinu. Pronalaženje i matematičko opisivanje ovog funkcionala je veoma zahtevno, tako da su razvijeni brojni aproksimativni funkcionali za uključivanje ovih efekata u DFT formalizam. Na osnovi teorijskih postavki na kojima se zasnivaju, aproksimativni funkcionali se mogu podeliti u tri velike grupe: aproksimacija lokalne gustine (Local Density Approximation - LDA), aproksimacija generalizovanog gradijenta (Generalized-Gradient Approximation - GGA) i hibridni funkcionali (Hybrid Functional).

Aproksimativni funkcionali

Prvi pokušaji da se proceni vrednost funkcionala izmene-korelacije su se zasnivali na aproksimaciji lokalne gustine. U LDA metodi E_{xc} se računa pod predpostavkom da se sistem lokalno ponaša kao uniformni elektronski gas, odnosno:

$$E_{xc} = \int \rho\,(\boldsymbol{r})\varepsilon_{xc}^{LDA}\big(\rho(\boldsymbol{r})\big)$$

gde je $\varepsilon_{xc}^{LDA}(\rho)$ energija izmene-korelacije jednog elektrona u uniformnom gasu gustine ρ. Proračuni ukupne elektronske energije dobijeni primenom aproksimacije lokalne gustine su bili iznenađujuće dobri, međutim, zbog toga što metoda sistematski precenjuje vrednosti energije veza i loše reprodukuje termohemijske osobine molekula, njihova upotreba u računarskoj hemiji je veoma mala.

Drugu klasu funkcionala, koji imaju znatno veću primenu u računarskoj hemiji i daju bolje rezultate u odnosu na LDA funkcional, čine funkcionali koji se zasnivaju na aproksimaciji generalizovanog gradijenta. U ovoj aproksimaciji funkcional izmene-korelacije zavisi i od vrednosti elektronske gustine i od njenog gradijenta:

$$E_{xc} = \int \rho\,(\boldsymbol{r})\varepsilon_{xc}^{GGA}\big(\rho(\boldsymbol{r}), \nabla\rho(\boldsymbol{r})\big)d\boldsymbol{r}$$

Lokalne nehomogenosti elektronske gustine se mogu uzeti u obzir tako što će energija izmene-korelacije zavisiti od gradijenta elektronske gustine. Za razliku od LDA funkcionala, izraz za određivanje ε_{xc}^{GGA} nije jedinstven, tako da postoje brojni funkcionali koji se zasnivaju na aproksimaciji generalizovanog gradijenta. Ovi funkcionali se razlikuju po broju ograničenja koja ispunjavaju, po broju parametara koje poseduju kao i u količini empirijskih podataka koji su korišćeni prilikom njihove konstrukcije. Najpoznatiji i najčešće korišćeni GGA funkcionali su PW91[3], PBE[4] i BLYP[5].

U suštini GGA funkcionali daju znatno bolje rezultate u odnosu na LDA funkcionale ali se ne mogu koristiti pri računanju stanja daleko od minimuma, kao što su energije hemijskih reakcija. GGA funkcionali se se pokazali veoma dobro pri računanju molekula u čvrstom stanju jer daju precizne geometrije, elastične osobine periodičnih čvrstih tela i kvalitativno ispravnu strukturu elektronskih traka. Ipak, ovi funkcionali sistematski podcenjuju razliku u energiji između elektronskih traka.

Meta-GGA funkcionali povećavaju fleksibilnost funkcionala izmene-odbijanja dodajući Kon-Šamovu gustinu kinetičke energije (τ_{KS}) elektronskoj gustini i njenom izvodu:

$$E_{xc} = \int \rho\,(\boldsymbol{r})\varepsilon_{xc}^{GGA}\big(\rho(\boldsymbol{r}), \nabla\rho(\boldsymbol{r}), \nabla^2\rho(\boldsymbol{r}), \tau_{KS}(\boldsymbol{r})\big)d\boldsymbol{r}$$

$$\tau_{KS}(\boldsymbol{r}) = -\frac{1}{2}\sum_i |\nabla_i(\boldsymbol{r})|$$

Zbog te povećane fleksibilnosti meta-GGA funkcionali su tačniji prilikom izračunavanja osobina molekula u odnosu na GGA i LDA funkcionale.

Pomenuti funkcionali (LDA, GGA i meta-GGA) su funkcionali semilokalnog tipa. To znači da gustina eneregije izmene-korelacije u nekoj delu prostora zavisi samo od osobina tog dela prostora. Beke je pokazao[6] da je moguće značajno poboljšati proračune termohemijskih osobina molekula korišćenjem GGA funkcionala uz dodatak dela energije izmene izračunate Hartri-Fok metodom na Kon-Šam orbitalama.

Upotreba ove dodate Hartri-Fok izmene se može opravdati uvođenjem formule adijabatskog povezivanja[7,8]:

$$E_{xc}[\rho] = \int_0^1 \left(\langle \sum_{i>j} r_{ij}^{-1} \rangle_\lambda - J\left[\rho^\lambda\right] \right) d\lambda = \int_0^1 U_{xc}^\lambda d\lambda$$

gde vrednost parametra λ = 0 predstavlja neinteragujući Kon-Šamov sistem, dok λ = 1 predstavlja realan sistem. To znači da se pomoću parametra λ može uključivati ili isključivati računanje elektronske korelacije. Potencijal energije izmene-korelacije (U_{xc}) na vrednosti λ = 0 predstavlja tačnu Hartri-Fokovu energiju izmene računatu sa Kon-Šamovim orbitalama.

$$U_{xc}^{0} = -\frac{1}{2}\sum_{ij}^{occ}\int \frac{\Psi_i^*(\boldsymbol{r}_1)\Psi_j^*(\boldsymbol{r}_2)\Psi_j^*(\boldsymbol{r}_1)\Psi_i^*(\boldsymbol{r}_2)}{\boldsymbol{r}_{12}} d\boldsymbol{r}_1 d\boldsymbol{r}_2$$

Funkcional izmene-korelacije se onda može aproksimirati interpolacijom između poznatog λ = 0 limita (Hartri-Fock izmena) i λ = 1 predstavljenog semilokalnim funkcionalom izmene-korelacije.

$$E_{xc}[\rho] = a_x U_{xc}^{0} + (1 - a_x)E_{xc}^{semilocal}[\rho]$$

Funkcionali koji koriste deo Hartri-Fok izmene se zovu hibridni funkcionali. Ovi funkcionali nisu semilokalni jer računanje Hartri-Fock izmene zahteva dvostruko integraljenje celog realnog prostora. Zbog toga upotreba ovih funkcionala zahteva više računarskog vremena. Najpoznatiji hibridni funkcionali su B3LYP[9], TPSSh[10], PBE1PBE[11] i M06[12].

1 P. Hohenberg and W. Kohn, *Physical Review*, 1964, **136**, B864-B871.

2. W. Kohn and L. J. Sham, *Physical Review*, 1965, **140**, A1133-A1138.

3 J. P. Perdew, J. A. Chevary, S. H. Vosko, K. A. Jackson, M. R. Pederson, D. J. Singh, and C. Fiolhais "Atoms, molecules, solids, and surfaces: Applications of the generalized gradient approximation for exchange and correlation" Phys. Rev. B **1992**, 46, 6671.

4 J. P. Perdew, K. Burke, and M. Ernzerhof "Generalized Gradient Approximation Made Simple" Phys. Rev. Lett. **1996**, 77, 3865.

5 A. D. Becke "Exchange: Density-functional exchange-energy approximation with correct asymptotic behavior" Phys. Rev. A **1988**, 38, 3098.

6 A. D. Becke, *The Journal of chemical physics*, 1993, **98**, 1372-1377.

7 O. Gunnarsson and B. I. Lundqvist, *Phys. Rev. B*, 1976, **13**, 4274-4298.

8 R. Harris and B. G. Mulimani, *J. Phys. F*, 1974, **4**, 703-710.

9 A. D. Becke "Density-functional thermochemistry. III. The role of exact exchange" J. Chem. Phys. **1993**, 98, 5648.

10 V. N. Staroverov, G. E. Scuseria, J. Tao, and J. P. Perdew "Comparative assessment of a new nonempirical density functional: Molecules and hydrogen-bonded complexes" J. Chem. Phys. **2003**, 119, 12129.

11 C. Adamo, V. Barone, "Toward reliable density functional methods without adjustable parameters: The PBE0 model" J. Chem. Phys. **1999**, 110 6158-69.

12 Y. Zhao, D. G. Truhlar, "The M06 suite of density functionals for main group thermochemistry, thermochemical kinetics, noncovalent interactions, excited states, and transition elements: two new functionals and systematic testing of four M06-class functionals and 12 other functionals," Theor. Chem. Acc. **2008**, 120, 215-41.

3 EXPERIMENTAL PART

3.1 Materials

All used materials and solvents (UV spectrophotometric grade) were obtained commercially (Fluka and Sigma-Aldrich), and used without purification.

3.2 Equipment

All Fourier-transform infrared (FTIR) spectra were obtained using FTIR BOMEM MB 100 in the form of KBr pellets. The purity of the obtained compounds was confirmed by elemental analysis. Elemental analysis (C, H, N and O) was performed using a VARIO EL III Elemental analyzer, and F, Cl, Br and I content was calculated as substraction.

6(2)-Hydroxy-4-methyl-2(6)-oxo-1-(substituted phenyl)-1,2(1,6)-dihydropyridine-3-carbonitriles and 5-arylazo-6(2)-hydroxy-4-methyl-3-cyano-*N*(1)-phenyl-2(6)-oxo-pyridine-3-carbonitrile dyes: NMR spectral measurements were performed on a Bruker Avance III 500 spectrometer (500.26 MHz for ^{1}H, 125.80 MHz for ^{13}C) equipped with broadband 5 mm probe (BBO). The spectra were recorded at room temperature in deuterated dimethyl sulfoxide (DMSO-d_6). The chemical shifts were expressed in ppm values referenced to δ_H = 2.5 and δ_C = 39.5 ppm in ^{1}H and ^{13}C NMR spectra, respectively. Coupling constants *J* were expressed in Hz. ^{1}H NMR spectra of compound **1** were recorded at 343 K. 2D COSY, HMBC and HSQC spectra were also recorded on a Bruker Avance III 500 spectrometer. Standard pulse sequences were used for 2D spectra. COSY spectra were recorded at spectral widths of 5 kHz in both *F*2 and *F*1 domains; 1K × 512 data points were acquired with 32 scans per increment and the relaxation delays of 2.0 s. Data processing was performed on a 1K × 1K data matrix. Inverse-detected 2D heteronuclear correlated spectra were measured over 512 complex points in *F*2 and 256 increments in *F*1, collecting 128 (HSQC) or 256 (HMBC) scans per increment with the relaxation delays of 1.0 s. The HMBC experiments, the long-range ^{13}C–^{1}H chemical shifts correlations, were obtained by optimizing for a coupling of 8 Hz. Fourier transform was done on a 512 × 512 data matrix. π/2 shifted sine squared window functions were used along *F*1 and *F*2 axes for all 2D spectra.

3-Cyano-4-(substituted phenyl)-6-phenyl-2(1*H*)-pyridones: ^{1}H and ^{13}C NMR characterizations were performed on a Varian Gemini 2000 (200/50 MHz) instrument at 25 ^{o}C. Chemical shifts (δ) were reported in part per million (ppm) relative to tetramethylsilane (δ_H=0 ppm) in ^{1}H NMR, and to dimethyl sulfoxide (δ_C=39.5 ppm) in ^{13}C NMR, using the residual solvent peak as a reference standard. 2D Nuclear Overhauser effect spectroscopy (NOESY), Heteronuclear Multiple Bond Correlation (HMBC) and Heteronuclear single quantum coherence spectroscopy (HSQC) spectra were recorded on a Bruker Avance 500 spectrometer (500/125 MHz) equipped with inverse detection triple resonance 5 mm probe (TXI). Standard pulse sequences were used for 2D spectra [192].

The UV absorption spectra were recorded in the range from 200 to 600 nm in solvents of different polarity using UV-Vis Shimadzu 1700A spectrophotometer. Spectra were recorded at different conditions, *e.g.* variable temperature and concentration, as well as solvent mixtures, which were expected to have effect on the tautomer ratio and extent of dimerization: concentration was changed in the range from 1.00 x 10^{-4} to 1.00 x 10^{-7} mol dm^{-3}, and at temperature of 25, 35, 45 and 55 ± 0.1 ^{o}C. The constant, K_T = [**6-PY**]/[**2-PY**] ([**b**]/[**a**]) for 6(2)-hydroxy-4-methyl-2(6)-oxo-1-(substituted phenyl)-1,2(1,6)-dihydropyridine-3-carbonitriles, and K_T = [**PY**]/[**HP**] for 3-cyano-4-(substituted phenyl)-6-phenyl-2(1*H*)-pyridones, represent proportion of the area in UV spectra of the corresponding tautomeric form.

The mass spectra were obtained on a FinniganMAT 8230 (EI, 70 eV) and on Agilent technologies 6210 TOF LC/MS (high resolution mass spectrometry - HRMS) instrument (LC: series 1200). Microwave synthesis was performed in Milestone MycroSYNTH reactor.

3.3 Synthesis

3.3.1 Synthesis of 6(2)-hydroxy-4-methyl-2(6)-oxo-1-(substituted phenyl)-1,2(1,6)-dihydropyridine-3-carbonitriles

Synthesis of 6(2)-hydroxy-4-methyl-2(6)-oxo-1-(substituted phenyl)-1,2(1,6)-dihydropyridine-3-carbonitriles was done on 2 ways [193,194]:

General procedure for the pyridones synthesis under microwave irradiation: A mixture of ethyl acetoacetate (4.9 mmol), 2-cyano-*N*-(substituted phenyl)ethanamides (1.25 mmol) and freshly powdered potassium hydroxide (2.5 mmol) was placed in a glass vial, equipped with condenser and irradiated with stirring using the following method: ramp time 1 min at 150 W and hold time 10 min at 150 W. The obtained product was suspended in hot water, acidified with diluted HCl, filtrated and washed with water and chloroform.

General procedure for the conventional pyridones synthesis: A mixture of ethyl acetoacetate (30.0 mmol), 2-cyano-*N*-(substituted phenyl)ethanamides (12.0 mmol) and freshly powdered potassium hydroxide (20.0 mmol) was placed in a three-necked flask, equipped with condenser, thermometer and magnetic stirrer, and heated for 3 h under reflux. The obtained product was suspended in hot water, acidified with diluted HCl, filtrated and washed with water and chloroform.

3.3.2 Synthesis of 2(1*H*)-pyridones

2-Cyano-*N*-(substituted phenyl)-ethanamides as well as methoxy, nitro and chloro derivatives of 3-cyano-4-(2-, 3-, and 4-substituted phenyl)-6-phenyl-2(1*H*)-pyridones are synthesized according to literature method [194].

3.3.4 Synthesis of 5-arylazo-6(2)-hydroxy-4-methyl-3-cyano-*N*(1)-phenyl-2(6)-oxo-pyridine-3-carbonitrile dyes

(Z)-4-methyl-5-[2-(3 or 4-substituted phenyl)hydrazono]-2,6-dioxo-1-phenyl-1,2,5,6-tetrahydro-3-carbonitriles are synthesized according to literature methods [Ertan N, Gürkan P (1997) Dyes Pigments 33:137].

1-(3- or 4-substituted aniline)-3-cyano-6-hydroxy-4-methyl-2-pyridone (2.26 g, 0.005mole) was dissolved in a solution of KOH (0.28 g, 0.005mole) in 2ml water. The resulting solution was cooled to 0-5 ºC and was stirred with a cold (0-5 ºC) solution of the appropriate diazonium prepared by diazotizing the substituted aniline (0.005mole) in 1.25ml concentrated HCl with (0.38gm, 0.005mole) $NaNO_2$ in 2ml water. The resulting diazonium salt was then slowly added to the vigorously stirred solution of the pyridine and the mixture was stirred for more than 3 hours. The precipitated was collected and washed thoroughly with cold water and dried. Crystallization has been down in two steps:

Firstly the dyes were dissolved in methanol and then filtrated and it was left to dry.

Secondly, the filter paper was dissolved in acetone and left to evaporate and then the precipitated solid was collected.

The obtained material was filtrated, washed with distilled water, and recrystalled from methanol and finally purified by flash chromatography.

Microwave synthesis was performed in Milestone MycroSYNTH reactor.

3.4 Characteristics of 6(2)-hydroxy-4-methyl-2(6)-oxo-1-(substituted phenyl)-(1,2 or 1,6)-dihydropyridine-3-carbonitriles

6-hydroxy-4-methyl-2-oxo-1-phenyl-1,2-dihydropyridine-3-carbonitriles (**1a**, $C_{13}H_{10}N_2O_2$) and *2-hydroxy-4-methyl-6-oxo-1-phenyl-1,6-dihydro- pyridine-3-carbonitriles* (**1b,** $C_{13}H_{10}N_2O_2$)

White-yellowish crystalline solid; yield 78%, m.p.: 281-283ºC (Ref. [195] 280-283ºC);

6-hydroxy-4-methyl-2-oxo-1-(4-methylphenyl)-1,2-dihydropyridine-3-carbonitriles (**2a**, $C_{14}H_{12}N_2O_2$) and *2-hydroxy-4-methyl-6-oxo-1-(4-methylphenyl)-1,6-dihydropyridine-3-carbonitriles* (**2b**, $C_{14}H_{12}N_2O_2$)

White-yellowish crystalline solid; yield 72%, m.p.: 284-285ºC;

HRMS: *m/z* (MH^+) calcd for $C_{14}H_{13}N_2O_2$ 241.0996, found 241.0972; IR (KBr): $\bar{\nu}$ = 514, 655, 816, 1036, 1104, 1131, 1181, 1232, 1415, 1538, 1664 (C=O), 2216 (C≡N), 2507, 2608, 2932, 3078, 3419 (O-H) cm^{-1}; UV-Vis (ethanol, $c = 5.10^{-5}$ mol dm^{-3}): λ_{max} (ε) = 326 (16420) nm (mol^{-1} dm^3 cm^{-1}); Elemental Analysis:

Calculated: %C 69.99, %H 5.03, %N 11.66, %O 13.32

Found: %C 69.80, %H 5.22, %N 11.50, %O 13.48

2a) ^{1}H NMR (500 MHz, DMSO-d_6): δ = 2.27 (s, 3H, 4-CH_3), 2.35 (s, 3H, 4'-CH_3), 5.69 (s, 1H, 5-H), 7.07 (AA'XX', J = 8.2 Hz, 2H, $C_6H_4CH_3$), 7.27 (AA'XX', J = 8.6 Hz, 2H, $C_6H_4CH_3$), 12.60 (bs, 1H, OH) ppm; ^{13}C NMR (125 MHz, DMSO-d_6): δ = 20.9 (4-CH_3), 21.0 (4'-CH_3), 88.6 (C3), 92.7 (C5), 117.8 (C≡N), 128.4 (C2', C6'), 129.7 (C3', C5'), 133.0 (C1'), 138.0 (C4'), 159.4 (C4), 161.1 (C2), 162.5 (C6) ppm.

2b) ^{1}H NMR (500 MHz, DMSO-d_6): δ = 1.90 (s, 3H, 4-CH_3), 2.36 (s, 3H, 4'-CH_3), 6.08 (s, 1H, 5-H), 7.14 (AA'XX', J = 8.4 Hz, 2H, $C_6H_4CH_3$), 7.31 (AA'XX', J = 8.4 Hz, 2H, $C_6H_4CH_3$), 12.60 (bs, 1H, OH) ppm; ^{13}C NMR (125 MHz, DMSO-d_6): δ = 21.0 (4'-CH_3), 21.9 (4-CH_3), 83.6 (C3), 99.0 (C5), 115.5 (C≡N), 128.3 (C2', C6'), 130.2 (C3', C5'), 135.2 (C1'), 138.6 (C4'), 153.3 (C4), 161.2 (C6), 171.9 (C2) ppm.

6-hydroxy-4-methyl-2-oxo-1-(4-methoxyphenyl)-1,2-dihydropyridine-3-carbonitriles (**3a**, $C_{14}H_{12}N_2O_3$) and *2-hydroxy-4-methyl-6-oxo-1-(4-methoxy- phenyl) -1,6-dihydropyridine-3-carbonitriles* (**3b**, $C_{14}H_{12}N_2O_3$)

Yellowish crystalline solid; yield 60%, m.p.: 270-273ºC;

3a) ^{1}H NMR (500 MHz, DMSO-d_6): δ = 2.28 (s, 3H, CH_3), 3.79 (s, 3H, OCH_3), 5.69 (s, 1H, 5-H), 7.00 (AA'XX', J = 7.2 Hz, 2H, $C_6H_4OCH_3$), 7.12 (AA'XX', J = 7.2 Hz, 2H, $C_6H_4OCH_3$),

12.73 (bs, 1H, OH) ppm; ^{13}C NMR (125 MHz, DMSO-d_6): δ = 21.0 (CH_3), 55.5 (OCH_3), 89.0 (C3), 92.6 (C5), 114.4 (C3', C5'), 117.8 (C≡N), 128.0 (C1'), 129.6 (C2', C6'), 159.3 (C4), 159.4 (C4'), 161.2 (C2), 162.7 (C6) ppm.

3b) ^{1}H NMR (500 MHz, DMSO-d_6): δ = 1.91 (s, 3H, CH_3), 3.78 (s, 3H, OCH_3), 6.07 (s, 1H, 5-H), 7.03 (AA'XX', J = 7.4 Hz, 2H, $C_6H_4OCH_3$), 7.18 (AA'XX', J = 7.4 Hz, 2H, $C_6H_4OCH_3$), 12.73 (bs, 1H, OH) ppm; ^{13}C NMR (125 MHz, DMSO-d_6): δ = 22.0 (CH_3) 55.6 (OCH_3), 83.6 (C3), 99.0 (C5), 114.8 (C3', C5'), 115.6 (C≡N), 129.7 (C2', C6'), 130.3 (C1'), 153.6 (C4), 159.5 (C4'), 161.5 (C6), 171.9 (C2) ppm.

HRMS: *m/z* (MH^+) calcd for $C_{14}H_{13}N_2O_3$ 255.0751, found 255.0762; IR (KBr): $\bar{\nu}$ =551, 633, 770, 825, 1036, 1172, 1255, 1302, 1410, 1512, 1665 (C=O), 2218 (C≡N), 2514, 2605, 2835, 2972, 3074, 3422 (O-H) cm^{-1}; UV-Vis (ethanol, c = 5.10^{-5} mol dm^{-3}): λ_{max} (ε) = 323 (18460) nm (mol^{-1} dm^3 cm^{-1}); Elemental Analysis:

Calculated: %C 65.62, %H 4.72, %N 10.93, %O 18.73

Found: %C 65.50, %H 4.84, %N 10.90, %O 18.76

6-hydroxy-4-methyl-2-oxo-1-(4-nitrophenyl)-1,2-dihydropyridine-3-carbonitriles

(**4a,** $C_{13}H_9N_3O_4$) and *2-hydroxy-4-methyl-6-oxo-1-(4-nitrophenyl)-1,6-dihydro pyridine-3-carbonitriles* (**4a,** $C_{13}H_9N_3O_4$)

Yellow crystalline solid; yield 73%, m.p.: 238-242ºC;

4a) ^{1}H NMR (500 MHz, DMSO-d_6): δ = 2.28 (s, 3H, CH_3), 5.69 (s, 1H, 5-H), 7.65 (AA'XX', J = 10 Hz, 2H, $C_6H_4NO_2$), 8.32 (AA'XX', J = 10 Hz, 2H, $C_6H_4NO_2$), 12.10 (bs, 1H, OH) ppm; ^{13}C NMR (125 MHz, DMSO-d_6): δ = 20.9 (CH_3), 88.1 (C3), 95.9 (C5), 118.0 (C≡N), 124,1 (C3', C5'), 130.3 (C2', C6'), 141.0 (C4'), 146.3 (C1'), 159.0 (C4), 160.9 (C2), 161.3 (C6) ppm.

4b) ^{1}H NMR (500 MHz, DMSO-d_6): δ = 1.93 (s, 3H, CH_3), 6.13 (s, 1H, 5-H), 7.76 (AA'XX', J = 10 Hz, 2H, $C_6H_4NO_2$), 8.36 (AA'XX', J = 10 Hz, 2H, $C_6H_4NO_2$), 12.10 (bs, 1H, OH) ppm; ^{13}C NMR (125 MHz, DMSO-d_6): δ = 21.5 (CH_3), 83.4 (C3), 99.4 (C5), 114.9 (C≡N), 124.7 (C3', C5'), 130.4 (C2', C6'), 143.2 (C4'), 147.6 (C1'), 152.1 (C4), 162.0 (C6), 172.1 (C2) ppm.

HRMS: *m/z* (MH^+) calcd for $C_{13}H_{10}N_3O_4$ 272.0691, found 272.0666; IR (KBr): $\bar{\nu}$ = 639, 751, 856, 1112, 1346, 1411, 1514, 1575, 1654 (C=O), 1718, 2221(C≡N), 2501, 2594, 3085, 3308, 3426 (O-H) cm^{-1}; UV-Vis (ethanol, c = 5.10^{-5} mol dm^{-3}): λ_{max} (ε) = 335 (15760) nm (mol^{-1} dm^3 cm^{-1}); Elemental Analysis:

Calculated: %C 57.57, %H 3.34, %N 15.49, %O 23.60

Found: %C 57.66, %H 3.29, %N 15.40, %O 23.65

6-hydroxy-4-methyl-2-oxo-1-(4-acetylphenyl)-1,2-dihydropyridine-3-carbonitriles (**5a**, $C_{15}H_{12}N_2O_3$) and *2-hydroxy-4-methyl-6-oxo-1-(4-acetylphenyl)-1,6-dihydro pyridine-3-carbonitriles* (**5b**, $C_{15}H_{12}N_2O_3$)

Brownish crystalline solid; yield 42%, m.p.: 227-230ºC;

5a) ^{1}H NMR (500 MHz, DMSO-d_6): δ = 2.27 (s, 3H, CH_3), 2.62 (s, 3H, C(O)CH_3), 5.66 (s, 1H, 5-H), 7.38 (AA'XX', J = 8.5 Hz, 2H, C_6H_4C(O)CH_3), 8.03 (AA'XX', J = 8.5 Hz, 2H, C_6H_4C(O)CH_3) ppm; ^{13}C NMR (125 MHz DMSO-d_6): δ = 20.8 (CH_3), 26.9 (C(O)CH_3), 87.3 (C3), 93.2 (C5), 117.8 (C≡N), 128.8 (C3', C5'), 129.0 (C2', C6'), 136.5 (C4'), 139.9 (C1'), 158.9 (C4), 160.7 (C2), 161.0 (C6), 197.4 (C(O)CH_3) ppm.

5b) ^{1}H NMR (500 MHz, DMSO-d_6): δ = 1.92 (s, 3H, CH_3), 2.63 (s, 3H, C(O)CH_3), 6.13 (s, 1H, 5-H), 7.47 (AA'XX', J = 8.5 Hz, 2H, C_6H_4C(O)CH_3), 8.08 (AA'XX', J = 8.5 Hz, 2H, C_6H_4C(O)CH_3) ppm; ^{13}C NMR (125 MHz, DMSO-d_6): δ = 21.6 (CH_3), 26.9 (C(O)CH_3), 83.41 (C3), 99.1 (C5), 115.1 (C≡N), 129.0 (C2', C6') 129.3 (C3', C5'), 137.0 (C4'), 141.5 (C1'), 152.3 (C4), 162.0 (C6), 171.9 (C2), 197.4 (C(O)CH_3) ppm.

HRMS: *m/z* (MH^+) calcd for $C_{15}H_{13}N_2O_3$ 269.0927, found 269.0921; IR (KBr): $\bar{\nu}$ = 643, 822, 958, 1010, 1267, 1450, 1531, 1666, 1687, (C=O), 2219 (C≡N), 2489, 2593, 3071, 3433 (O-H) cm^{-1}; UV-Vis (ethanol, c = 5.10^{-5} mol dm^{-3}): λ_{max} (ε) = 331 (24040) nm (mol^{-1} dm^3 cm^{-1}); Elemental Analysis:

Calculated: %C 67.16, %H 4.51, %N 10.44, %O 17.89

Found: %C 67.20, %H 4.49, %N 10.40, %O 17.91

6-hydroxy-4-methyl-2-oxo-1-(4-hydroxyphenyl)-1,2-dihydropyridine-3-carbonitriles (**6a**, $C_{13}H_{10}N_2O_3$)

Gray-brownish crystalline solid; yield 50%, m.p.: 286-288ºC;

6a) ^{1}H NMR (500 MHz, DMSO-d_6): δ = 2.27 (s, 3H, CH_3), 5.69 (s, 1H, 5-H) 6.82 (AA'XX', J = 8.6 Hz, 2H, C_6H_4OH), 6.98 (AA'XX', J = 8.8 Hz, 2H, C_6H_4OH) ppm; ^{13}C NMR (125 MHz, DMSO-d_6): δ = 21.0 (CH_3), 89.1 (C3), 92.5 (C5), 115.7 (C3', C5'), 117.8 (C≡N), 126.4 (C1'), 129.5 (C2', C6'), 157.6 (C4'), 159.5 (C4,), 161.3 (C2) 161.4 (C6) ppm.

HRMS: *m/z* (MH^-) calcd for $C_{13}H_9N_2O_3$ 241.0612, found 241.0618; IR (KBr): $\bar{\nu}$ = 543, 633, 768, 830, 1030, 1127, 1168, 1281, 1407, 1442, 1511, 1528, 1665 (C=O), 2220 (C≡N), 2513,

2612, 3060, 3519 (O-H) cm^{-1}; UV-Vis (ethanol, $c = 5.10^{-5}$ mol dm^{-3}): λ_{max} (ε) = 331 (23080) nm (mol^{-1} dm^3 cm^{-1}); Elemental Analysis:

Calculated: %C 64.46, %H 4.16, %N 11.56, %O 19.82

Found: %C 64.52, %H 4.07, %N 11.50, %O 19.91

6-hydroxy-4-methyl-2-oxo-1-(4-iodophenyl)-1,2-dihydropyridine-3-carbonitriles (**7a**, $C_{13}H_9IN_2O_2$) and 2-*hydroxy-4-methyl-6-oxo-1-(4-iodophenyl)-1,6-dihydro pyridine-3-carbonitriles* (**7b**, $C_{13}H_9IN_2O_2$)

Grayish crystalline solid; yield 57%, m.p.: 288-289ºC;

7a) ^{1}H NMR (500 MHz, DMSO-d_6): δ = 2.27 (s, 3H, CH_3), 5.66 (s, 1H, 5-H), 7.05 (AA'XX', J = 10 Hz, 2H, C_6H_4I), 7.82 (AA'XX', J = 10 Hz, 2H, C_6H_4I), 8.65 (bs, 1H, OH) ppm; ^{13}C NMR (125 MHz, DMSO-d_6): δ = 20.8 (CH_3), 88.0 (C3), 92.8 (C5), 94.6 (C4'), 117.5 (C≡N), 130.8 (C2', C6'), 135.3 (C1'), 137.8 (C3', C5'), 159.2 (C4), 160.6 (C2), 160.8 (C6) ppm.

7b) ^{1}H NMR (500 MHz, DMSO-d_6): δ = 1.91 (s, 3H, CH_3), 6.08 (s, 1H, 5-H), 7.11 (AA'XX', J = 10 Hz, 2H, C_6H_4I), 7.87 (AA'XX', J = 10 Hz, 2H, C_6H_4I), 8.65 (bs, 1H, OH) ppm; ^{13}C NMR (125 MHz, DMSO-d_6): δ = 21.7 (CH_3), 83.4 (C3), 99.0 (C5), 95.4 (C4'), 115.1 (C≡N), 130.7 (C2', C6'), 137.3 (C1'), 138.3 (C3', C5'), 152.5 (C4), 162.1 (C6), 171.8 (C2) ppm.

HRMS: *m/z* (MH^+) calcd for $C_{13}H_{10}IN_2O_2$ 352.9806, found 352.9782; IR (KBr): $\bar{\nu}$ = 512, 590, 637, 760, 811, 1009, 1231, 1269, 1416, 1524, 1665 (C=O), 2480, 2223 (C≡N), 2664, 3091, 3426 (O-H) cm^{-1}; UV-Vis (ethanol, $c = 5.10^{-5}$ mol dm^{-3}): λ_{max} (ε) = 328 (6720) nm (mol^{-1} dm^3 cm^{-1}); Elemental Analysis:

Calculated: %C 44.34, %H 2.58, %N 7.96, %O 9.09, %I 36.04

Found: %C 44.43, %H 2.62, %N 7.85, %O 9.00, %I 36.10

6-hydroxy-4-methyl-2-oxo-1-(4-chlorophenyl)-1,2-dihydropyridine-3-carbonitriles (**8a**, $C_{13}H_9ClN_2O_2$) and *2-hydroxy-4-methyl-6-oxo-1-(4-chlorophenyl)-1,6-dihydropyridine-3-carbonitriles* (**8a**, $C_{13}H_9ClN_2O_2$)

White crystalline solid; yield 64%, m.p.: 285-287ºC;

8a) ^{1}H NMR (500 MHz, DMSO-d_6): δ = 2.27 (s, 3H, CH_3), 5.66 (s, 1H, 5-H), 7.28 (AA'XX', J = 8.6 Hz, 2H, C_6H_4Cl), 7.53 (AA'XX', J = 8.6 Hz, 2H, C_6H_4Cl) ppm; ^{13}C NMR (125 MHz, DMSO-d_6): δ = 21.0 (CH_3), 88.2 (C3), 93.1 (C5), 117.9 (C≡N), 129.3 (C3', C5'), 130.7 (C2', C6'), 133.2 (C4'), 134.7 (C1'), 159.5 (C4), 161.0 (C2), 161.2 (C6) ppm.

8b) ^{1}H NMR (500 MHz, DMSO-d_6): δ = 1.92 (s, 3H, CH_3), 6.10 (s, 1H, 5-H), 7.36 (AA'XX', J = 8.8 Hz, 2H, C_6H_4Cl), 7.55 (AA'XX', J = 8.4 Hz, 2H, C_6H_4Cl) ppm; ^{13}C NMR (125 MHz, DMSO-d_6): δ = 21.9 (CH_3), 83.5 (C3), 99.3 (C5), 115.4 (C≡N), 129.8 (C3', C5'), 130.7 (C2', C6'), 133.8 (C4'), 136.6 (C1'), 152.9 (C4), 162.5 (C6), 172.1 (C2) ppm.

HRMS: *m/z* (MH^+) calcd for $C_{13}H_{10}ClN_2O_2$ 261.0450, found 261.0425; IR (KBr): $\bar{\nu}$ = 515, 638, 738, 817, 1021, 1094, 1232, 1312, 1416, 1492, 1536, 1665 (C=O), 2218 (C≡N), 2507, 2612, 2928, 3074, 3428 (O-H) cm^{-1}; UV-Vis (ethanol, c = 5.10^{-5} mol dm^{-3}): λ_{max} (ε) = 328 (24040) nm (mol^{-1} dm^3 cm^{-1}); Elemental Analysis:

Calculated: %C 59.90, %H 3.48, %N 10.75, %O 12.28, %Cl 13.60

Found: %C 59.97, %H 3.41, %N 10.64, %O 12.32, %Cl 13.66

6-hydroxy-4-methyl-2-oxo-1-(4-bromophenyl)-1,2-dihydropyridine-3-carbonitriles (**9a**, $C_{13}H_9BrN_2O_2$) and *2-hydroxy-4-methyl-6-oxo-1-(4-bromophenyl)-1,6-dihydro pyridine-3-carbonitriles* (**9b**, $C_{13}H_9BrN_2O_2$)

White crystalline solid; yield 64%, m.p.: 276-278ºC;

9a) ^{1}H NMR (500 MHz, DMSO-d_6): δ = 2.26 (s, 3H, CH_3), 5.66 (s, 1H, 5-H), 7.24 (AA'XX', J = 8.4 Hz, 2H, C_6H_4Br), 7.66 (AA'XX', J = 8.4 Hz, 2H, C_6H_4Br), 12.80 (bs, 1H, OH) ppm; ^{13}C NMR (125 MHz DMSO-d_6): δ = 21.0 (CH_3), 88.0 (C3), 93.1 (C5), 117.9 (C≡N), 122.4 (C4'), 131.1 (C3', C5'), 132.7 (C2', C6'), 135.2 (C1'), 159.4 (C4), 160.9 (C2), 162.4 (C6) ppm.

9b) ^{1}H NMR (500 MHz, DMSO-d_6): δ = 1.92 (s, 3H, CH_3), 6.09 (s, 1H, 5-H), 7.28 (AA'XX', J = 8.4 Hz, 2H, C_6H_4Br), 7.72 (AA'XX', J = 8.6 Hz, 2H, C_6H_4Br), 12.80 (bs, 1H, OH) ppm; ^{13}C NMR (125 MHz DMSO-d_6): δ = 21.9 (CH_3), 83.6 (C3), 99.3 (C5), 115.4 (C≡N), 121.7 (C4'), 131.1 (C3', C5'), 132.2 (C2', C6'), 137.1 (C1'), 152.9 (C4), 161.2 (C6), 172.1 (C2) ppm.

HRMS: *m/z* (MH^+) calcd for $C_{13}H_{10}BrN_2O_2$ 302.9750, found 302.9762; IR (KBr): $\bar{\nu}$ = 513, 596, 633, 770, 812, 1017, 1133, 1246, 1416, 1488, 1545, 1663 (C=O), 2219 (C≡N), 2616, 3419 (O-H) cm^{-1}; UV-Vis (ethanol, c = 5.10^{-5} mol dm^{-3}): λ_{max} (ε) = 323 (15360) nm (mol^{-1} dm^3 cm^{-1}); Elemental Analysis:

Calculated: %C 51.17, %H 2.97, %N 9.18, %O 10.49, %Br 26.19

Found: %C 51.11, %H 2.94, %N 9.24, %O 10.59, %Br 26.12

6-hydroxy-4-methyl-2-oxo-1-(4-fluorophenyl)-1,2-dihydropyridine-3-carbonitriles (**10a**, $C_{13}H_9FN_2O_2$) and *2-hydroxy-4-methyl-6-oxo-1-(4-fluorophenyl)-1,6-dihydropyridine-3-carbonitriles* (**10b**, $C_{13}H_9FN_2O_2$)

White-brownish crystalline solid; yield 74%, m.p.: 284-285ºC;

10a) ^{1}H NMR (500 MHz, DMSO-d_6): δ = 2.27 (s, 3H, CH_3), 5.67 (1H, s, 5-H), 7.29 (t, J = 5 Hz, 4H, C_6H_4F), 12.7 (bs, 1H, OH) ppm; ^{13}C NMR (125 MHz DMSO-d_6): δ = 20.8 (CH_3), 87.8 (C3), 92.8 (C5), 115.7 (C3') 116.2 (C5'), 117.6 (C≡N), 130.7 (C6'), 131.6 (C2'), 133.6 (C1'), 159.1 (C4), 160.6 (C2), 161.1 (C6), 162.8 (C4') ppm.

10b) ^{1}H NMR (500 MHz, DMSO-d_6): δ = 1.92 (s, 3H, CH_3), 6.09 (s, 1H, 5-H), 7.35 (t, J = 5 Hz, 4H, C_6H_4F), 12.7 (bs, 1H, OH) ppm; ^{13}C NMR (125 MHz, DMSO-d_6): δ = 21.7 (CH_3), 83.4 (C3), 99.0 (C5), 115.0 (C≡N), 115.9 (C3') 116.4 (C5'), 130.5 (C2'), 130.6 (C6'), 133.7 (C1'), 152.9 (C4), 160.8 (C6), 162.3 (C4'), 171.7 (C2) ppm.

HRMS: *m/z* (MH^+) calcd. for $C_{13}H_{10}FN_2O_2$ 245.0746, found 245.0721; IR (KBr): $\bar{\nu}$ = 537, 643, 655, 797, 832, 1132, 1156, 1224, 1380, 1408, 1509, 1572, 1637, 1663 (C=O), 1637, 2221 (C≡N), 3434 (O-H) cm^{-1}; UV-Vis (ethanol, c = 5.10^{-5} mol dm^{-3}): λ_{max} (ε) = 321 (17980) nm (mol^{-1} dm^3 cm^{-1}); Elemental Analysis:

Calculated: %C 63.93, %H 3.71, %N 11.47, %O 13.10, %F 7.78

Found: %C 63.89, %H 3.75, %N 11.40, %O 13.14, %F 7.82

6-hydroxy-4-methyl-2-oxo-1-(3-(tifluoromethyl)phenyl)-1,2-dihydropyridine-3-carbonitriles

(**11b**, $C_{14}H_9F_3N_2O_2$)

Grayish crystalline solid; yield 66%, m.p.: 315-317ºC;

11b) ^{1}H NMR (500 MHz, DMSO-d_6): δ = 1.92 (s, 3H, CH_3), 6.18 (s, 1H, 5-H**)**, 7.67 (d, J=7.6 Hz, 6'-H), 7.76 (d, J=7.4 Hz, 4'-H), 7.82-7.89 (m, 2H, 2'-H, 5'-H), 12.81 (bs, 1H, OH) ppm; ^{13}C NMR (125 MHz, DMSO-d_6): δ = 21.9 (CH_3), 83.6 (C3), 99.5 (C5), 115.3 (C≡N), 126.1 (C4'), 126.7 (CF_3), 130.2 (C2'), 130.8 (C5'), 131.0 (C6'), 133.3 (C3'), 138.5 (C1'), 152.7 (C4), 162.5 (C6), 172.3 (C2) ppm.

HRMS: *m/z* (MH^-) calcd for $C_{14}H_8F_3N_2O_2$ 293.0519, found 293.0543; IR (KBr): $\bar{\nu}$ = 570, 626, 657, 706, 807, 1071, 1133, 1249, 1330, 1405, 1461, 1570, 1645 (C=O), 2229 (C≡N), 2610, 2851, 3077, 3431 (O-H) cm^{-1}; UV-Vis (ethanol, c = 5.10^{-5} mol dm^{-3}): λ_{max} (ε) = 303 (7940) nm (mol^{-1} dm^3 cm^{-1}); Elemental Analysis:

Calculated: %C 57.15, %H 3.08, %N 9.52, %O 10.88, %F 19.37

Found: %C 57.18, %H 3.02, %N 9.48, %O 10.91, %F 19.41

6-hydroxy-4-methyl-2-oxo-1-(3-chlorophenyl)-1,2-dihydropyridine-3-carbonitriles (**12a**, $C_{13}H_9ClN_2O_2$) and *2-hydroxy-4-methyl-6-oxo-1-(3-chlorophenyl)-1,6-dihydropyridine-3-carbonitriles* (**12b**, $C_{13}H_9ClN_2O_2$)

Grayish crystalline solid; yield 59%, m.p.: 275-278ºC;

12a) ^{1}H NMR (500 MHz, DMSO-d_6): δ = 2.28 (s, 3H, CH_3), 5.67 (s, 1H, 5-H), 7.21-7.26 (m, 1H, 6'-H), 7.42 (t, *J*=2.2 Hz, 1H, 4'-H), 7.50-7.54 (m, 1H, 2'-H), 7.55 (d, *J*=1.2 Hz, 1H, 5'-H), 12.90 (bs, 1H, OH) ppm; ^{13}C NMR (125 MHz DMSO-d_6): δ = 21.0 (CH_3), 88.6 (C3), 93.2 (C5), 117.9 (C≡N), 127.7 (C6'), 128.7 (C4'), 130.7 (C5'),130.8 (C2'), 133.3 (C3'), 137.2 (C1'), 159.42 (C4), 161.3 (C2), 162.4 (C6) ppm.

12b) ^{1}H NMR (500 MHz, DMSO-d_6): δ = 1.94 (s, 3H, CH_3), 6.10 (s, 1H, 5-H), 7.28-7.34 (m, 1H, 6'-H), 7.49 (t, *J*=2.2 Hz, 1H, 4'-H), 7.50-7.54 (m, 1H, 2'-H), 7.57 (d, *J*=1.2 Hz, 1H, 5'-H), 12.90 (bs, 1H, OH) ppm; ^{13}C NMR (125 MHz, DMSO-d_6): δ = 21.8 (CH_3), 83.6 (C3), 99.3 (C5), 115.3 (C≡N), 127.8 (C6'), 129.0 (C4'), 129.4 (C2'), 131.3 (C5'), 133.9 (C3'), 139.1 (C1'), 152.81 (C4), 161.0 (C6), 172.1 (C2) ppm.

HRMS: *m/z* (MH^-) calcd for $C_{13}H_8ClN_2O_2$ 259.0255, found 259.0279; IR (KBr): $\bar{\nu}$ = 581, 627, 690, 745, 789, 818, 1078, 1134, 1297, 1379, 1406, 1489, 1546, 1662 (C=O), 2219 (C≡N), 2594, 3073, 3445 (O-H) cm^{-1}; UV-Vis (ethanol, $c = 5.10^{-5}$ mol dm^{-3}): λ_{max} (ε) = 323 (12080) nm (mol^{-1} dm^3 cm^{-1});

Elemental Analysis:

Calculated: %C 59.90, %H 3.48, %N 10.75, %O 12.28, %Cl 13.60

Found: %C 59.85, %H 3.53, %N 10.65, %O 12.32, %Cl 13.65

6-hydroxy-4-methyl-2-oxo-1-(3-bromophenyl)-1,2-dihydropyridine-3-carbonitriles (**13a**, $C_{13}H_9BrN_2O_2$) and *2-hydroxy-4-methyl-6-oxo-1-(3-bromophenyl)-1,6-dihydropyridine-3-carbonitriles* (**13b**, $C_{13}H_9BrN_2O_2$)

Grayish crystalline solid; yield 52%, m.p.: 278-280ºC;

13a) ^{1}H NMR (500 MHz, DMSO-d_6): δ = 2.26 (s, 3H, CH_3), 5.65 (s, 1H, 5-H), 7.35 (d, *J*=7.8 Hz, 1H, 6'-H), 7.46-7.51(m, 1H, 4'-H), 7.61-7.72 (m, 2H, 2'-H, 5'-H), 12.88 (bs, 1H, OH) ppm; ^{13}C NMR (125 MHz DMSO-d_6): δ = 21.0 (CH_3), 87.6 (C3), 93.3 (C5), 117.9 (C≡N), 121.5 (C2'), 128.2 (C6'), 128.3 (C4'), 131.5 (C5'), 131.7 (C3'), 137.4 (C1'), 159.2 (C4), 161.1 (C2), 162.5 (C6) ppm.

13b) ^{1}H NMR (500 MHz, DMSO-d_6): δ = 1.93 (s, 3H, CH_3), 6.10 (s, 1H, 5-H), 7.27 (d, J=6.8 Hz, 1H, 6'-H), 7.40-7.45 (m, 1H, 4'-H), 7.52-7.60 (m, 2H, 2'-H, 5'-H), 12.88 (bs, 1H, OH). ^{13}C NMR (125 MHz DMSO-d_6): δ = 21.8 (CH_3), 83.5 (C3), 99.3 (C5), 115.30 (C≡N), 122.04 (C2'), 128.1 (C6'), 128.6 (C4'), 131.0 (C5'), 132.2 (C3'), 139.2 (C1'), 152.8 (C4), 161.3 (C6), 172.1 (C2) ppm.

HRMS: *m/z* (MH^-) calcd for $C_{13}H_8BrN_2O_2$ 302.9750, found 302.9775; IR (KBr): $\bar{\nu}$ = 676, 685, 730, 770, 786, 825, 1036, 1070, 1134, 1229, 1246, 1311, 1408, 1474, 1545, 1660 (νC=O), 2219 (νC≡N), 2593, 2924 (νasCH$_3$), 3066, 3435 (νO-H) cm^{-1}; UV-Vis (ethanol, c = 5.10^{-5} mol dm^{-3}): λ_{max} (ε) = 323 (9480) nm (mol^{-1} dm^3 cm^{-1}); Elemental Analysis:

Calculated: %C 51.17, %H 2.97, %N 9.18, %O 10.49, %Br 26.19

Found: %C 51.22, %H 2.92, %N 9.09, %O 10.54, %Br 26.23

6-hydroxy-4-methyl-2-oxo-1-(3-methoxyphenyl)-1,2-dihydropyridine-3-carbonitriles (**14a**, $C_{14}H_{12}N_2O_3$) and *2-hydroxy-4-methyl-6-oxo-1-(3-methoxy phenyl)-1,6-dihydropyridine-3-carbonitriles* (**14b**, $C_{14}H_{12}N_2O_3$)

Gray crystalline solid; yield 47%, m.p.: 250-252ºC;

14a) ^{1}H NMR (500 MHz, DMSO-d_6): δ = 2.29 (s, 3H, 4-CH_3), 3.75 (s, 3H, 3'-OCH_3), 5.70 (s, 1H, 5-H), 6.79 (dd, J = 0.75 Hz, J =7 Hz, 1H, 6'-H), 6.84 (t, J = 2.2 Hz, 1H, 2'-H), 7.00 (dd, J = 2 Hz, J = 6 Hz, 1H, 4'-H), 7.38 (t, J = 8.2 Hz, 1H, 5'-H), 12.70 (bs, 1H, OH) ppm; ^{13}C NMR (125 MHz, DMSO-d_6): δ = 20.8 (4-CH_3), 55.3 (3'-OCH_3), 88.9 (C3), 92.3 (C5), 114.1 (C2'), 114.2 (C4'), 117.4 (C≡N), 120.5 (C6'), 129.7 (C5'), 136.4 (C1'), 159.5 (C4), 159.8 (C3'), 160.8 (C2), 162.1 (C6) ppm.

14b) ^{1}H NMR (500 MHz, DMSO-d_6): δ = 1.94 (s, 3H, 4-CH_3), 3.77 (s, 3H, 3'-OCH_3), 6.08 (s, 1H, 5-H), 6.82 (d, J = 1 Hz, 1H, 6'-H), 6.90 (t, J = 2.2 Hz, 1H, 2'-H), 7.03 (dd, J = 2 Hz, J =6.5 Hz, 1H, 4'-H), 7.41 (t, J = 8.3 Hz, 1H, 5'-H), 12.70 (bs, 1H, OH) ppm; ^{13}C NMR (125 MHz, DMSO-d_6): δ = 21.5 (4-CH_3), 55.4 (C3'-OCH_3), 83.4 (C3), 98.8 (C5), 114.1 (C2'), 114.7 (C4'), 115.2 (C≡N), 120.4 (C6'), 130.2 (C5'), 138.6 (C1'), 152.9 (C4), 160.1 (C3'), 160.6 (C6), 171.7 (C2) ppm.

HRMS: *m/z* (MH^-) calcd for $C_{14}H_{11}N_2O_3$ 255.0751, found 255.0775; IR (KBr): $\bar{\nu}$ = 513, 636, 701, 768, 821, 1050, 1120, 1289, 1412, 1491, 1539, 1609, 1663 (C=O), 2218 (C≡N), 3072, 3436 (O-H) cm^{-1}; UV-Vis (ethanol, c = 5.10^{-5} mol dm^{-3}): λ_{max} (ε) = 316 (10580) nm (mol^{-1} dm^3 cm^{-1}); Elemental Analysis:

Calculated: %C 65.62, %H 4.72, %N 10.93, %O 18.73

Found: %C 65.58, %H 4.69, %N 10.97, %O 18.76

6-hydroxy-4-methyl-2-oxo-1-(3-methylphenyl)-1,2-dihydropyridine-3-carbonitriles (**15a**, $C_{14}H_{12}N_2O_2$) and *2-hydroxy-4-methyl-6-oxo-1-(3-methylphenyl)-1,6-dihydro- pyridine-3-carbonitriles* (**15b**, $C_{14}H_{12}N_2O_2$)

Grayish crystalline solid; yield 54%, m.p.: 284-285ºC (Ref. [196] 278-281ºC);

15a) ^{1}H NMR (500 MHz, DMSO-d_6): δ = 2.28 (s, 3H, 4-CH_3), 2.33 (s, 3H, 3'-CH_3), 5.69 (s, 1H, 5-H), 6.99-7.02 (m, 2H, 2'-H, 4'-H), 7.22 (d, J = 8 Hz, 1H, 6'-H,), 7.35 (t, J = 7.8 Hz, 1H, 5'-H), 12.70 (bs, 1H, OH) ppm; ^{13}C NMR (125 MHz, DMSO-d_6): δ = 20.7 (3'-CH_3), 20.8 (4-CH_3), 88.5 (C3), 92.5 (C5), 117 (C≡N), 125.4 (C4'), 128.8 (C2'), 129.0 (C5'), 129.2 (C6'), 135.3 (C1'), 138.4 (C3'), 159.2 (C4), 160.7 (C2), 162.2 (C6) ppm.

15b) ^{1}H NMR (500 MHz, DMSO-d_6): δ = 1.91 (s, 3H, 4-CH_3), 2.34 (s, 3H, 3'-CH_3), 6.08 (s, 1H, 5-H), 7.04-7.08 (m, 2H, 2'-H, 4'-H), 7.28 (d, J = 8 Hz, 1H, 6'-H), 7.39 (t, J = 7.8 Hz, 1H, 5'-H), 12.70 (bs, 1H, OH) ppm; ^{13}C NMR (125 MHz, DMSO-d_6): δ = 20.7 (3'-CH_3), 21.7 (4-CH_3), 83.4 (C3), 98.8 (C5), 115 (C≡N), 125.3 (C4'), 128.7 (C2'), 129.2 (C5'), 129.5 (C6'), 137.4 (C1'), 139.1(C3'), 152.8 (C4), 160.9 (C6), 171.6 (C2) ppm.

HRMS: *m/z* (MH^-) calcd for $C_{14}H_{11}N_2O_2$ 239.0801, found 239.0826; IR (KBr): $\bar{\nu}$ = 581, 626, 703, 769, 832, 879, 1046, 1132, 1245, 1337, 1379, 1407, 1458, 1552, 1648 (C=O), 2223 (C≡N), 2608, 2861, 2928, 3084, 3433 (O-H) cm^{-1}; UV-Vis (ethanol, c = 5.10^{-5} mol dm^{-3}): λ_{max} (ε) = 300 (2980) nm (mol^{-1} dm^3 cm^{-1}); Elemental Analysis:

Calculated: %C 69.99, %H 5.03, %N 11.66, %O 13.32

Found: %C 69.85, %H 5.12, %N 11.73, %O 13.30

6-hydroxy-4-methyl-2-oxo-1-(3-acetylphenyl)-1,2-dihydropyridine-3-carbonitriles (**16a**, $C_{15}H_{12}N_2O_3$) and *2-hydroxy-4-methyl-6-oxo-1-(3-acetylphenyl)-1,6-dihydropyridine-3-carbonitriles* (**16b**, $C_{15}H_{12}N_2O_3$)

Gray crystalline solid; yield 52%, m.p.: 243-245ºC;

16a) ^{1}H NMR (500 MHz, DMSO-d_6): δ = 2.29 (s, 3H, CH_3), 2.61 (s, 3H, C(O)CH_3), 5.70 (s, 1H, 5-H), 7.53 (d, J=8 Hz, 1H, 6'-H), 7.64-7.62 (m, 1H, 2'-H), 7.89 (t, J = 2 Hz, 4'-H), 8.03 (t, J = 7.7 Hz, 5'-H) ppm; ^{13}C NMR (125 MHz, DMSO-d_6): δ = 21.1 (CH_3), 27.1 (C(O)CH_3), 88.2 (C3), 93.2 (C5**),** 117.9 (C≡N), 128.4 (C2'), 128.8 (C4'), 130.2 (C6'), 133.5 (C5'), 136.29 (C1'), 138.4 (C3'), 159.6 (C4), 161.1 (C2), 162.6 (C6), 197.5 (C(O)CH_3) ppm.

16b) ^{1}H NMR (500 MHz, DMSO-d_6): δ = 1.93 (s, 3H, CH_3), 2.59 (s, 3H, C(O)CH_3), 6.13 (s, 1H, 5-H), 7.58 (d, J = 8 Hz, 1H, 6'-H), 7.64-7.62 (m, 1H, 2'-H), 7.82 (t, J=2 Hz, 4'-H), 8.03 (t, J = 7.7 Hz, 5'-H) ppm; ^{13}C NMR (125 MHz, DMSO-d_6): δ = 22.0 (CH_3), 27.0 (C(O)CH_3), 83.7 (C3), 99.4 (C5), 115.4 (C≡N), 128.5 (C2'), 128.6 (C4'), 129.7 (C6'), 133.7 (C5'), 138.02 (C1'), 138.2 (C3'), 153.0 (C4), 161.4 (C6), 172.2 (C2), 197.5 (C(O)CH_3) ppm.

HRMS: *m/z* (M+CH_3COO –H_2O–H^-) calcd for $C_{17}H_{11}N_2O_4$ 267.0751, found 267.0775; IR (KBr): $\bar{\nu}$ = 589, 635, 698, 757, 820, 1037, 1133, 1239, 1281, 1412, 1557, 1662 (C=O) , 2216 (C≡N), 2356, 2598, 3446 (O-H), 3537 cm^{-1}; UV-Vis (ethanol, c = 5.10^{-5} mol dm^{-3}): λ_{max} (ε) = 324 (10380) nm (mol^{-1} dm^3 cm^{-1}); Elemental Analysis:

Calculated: %C 67.16, %H 4.51, %N 10.44, %O 17.89

Found: %C 67.11, %H 4.55, %N 10.41, %O 17.93

Synthesis of (Z)-4-methyl-5-[2-(4-nitrophenyl)hydrazono)]-2,6-dioxo-1-phenyl-1,2,5,6-tetrahydro-3-carbonitriles

The azo dye was synthesized by the diazotization of pyridone **1** by using 4-nitrophenyldiazonium chloride [197]. The obtained material was filtrated, washed with distilled water, and recrystalled from methanol and finally purified by flash chromatography.

(Z)-4-methyl-5-[2-(4-nitrophenyl)hydrazono]-2,6-dioxo-1-phenyl-1,2,5,6-tetrahydro-3-carbonitriles (**17**, $C_{19}H_{13}N_5O_4$)

Red dark powder; yield 64%, m.p.: >300ºC;

^{1}H NMR (500 MHz, DMSO-d_6): δ = 2.63 (s, 3H, 4-CH_3), 7.32-7.34 (m, 2H, 5'-H, 3'-H), 7.46-7.49 (m, 1H, 4'-H), 7.51-7.54 (m, 2H, 2'-H, 6'-H), 7.91 (AA'XX', J = 9.0 Hz, 2H, C_6H_4- NO_2), 8.30 (AA'XX', J = 9.5 Hz, 2H, C_6H_4- NO_2), 14.26 (s, 1H, OH) ppm; ^{13}C NMR (125 MHz, DMSO-d_6): δ = 16.6 (CH_3), 103.4 (C5), 114.7 (C3), 117.6 (C≡N), 125.5 (C_6H_4-NO_2), 125.9 (C4'), 128.8 (C_6H_4-NO_2), 128.8 (C3', C5'), 129.0 (C2', C6'), 133.8 (C1'), 144.4 (C_6H_4-NO_2), 146.5 (C_6H_4-NO_2), 159.6 (C2), 159.9 (C4), 160.2 (C6) ppm. IR (KBr): $\bar{\nu}$ = 586, 632, 689, 700, 739, 749, 771, 796, 847, 872, 952, 1110, 1152, 1167, 1214, 1260, 1339, 1407, 1423, 1507, 1644, 1697 (C=O) , 2221 (C≡N), 2852, 2923, 3082, 3116, 3444 (O-H) cm^{-1}; UV-Vis (ethanol, c = 5.10^{-5} mol dm^{-3}): λ_{max} (ε) = 430 (24560) nm (mol^{-1} dm^3 cm^{-1});

Elemental Analysis:

Calculated: %C 60.80, %H 3.49, %N 18.66, %O 17.05

Found: %C 60.76, %H 3.42, %N 18.71, %O 17.11

3.5 Characteristics of 5-arylazo-6(2)-hydroxy-4-methyl-3-cyano-*N*(1)-phenyl-2(6)-oxo-pyridine-3-carbonitrile dyes

(Z)-4-methyl-5-[2-phenylhydrazono]-2,6-dioxo-1-phenyl-1,2,5,6-tetrahydro-3-carbonitriles (**1**, $C_{19}H_{14}N_4O_2$).

Yellow-orange powder; yield 78%, m.p.: 271-3ºC;

^{1}H NMR (500 MHz, DMSO-d_6): δ = 2.62 (s, 3H, 4-CH_3), 7.28-7.33 (m, 3H, 3'-H, 5'-H, 4"-H), 7.44-7.53 (m, 5H, 2'-H, 4'-H, 6'-H, 3"-H, 5"-H), 7.70-7.72 (m, 2H, 2"-H, 6"-H), 14.47 (s, 1H, N-H) ppm; ^{13}C NMR (125 MHz, DMSO-d_6): δ = 16.5 (CH_3), 100.8 (C5), 115.1 (C≡N), 117.45 (4-C_6H_5), 123.4 (C3), 127.0 (C4"), 128.6 (C4'), 128.8 (4-C_6H_5), 128.8 (C5', C3') 129.8 (C2', C6'), 134.1 (C1'), 141.2 (C1"), 159.8 (C2), 160.2 (C4), 160.6 (C6) ppm. IR (KBr): $\bar{\nu}$ = 685, 693, 773, 761, 773, 824, 863, 907, 953, 1002, 1071, 1153, 1172, 1214, 1279, 1311, 1332, 1399, 1435, 1461, 1491, 1505, 1572, 1590, 1632, 1682 (C=O) , 2226 (C≡N), 2505, 2952, 3444 (O-H) cm^{-1}; UV-Vis (ethanol, $c = 5.10^{-5}$ mol, dm^{-3}): λ_{max} (ε) = 430 (24560) nm (mol^{-1} dm^3 cm^{-1});

Elemental Analysis:

Calculated: %C 60.08, %H 4.27, %N 16.96, %O 9.69

Found: %C 60.07, %H 4.28, %N 16.94, %O 9.70

(Z)-4-methyl-5-[2-(4-methylphenyl)hydrazono]-2,6-dioxo-1-phenyl-1,2,5,6-tetrahydro-3-carbonitriles (**2**, $C_{20}H_{16}N_4O_2$)

Brownish powder; yield 63%, m.p.: 229-31ºC;

^{1}H NMR (500 MHz, DMSO-d_6): δ = 2.32 (s, 3H, 4-CH_3), 2.60 (s, 3H, 4"- CH_3), 6.92-6.96 (m, 2H, 2"-H, 6"-H), 7.15-7.32 (m, 3H, 4'-H, 3"-H, 5"-H), 7.54-7.62 (m, 4H, 2'-H, 3'-H, 5'-H, 6'-H), 14.53 (s, 1H, N-H) ppm; ^{13}C NMR (125 MHz, DMSO-d_6): δ = 16.6 (CH_3), 20.8 (4"-CH_3), 100.4 (C5), 115.4 (C≡N), 117.6 (4-CH_3-C_6H_4), 123.1 (C3), 128.6 (C4'), 128.8 (C3', C5'), 129.2 (4-CH_3-C_6H_4), 129.6 (C2', C6'), 130.2 (C4"), 134.3 (C1'), 139.1 (C1"), 159.9 (C2), 160.4 (C4), 160.8 (C6) ppm. IR (KBr): $\bar{\nu}$ = 455, 509, 669, 692, 767, 809, 832, 954, 1072, 1215, 1291, 1335, 1491, 1515, 1578 1662, 1683 (C=O) , 2223 (C≡N), 2894, 2928, 3447 (O-H) cm^{-1}; UV-Vis (ethanol, $c = 5.10^{-5}$ mol dm^{-3}): λ_{max} (ε) = 430 (24560) nm (mol^{-1} dm^3 cm^{-1});

Elemental Analysis:

Calculated: %C 69.76, %H 4.68, %N 16.27, %O 9.29

Found: %C 69.74, %H 4.66, %N 16.25, %O 9.26

(Z)-4-methyl-5-[2-(4-methoxyphenyl)hydrazono]-2,6-dioxo-1-phenyl-1,2,5,6-tetrahydro-3-carbonitriles (**3**, $C_{20}H_{16}N_4O_3$)

Red powder; yield 66%, m.p.: 247-9ºC;

^{1}H NMR (500 MHz, DMSO-d_6): δ = 2.50 (s, 3H, 4-CH_3), 3.79 (s, 3H, 4”- OCH_3), 7.29-7.33 (m, 2H, 2’-H, 6’-H), 7.48-7.52 (m, 3H, 4’-H, 3’-H, 5’-H), 7.06 (AA’XX’, J = 8.8 Hz, 2H, C_6H_4-OCH_3), 7.69 (AA’XX’, J = 8.8 Hz, 2H, C_6H_4- OCH_3), 14.69 (s, 1H, N-H) ppm; ^{13}C NMR (125 MHz, DMSO-d_6): δ = 16.6 (CH_3), 55.7 (4”-OCH_3), 99.5 (C5), 115.3 (C≡N), 119.4 (4-OCH_3-C_6H_4), 122.6 (C3), 128.7 (C4’), 128.8 (4-OCH_3-C_6H_4), 129.0 (C3’, C5’), 129.1 (C2’, C6’), 134.4 (C1’), 134.8 (C1”) 139.1 (C4”), 158.9 (C2), 159.7 (C4), 160.8 (C6) ppm. IR (KBr): $\bar{\nu}$ = 417, 514, 570, 597, 637, 671, 702, 763, 832, 1009, 1090, 1211, 1278, 1397, 1418, 1508, 1585 1638, 1686 (C=O), 2222 (C≡N), 2924, 3446 (O-H) cm^{-1}; UV-Vis (ethanol, c = 5.10^{-5} mol dm^{-3}): λ_{max} (ε) = 430 (24560) nm (mol^{-1} dm^3 cm^{-1});

Elemental Analysis:

Calculated: %C 66.66, %H 4.48, %N 15.55, %O 13.32

Found: %C 66.67, %H 4.46, %N 15.56, %O 13.31

(Z)-4-methyl-5-[2-(4-nitrophenyl)hydrazono]-2,6-dioxo-1-phenyl-1,2,5,6-tetrahydro-3-carbonitriles (**4**, $C_{19}H_{13}N_5O_4$)

Red dark powder; yield 64%, m.p.: >300ºC;

^{1}H NMR (500 MHz, DMSO-d_6): δ = 2.63 (s, 3H, 4-CH_3), 7.32-7.34 (m, 2H, 5’-H, 3’-H), 7.46-7.49 (m, 1H, 4’-H), 7.51-7.54 (m, 2H, 2’-H, 6’-H), 7.91 (AA’XX’, J = 9.0 Hz, 2H, C_6H_4- NO_2), 8.30 (AA’XX’, J = 9.5 Hz, 2H, C_6H_4-NO_2), 14.26 (s, 1H, OH) ppm; ^{13}C NMR (125 MHz, DMSO-d_6): δ = 16.6 (CH_3), 103.4 (C5), 114.7 (C3), 117.6 (C≡N), 125.5 (4-NO_2-C_6H_4), 125.9 (C4’), 128.8 (4-NO_2-C_6H_4), 128.8 (C3’, C5’), 129.0 (C2’, C6’), 133.8 (C1’), 144.4 (C4”), 146.5 (C1”), 159.6 (C2), 159.9 (C4), 160.2 (C6) ppm. IR (KBr): $\bar{\nu}$ = 586, 632, 689, 700, 739, 749, 771, 796, 847, 872, 952, 1110, 1152, 1167, 1214, 1260, 1339, 1407, 1423, 1507, 1644, 1697 (C=O) , 2221 (C≡N), 2852, 2923, 3082, 3116, 3444 (O-H) cm^{-1}; UV-Vis (ethanol, c = 5.10^{-5} mol dm^{-3}): λ_{max} (ε) = 430 (24560) nm (mol^{-1} dm^3 cm^{-1});

Elemental Analysis:

Calculated: %C 60.80, %H 3.49, %N 18.66, %O 17.05

Found: %C 60.76, %H 3.42, %N 18.71, %O 17.11

(Z)-4-methyl-5-[2-(4-fluorophenyl)hydrazono]-2,6-dioxo-1-phenyl-1,2,5,6-tetrahydro-3-carbonitriles (**5**, $C_{19}H_{13}N_4O_2F$).

Yellow powder; yield 65%, m.p.: 265-8ºC;

^{1}H NMR (500 MHz, DMSO-d_6): δ = 2.61 (s, 3H, 4-CH_3), 7.30-7.35 (m, 4H, 2'-H, 3'-H,5'-H, 6'-H), 7.44-7.47 (m, 1H, 4'-H), 7.49-7.52 (m, 2H, 2"-H, 6"-H), 7.76-7.79 (3"-H, 5"-H), 14.5 (s, 1H, N-H) ppm; ^{13}C NMR (125 MHz, DMSO-d_6): δ = 16.5 (CH_3), 100.7 (C5), 115.1 (C≡N), 116.54 (4-F-C_6H_4), 116.72 (4-F-C_6H_4), 119.4 (4-F-C_6H_4), 119.6 (4-F-C_6H_4), 123.4 (C3), 128.5 (C4'), 128.8 (C3', C5'), 129.0 (C2', C6'), 134.1 (C1'), 137.9 (C4"), 159.6 (C1"), 159.7 (C2), 160.1(C4), 160.4(C6) ppm. IR (KBr): $\bar{\nu}$ = 512, 635, 670, 692, 736, 749, 770, 791, 837, 871, 954, 1033,1073,1100, 1152, 1206,1234, 1288, 1333,1398, 1425, 1447, 1508,1578, 1638, 1680 (C=O), 2221 (C≡N), 3075, 3448 (O-H) cm^{-1}; UV-Vis (ethanol, c = 5.10^{-5} mol dm^{-3}): λ_{max} (ε) = 430 (24560) nm (mol^{-1} dm^3 cm^{-1});

Elemental Analysis:

Calculated: %C 65.51, %H 3.76, %N 16.08, %O 9.19, %F 5.45.

Found: %C 65.49, %H 3.72, %N 16.05, %O 9.17, %F 5.42.

(Z)-4-methyl-5-[2-(4-bromophenyl)hydrazono]-2,6-dioxo-1-phenyl-1,2,5,6-tetrahydro-3-carbonitriles (**6**, $C_{19}H_{13}N_4O_2$ Br)

Red powder; yield 60%, m.p.: 275-7ºC;

^{1}H NMR (500 MHz, DMSO-d_6): δ = 2.61 (s, 3H, 4-CH_3), 7.27-7.33 (m, 3H, 4'-H, 2"-H, 6"-H), 7.46-7.53 (m, 4H, 2'-H, 6'-H, 5'-H, 3'-H), 7.647-7.693 (m, 2H, 3"-H, 5"-H) 14.35 (s, 1H, N-H) ppm; ^{13}C NMR (125 MHz, DMSO-d_6): δ = 16.4 (CH_3), 101.3 (C5), 114.9 (C≡N), 119.0 (4-Br-C_6H_4) 123.7 (C3), 128.1 (4-Br-C_6H_4), 128.5 (C4'), 128.6 (4-Br-C_6H_4), 128.8 (C3', C5'), 129.3 (C2', C6'), 132.3 (C1'), 140.4 (C1"), 152.3 (C4"), 159.4 (C2), 159.9 (C4), 160.4 (C6) ppm. IR (KBr): $\bar{\nu}$ = 506, 558, 691,667, 700, 755, 771, 796, 825, 831, 953, 1006, 1169, 1172, 1243, 1275, 1301, 1391, 1437, 1479, 1505, 1593,1638, 1689 (C=O), 2219 (C≡N), 2923, 3070, 3116, 3435 (O-H) cm^{-1}; UV-Vis (ethanol, c = 5.10^{-5} mol dm^{-3}): λ_{max} (ε) = 430 (24560) nm (mol^{-1} dm^3 cm^{-1});

Elemental Analysis:

Calculated: %C 5576, %H 3.20, %N 13.69, %O 7.82, %Br 19.53.

Found: %C 60.73, %H 3.18, %N 13.71, %O 7.81 , %Br 19.50

(Z)-4-methyl-5-[2-(4-iodophenyl)hydrazono]-2,6-dioxo-1-phenyl-1,2,5,6-tetrahydro-3-carbonitriles (**7**, $C_{19}H_{13}N_4O_2I$).

Red powder; yield 71%, m.p.: 273-5ºC;

^{1}H NMR (500 MHz, DMSO-d_6): δ = 1.89 (s, 3H, 4-CH_3), 7.29-7.33 (d, 2H, 2”-H, 6”-H), 7.48-7.52 (m, 5H, 2’-H, 3’-H, 4’-H, 5’-H, 6’-H), 7.31-7.79 (m, 2H, 2”-H, 6”-H), 14.29 (s, 1H, N-H) ppm; ^{13}C NMR (125 MHz, DMSO-d_6): δ = 16.7 (CH_3), 92.08 (C4”), 101.5 (C5), 115.2 (C≡N), 119.6 (4-I- C_6H_4), 124.0 (C3), 128.6 (C4’), 128.8 (4-I-C_6H_4), 129.0 (C2’, C6’), 129.21 (C3’, C5’), 138.5 (4-I-C_6H_4), 141.2 (C1’), 159.8 (C2), 160.7 (C4), 162.4 (C6) ppm. IR (KBr): $\bar{\nu}$ = 694, 771, 953, 1001, 1210, 1273, 1393, 1413, 1508, 1576 1638, 1690 (C=O), 2219 (C≡N), 3452 (O-H) cm^{-1}; UV-Vis (ethanol, c = 5.10^{-5} mol dm^{-3}): λ_{max} (ε) = 430 (24560) nm (mol^{-1} dm^3 cm^{-1});

Elemental Analysis:

Calculated: %C 50.05, %H 2.87, %N 12.28, %O 7.01, %I 27.82.

Found: %C 50.03, %H 2.85, %N 12.30, %O 7.02, %I 27.83.

(Z)-4-methyl-5-[2-(4-clorophenyl)hydrazono]-2,6-dioxo-1-phenyl-1,2,5,6-tetrahydro-3-carbonitriles (**8**, $C_{19}H_{13}N_4O_2Cl$).

Brownish powder; yield 69%, m.p.: 226-8ºC;

^{1}H NMR (500 MHz, DMSO-d_6): δ = 2.59 (s, 3H, 4-CH_3), 7.42-7.45 (m, H, 4’-H), 7.49-7.51 (m, 4H, 2’-H, 3’-H, 5’-H, 6’-H), 7.31 (AA’XX’, J = 7.0 Hz, 2H, C_6H_4- Cl), 7.72 (AA’XX’, J = 9.0 Hz, 2H, C_6H_4- Cl), 14.34 (s, 1H, N-H) ppm; ^{13}C NMR (125 MHz, DMSO-d_6): δ = 16.5 (CH_3), 101.2 (C5), 114.9 (C≡N), 119.0 (4-Cl-C_6H_4), 123.7 (C3), 128.9 (C4’), 128.4 (4-ClC_6H_4), 128.8 (C3’, C5’), 129.2 (4-Cl-C_6H_4) 129.4 (C2’, C6’), 129.6 (4-Cl-C_6H_4), 130.8 (C4”), 134.0 (C1’), 140.2 (C1”), 159.6 (C2), 160.0 (C4), 160.4 (C6) ppm. IR (KBr): $\bar{\nu}$ = 415, 506, 654, 691, 773, 830, 954, 1091, 1213, 1277, 1389, 1407, 1418, 1491, 1511, 1585, 1638, 1686 (C=O), 2220 (C≡N), 3441 (O-H) cm^{-1}; UV-Vis (ethanol, c = 5.10^{-5} mol dm^{-3}): λ_{max} (ε) = 430 (24560) nm (mol^{-1} dm^3 cm^{-1});

Elemental Analysis:

Calculated: %C 62.56, %H 3.59, %N 15.36, %O 9.77, %Cl 9.72.

Found: %C 62.54, %H 3.56, %N 15.34, %O 9.75 , %Cl 9.70.

(Z)-4-methyl-5-[2-(3-(tifluoromethyl)phenyl)hydrazono]-2,6-dioxo-1-phenyl-1,2,5,6-tetrahydro-3-carbonitriles (**9**, $C_{20}H_{13}N_4O_2$ F3).

Yellow-orange powder; yield 76%, m.p.: 259-61ºC;

^{1}H NMR (500 MHz, DMSO-d_6): δ = 2.63 (s, 3H, 4-CH_3), 7.26-7.33 (m, 2H, 2'-H, 6'-H), 7.45-7.53 (m, 3H, 3'-H, 4'-H, 5'-H), 7.61 (d, 1H, *J* = 7.5 , 6"-H), 7.70 (t, 1H, *J* = 16, 5"-H), 8.02 (d, 1H, *J* = 8.5, 4"-H), 8.08 (s, 1H, 2"-H), 14.37 (s, 1H, N-H) ppm; ^{13}C NMR (125 MHz, DMSO-d_6): δ = 16.6 (CH_3), 101.7 (C5), 114.9 (3-CF_3-C_6H_4), 116.4 (C≡N), 120.9 (3-CF_3-C_6H_4) 122.7 (3-CF_3-C_6H_4), 122.5 (C3), 124.2 (CF_3), 128.7 (C4'), 128.8 (C3', C5'), 128.9 (C2', C6'), 131.6 (3-CF_3-C_6H_4), 134.0 (C1'), 137.5 (3-CF_3-C_6H_4), 142.8 (C1"), 159.6 (C2), 160.1 (C4), 160.4 (C6) ppm. IR (KBr): $\bar{\nu}$ = 531, 685, 737, 778, 801, 838, 894, 954, 921, 955, 1002, 1033, 1097, 1123, 1156, 1223, 1278, 1329, 1405, 1465, 1489, 1509, 1581, 1640, 1693 (C=O) , 2221 (C≡N), 3067, 3448 (O-H) cm^{-1}; UV-Vis (ethanol, *c* = 5.10^{-5} mol dm^{-3}): λ_{max} (ε) = 430 (24560) nm (mol^{-1} dm^3 cm^{-1});

Elemental Analysis:

Calculated : %C 60.30, %H 3.29, %N 14.07, %O 8.03, %F 14.31.

Found: %C 60.31, %H 3.27, %N 14.08, %O 8.01 ,%F 14.29

(Z)-4-methyl-5-[2-(3-bromophenyl)hydrazono]-2,6-dioxo-1-phenyl-1,2,5,6-tetrahydro-3-carbonitriles (**10**, $C_{19}H_{13}N_4O_2Br$).

Orange powder; yield 66%, m.p.: 278-80ºC;

^{1}H NMR (500 MHz, DMSO-d_6): δ = 2.61 (s, 3H, 4-CH_3),), 7.31-7.32 (m, 1H, 2'-H, 5'-H), 7.39-7.47 (m, 3H, 3'-H, 4'-H, 5'-H), 7.50-7.53 (m, 2H , 2"-H, 5"-H), 7.70-7.72 (m, 1H, 6"-H), 7.922-7.929 (m, 1H, 4"-H), 14.29 (s, 1H, N-H) ppm ^{13}C NMR (125 MHz, DMSO-d_6): δ = 16.6 (CH_3), 101.7 (C5), 114.9 (3-Br-C_6H_4), 116.4 (C≡N), 119.85 (3-Br-C_6H_4) 122.5 (C3), 124.2 (C4"), 128.7 (C4'), 128.8 (C3', C5'), 128.9 (C2', C6'), 129.1 (3-Br-C_6H_4), 131.6 (3-Br-C_6H_4), 134.6 (C1'), 134.0 (3-Br-C_6H_4), 142.8 (C1") 159.6 (C2), 160.1 (C4), 160.4 (C6) ppm. IR (KBr): $\bar{\nu}$ = 677, 689, 743, 777, 835, 870, 895, 954, 993, 1034, 1065, 1095, 1155, 1208, 1276, 1303, 1330, 1404, 1426, 1511, 1578, 1638, 1689 (C=O) , 2222 (C≡N), 3073, 3451 (O-H) cm^{-1}; UV-Vis (ethanol, *c* = 5.10^{-5} mol dm^{-3}): λ_{max} (ε) = 430 (24560) nm (mol^{-1} dm^3 cm^{-1});

Elemental Analysis:

Calculated: %C 55.76, %H 3.20, %N 13.69, %O 7.82, %Br 19.53.

Found: %C 55.75, %H 3.22, %N 13.70, %O 7.80, %Br 19.52.

(Z)-4-methyl-5-[2-(3-clorophenyl)hydrazono]-2,6-dioxo-1-phenyl-1,2,5,6-tetrahydro-3-carbonitriles (**11**, $C_{19}H_{13}N_4O_2Cl$).

Brownish-red powder; yield 72%, m.p.: 235-7ºC;

^{1}H NMR (500 MHz, DMSO-d_6): δ = 2.60 (s, 3H, 4-CH_3),), 7.29-7.32 (m, 2H, 2'-H, 6'-H), 7.45-7.52(m, 3H, 3'-H, 4'-H, 5'-H), 7.63-7.66 (m, 1H, 6"-H), 7.84-7.87 (m, 1H, 5"-H), 8.00 (d, 1H, *J* = 7, 4"-H), 8.07 (s, 1H, 2"-H), 14.28 (s, 1H, N-H) ppm ^{13}C NMR (125 MHz, DMSO-d_6): δ = 16.6 (CH_3), 101.8 (C5), 114.9 (3-Cl- C_6H_4), 116.9 (C≡N), 117.0 (3-Cl- C_6H_4), 124.1 (C3), 126.2 (3-Cl-C_6H_4), 128.7 (3-Cl-C_6H_4), 128.8 (C3', C5'), 128.9 (C2', C6'), 131.3 (C1'), 133.9 (3-Cl- C_6H_4), 134.2 (3-Cl-C_6H_4), 142.7 (3-Cl-C_6H_4), 159.6 (C2), 160.0 (C4), 160.4 (C6) ppm. IR (KBr): $\bar{\nu}$ = 592, 632, 676, 691, 704, 745, 784, 836, 868, 955, 996, 1033, 1071, 1095, 1156, 1211, 1283, 1332, 1405, 1432, 1455 1509, 1581 1642, 1690 (C=O) , 2221 (C≡N), 2851, 2922, 3073, 3443 (O-H) cm^{-1}; UV-Vis (ethanol, c = 5.10^{-5} mol dm^{-3}): λ_{max} (ε) = 430 (24560) nm (mol^{-1} dm^3 cm^{-1});

Elemental Analysis:

Calculated: %C 62.56, %H 3.59, %N 15.36, %O 9.77, %Cl 9.72.

Found: %C 62.55, %H 3.57, %N 15.37, %O 9.79, %Cl 9.74.

3.6 Theoretical calculations

3.6.1 *Ab-initio* theoretical calculation method

The geometry optimizations were carried out by B3LYP method with standard basis set, 6-311G(d,p). Harmonic vibrational frequencies were evaluated at same level to confirm the nature of the stationary points found (to confirm that optimized geometry corresponds to local minimum that has only real frequencies), and to account for the zero point vibrational energy (ZPVE) correction. Global minima were found for every molecule considering pyridone tautomeric forms **a** and **b**, and rotational isomer of *meta*-substituted derivatives. Solvent (DMSO) was simulated with standard polarized continuum model (PCM). Theoretical calculation of chemical shifts on optimized geometries can provide good basis for estimation of experimental data. Quantum-chemical calculation of ^{1}H and ^{13}C NMR chemical shifts (method GIAO, WP04 functional and aug-cc-pVDZ basis set, and PCM for inclusion of solvation effect) were done. Tautomer electronic energies and atomic charges (ChelpG method) were calculated on B3LYP/6-311G(d,p) optimized geometries with B3LYP/6-311++G(3df,3pd) method. All calculations were done with Gaussian03 program package [198].

3.6.2 Molecular geometry optimization and theoretical absorption spectra calculation

The ground state geometries of compounds **1-9** were fully optimized with DFT method (more specifically the Becke three-parameter exchange functional (B3) and the Lee-Yang-Parr correlation functional (LYP)) with 6-311G(d,p) basis set without symmetry constrain, and with default tight convergence criteria. Global minima were found for each molecule. Harmonic vibrational frequencies have been evaluated at the same level to confirm the nature of the stationary points found (to confirm that optimized geometry corresponding to minimum that has only real frequencies), and to account for the zero point vibrational energy (ZPVE) correction. Solvents have been simulated with standard static isodensity surface polarized continuum model (IPCM). Theoretical absorption spectra of both tautomeric forms were calculated in gas phase, ethanol, tetrahydrofuran, acetonitrile and dimethylsulfoxide with TD-DFT method. The frontier molecular orbital energies: E_{HOMO} for highest occupied molecular orbital (HOMO) and E_{LUMO} for

lowest unoccupied molecular orbital (LUMO) and HOMO-LUMO energy gaps (E_{gap}) were also calculated with the same methods. All calculations were done with Gaussian03 software [28]. The Bader`s analysis were done on charge density grid with program "Bader" [199]. The ground state and excited state electron densities were calculated on ground state optimized geometries with B3LYP/6-311(d,p) method. Density difference maps were plotted as difference between electron densities of the excited state and the ground state, in program gOpenMol [200].

3.6.3 Regression Analysis

SCS were regressed on the $\rho(\sigma^0 + r^+\Delta\sigma_R^+)$ term varying r^+ value from 0.1 to 2.0 for 0.1 [neka ref iz rada, dodati]. Afterwards, the r^+ value which gave the best correlation was chosen to be expanded to two decimals by scanning the best one higher and lower by 0.01. This was repeated with a 0.01 increment until we reached the two decimal r^+ values which gave the best correlation coefficient. The Reynolds DSP model was obtained by regressing ^{13}C SCS on σ_I and σ_R constants [201].

The correlation analysis was carried out using Microsoft Excel software, considering 95% confidence level. The quality of correlations was evaluated by the correlation coefficient (*R*), standard error of the estimate (*Sd*), and Fisher's test of significance (*F*).

Table 3.6.1 Solvent parameters used in Kamlet–Taft equation [201]

Solvent	**π^***	**α**	**β**
Ethanol	0.54	0.83	0.77
Methanol	0.6	0.93	0.62
2-Propanol	0.48	0.76	0.95
1-Propanol	0.52	0.78	0.83
1-Butanol	0.47	0.79	0.88
2-Butanol	0.4	0.69	0.8
DMSO	1	0	0.76
THF	0.58	0	0.55
AcN	0.75	0.19	0.31
Acetone	0.71	0.08	0.48
Anisole	0.73	0	0.32
DMAc	0.88	0	0.76
DMF	0.88	0	0.69
NMF	0.90	0.62	0.80
EtAc	0.55	0	0.45
Chl	0.58	0.44	0
Dioxane	0.55	0	0.37
DCM	0.82	0.30	0
DEE	0.27	0	0.47

Table 3.6.2 Solvent parameters used in Catalán equation [videti koja je od vec navedenih]

Solvent	SP	SdP	SA	SB
Ethanol	0.633	0.783	0.4	0.658
Methanol	0.608	0.904	0.605	0.545
2-Propanol	0.633	0.808	0.283	0.83
1-Propanol	0.658	0.748	0.367	0.782
1-Butanol	0.674	0.655	0.341	0.809
2-Butanol	0.656	0.706	0.221	0.888
DMSO	0.83	1	0.072	0.647
THF	0.714	0.634	0	0.591
AcN	0.645	0.974	0.044	0.286
Acetone	0.651	0.907	0.000	0.475
Anisole	0.82	0.543	0.084	0.299
DMAc	0.763	0.987	0.028	0.65
DMF	0.759	0.977	0.031	0.613
EtAc	0.656	0.603	0	0.542
Chl	0.783	0.614	0.047	0.071
Dioxane	0.737	0.312	0	0.444
DCM	0.761	0.769	0.040	0.178
DEE	0.617	0.385	0	0.562

Table 3.6.3 Substituent constants σ, σ_I, σ_R^0 and σ_R for derivates of (6 or 2)-hydroxy-4-methyl-(2 or 6)-oxo-1-(substituted phenyl)-(1,2 or 1,6)-dihydropyridine-3-carbonitriles [videti koja je od vec navedenih]

Comp.	σ	σ_I	σ_R^0	σ_R	Comp.	σ	σ_I	σ_R^0	σ_R
1	0	0	0	0	**9**	0.23	0.44	-0.25	-0.19
2	-0.17	-0.04	-0.14	-0.10	**10**	0.06	0.52	-0.48	-0.37
3	-0.27	0.27	-0.43	-0.66	**11**	0.43	0.40	0.15	0.15
4	0.78	0.64	0.15	0.15	**12**	0.37	0.47	-0.25	-0.21
5	0.5	0.30	0.20	0.06	**13**	0.39	0.44	-0.25	-0.19
6	-0.37	0.29	-0.43	-0.64	**14**	0.12	0.27	-0.43	-0.66
7	0.18	0.39	-0.16	-0.18	**15**	-0.07	-0.04	-0.14	-
8	0.23	0.47	-0.25	-0.21	**16**	0.38	0.30	0.20	0.06

Compound	**1**	**2**	**3**	**4**	**5**	**6**	**7**	**8**	**9**
σ	0.06	0.12	-0.27	0.40	0.37	0.23	1.05	0.71	0.78

4 RESULTS AND DISCUSSION

4.1 A simple and convenient synthesis of tautomeric 6(2)-hydroxy-4-methyl-(2 or 6)-oxo-1-(substituted phenyl)-(1,2 or 1,6)-dihydropyridine-3-carbonitriles

4.1.1 Results of classical and MW synthesis

A series of sixteen reaction products, consisting of a mixture of tautomers **a** and **b** (Figure 4.1.1), was synthesized using microwave irradiation starting from ethyl acetoacetate and corresponding 2-cyano-*N*-(substituted phenyl)etanamides in the presence of freshly powdered potassium hydroxide.

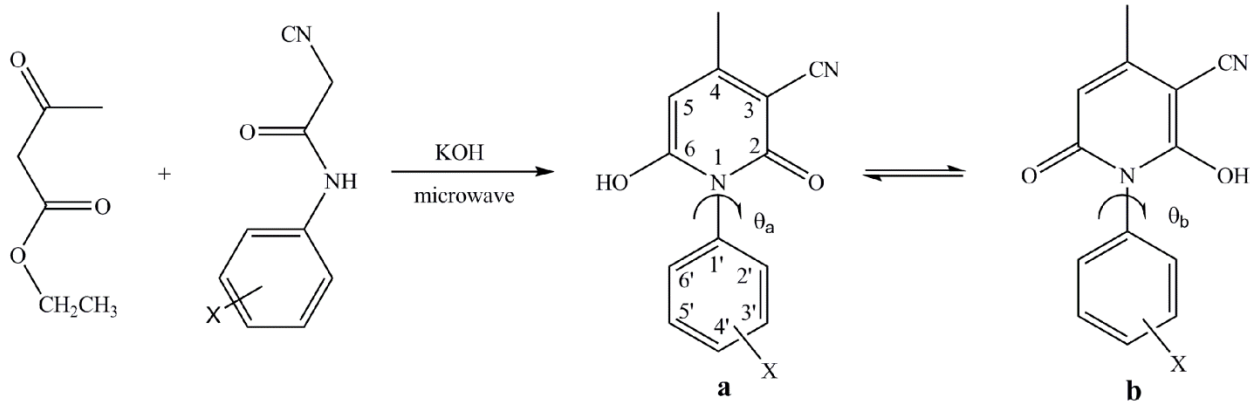

Figure 4.1.1 Microwave assisted synthesis of tautomeric pyridones

Starting 2-cyano-*N*-(substituted phenyl)ethanamides were synthesized according to previously published methods [194]. Microwave synthesis (MW) was performed in a dedicated microwave reactor in an open vessel. An attempt was made to perform synthesis in a closed vessel but much lower yields were obtained. Reactions were also carried out in a domestic commercial microwave oven as well. The conventional synthesis was also performed.

In order to optimize reaction conditions: irradiation power (100-600 W), reaction time (1-30 min), and reactant molar ratio for the reaction between 2-cyano-*N*-phenyletanamide, ethyl acetoacetate and freshly powdered potassium hydroxide was used as a model reaction. The optimized reactant ratios were found to be 1.0 equiv. 2-cyano-*N*-phenyletanamide, 3.9 equiv. ethyl acetoacetate, and 2.0 equiv. potassium hydroxide in the open vessel conducting reaction in

a dedicated microwave reactor. Optimized reaction time was found to be 10 min at 150 W. The isolated yield of the product **1** is 78 %. All other products were synthesized, according to established optimized reaction conditions, and results are given in Table 4.1.1

Table 4.1.1 Yields and melting points of the obtained product (MW synthesis)

Comp.	X	Yield / %*	M.p. / °C	Comp.	X	Yield /	M.p. / °C
1	H	78	281-3	**9**	4-Br	64	276-8
2	4-CH_3	72	284-5	**10**	4-F	74	284-5
3	4-OCH_3	60	270-3	**11**	3-CF_3	66	315-7
4	4-NO_2	73	238-42	**12**	3-Cl	59	275-8
5	4-$COCH_3$	42	227-30	**13**	3-Br	52	278-80
6	4-OH	50	286-8	**14**	3-OCH_3	47	250-2
7	4-I	57	288-9	**15**	3-CH_3	54	284-5
8	4-Cl	64	285-7	**16**	3-$COCH_3$	52	243-5

*purification performed by chloroform washing

The obtained products were characterized by melting point, FTIR, NMR, UV and MS data, as well as elemental analysis. When reactions were run in the closed vessel, ethanol was used as solvent. Reactions were performed at 140 °C but the isolated yields (20-25%) were several times lower than in the open vessel. Also reactions were run in an open vessel in the domestic commercial microwave oven. These reactions were run, using the optimized reactant ratio obtained in the dedicated microwave reactor, without stirring during irradiation (10 min). The higher irradiation power (300 W) than in the dedicated microwave reactor was needed to obtain the yields of 30-50 %. Although not much lower yields were obtained in comparison to the dedicated microwave reactor, synthesis in domestic commercial microwave ovens can not be suggested due to the safety and reproducibility reasons [203]. In addition, conventional synthesis of all pyridones was performed using optimal reactant ratio in ethanol at the reflux temperature. In comparison to the conventional, microwave synthesis gives products in higher yields (example compound **1**: 78% in the microwave *vs.* 40% in the conventional synthesis), and in a shorter reaction time (10 min *vs.* 3 h). The similar trend was found for other compounds, and results are given in Table 4.1.2.

Table 4.1.2 Yields and melting points of the obtained product in conventional synthesis

Comp.	X	Yield / %	M.p. / ^{o}C	Comp.	X	Yield /	M.p. / ^{o}C
1	H	40	280-2	**9**	4-Br	36	275-7
2	4-CH_3	38	283-5	**10**	4-F	41	282-4
3	4-OCH_3	41	270-2	**11**	3-CF_3	37	314-5
4	4-NO_2	32	236-40	**12**	3-Cl	34	273-6
5	4-$COCH_3$	25	226-9	**13**	3-Br	36	277-80
6	4-OH	24	284-6	**14**	3-OCH_3	28	250-2
7	4-I	38	286-7	**15**	3-CH_3	29	281-3
8	4-Cl	40	285-7	**16**	3-$COCH_3$	27	242-4

The preliminary study of the ^{1}H and ^{13}C NMR spectra of the obtained products indicated existence of two compounds that could not be separated using chromatographic techniques. A detail study, using homonuclear correlated spectroscopy (H,H-COSY), heteronuclear single quantum coherence (^{1}H-^{13}C HSQC), and heteronuclear multiple bond correlation (^{1}H-^{13}C HMBC) techniques, on assignments of ^{1}H and ^{13}C NMR signals of synthesized compounds was undertaken. The results were used for characterization and study of the state of equilibrium, *i.e.* state of tautomeric interconversion forms **a** and **b** (Figure 4.1.1), in DMSO-d_6 solution. Most of the synthesized compounds, according to our knowledge, are reported for the first time, and for known compounds **2-4**, **8**, **12, 15** and **17** corresponding NMR spectral data are not available in the literature.

4.1.2 ^{1}H and ^{13}C NMR spectral analysis

It was not new notion that pyridones exist in solution or in the solid state as an appropriate equilibrium of tautomeric or dimeric forms [124,204]. This equilibrium in solution is mainly affected by substituent electronic effects as well as solvent properties [205,206]. Slow proton exchange in prototropic equilibrium allowed observation of separate signals in ^{1}H and ^{13}C NMR spectra which were used for qualitative and quantitative determination of each forms in tautomeric mixture. The integral of H5 NMR signal was the main indication and the parameter used for determination of pyridone tautomer ratio in DMSO-d_6. In the ^{1}H NMR spectra of compound **1** singlet at 5.69 and 6.09 are unequivocally assigned to H5 of **1a** and **1b** forms, respectively. This methodology was applied to the NMR data of other compounds, and results of tautomer percentages and K_T determination are given in Table 4.1.5. Additionally, quantitative

^{13}C NMR spectra with inverse-gated ^{1}H decoupling were recorded. Analysis of the obtained results indicated that a good agreement of the tautomer determination existed for the methyl group proton at C4 and C2-C6 carbon atoms of the pyridone ring (example given for comp. **1**; Fig. 4.1.2).

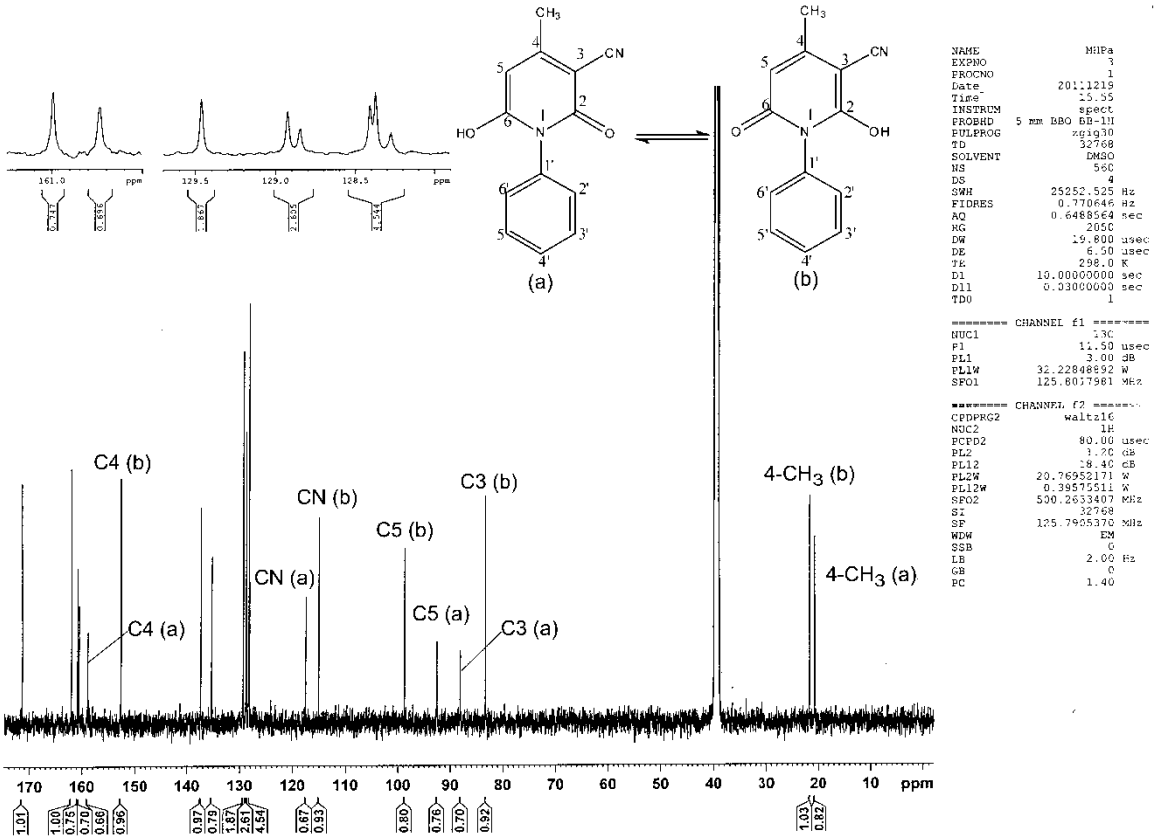

Fig. 4.1.2 Quantitative ^{13}C NMR spectrum of compound **1**

Results of DFT calculation of ^{1}H and ^{13}C NMR chemical shifts (performed by GIAO/WP04/aug-cc-pVDZ model and PCM-type calculation to include DMSO solvation), are given in Tables 4.1.3 and 4.1.4.

Table 4.1.3 Results of calculations of ^{1}H and ^{13}C NMR chemical shifts for tautomer **a**

No.	Substituent	q_{C5}	C4		C3		C2		C6		C5		H5		C4'		4-CH_3	
			calc	exp	calc	exp	calc	exp	calc	exp	calc	exp	calc	exp	calc	exp	calc	exp
1	H	-0.602	158.9	159.1	93.3	88.2	154.6	160.7	154.4	161.0	89.4	92.6	5.89	5.69	124.5	128.2	19.2	20.8
2	4-CH_3	-0.601	158.9	159.4	93.1	88.6	154.8	161.1	154.6	162.5	89.5	92.7	5.88	5.69	137.3	138.0	19.3	20.9
3	4-OCH_3	-0.588	158.8	159.3	93.2	89.0	154.9	161.2	154.7	162.7	89.6	92.6	5.89	5.69	155.1	159.4	19.2	21.0
4	4-NO_2	-0.581	160.0	159.0	93.9	88.1	154.0	160.9	153.4	161.3	90.1	95.9	5.97	5.69	147.4	141.0	19.3	20.9
5	4-$COCH_3$	-0.579	159.4	158.9	93.7	87.3	154.2	160.7	153.7	161.0	89.9	93.2	5.94	5.66	132.9	136.5	19.3	20.8
6	4-OH	-0.602	158.7	159.5	93.2	89.1	154.9	161.3	154.7	161.4	89.5	92.5	5.87	5.69	152.5	157.6	19.1	21.0
7	4-I*	-	-	159.2	-	88.0	-	160.6	-	160.8	-	92.8	-	5.66	-	159.2	-	20.8
8	4-Cl	-0.598	159.4	159.5	93.5	88.2	154.5	161.0	154.0	161.2	89.7	93.1	5.91	5.66	131.7	133.2	19.2	21.0
9	4-Br	-0.600	159.3	159.4	93.4	88.0	154.4	160.9	154.0	162.4	89.7	93.1	5.92	5.66	124.9	122.4	19.3	21.0
10	4-F	-0.615	159.2	159.1	93.4	87.8	154.7	160.6	154.3	161.1	89.6	92.8	5.90	5.67	159.0	162.8	19.2	20.8
11	3-CF_3	-0.600	159.4	-	93.4	-	154.3	-	153.8	-	89.8	-	5.94	-	132.9	-	19.3	-
12	3-Cl	-0.602	159.3	159.4	93.4	88.6	154.4	161.3	153.9	162.4	89.6	93.2	5.91	5.67	124.8	128.7	19.3	21.0
13	3-Br	-0.601	159.3	159.2	93.4	87.6	154.4	161.1	153.9	152.5	89.6	93.3	5.90	5.65	127.4	128.3	19.2	21.0
14	3-OCH_3	-0.613	158.9	159.5	93.3	88.9	154.6	160.8	154.4	162.1	89.6	92.3	5.89	5.70	115.8	114.2	19.1	20.8
15	3-CH_3	-0.621	158.9	159.2	93.1	88.5	154.6	160.7	154.4	162.2	89.6	92.5	5.89	5.69	124.9	125.4	19.2	20.7
16	3-$COCH_3$	-0.586	159.2	159.6	93.3	88.2	154.4	161.1	153.9	162.6	89.9	93.2	5.95	5.70	126.3	128.8	19.2	21.1

*basis set for I substituent is not available

Table 4.1.4 Results of calculations of ^{1}H and ^{13}C NMR chemical shifts for tautomer **b**

No.	Substituent	q_{C5}	C3		C2		C4		C5		C6		H5		C4'		4-CH_3	
			calc	exp	calc	exp	calc	exp	calc	exp	calc	exp	calc	exp	calc	exp	calc	exp
1	H	-0.562	76.3	83.4	159.0	171.6	148.4	152.8	107.3	98.8	153.4	162.2	6.10	6.09	132.5	128.8	19.5	21.7
2	4-CH_3	-0.534	76.2	83.6	159.1	171.9	148.3	153.3	108.3	99.0	153.6	161.2	6.09	6.08	137.6	138.6	19.4	21.9
3	4-OCH_3	-0.559	76.3	83.6	159.3	171.9	148.2	153.6	108.4	99.0	153.6	161.5	6.09	6.07	155.2	159.5	19.4	22.0
4	4-NO_2	-0.564	76.3	83.4	158.3	172.1	149.3	152.1	107.5	99.4	152.5	162.0	6.18	6.13	147.5	143.2	19.5	21.5
5	4-$COCH_3$	-0.525	76.9	83.4	158.6	171.9	148.8	152.3	107.4	99.1	152.9	162.0	6.15	6.13	133.1	137.0	19.4	21.6
6	4-OH	-0.529	76.3	-	159.3	-	148.1	-	107.2	-	153.6	-	6.08	-	152.6	-	19.4	-
7	4-I*	-	-	83.4	-	171.8	-	152.5	-	99.0	-	162.1	-	6.08	-	95.4	-	21.7
8	4-Cl	-0.561	76.7	83.5	158.8	172.1	148.7	152.9	107.3	99.3	153.1	162.5	6.12	6.10	131.4	133.8	19.4	21.9
9	4-Br	-0.552	76.7	83.6	158.8	172.1	148.7	152.9	107.3	99.3	153.1	161.2	6.12	6.09	124.7	121.7	19.4	21.9
10	4-F	-0.553	76.6	83.4	159.0	171.7	148.6	152.9	107.3	99.0	153.3	160.8	6.11	6.09	159.2	162.3	19.4	21.7
11	3-CF_3	-0.546	76.9	83.6	158.7	172.3	148.8	152.7	107.3	99.5	152.9	162.5	6.16	6.18	123.4	126.1	19.5	21.9
12	3-Cl	-0.555	76.7	83.6	158.7	172.1	148.8	152.8	107.4	99.3	153.0	161.0	6.12	6.10	125.0	129.0	19.5	21.8
13	3-Br	-0.552	76.6	83.5	158.7	172.1	148.7	152.8	107.3	98.3	153.0	161.3	6.13	6.10	127.8	128.6	19.5	21.8
14	3-OCH_3	-0.549	76.2	83.4	159.1	171.7	148.4	152.9	107.4	98.8	153.3	160.6	6.10	6.08	113.8	114.7	19.4	21.5
15	3-CH_3	-0.574	76.2	83.4	159.1	171.6	148.2	152.8	107.5	98.8	153.5	160.9	6.09	6.08	125.4	125.3	19.5	21.7
16	3-$COCH_3$	-0.545	76.9	83.7	158.7	172.2	148.7	153.0	107.3	99.4	153.0	161.4	6.16	6.13	126.6	128.6	19.5	22.0

*basis set for I substituent is not available

The analysis of the ^{1}H-^{13}C correlated spectra provided precise protons and carbons signals assignments. Examples are given for compound **15**: HMBC at Fig. 4.1.3, and HSQC at Fig. 4.1.4. Connectivity found in the HMBC spectra helped to distinguish the quartenary carbons of the pyridone core.

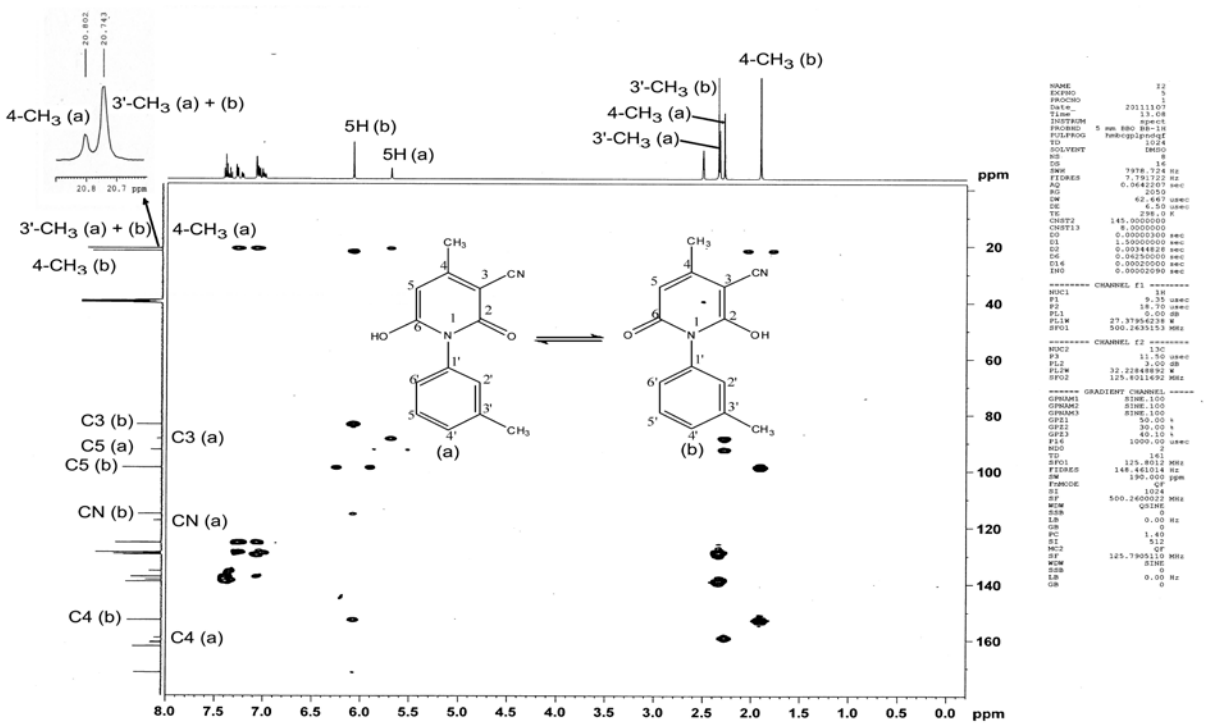

Fig. 4.1.3 HMBC spectrum of compound **15**

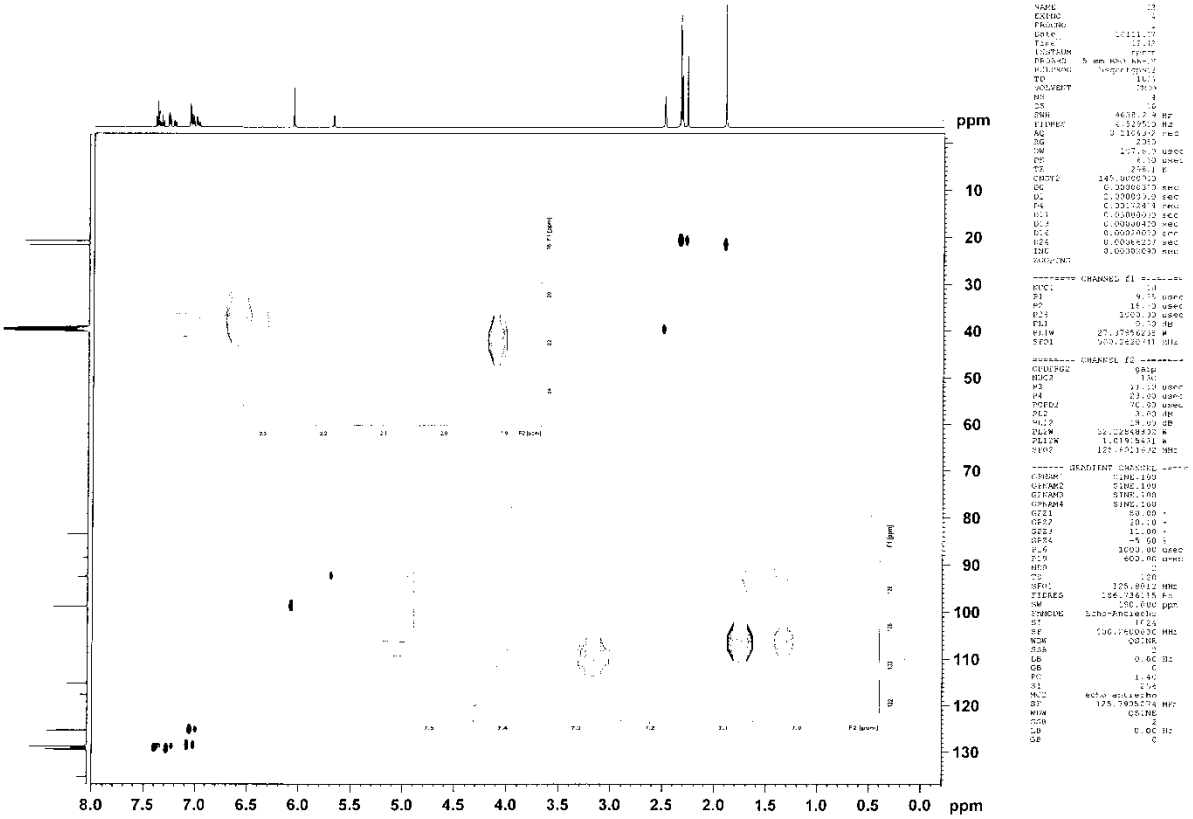

Fig. 4.1.4 HSQC spectrum of compound **15**

Table 4.1.5 Percentage of tautomers **a** and **b** and equilibrium constant K_T

Comp.	**a** (%)	**b** (%)	K_T[a]	Comp.	**a** (%)	**b** (%)	K_T[a]
1	43	57	1.33	**9**	60	40	0.67
2	70	30	0.43	**10**	41	59	1.44
3	23	77	3.35	**11**	0	100	-
4	27	73	2.70	**12**	45	55	1.22
5	73	27	0.37	**13**	54	46	0.85
6	100	0	0.00	**14**	80	20	0.25
7	75	25	0.33	**15**	30	70	2.33
8	68	32	0.47	**16**	43	57	1.33

K_T = **[b]**/**[a]**; proportion are determined by ratio of integrated 5H signal in DMSO-d_6

Results from Table 4.1.2 indicate complex influence of electronic substituent effects on tautomeric equilibriums. Linear correlations of negative logarithm value of the equilibrium constant, pK_T, with Hammett substituent constant, $\sigma_{m/p}$ [207], was found for electron-acceptor substituted compounds (Fig. 4.1.5 and Table 4.1.6).

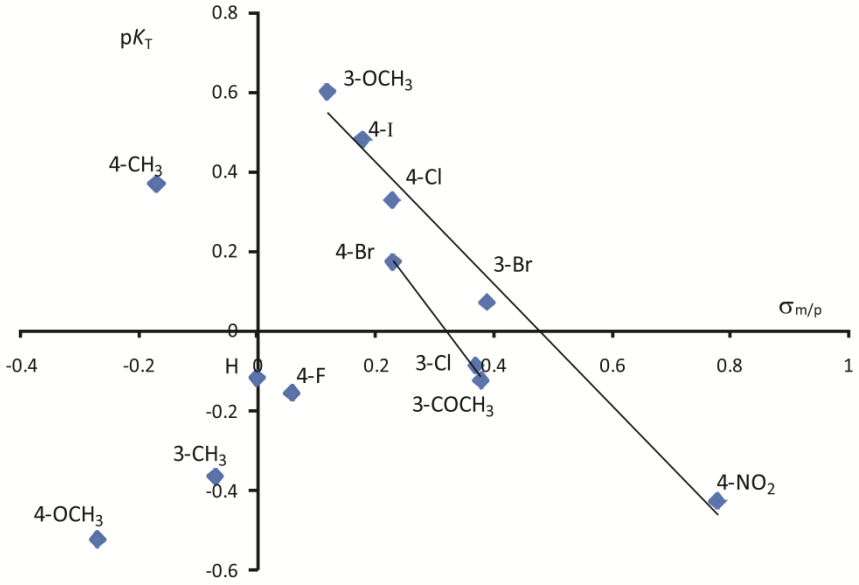

Fig. 4.1.5 Graphical presentation of relation pK_T *vs* $\sigma_{m/p}$

Table 4.1.6 Results of Hammett[a] correlations pK_T *vs* $\sigma_{m/p}$ for electron-acceptor substituted compounds **4**, **7**-**9**, **12**-**14** and **16**

scale	h[b]	ρ[c]	r[d]	sd[e]	F[f]	n[g]
$\sigma_{m/p}$	0.638 (±0.102)	-1.528 (±0.264)	0.92	0.143	33	8
$\sigma_{m/p}$	0.475 (±0.021)	-0.642 (±0.048)	0.99	0.039	175	5[h]
$\sigma_{m/p}$	0.618 (±0.036)	-1.931 (±0.109)	0.99	0.013	311	3[i]

[a] pK_T = $\rho\sigma + h$; [b]intercept; [c]proportionality constant; [d] Correlation coefficient; [e] Standard deviation; [f] Fisher test of significance; [g] number of data included in correlation; [h] compounds **4**, **7**, **8**, **13** and **14**; [i] compounds **9**, **12** and **16.**

The slopes of correlation lines pK_T - $\sigma_{m/p}$ are negative, and the proportionality constants ρ indicate significant sensitivity of pK_T to substituent effects. The negative sign means reverse behavior, *i.e.*, the contribution of tautomer **b** in equilibrium increases, although the electron–withdrawing ability of the substituents, measured by σ, increases. Non-linear relation pK_T - $\sigma_{m/p}$, which includes fluoro substituted pyridone due to its significant electron-donating character [207], was found for electron-donor substituted compounds (Fig. 4.1.5). Transmission of the resonance substituent effect is significantly affected by the non-planarity of the molecule (Table 4.17; angles θ_a and θ_b), in that way influencing the π-electron delocalization and the state of tautomeric equilibrium. Moreover, it could not neglected contributions of the solvent effects (DMSO): dipolarity, polarizability and solute/solvent hydrogen bonding interaction (hydrogen

bond donor HBD and hydrogen bond acceptor HBA interaction) which significantly contribute to the tautomer stability. Generally, it could be observed that solvent HBA effect is more pronounced for compound **6** influencing that tautomer **a** predominate (Table x?) due to presence of proton-donating site, *i.e*. OH group. As the contribution of solvent HBA effect decreases, due to decreasing substituent proton donating capabilities (comps. **2**, **1, 10, 15** and **3,** respectively. Fig 4.1.5) K_T increase, *i.e*. contribution of tautomer **b** increases.

4.1.3 Elements of geometry

Table 4.1.7 Elements of geometry of the tautomer **a** obtained by the use of B3LYP/6-11++G(d,p) method

No.	Sub.	Torsion angle	Charge	Bond length				
		θ	q_{C5}	N1-C2	N1-C6	N1-C1'	C6-O	C2-O
1	H	79.65	-0.602	1.441	1.363	1.449	1.347	1.218
2	4-CH_3	80.18	-0.601	1.441	1.363	1.448	1.347	1.219
3	4-OCH_3	76.25	-0.588	1.442	1.363	1.447	1.347	1.219
4	4-NO_2	66.55	-0.581	1.444	1.367	1.443	1.346	1.218
5	4-$COCH_3$	68.93	-0.579	1.443	1.365	1.446	1.346	1.219
6	4-OH	73.35	-0.602	1.442	1.364	1.446	1.347	1.219
7	4-I*	-	-	-	-	-		
8	4-Cl	73.05	-0.598	1.442	1.365	1.446	1.347	1.218
9	4-Br	73.05	-0.600	1.442	1.365	1.446	1.346	1.218
10	4-F	75.69	-0.615	1.442	1.364	1.446	1.347	1.217
11	3-CF_3	68.54	-0.600	1.443	1.363	1.445	1.346	1.219
12	3-Cl	73.57	-0.602	1.442	1.365	1.446	1.346	1.218
13	3-Br	72.50	-0.601	1.442	1.365	1.446	1.346	1.218
14	3-OCH_3	74.09	-0.613	1.441	1.363	1.449	1.346	1.219
15	3-CH_3	77.42	-0.621	1.441	1.363	1.449	1.347	1.219
16	3-$COCH_3$	66.19	-0.586	1.443	1.366	1.446	1.346	1.219

*basis set for I substituent is not available; [a] torsional angle C2-N1-C1'-C2'; [b] torsional angle C6-N1-C1'-C6'

Table 4.1.8 Elements of geometry of the tautomer **b** obtained by the use of B3LYP/6-311++G(d,p) method

No.	Sub.	Torsional angle	Charge	Bond length				
		θ	q_{C5}	N1-C2	N1-C6	N1-C1'	C6-O	C2-O
1	H	78.19	-0.562	1.356	1.452	1.448	1.219	1.338
2	4-CH_3	77.85	-0.534	1.356	1.452	1.448	1.220	1.338
3	4-OCH_3	74.04	-0.559	1.356	1.453	1.446	1.220	1.338
4	4-NO_2	66.07	-0.564	1.360	1.457	1.443	1.219	1.338
5	4-$COCH_3$	68.58	-0.525	1.358	1.455	1.446	1.219	1.338
6	4-OH	73.44	-0.529	1.357	1.453	1.446	1.220	1.338
7	4-I*	-	-	-	-	-		
8	4-Cl	71.82	-0.561	1.358	1.454	1.446	1.219	1.338
9	4-Br	71.46	-0.552	1.358	1.455	1.446	1.219	1.338
10	4-F	67.22	-0.553	1.357	1.454	1.446	1.219	1.338
11	3-CF_3	69.63	-0.546	1.358	1.455	1.445	1.219	1.338
12	3-Cl	73.16	-0.555	1.358	1.454	1.446	1.219	1.338
13	3-Br	73.86	-0.552	1.358	1.454	1.446	1.219	1.338
14	3-OCH_3	82.77	-0.549	1.356	1.452	1.450	1.220	1.338
15	3-CH_3	80.91	-0.574	1.356	1.452	1.449	1.219	1.338
16	3-$COCH_3$	67.22	-0.545	1.358	1.454	1.446	1.220	1.338

*basis set for I substituent is not available; [a] torsional angle C2-N1-C1'-C2'; [b] torsional angle C6-N1-C1'-C6'

Also, we carried out *ab-initio* studies to calculate energies of both tautomers. The obtained results in gas phase indicates higher stability of tautomer **b** (0.5-11.4 kJ/mol) for all compounds due to existence of intramolecular hydrogen bond between hydroxy and cyano groups. On the other hand, calculations of the solvation free energy have shown that **a** tautomers are better solvated in DMSO (difference in solvation free energy between tautomer **a** and **b** is from 0.1 to 8.9 kJ/mol), thus indicating a higher stability of **a** form in solution. Detailed experimental and theoretical investigation on solvent- and temperature-dependent pyridone tautomeric equilibrium, and tautomerization mechanism is a matter of current study. In Fig. 4.1.6 the optimized geometry of tautomers **1a** and **1b**, obtained by the use of B3LYP method with 6-311G(d,p) basis set, is given. Also, some elements of optimized geometries are given in Table x?.

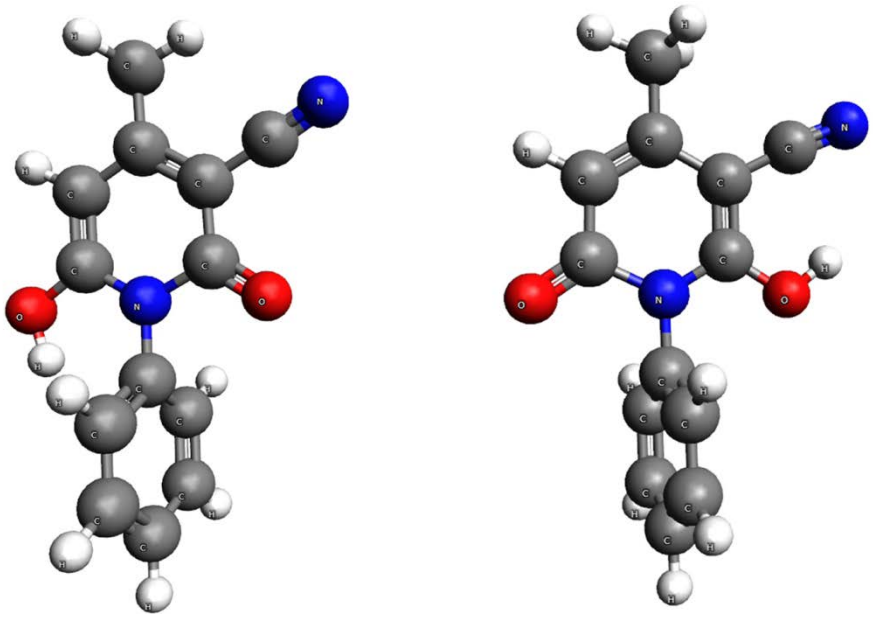

Fig. 4.1.6 Optimized geometries of tautomers **1a** and **1b**

The determination of thermodynamic parameters for the keto-enol equilibrium (comp. **1**) in DMSO-d_6 indicated an endothermic character of such process [208], which is in accordance with low temperature influence on equilibrium shift observed in NMR spectra (Fig. x?). The NMR spectra of compound **1** were recorded at 343 K to confirm thermally induced tautomerization, *i.e.* slow proton exchange in prototropic equilibrium of compound **1**. The prototropic interconversion could be accomplished *via* [1,5]- [209], or less probably [1,7]-hydrogen transfer, as well as by intermolecular double proton transfer,

prototropic interconversion with cyclic associate participation [210], supported by high pyridone tendency to create dimer (self-association) [211].

The synthesized pyridones showed an interesting feature (presented in case of pyridone **1**): its diazotization (Figure 4.1.7) produced azo derivatives which are easily rearranged to more stable hydrazone form [208].

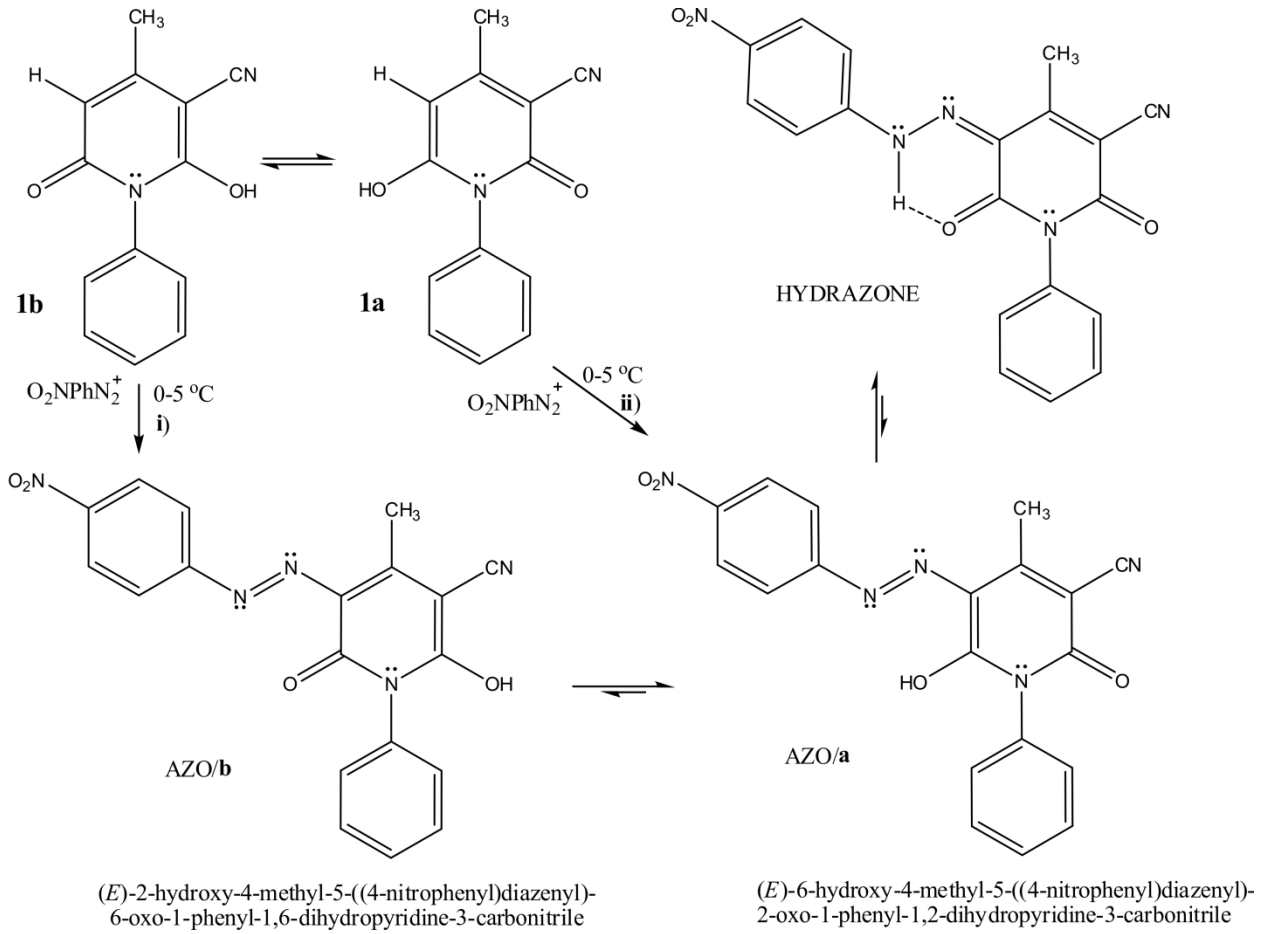

Figure 4.1.7 The proposed reaction pathways and equilibria shift during synthesis of (*Z*)-4-methyl-5-[2-(4-nitrophenyl)hydrazono]-2,6-dioxo-1-phenyl-1,2,5,6-tetrahydro-3-carbonitriles

Spectral assignments of (*Z*)-6-hydroxy-4-methyl-5-[2-(4-nitrophenyl)-hydrazono]-2,6-dioxo-1-phenyl-1,2,5,6-tetrahydro-3-carbonitriles is given in ^{1}H NMR spectrum of unpurified, as well as purified product (Figs. 4.18 and 4.1.9, respectively).

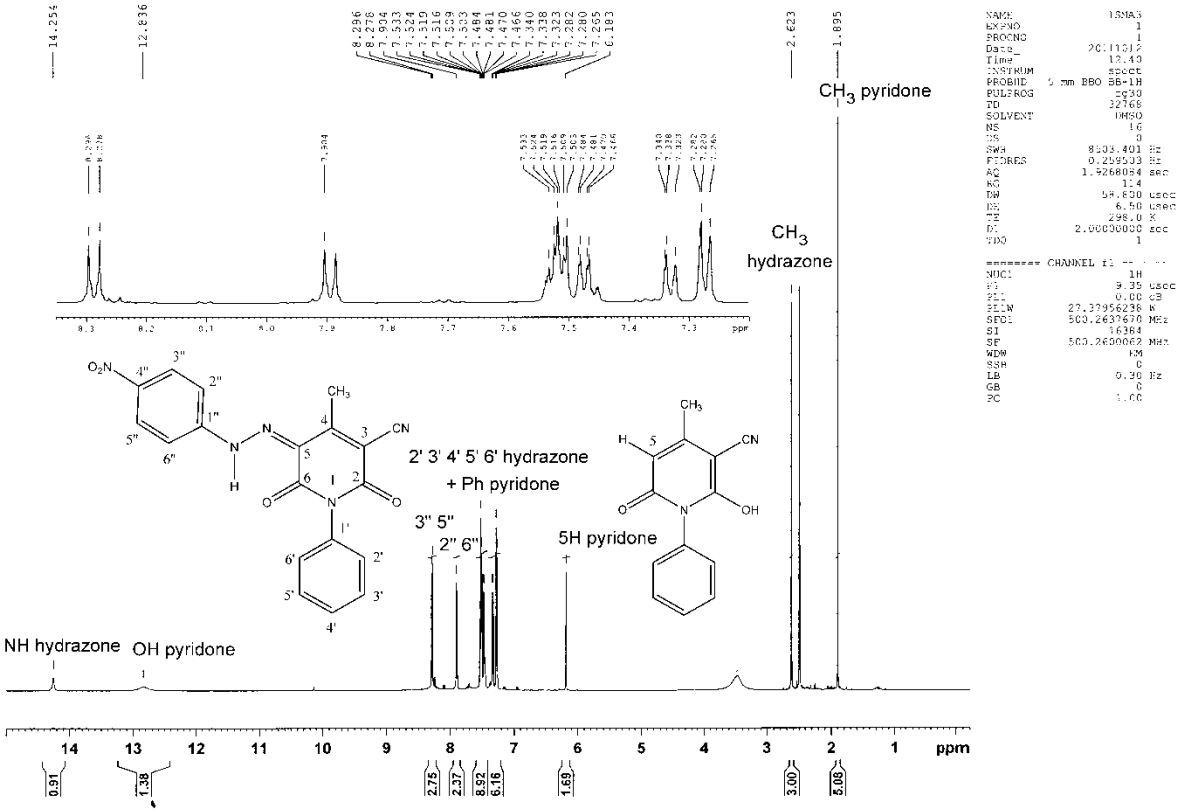

Fig. 4.1.8 ^{1}H NMR spectrum of unpurified product from (*Z*)-4-methyl-5-[2-(4-nitrophenyl)hydrazono]-2,6-dioxo-1-phenyl-1,2,5,6-tetrahydro-3-carbonitriles synthesis

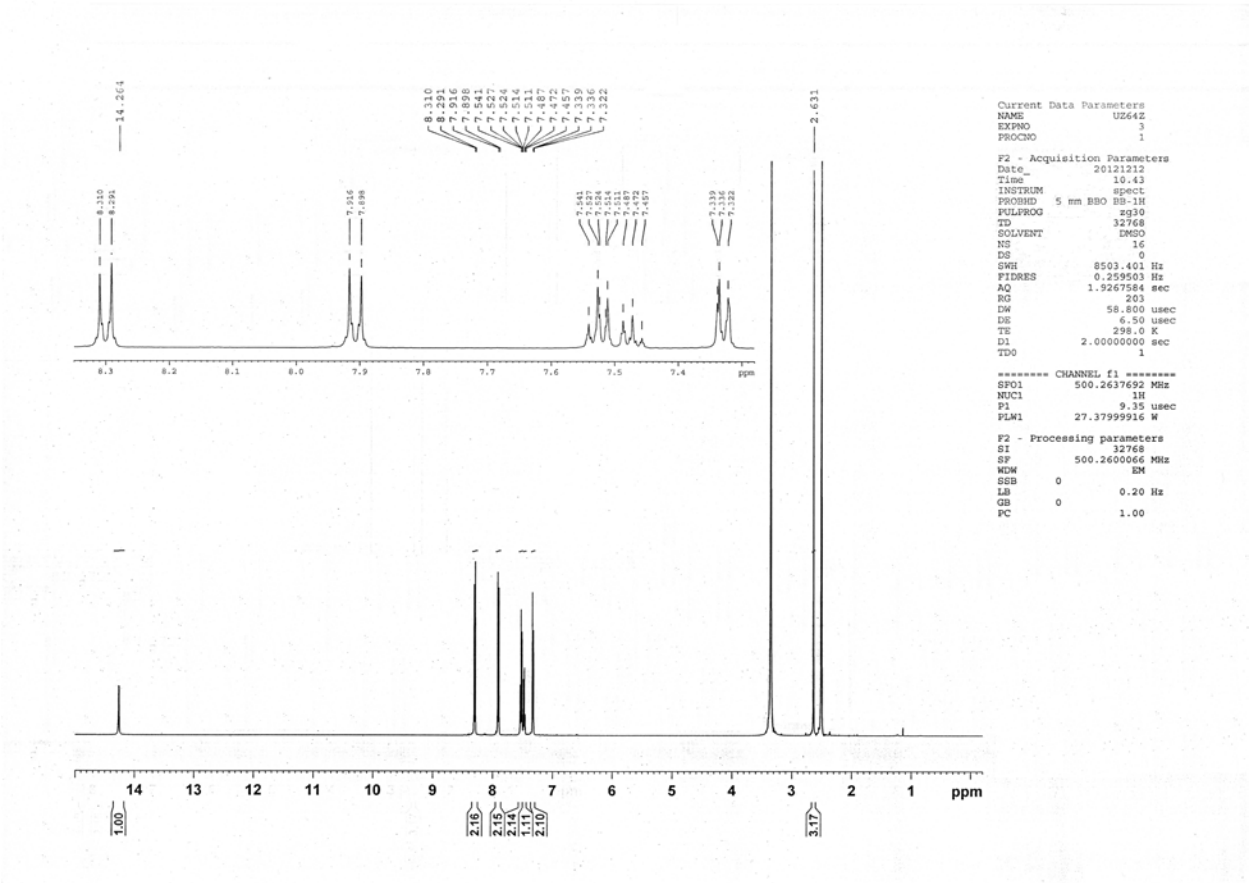

Fig. 4.1.9 ^{1}H NMR spectrum of (*Z*)-4-methyl-5-[2-(4-nitrophenyl)hydrazono]-2,6-dioxo-1-phenyl-1,2,5,6-tetrahydro-3-carbonitriles

Additionally, the theoretical calculations showed that HYDRAZONE form is for 15 kcal/mol more stable than AZO/**b** form mainly because of the formation of intramolecular hydrogen bond (Scheme x?). On the other hand, calculations have shown that AZO/**a** tautomer is not a minimum on potential energy surface. All B3LYP/6-311++G(d,p) optimizations, which started from AZO/**a** geometry, optimized to much more stable HYDRAZONE geometry. Theoretical calculations and NMR results clearly indicate that if both tautomers (AZO/**a** and AZO/**b**; Scheme 2) are obtained by pyridone **1** diazotization subsequent hydrogen rearrangements drive the equilibrium to more stable HYDRAZONE form. Diazotization of **1b** form could take place either following path **i**) and consecutive tautomerization AZO/**b** to AZO/**a** or by prototropic equilibrium shifts to **1a** form followed by diazotization (path **ii**) (Figure 4.1.6). Reactivity of diazonium salt depends on the substituent groups that are present on starting pyridone. From the

kinetically point of view electrophilic attack at C5 by *para*-nitrophenyldiazonium ion significantly depends on charge density at this carbon. DFT calculation showed higher negative charges at C5 for tautomer **a** in all compounds (Tables x and x?), and thus, it could be supposed higher probability that reaction take place at C5 of **a** form.

Moreover, the results of pyridone geometry optimization showed that hydroxyl group at C6 and pyridone ring are *co*-planar on that way higher extent of overlapping (n,π-conjugation) of oxygen lone pairs (*p*-orbitals) and π–electrons of the pyridone ring contribute to an increased electron density at C5 carbon. It is expected that close vicinity of electron-donating hydroxyl group in **a** form at C6 could participate in a stabilization of activated complex, and more favorable reaction pathways **ii**) could be operative in that way. Studies of solvent and substituent intramolecular charge transfer properties of pyridones and dyes, using UV and time-dependent density functional theory (TD-DFT) methods, will be focus of forthcoming work. Generally speaking, result of dye synthesis gave a product containing non-reacted pyridone **b** form and azo dye product. The pure pyridone azo dye absorbed at a higher wavelength (batochromic shift; λ_{max}= 430 nm) due to larger mobility of electronic densities (extended π-resonance) through overall π-electronic systems. Obtained dye exhibit their color hue in red comparing to white-yellowish of starting pyridone. High commercial importance of these dyes as coloring material undisputedly set further demands for intensive dye synthesis and azo-hydrazone tautomerism study, as well as their solvatochromic and substituent dependent properties.

In summary, this simple, convenient and rapid one-pot microwave procedure, which gives the title tautomeric pyridones product in good yield with high purity, can be useful in the preparation of dyes and pigments as well as pharmaceutically important compounds.

4.2 Solvent and structural effects in tautomeric 3-cyano-4-(substituted phenyl)-6-phenyl-2(1*H*)-pyridones: experimental and quantum chemical study

4.2.1 Resolution of UV spectra

2(1*H*)-Pyridones exist in a solution as the equilibrium of tautomeric and/or dimer forms [130, 212], and these phenomena have significant influences on their physico-chemical properties. The tautomeric equilibrium is affected by the factors inherent to studied molecules, geometries and substituent effects, while others are associated to solvent properties like polarity, stabilization of the charges in the solvation sphere and from alteration of a solute's electronic structure in the ground and excited states due to both short- and long-range interactions with surrounding solvent molecules [193,212].

A study of the mechanism of proton-transfer and state of equilibria in solution is an interesting and complex phenomenon which needs careful analysis to avoid misinterpretation of the results obtained. Different spectroscopic techniques were used for studying solvent–solute interactions and state of tautomeric equilibria. Slow proton exchange allows observation of distinct signals in ^{1}H NMR spectra, which could be used for qualitative and quantitative determination of each tautomeric form [213]. When the proton exchange is fast comparing with NMR timescale, in the NMR spectrum of a tautomeric mixture only one, average, signal can be observed. Fast proton exchange limited applicability of NMR spectroscopy for the study of prototropic equilibria in the case of studied 2(1*H*)-pyridones. Therefore, we used advantages of the UV/Vis absorption spectroscopy in following: tautomeric forms have different spectral characteristics and the tautomeric equilibrium is influenced by various external factors like environment (solvent), substituent effect, acidity, temperature, *etc*. Consequently, examination of the tautomeric equilibria, solvatochromism and transmission of substituent effects through appropriate tautomeric forms of compounds **1**-**9** was performed by analyzing UV/Vis spectra. Resolution of individual bands in UV-Vis spectra was best described with the pure Gauss or with the mixed Gauss-Lorentz functions [214]. Spectral properties determination was based on various assumptions and approximations [215].

In general, tautomeric equilibrium is shifted towards more dipolar **PY** form with increasing solvent polarity due to the larger contribution of the charge-separated mesomeric form (Fig. 4.2.1c) [uzeti ref iz rada], while the opposite is true for non-polar solvents.

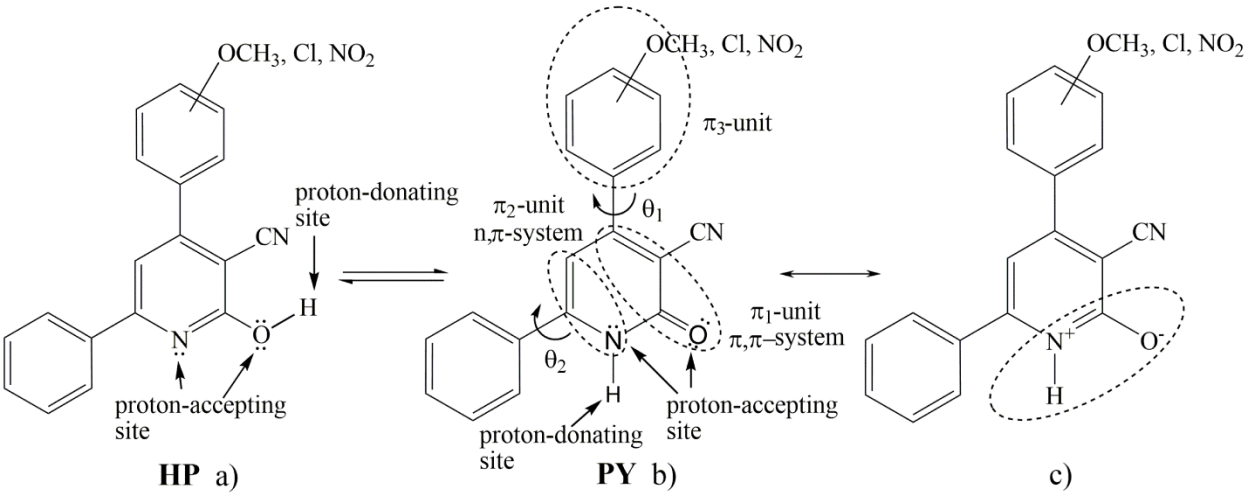

Fig. 4.2.1 Tautomeric equilibria of **2-HP** a), **2-PY** b), and zwitter-ion structure c) of investigated compounds

Absorption spectra of the investigated compounds were recorded in seventeen solvents. It was found that spectra consist of two overlapped bands in the region 300-500 nm. Mutual ratio of the bands depends on both the substituent effects and the solvent properties. Influences of solvent–solute interactions on molecular associations (dimer formation) have been thoroughly investigated [121-123]. To study the appearance of dimerization and its influence on spectroscopic properties, the UV/Vis spectra of 2(1*H*)-pyridones were recorded at different concentrations and temperatures (Fig. 4.2.2). The results showed no effect on K_T at concentrations lower than 1×10^{-5} mol dm^{-3}, indicating no monomer content rising upon dilution. Therefore, the presence of dimeric forms did not affect UV spectra at concentration of 1×10^{-5} mol dm^{-3}. Also, negligible influences of temperature changes were observed (Fig. 4.2.2) [216-218].

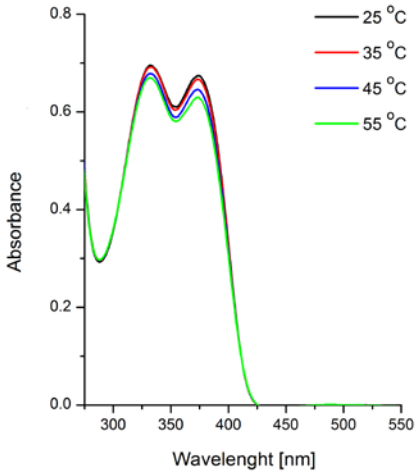

Fig. 4.2.2 Temperature-dependent UV spectra of compound **3** in DMF

The absorption maxima of both **PY** (higher wavelength energy band) and **HP** forms (lower one) in the set of selected solvents are given in Tables 4.2.1 and 4.2.2. The characteristic absorption spectra in ethanol, THF and NMF are shown in Fig. 4.2.3 and Fig. 4.2.4.

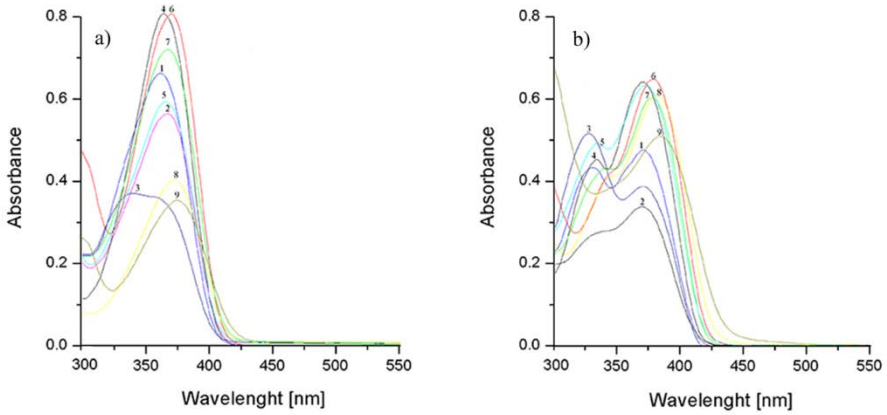

Fig. 4.2.3 Absorption spectra of compounds **1** - **9** in a) ethanol and b) THF

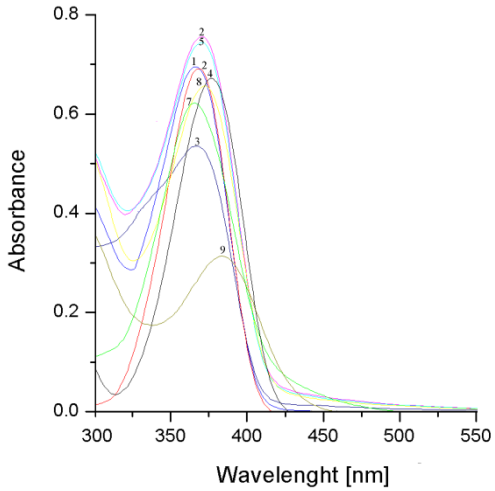

Fig. 4.2.4 Absorption spectra of compounds **1**-**9** in NMF

The spectra consisting of overlapped bands were analysed by a stepwise procedure, whereby an estimation of both tautomerization constants and individiual spectra of the tautomers were obtained from experimental data and DFT calculation. Because of the shape of spectra shown in Fig. 4.2.3., and the observation that overlapped bands were present in a UV/Vis spectra, we performed detailed analysis of the structure of spectral bands. The resolution of the individual bands was a complex task due to high extent of the overlapping of absorption bands and difficulties related to estimation of their number. Derivative spectroscopy was a very useful tool in determining the number and approximate position of the absorption bands.

In the first step, we determined the approximate number of bands and the position of each band, by applying second and fourth derivative spectroscopy [217]. In the second step, the initial approximation of the band intensities and band widths, and assignment to the appropriate tautomeric form was performed. The final refinement is performed by simultaneous resolution of the whole set of spectra according to literature procedures described in references [217-219]. Results are exemplified in Figs. 4.2.5 and 4.2.6, and results obtained are given in Tables 4.2.1 and 4.2.2. Such methodology provides differentiation without loss of the terminal spectral points [220].

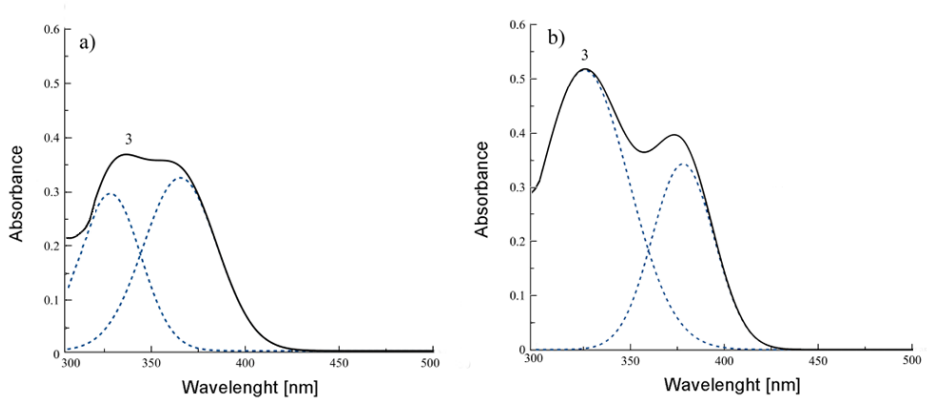

Fig. 4.2.5 Resolved overlapping bands of compound **3** in ethanol a) and THF b) (spectra given in Fig. 4.2.3)

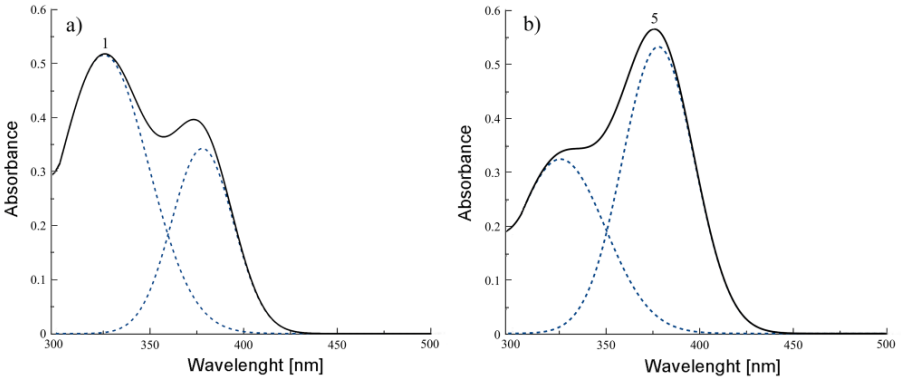

Fig. 4.2.6 a) Resolved overlapping bands in spectrum of compound **3** recorded in THF (spectrum 1 in Fig. 3 a), and b) in a mixture of THF/NMF (10/90 v/v) (spectrum 5 in Fig. 4.2.4)

Table 4.2.1 Absorption frequencies of the **PY** form in selected solvents

Solvent/compound	$\nu_{max} \times 10^{-3}$ (cm^{-1})									
	0*	**1-PY**	**2-PY**	**3-PY**	**4-PY**	**5-PY**	**6-PY**	**7-PY**	**8-PY**	**9-PY**
Methanol	27.55	27.78	27.53	27.03	27.53	27.43	27.23	27.47	27.11	26.84
Ethanol	27.47	27.64	27.23	26.74	27.49	27.41	27.03	27.19	26.87	26.75
1-Propanol	27.25	27.22	26.95	26.69	27.47	27.13	27.03	27.38	26.75	26.78
2-Propanol	27.32	27.13	26.83	26.69	27.20	27.25	27.17	27.25	26.88	26.52
1-Butanol	27.25	27.05	26.75	26.67	27.46	27.40	27.32	27.20	26.81	26.48
2-Butanol	27.28	26.97	26.79	26.96	27.46	27.26	27.08	27.23	26.68	26.57
1,4-Dioxane (Dioxane)	26.78	26.55	26.41	26.42	26.99	27.06	26.74	26.42	26.70	26.56
Ethyl acetate (EtAc**)	26.95	26.55	26.47	26.46	26.82	26.88	26.95	26.82	26.52	26.27
Tetrahydrofuran (THF)	26.74	26.50	26.54	26.41	26.66	26.04	26.71	26.27	25.80	25.80
Acetonitrile (AcN)	26.87	27.40	27.01	26.55	27.12	26.99	26.81	26.79	26.67	25.64
Acetone	27.08	27.19	26.87	27.04	27.01	26.88	26.74	26.90	26.52	26.25
Dimethyl sulfoxide (DMSO)	26.65	26.35	26.16	26.02	26.53	26.49	26.38	27.12	26.11	24.60
N,*N*-Dimethylformamide (DMF)	26.60	26.28	26.03	25.97	26.64	26.52	26.38	26.94	26.18	24.45
N,*N*-Dimethylacetamide (DMAc)	26.52	26.32	26.11	26.11	26.71	26.45	26.45	27.23	26.05	24.04
N-Methylformamide (NMF)	27.51	27.35	26.98	27.30	27.08	27.06	26.94	27.43	26.50	26.05
Dichloromethane (DCM)	27.30	27.11	27.17	26.98	27.08	27.16	26.95	27.23	26.79	26.48
Chloroform (Chl)	27.41	27.70	27.35	27.56	27.43	27.32	27.17	27.16	26.68	26.51

* Unsubstituted compounds

** Abbreviations taken from www.chemnetbase.com.

Table 4.2.2 Absorption frequencies of the **HP** form in selected solvents

Solvent/compound	ν_{max} x 10^{-3} (cm^{-1})									
	0*	**1-HP**	**2-HP**	**3-HP**	**4-HP**	**5-HP**	**6-HP**	**7-HP**	**8-HP**	**9-HP**
Methanol	30.31	29.91	29.91	29.99	29.99	29.73	29.75	30.25	29.21	29.13
Ethanol	29.99	29.82	29.51	30.03	29.35	29.56	29.80	29.78	28.93	28.52
1-Propanol	29.39	29.79	29.64	30.00	29.76	29.70	29.13	29.57	28.67	28.67
2-Propanol	29.68	30.13	29.75	30.18	29.23	29.63	29.25	29.56	29.01	28.99
1-Butanol	30.17	29.81	29.43	30.47	29.18	29.13	29.20	30.06	28.51	28.94
2-Butanol	30.18	29.83	29.68	30.43	29.13	29.67	29.43	30.13	29.60	29.51
Dioxane	29.88	29.80	29.51	30.53	29.31	29.80	29.62	29.58	29.82	29.63
EtAc	30.13	29.63	29.62	30.73	29.40	29.43	29.31	30.25	29.37	29.15
THF	30.47	29.99	29.93	30.63	29.80	29.56	28.67	30.08	29.28	29.50
AcN	27.13	29.03	28.80	30.30	29.00	29.10	28.17	27.05	27.98	28.12
Acetone	29.05	29.32	29.00	30.21	28.80	28.93	28.95	28.98	28.90	28.21
DMSO	28.31	28.98	28.31	29.75	27.63	29.09	28.90	27.73	28.13	25.20
DMF	28.70	29.27	28.64	29.81	27.91	29.13	28.95	28.80	27.50	25.33
DMAc	27.36	29.65	29.00	30.13	28.52	29.12	28.10	28.01	27.45	27.31
NMF	28.77	29.57	28.98	30.52	28.51	28.91	29.57	28.67	27.64	29.81
DCM	28.15	28.67	28.50	29.90	28.42	28.71	28.42	27.95	28.37	28.03
Chl	29.21	29.07	29.52	30.21	30.05	29.30	29.07	28.92	28.72	28.71

* Unsubstituted compound

The absorption maxima shifts showed low dependence with respect to both solvent and substituent effects (Tables 4.2.1 and 4.2.2), and the lower values of ν_{max} were found for electron-acceptor substituted compounds (lowest for compound **9**). The ν_{max} shifts are influenced by solvent–solute non-specific (dipolarity/polarizability) and specific (HBA/HBD) interactions. The solvent hydrogen-bonding ability plays a specific role in solvation of appropriate tautomeric forms: HBD solvent effect contribute to better stabilization of the oxo form (**PY**), whereas HBA stabilizes better the hydroxy form (**HP**) [221], on that way their balanced contribution cause state of tautomeric equilibria.

4.2.2 LSER analysis of UV data

The influence of various types of solvent–solute interactions on the absorption maxima shifts was interpreted by means of the LSER models of Kamlet-Taft (Eq. 2.6.13) and Catalán (Eq. 2.6.14). The Kamlet–Taft and the Catalan parameters [191,207,222], given in Tables 3.5.1 and 3.5.2, were used for the evaluation of the solute–solvent interactions and the solvatochromic shifts of the UV/Vis absorption maxima of the investigated compounds. In general, the correlation results supports conclusions about relation between the solvent–solute interactions and the state of tautomeric equilibria. The values of the correlation coefficients, obtained according to Kamlet–Taft and the Catalán equations, are collected in Tables 4.2.3 and 4.2.5 for the **PY** form, and Tables 4.2.4 and 4.2.6 for **HP** form, respectively.

Table 4.2.3 The results of the correlation analysis for **PY** tautomer obtained according to Kamlet–Taft equation

Comp.	$\nu_0\times10^{-3}$ (cm^{-1})	$s\times10^{-3}$ (cm^{-1})	$a\times10^{-3}$ (cm^{-1})	$b\times10^{-3}$ (cm^{-1})	R^a	Sd^b	F^c	Solvent excluded from correlation
0[d]	27.20 ±0.16	–0.26 ±0.18	0.86 ±0.09	–0.50 ±0.08	0.96	0.09	66.71	NMF, Acetone, Dioxane
1	27.66 ±0.15	–0.66 ±0.19	0.73 ±0.10	–0.30 ±0.11	0.95	0.12	41.08	–
2	27.35 ±0.10	–0.51 ±0.13	0.81 ±0.07	–0.54 ±0.07	0.98	0.08	95.16	–
3	27.54 ±0.13	–0.59 ±0.16	1.02 ±0.09	–0.37 ±0.10	0.98	0.10	88.12	–
4	27.53 ±0.12	–0.65 ±0.15	0.58 ±0.08	–0.29 ±0.08	0.96	0.09	50.09	–
5	27.43 ±0.11	–0.59 ±0.14	0.72 ±0.07	–0.47 ±0.08	0.97	0.08	73.13	–
6	27.35 ±0.14	–0.70 ±0.18	0.54 ±0.09	–0.32 ±0.10	0.94	0.11	33.11	–
7	26.88 ±0.26	-[e]	0.71 ±0.10	–0.22 ±0.14	0.93	0.10	20.25	DMSO, DMF, DMAc
8	27.13 ±0.12	–0.56 ±0.14	0.62 ±0.08	–0.62 ±0.11	0.96	0.09	40.05	DMF, Chl
9	28.39 ±0.59	–3.09 ±0.74	1.10 ±0.36	–1.35 ±0.37	0.92	0.39	22.73	NMF

[a] Correlation coefficient
[b] Standard deviation
[c] Fisher test of significance
[d] Unsubstituted compound
[e] Negligible values with high standard errors

Table 4.2.4 Results of the correlatin analysis of compounds in the **HP** form obtained according to Kamlet–Taft equation

No.	ν_0 x 10^{-3} (cm^{-1})	s x 10^{-3} (cm^{-1})	a x 10^{-3} (cm^{-1})	b x 10^{-3} (cm^{-1})	R	Sd	F	Solvent excluded from correlation
0[a]	32.33 ±0.47	-4.64 ±0.61	-1.07 ±0.32	0.73 ±0.30	0.94	0.29	23.31	Methanol, AcN, NMF, DMAc
1-HP	30.57 ±0.24	-2.20 ±0.31	-0.53 ±0.15	0.98 ±0.15	0.95	0.15	32.19	Methanol, 2-Butanol, NMF
2-HP	30.81 ±0.35	-2.51 ±0.44	-[b]	-[b]	0.89	0.26	15.23	1-Butanol
3-HP	31.70 ±0.20	-1.93 ±0.25	-0.68 ±0.12	-[b]	0.91	0.13	20.56	NMF
4-HP	31.42 ±0.44	-2.72 ±0.60	0.55 ±0.30	-1.17 ±0.38	0.92	0.32	19.38	2-Butanol, DCM
5-HP	30.28 ±0.22	-1.69 ±0.28	-0.27 ±0.16	0.45 ±0.16	0.90	0.17	15.43	Methanol, 1-Butanol
6-HP	29.24 ±0.61	-0.71 ±0.73	0.57 ±0.36	-[b]	0.72	0.35	3.96	Dioxane, NMF
7-HP	31.61 ±0.82	-4.41 ±1.01	-[b]	0.89 ±0.59	0.82	0.62	9.22	-
8-HP	31.79 ±0.57	-3.98 ±0.67	-0.68 ±0.41	-[b]	0.88	0.40	12.62	Methanol, Chl
9-HP	34.04 ±0.89	-7.58 ±1.11	-[b]	-1.24 ±0.56	0.92	0.58	22.12	NMF

[a] Unsubstituted compound [114]

[b] Negligible values with high standard errors

The correlation results helped us to evaluate the contribution of the each type of solvent–solute interactions on the spectral shift change of the appropriate tautomeric form. The positive value of the coefficient *a*, obtained for the **PY** form, indicate better stabilization of the molecule in the ground state (Table 4.2.3). Oppositely, negative sign of the coefficient *a*, obtained for the **HP** form (Table 4.2.4; except comps. **4** and **6**), indicate batochromic shift in relation to increased contribution of the HBD effect. It means that proton-accepting capabilities of both pyridine nitrogen and hydroxyl group in the **HP** form contribute in moderate extent to the solute stabilization in excited state (Table 4.2.4).

A negative sign of the coefficients *s* and *b*, obtained in correlations for the **PY** form (Table 4.2.3), indicate a batochromic shift of the absorption maxima with the increasing contribution of solvent dipolarity/polarizability and hydrogen-accepting capability. The largest value of coefficients *s* and *b* of the **PY** form was found in compound **9** (Table

4.2.3). It means that the most effective transmission of the substituent effect, *i.e.* electron-accepting ability of the nitro group, from *para*-position to the amide NH group increase dipolarity/polarizability and hydrogen-bonding capability of compound **9**. In the case of the compounds in the **HP** forms, non-specific solvent effect is the main contributing factor influencing batochromic shift, while specific solvent effects showed a lower and complex influence on solvatochromism of the investigated compounds (Table x?). Non-specific solvent effect is more pronounced in compounds in the **HP** form, comparing to the **PY** form, and largest effect was obtained for nitro-substituted compounds **7**-**9**.

The correlation results, obtained following Eq. 2.6.14, implied that the solvent dipolarity is the principal factor influencing the batochromic shift (Table 4.2.5).

Table 4.2.5 The results of the correlation analysis for PY tautomers obtained according to Catalán equation

Comp.	$v_0\times10^{-3}$ (cm^{-1})	$a\times10^{-3}$ (cm^{-1})	$b\times10^{-3}$ (cm^{-1})	$c\times10^{-3}$ (cm^{-1})	$d\times10^{-3}$ (cm^{-1})	*R*	*Sd*	*F*	Solvent excluded from correlation[a]
0[b]	28.13 ±0.66	1.57 ±0.32	–0.61 ±0.20	–1.01 ±0.31	–[c]	0.92	0.16	13.34	Acetone, Dioxane
1	29.50 ±0.44	0.88 ±0.21	–[c]	–0.33 ±0.17	–3.02 ±0.62	0.95	0.12	37.2	Chl
2	28.81 ±0.60	1.41 ±0.29	–0.82 ±0.21	–0.81 ±0.30	–1.34 ±0.79	0.93	0.16	15.7	2-Butanol, Dioxane
3	29.26 ±0.69	1.82 ±0.34	–0.58 ±0.23	–0.55 ±0.26	–2.09 ±0.91	0.93	0.18	18.2	–
4	28.48 ±0.60	1.67 ±0.42	–0.68 ±0.28	–0.49 ±0.23	–1.10 ±0.83	0.90	0.16	9.19	Methanol, Chl
5	28.66 ±0.53	1.33 ±0.26	–0.71 ±0.19	–0.74 ±0.20	–1.28 ±0.70	0.93	0.14	17.1	2-Butanol
6	28.83 ±0.43	0.86 ±0.21	–0.35 ±0.14	–1.27 ±0.21	–1.21 ±0.57	0.95	0.11	22.4	Dioxane
7	25.73 ±0.70	1.22 ±0.22	–[c]	–[c]	1.49 ±0.86	0.92	0.11	10.8	DMSO, DMAc, DCM
8	28.48 ±0.32	0.95 ±0.15	–0.43 ±0.11	–0.52 ±0.12	–1.97 ±0.41	0.97	0.08	33.7	DMAc, DCM
9	32.78 ±1.57	2.21 ±0.76	–1.38 ±0.53	–2.72 ±0.59	–6.05 ± 2.07	0.92	0.42	14.6	–

[a] No available literature data of solvent parameters for NMF; excluded from Catalán correlation
[b] Unsubstituted compound
[c] Negligible values with high standard errors

Table 4.2.6 Regression fits to the solvatochromic parameters for HP tautomer obtained according to Catalán equation

No.	v_0 x 10^{-3} (cm^{-1})	a x 10^{-3} (cm^{-1})	b x 10^{-3} (cm^{-1})	c x 10^{-3} (cm^{-1})	d x 10^{-3} (cm^{-1})	*R*	*Sd*	*F*	Solvent excluded from correlation
0[a]	34.86 ± 2.10	1.60 ± 0.99	-[b]	-3.27 ± 1.13	-5.03 ± 2.92	0.92	0.48	9.22	THF, AcN, Dioxane, 1-Propanol
1-HP	31.26 ± 0.68	0.55 ± 0.33	0.87 ± 0.23	-1.01 ± 0.26	-2.26 ± 0.87	0.94	0.17	18.83	THF, DMAc
2-HP	32.49 ± 0.76	0.55 ± 0.39	0.71 ± 0.31	-1.16 ± 0.30	-4.14 ± 1.06	0.95	0.26	19.48	THF, Chl
3-HP	33.00 ± 0.61	-0.85 ± 0.29	-[b]	-1.06 ± 0.23	-2.82 ± 0.79	0.91	0.16	10.27	1-Propanol, DMAc
4-HP	34.28 ± 0.96	1.05 ± 0.50	-[b]	-1.41 ± 0.37	-6.07 ± 1.33	0.95	0.25	19.55	THF, Chl
5-HP	30.00 ± 0.59	0.83 ± 0.29	0.59 ± 0.20	-1.17 ± 0.23	-[b]	0.92	0.16	13.57	1-Butanol
6-HP	32.32 ± 1.32	1.25 ± 0.52	-[b]	-2.94 ± 1.70	-2.49 ± 0.40	0.91	0.26	7.24	DMSO, DCM, 1-Propanol, 1-Butanol, THF
7-HP	36.16 ± 1.80	-[b]	0.75 ± 0.59	-3.06 ± 0.90	-7.09 ± 2.50	0.92	0.42	12.72	Dioxane, AcN
8-HP	35.35 ± 1.42	0.45 ± 0.70	0.34 ± 0.49	-3.00 ± 0.54	-3.61 ± 1.88	0.94	0.31	15.94	1-Butanol, DMSO
9-HP	42.26 ± 2.20	-[b]	-1.10 ± 0.73	-5.29 ± 0.83	-13.48 ± 2.83	0.94	0.56	18.09	DMA

[a] Unsubstituted compound [ref iz rada]

[b] Negligible values with high standard errors

Quantitative separation of the non-specific solvent effect (coefficient *s*; Tables 4.2.3 and 4.2.4) on polarizability and dipolarity term (coefficients *c* and *d*, Tables 4.2.5 and 4.2.6), showed high significance of the solvent dipolarity on stabilization of the excited state in both forms. High values of coefficient *d* and lower values of coefficient *c*, obtained for all compounds in the **HP** form (Table 4.2.6), indicate pronounced influence of solvent dipolarity and less polarizability effects on ν_{max} change. This means that strong electron-withdrawing character of the nitro group causes high extent of π-electron delocalization which contributes to larger dipolarity and π-electron polarizability of compunds in the **HP** form. This could not be applied for compounds in the **PY** form where the most pronounced non-specific solvent effect was noticed only for compound **9**. It means that contribution of zwitter-ionic structure (Fig. 4.2.1c) in an overall resonance hybrid of compound **9** in the **PY** form causes increased molecule dipolarity.

Solvent hydrogen-bonding interactions have moderate to low contribution on the absorption maxima shift and preferentially acts through hydrogen-bonding with the hydroxyl and the pyridine aza groups of the solutes in the **HP** form (Table 4.2.5). Significant number of compound show negligible values and complex influence of specific solvent effects on solvatochromism of the investigated compounds (Table 4.2.5). Negative values of the coefficient *b* indicate higher stabilization of the excited state in **PY** form, while opposite is true for HBD solvent effect.

The comparison of the correlation results obtained for unsubstituted compound in the **PY** form indicate low contribution of non-specific solvent effect (Table 4.2.3). Similar results, negligible *d* and moderate value of coefficient *c*, were obtained according to Catalán equation (Table 4.2.5). Such result strongly indicates low contribution of zwitter-ionic structure c) (Fig. x?) to overall resonance hybrid of this compound in the **PY** form. Solvent dipolarity and polarizability are dominant effects contributing to higher stabilization of excited state of unsubstituted compound in the **HP** form (Tables 4.2.4 and 4.2.6). Larger dipolarity and π-electron mobility of the **HP** form is a mainly consequence of appropriate molecular geometry which enable larger extent of π-electron conjugative transfer. Introduction of electron-donating substituents cause decreases of π-electron mobility, *i.e.* decreases of contribution of dipolarity and polarizability effects. Oppositely, introduction of electron-accepting substituents, from chloro to nitro, causes significant increases of coefficients *c* and *d* (Table 4.2.6; except comps. **6** and **8**).

In order to examine influence of HBD solvent effect on the state of tautomeric equilibria, UV/Vis spectra of some compounds were recorded in a different set of solvent mixtures. Representative examples of UV spectra of compound **3,** recorded in a mixture of THF/NMF, are shown on Fig. 4.2.7 a). The second derivative of the spectra are presented in Fig. 4.2.7 b). An example of the K_T evaluation is given in Fig. 4.2.6, and the determined K_T values are: K_T=0.46 (100 % THF); K_T=0.53 (70 % THF); K_T=0.82 (50 % THF); K_T=0.96 (30 % THF); and K_T=1.40 (10 % THF). Obtained results showed appropriate relation between **PY/HP** tautomer and the contribution of appropriate solvent effects [219].

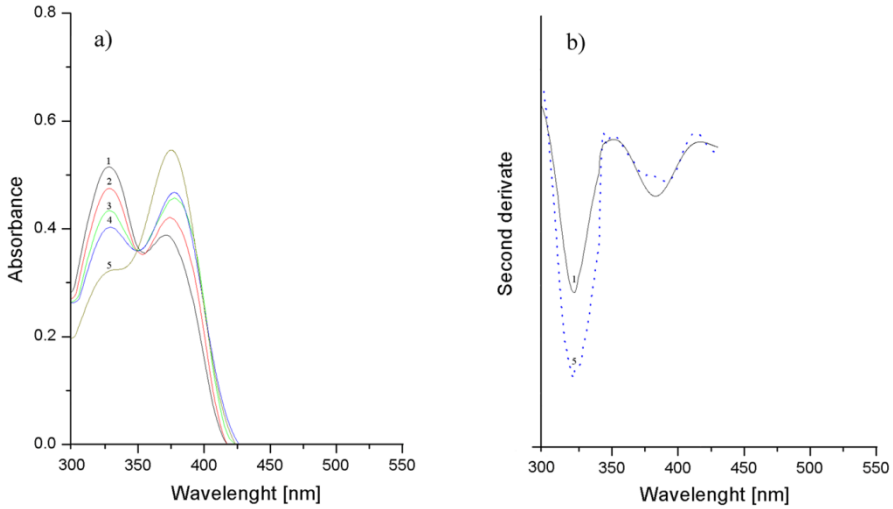

Fig. 4.2.7 Absorption spectra of comp. **3** in a different v/v ratio of THF/NMF: a) 100%; 2) 70%; 3) 50%; 4) 30%; 5), and 10% THF; b) Second derivate of spectra **1** and **5**

It is noticeable that tautomeric forms exist in the different ratio in appropriate solvent mixture. Increasing proportion of protic solvent, *i.e.* increasing of hydrogen-bonding capability of solvent mixture, causes increase of K_T value. Solvation phenomena refer to the interaction between dissolved molecule and solvents, which leads to the stabilization of the system by formation of solvation shells. In binary mixtures of solvents, a solute could form different types of preferential interactions with surrounding solvent molecules in different extent. This is in accordance with the fact that higher HBD ability of solvent mixture shift equilibrium toward the lactam form [9]. Also, this is an example how adjustment of HBD/HBA properties of solvent mixture could control the state of tautomeric equilibria.

The success of the quantification and interpretation of solvent effects on the position of the absorption maxima of the investigated molecules (Fig. 4.2.8) was evaluated by plotting the calculated frequency (ν_{calc}), obtained by Catalán parameter set, *versus* the measured frequency (ν_{exp}) (R=0.95, Sd=0.18, F=1295.6).

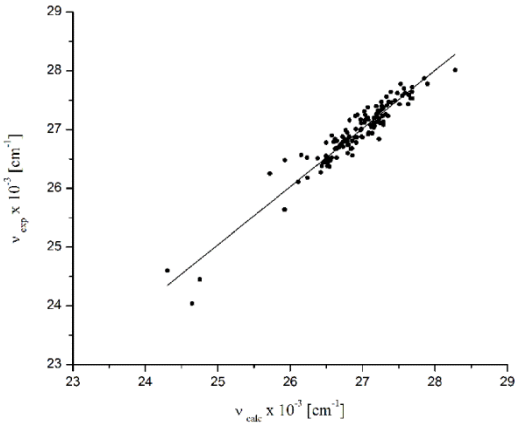

Fig. 4.2.8 The plot of ν_{exp} *vs.* ν_{calc}

According to the described method K_T values of the investigated compounds in all used solvents were determined, and the results are presented in Table 4.2.7.

Table 4.2.7 Equilibrum constants K_T in selected solvents

Solvent	Relative Permittivity*	K_T/compound								
		1	**2**	**3**	**4**	**5**	**6**	**7**	**8**	**9**
Methanol	32.66	1.42	1.26	1.41	1.35	1.21	1.27	1.33	1.25	1.40
Ethanol	24.55	1.08	1.17	2.00	1.06	1.05	1.17	1.46	1.09	1.28
1-Propanol	20.45	1.17	1.18	1.24	1.22	1.31	1.28	1.37	1.29	1.36
2-Propanol	19.92	1.23	1.19	1.05	1.03	1.17	1.21	1.05	1.07	1.11
1-Butanol	17.51	1.05	1.14	1.12	1.75	1.81	1.79	1.06	1.11	1.13
2-Butanol	16.56	1.19	1.80	1.99	1.93	1.89	1.91	1.32	1.45	1.49
Dioxane	2.21	0.76	0.79	0.58	0.80	0.73	0.61	0.63	0.59	0.60
EtAc	6.02	0.78	0.71	0.79	0.75	0.69	0.77	0.73	0.89	0.67
THF	7.58	0.66	0.65	0.46	0.82	0.65	0.67	0.61	0.69	0.59
ACN	35.94	0.63	0.79	0.70	0.65	0.81	0.72	0.73	0.77	0.81
Acetone	20.56	0.75	0.88	0.71	0.73	0.88	0.79	0.78	0.81	0.80
DMSO	46.45	0.72	0.55	0.41	0.68	0.61	0.59	0.79	0.75	0.69
DMF	36.71	0.70	0.51	0.34	0.65	0.60	0.58	0.74	0.72	0.67
DMAc	37.78	0.60	0.77	0.36	0.56	0.63	0.59	0.67	0.70	0.65
NMF	182.40	1.20	1.18	1.80	1.36	1.38	1.95	1.38	1.66	1.93
DCM	8.93	1.13	1.07	1.01	1.11	1.09	1.07	1.18	1.12	1.10
Chl	4.89	1.02	1.21	1.36	1.03	1.20	1.29	1.10	1.12	1.15

* Ref [iz rada Reichardt, 2003?]

The changes in the K_t values (Table 4.2.7) are consequence of the contribution of both solvent effects as well as the nature of the substituent present. Balanced contribution of protic solvent effects on K_T (increased contribution of HBD effect) cause shift of the tautomeric equilibria to the **PY** form (higher K_t values); opposite is true for aprotic solvents, *i.e*. solvent with increased dipolarity/polarizability and proton-accepting capability (lower K_t values). It could be postulated that such behavior is a consequence in the differences in conjugational ability of the π-electron densities through localized or delocalized π-electronic systems of the appropriate tautomeric forms.

4.2.3 LFER analysis of UV data

A comprehensive analysis of substituent effects on absorption spectra of the investigated molecules, by using LFER principles in the form of the Hammett equation (Eq. 2.6.1), was performed. The correlation results for **PY** and **HP** forms are given in Tables 4.2.8 and 4.2.9, respectively.

Table 4.2.8 Regression fits according to Hammett equation for the **PY** form of investigated compounds

Solvent/ Compound	ν_0 x 10^{-3} (cm^{-1})	ρ x 10^{-3} (cm^{-1})	*R*	*Sd*	*F*	ν_0 x 10^{-3} (cm^{-1})	ρ x 10^{-3} (cm^{-1})	*R*	*Sd*	*F*
	2, 3, 5, 6, 8, 9					**1, 4, 7**				
Methanol	27.67 ± 0.08	–0.97 ± 0.17	0.94	0.15	31.9	27.75 ± 0.08	-0.23 ± 0.09	0.93	0.09	6.2
Ethanol	27.50 ± 0.11	–0.93 ± 0.24	0.93	0.20	35.5	27.67 ± 0.01	-0.45 ± 0.01	0.99	0.01	7871
1-Propanol	27.40 ± 0.06	–0.88 ± 0.12	0.96	0.10	54.1	27.60 ± 0.05	-0.23 ± 0.08	0.95	0.05	8.9
2-Propanol	27.49 ± 0.07	–1.04 ± 0.15	0.96	0.13	45.9	27.57 ± 0.13	-0.38 ± 0.09	0.91	0.17	7.6
1-Butanol	27.45 ± 0.01	–0.94 ± 0.24	0.93	0.21	32.0	27.61 ± 0.01	-0.39 ± 0.01	0.99	0.01	1058.1
2-Butanol	27.39 ± 0.07	–0.97 ± 0.15	0.96	0.13	43.5	27.63 ± 0.02	-0.39 ± 0.03	0.99	0.02	174.3
EtAc	27.00 ± 0.07	–0.73 ± 0.15	0.92	0.13	22.4	27.29 ± 0.01	-0.43 ± 0.01	0.99	0.01	7871
THF	26.87 ± 0.19	–0.94 ± 0.40	0.91	0.15	30.2	26.98 ± 0.05	-0.20 ± 0.07	0.94	0.05	7.8
Acetone	26.93 ± 0.07	–0.66 ± 0.16	0.91	0.14	17.9	27.17 ± 0.06	-0.28 ± 0.09	0.95	0.06	9.3
DCM	27.19 ± 0.09	–0.67 ± 0.19	0.92	0.16	22.1	27.07 ± 0.05	-0.13 ± 0.07	0.92	0.06	5.9
	2, 3, 6, 8, 9					**1, 4, 5, 7**				
Dioxane	26.96 ± 0.05	–0.48 ± 0.09	0.94	0.08	24.5	27.21 ± 0.01	-0.36 ± 0.02	0.99	0.01	275.5
Chl	27.37 ± 0.05	–1.01 ± 0.10	0.98	0.09	95.9	27.63 ± 0.09	-0.49 ± 0.16	0.91	0.12	8.9
AcN	27.10 ± 0.22	–1.27 ± 0.44	0.92	0.40	18.2	27.34 ± 0.10	-0.56 ± 0.17	0.92	0.12	10.8
	2, 3, 6, 8, 9					**1, 4, 5**				
NMF	27.09 ± 0.09	–1.06 ± 0.19	0.95	0.17	29.65	27.40 ± 0.04	-0.85 ± 0.12	0.99	0.03	49.2
	2, 3, 6, 9					**1, 4, 5, 7, 8**				
DMSO	26.48 ± 0.25	–2.08 ± 0.58	0.93	0.41	13.3	26.75 ± 0.20	0.43 ± 0.33	0.91	0.20	7.5
DMF	26.44 ± 0.27	–2.18 ± 0.63	0.94	0.37	12.1	26.56 ± 0.30	0.10 ± 0.46	0.91	0.35	5.5
DMAc	26.52 ± 0.37	–2.68 ± 0.86	0.91	0.64	9.8	26.58 ± 0.22	0.55 ± 0.35	0.92	0.27	6.7

Table 4.2.9 Regression fits according to Hammett equation for the **HP** tautomer of investigated compounds

Solvent/ Compound	ν_0 x 10^{-3} (cm^{-1})	ρ x 10^{-3} (cm^{-1})	*R*	*Sd*	*F*	ν_0 x 10^{-3} (cm^{-1})	ρ x 10^{-3} (cm^{-1})	*R*	*Sd*	*F*
	1, 2, 3, 4					**5, 6, 8, 9**				
Methanol	29.94 ± 0.01	-0.14 ± 0.05	0.90	0.02	8.22	30.10 ± 0.10	-1.23 ± 0.17	0.98	0.08	52.21
	1, 2, 3, 4					**5, 6, 8, 9**				
Ethanol	29.76 ± 0.06	-1.05 ± 0.26	0.94	0.12	16.18	30.34 ± 0.17	-2.17 ± 0.29	0.98	0.13	55.81
	1, 2, 3, 6					**4, 5, 8, 9**				
1-Propanol	29.69 ± 0.12	-1.48 ± 0.62	0.86	0.23	5.62	30.82 ± 0.20	-2.87 ± 0.34	0.99	0.13	69.30
	1, 2, 3, 5					**4, 6, 8, 9**				
2-Propanol	29.89 ± 0.09	-0.89 ± 0.37	0.86	0.17	5.68	29.40 ± 0.05	-0.52 ± 0.08	0.98	0.04	40.33
	1, 2, 3, 6, 8					**4, 5, 9**				
1-Butanol	29.83 ± 0.08	-2.01 ± 0.24	0.98	0.17	72.11	29.36 ± 0.08	-0.53 ± 0.14	0.97	0.05	13.64
	1, 2, 3, 4, 6					**5, 8, 9**				
2-Butanol	29.91 ± 0.01	-1.96 ± 0.06	0.99	0.03	1192.86	29.80 ± 0.10	-0.33 ± 0.15	0.91	0.05	4.62
	1, 2, 3, 4, 6					**5, 7, 9**				
Dioxane	29.95 ± 0.08	-1.81 ± 0.32	0.96	0.16	32.54	29.91 ± 0.05	-0.33 ± 0.06	0.98	0.03	28.00
	1, 2, 3, 6					**4, 5, 8, 9**				
EtAc	29.92 ± 0.05	-2.87 ± 0.26	0.99	0.10	117.10	29.61 ± 0.15	-0.48 ± 0.26	0.80	0.09	3.47
	1, 2, 3, 5					**4, 8, 9**				
THF	30.14 ± 0.03	-1.68 ± 0.11	0.99	0.05	215.72	30.19 ± 0.48	-1.05 ± 0.74	0.82	0.21	2.06
	1, 2, 3, 6					**4, 5, 7**				
AcN	29.38 ± 0.15	-3.01 ± 0.78	0.94	0.30	15.04	30.21 ± 0.01	-3.11 ± 0.01	0.99	0.01	56012
	1, 2, 3, 6					**4, 5, 9**				
Acetone	29.46 ± 0.06	-2.67 ± 0.34	0.98	0.12	62.78	29.51 ± 0.10	-1.67 ± 0.17	0.99	0.06	90.84
	1, 2, 3, 6					**4, 5, 7, 8, 9**				
DCM	28.98 ± 0.08	-3.16 ± 0.45	0.98	0.17	48.62	28.95 ± 0.19	-0.98 ± 0.27	0.90	0.16	12.86
	1, 3, 5, 7					**2, 4, 6, 9**				
DMSO	29.32 ± 0.17	-1.44 ± 0.29	0.96	0.29	24.06	29.55 ± 0.57	-5.34 ± 1.24	0.95	0.62	18.47
	1, 3, 4, 7					**2, 5, 6, 8, 9**				
DMF	29.47 ± 0.10	-0.70 ± 0.17	0.94	0.17	16.18	29.57 ± 0.74	-4.25 ± 1.43	0.86	0.83	8.86
	1, 3, 5, 7					**2, 4, 6, 8, 9**				
DMAc	29.72 ± 0.02	-1.62 ± 0.03	0.99	0.03	3222	29.07 ± 0.31	-2.22 ± 0.60	0.91	0.35	13.61
	1, 6, 8, 9					**2, 3, 5, 7**				
Chl	29.16 ± 0.04	-0.59 ± 0.07	0.98	0.04	67.69	29.78 ± 0.12	-0.93 ± 0.22	0.95	0.21	18.46

The correlation results (Table 4.2.8), classified in the four sets of solvents and two groups (columns) of substituent-dependent correlation results, reflect the balanced interplay of solvent and substituent effects on absorption maxima shifts. The introduction of both electron-donating and electron-withdrawing substituents contributes to positive solvatochromism in all solvents, except for compounds **1, 4, 5, 7, 8** in DMSO, DMF and DMAc. Good correlation results were obtained in all solvents.

In the first set of protic solvent (comps. **2**, **3**, **5**, **6**, **8**, and **9**), as well as second and third sets of solvents (comps. **2**, **3**, **6**, **8**, and **9**) a similar correlation slopes were observed. Somewhat higher values were noticed for solvents which show increased HBD property: Chl, AcN and NMF. These results indicate that solvent effects: dipolarity/polarizability, HBD and HBA abilities cause appropriate sensitivity of the position of absorption maxima (ν_{max}) to substituent effect. In the last set of aprotic solvents (DMSO, DMF and DMAc), highest sensitivity of ν_{max} to substituent effect was found. Exceptionally higher value of correlation slope, found for compounds **2, 3, 6, 9** in DMSO, DMF and DMAc, indicate utmost significance of the solvent dipolarity/polarizabilty and proton-accepting capabilities to higher stabilization of excited state of these compounds.

Lower susceptibility of the ν_{max} shifts to the electronic substituent effects was found for *ortho*-substituted 2(1*H*)-pyridones, *i.e*. compounds **1**, **4** and **7 (**first set of solvents), for compounds **1**, **4**, **5**, and **7** (second set), and for compounds **1**, **4**, **5**, **7** and **8** (forth set; lower value was found for DMF). Significantly higher slope (ρ = –0.85) was noticed for NMF. These results showed specific influences of the *ortho*-substituents on the shift of absorption maxima. It is generally assumed that *ortho*-effect include electronic, steric and anisotropic factors [192]. Electronic and steric effects exert significant influence on solvatochromism. The electronic effect is not necessarily transmitted exclusively by polar (inductive) and π-electron delocalization (resonance) mechanisms, but could also be transmitted through space. Steric effect includes electronic density shift, bond length and bond angle change, and effect due to size of the *ortho*-substituent.

Results of LFER study clearly show higher stabilization of the **PY** form in the excited state, observed for compounds **2, 3, 6, 9** in DMSO, DMF and DMAc. Higher sensitivities of their absorption frequencies to substituent effects in these solvents might be explained in following way: at high relative permittivity of surrounding medium, the energy necessary to bring about

charge separation in the excited state is relatively small, which gives rise to a higher susceptibility to electronic substituent effects. Highly dipolar aprotic solvents (DMSO, DMF and DMAc) behave as poor anion solvators, while they usually better stabilize larger and more dispersible positive charges. The electronic systems of the investigated 2(1*H*)-pyridones, considering their *non*-planarity [as obtained from DFT calculation (Tables S9-S11?)], could be more susceptible to the substituent influence. Study of the transmission of substituent electronic effects through defined π-resonance units (Fig. 4.2.1b) showed that they behave either as isolated or conjugated fragments, and depend on substitution pattern under consideration [192].

Correlation obtained for the data derived in NMF, indicates significance of both HBD and non-specific solvent properties of NMF. Higher slope obtained for compounds **1**, **4** and **5** (second column) indicate that an appropriate balance of substituent and solvent effect may effectively contribute at different extent in the ground and in the excited states to the stabilization of solute. The complex influences of both solvent and substituent effect on UV/Vis absorption maxima of the **HP** forms (Table 4.2.9), confirmed such conclusions, contributing to higher sensitivity and larger stabilization of excited state.

4.2.4 DFT, TD-DFT and Bader's analysis. Evaluation of electronic transition and charge density change

An additional analysis of solvent and substituent effects on absorption frequencies, tautomeric equilibria and conformational changes of the studied compounds necessitated quantum-chemical calculations, *i.e.* geometry optimization and charge density analysis. Geometry optimization of the investigated molecules was performed by the use of B3LYP functional with 6-311G(d,p) basis set. The most stable conformations of compounds **1-3** in both **PY** and **HP** forms are presented in Fig. 4.2.9.

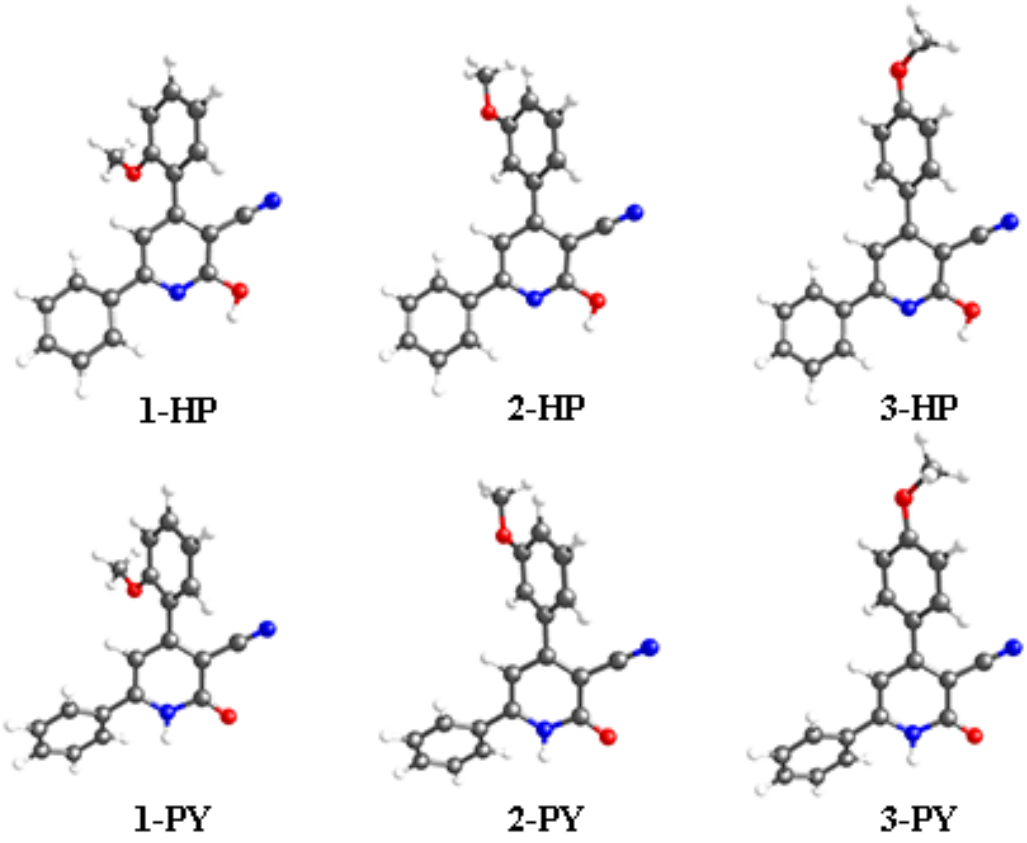

Fig. 4.2.9 Optimal geometries of both **HP** and **PY** forms of compounds **1 - 3**

Detailed information on elements of optimized geometries of compounds **1-9** are given in Tables 4.2.10-4.2.12.

Table 4.2.10 Elements of the optimized geometries of compounds **1 - 3** of both tautomers obtained by the use of DFT method

Bond/Compound	**1-PY**	**1-HP**	**2-PY**	**2-HP**	**3-PY**	**3-HP**
Interatomic distance (Å)						
N17-C16	1.4089	1.3215	1.4078	1.3224	1.4079	1.3222
C16-C15	1.4626	1.4155	1.4648	1.4155	1.4642	1.4152
C15-C14	1.3915	1.4122	1.3946	1.4123	1.3951	1.4143
C14-C13	1.4235	1.3996	1.4247	1.4004	1.4623	1.4024
C13-C12	1.3755	1.3982	1.3748	1.3997	1.3742	1.3987
C12-N17	1.3661	1.3506	1.3656	1.3495	1.3659	1.3500
C15-C19	1.4264	1.4278	1.4273	1.4276	1.4269	1.4273
C14-C23	1.4877	1.4864	1.4865	1.4856	1.4817	1.4805
C16=O21/C16-O21-H	1.2233	1.3463	1.2229	1.3454	1.2231	1.3458
Torsion angle θ (º)						
θ_1	36.42	21.65	36.75	20.18	37.20	20.98
θ_2	55.92	54.28	47.88	47.20	43.78	43.62
Energy (kcal/mol)						
Gas[a]	0	+0.91	0	+0.74	0	+0.88
Ethanol	-12.73	-10.26	-12.99	-10.49	-13.08	-10.55
THF	-10.92	-8.65	-11.16	-8.85	-11.24	-8.90
AcN	-13.05	-10.57	-13.31	-10.78	-13.41	-10.84
DMSO	-13.03	-10.67	-13.32	-10.76	-13.41	-13.41

[a] Relative ratio with respect to the form of higher stability

Table 4.2.11 Elements of the optimized geometries of compounds **4 - 6** compounds obtained by the use of DFT method

Bond/Compound	**4-PY**	**4-HP**	**5-PY**	**5-HP**	**6-PY**	**6-HP**
Interatomic distance (Å)						
N17-C16	1.4080	1.3181	1.4087	1.3187	1.4086	1.3187
C16-C15	1.4648	1.4134	1.4647	1.4135	1.4645	1.4134
C15-C14	1.3852	1.4058	1.3884	1.4087	1.3890	1.4092
C14-C13	1.4188	1.3940	1.4216	1.3971	1.4223	1.3978
C13-C12	1.3724	1.3980	1.3728	1.3982	1.3724	1.3978
C12-N17	1.3648	1.3468	1.3632	1.3461	1.3633	1.3462
C15-C19	1.4239	1.4241	1.4236	1.4239	1.4236	1.4239
C14-C23	1.4905	1.4891	1.4875	1.4858	1.4857	1.4842
C16=O21/C16-O21-H	1.2154	1.3426	1.2153	1.3422	1.2155	1.3423
Torsion angle θ (º)						
θ_1	36.81	21.07	36.94	19.97	37.17	20.91
θ_2	63.90	63.20	48.04	47.40	47.06	46.57
Energy (kcal/mol)						
Gas[a]	0	+1.01	0	+0.76	0	+0.74
Ethanol	-11.66	-9.49	-11.82	-9.54	-11.75	-9.65
THF	-10.01	-7.99	-9.99	-8.03	-10.09	-8.14
AcN	-11.96	-9.75	-12.11	-9.81	-12.03	-9.92
DMSO	-11.95	-9.73	-12.11	-9.77	-12.04	-9.90

[a] Relative ratio with respect to the form of higher stability

Table 4.2.12 Elements of the optimized geometries of compounds **7 - 9** investigated compounds obtained by the use of DFT method

Bond/Compound	**7-PY**	**7-HP**	**8-PY**	**8-HP**	**9-PY**	**9-HP**
Interatomic distance (Å)						
N17-C16	1.4085	1.3188	1.4088	1.3187	1.4093	1.3190
C16-C15	1.4645	1.4124	1.4649	1.4135	1.4651	1.4136
C15-C14	1.3840	1.4034	1.3882	1.4087	1.3877	1.4084
C14-C13	1.4182	1.3927	1.4206	1.3961	1.4207	1.3964
C13-C12	1.3717	1.3987	1.3735	1.3990	1.3735	1.3991
C12-N17	1.3639	1.3459	1.3627	1.3458	1.3628	1.3457
C15-C19	1.4235	1.4233	1.4233	1.4236	1.4233	1.4236
C14-C23	1.4923	1.4923	1.4881	1.4863	1.4878	1.4858
C16=O21/ C16-O21-H	1.2151	1.3418	1.2149	1.3415	1.2146	1.3411
Torsion angle θ (º)						
θ_1	39.10	22.74	37.21	20.43	36.92	20.51
θ_2	61.31	69.45	47.08	46.37	49.57	48.17
Energy (kcal/mol)						
Gas[a]	0	+1.18	0	+0.72	0	+0.65
Ethanol	-13.66	-11.71	-14.02	-11.58	-13.93	-11.89
THF	-11.70	-9.88	-11.70	-9.79	-11.99	-10.07
AcN	-14.01	-12.04	-14.36	-11.90	-14.26	-12.20
DMSO	-14.00	-12.00	-14.38	-11.88	-14.30	-12.19

[a] Relative ratio with respect to the form of higher stability

Molecular geometries parameters of the **PY** and **HP** forms are fairly similar, and despite on this, the relationship between structural elements and solvatohromism is not fully consistent. Theoretical absorption spectra of both tautomeric forms, *i.e.* the absorption frequencies ν_{max}, calculated in gas phase, ethanol, THF, AcN and DMSO with TD-DFT method are given in Tables 4.2.13 and 4.2.14.

Table 4.2.13 The absorption frequencies of the **PY** form of all compounds in selected solvents obtained by the use of DFT method

Solvent/ Compound	ν_{max} x10^{-3} (cm^{-1})								
	1-PY	**2-PY**	**3-PY**	**4-PY**	**5-PY**	**6-PY**	**7-PY**	**8-PY**	**9-PY**
Ethanol	27.30	27.53	28.01	28.59	28.26	28.17	24.13	25.50	24.50
THF	27.38	27.41	27.97	28.49	28.04	28.08	24.19	25.54	24.66
AcN	27.30	27.56	28.02	28.61	28.17	28.11	24.11	25.45	24.47
DMSO	27.25	27.51	27.92	28.48	28.14	28.05	24.14	25.44	24.41

Table 4.2.14 The absorption frequencies of the **HP** form of all compounds in selected solvents obtained by the use of DFT method

Solvent/ Compound	ν_{max} x10^{-3} (cm^{-1})								
	1-HP	**2-HP**	**3-HP**	**4-HP**	**5-HP**	**6-HP**	**7-HP**	**8-HP**	**9-HP**
Ethanol	28.56	28.81	28.78	31.23	30.80	30.76	26.13	27.01	26.32
THF	28.69	28.84	28.81	31.26	30.81	30.78	26.28	27.22	26.55
ACN	28.54	28.81	28.79	31.24	30.80	30.76	26.11	26.98	26.28
DMSO	28.46	28.78	28.72	31.10	30.66	30.62	26.10	26.98	26.24

The feature of the greatest interest in the ground state of investigated compounds is the values of torsion angle θ_1 (Fig. 4.2.1b), which are, among other factors, significantly influenced by the magnitude of substituent effects (Tables 4.2.10-4.2.12). It is generally accepted that higher planarity of molecule, *i.e*. lower torsional angle, induces red shift in the absorption spectra. In the investigated molecules, these values are somewhat larger for the **PY** than for the **HP** form, which means that transmission of the electronic substituent effects, mainly resonance interaction, is more suppressed in the **PY** form. Somewhat larger differences of θ_1 was noticed for compound **7** (Table 4.2.12: 39.10 for **7-PY** and 22.74 for **7-HP**), indicating significance of *ortho*-effect, *i.e.* vicinity of the substituent which exert large polar (inductive/field) and steric effects. It was also explained significance of the through-space field effect [192], which cause appropriate perturbation of π–electron density of the pyridone ring.

The results shown in Tables 4.2.10-4.2.12 indicate that bond lengths of the **PY** and **HP** forms are obviously different; while lower differences in bond lengths between *ortho*-, *meta*- and *para*-substituted compounds could be observed. In the **PY** form, low influences of the substituent electronic effects are observed, while in the **HP** form, a well-defined alternation could be noticed. Appropriate values of bond distances are in the frame of statistical errors and thus they are not suitable for evaluation purpose. Generally, the bond lengths of the carbonyl groups get longer,

while the bond length of C14–C23 (Fig. 4.2.10) gets shorter, and the deviation from the planarity (expressed in term of torsional angle θ_1) decreases with increasing electron-donating ability of the substituent. A decrease in the C14–C23 bond length, which is a bridging bond between π_1- and π_3-unit, indicates a greater extent of the extended π,π-delocalization. The results are opposite for the electron-acceptor substituted compounds **7**-**9** (Table 4.2.12). The common polarization of carbonyl groups is suppressed, and the slight decrease of the bond length was observed (Table 4.2.12). Generally, an electron-acceptor withdraw electron density from pyridone ring, causing decrease of the extent of π,π-conjugation in enone system (π_1-unit), and simultaneously exerts enhancement of n,π-conjugation in π_2-unit (Fig. 4.2.1). The largest contribution of solvent effects to stabilization of solvated molecules in ground state was obtained in polar aprotic solvents AcN and DMSO, ethanol exert somewhat lower influence, while lowest stabilization was found in THF (Tables 4.2.10-4.2.12).

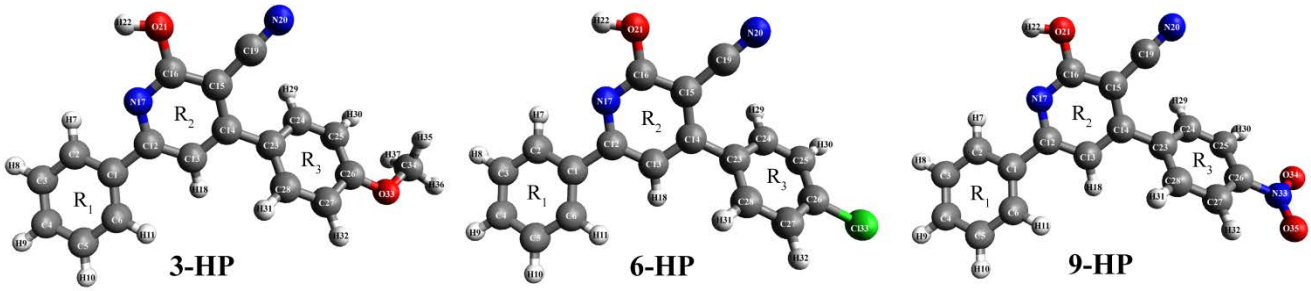

Fig. 4.2.10 Numbering of the atoms used in Bader's analysis for all investigated compounds (examples given for **3-HP**, **6-HP** and **9-HP** compounds)

Mechanism of electronic excitations and the electron density distribution in ground and excited states were studied by calculation of HOMO/LUMO energies (E_{HOMO}/ E_{LUMO}) and E_{gap} values (Tables 4.2.15-4.2.17, and Fig. 4.2.11).

Table 4.2.15 Calculated energies of the HOMO and LUMO orbitals and energy gap for compounds **1**, **2** and **3** in gas phase, ethanol, THF, AcN and DMSO

	Energy/Compound	**1-PY**	**1-HP**	**2-PY**	**2-HP**	**3-PY**	**3-HP**
Gas	E_{HOMO}	-6.35	-6.43	-6.34	-6.42	-6.22	-6.35
	E_{LUMO}	-2.35	-2.09	-2.49	-2.21	-2.40	-2.16
	E_{gap}	4.00	4.34	3.85	4.21	3.82	4.19
Ethanol	E_{HOMO}	-6.35	-6.37	-6.42	-6.40	-6.37	-6.34
	E_{LUMO}	-2.35	-2.19	-2.44	-2.26	-2.38	-2.22
	E_{gap}	4.00	4.18	3.98	4.14	3.99	4.12
THF	E_{HOMO}	-6.34	-6.37	-6.43	-6.40	-6.35	-6.33
	E_{LUMO}	-2.35	-2.17	-2.45	-2.25	-2.38	-2.21
	E_{gap}	3.99	4.20	3.98	4.15	3.97	4.12
AcN	E_{HOMO}	-6.35	-6.37	-6.42	-6.41	-6.37	-6.34
	E_{LUMO}	-2.35	-2.19	-2.44	-2.27	-2.38	-2.22
	E_{gap}	4.00	4.18	3.98	4.14	3.99	4.12
DMSO	E_{HOMO}	-6.35	-6.37	-6.43	-6.41	-6.38	-6.34
	E_{LUMO}	-2.35	-2.20	-2.44	-2.27	-2.38	-2.22
	E_{gap}	4.00	4.17	3.99	4.14	4.00	4.12

Table 4.2.16 Calculated energies of the HOMO and LUMO orbitals and energy gap for compounds **4**, **5** and **6** in gas phase, ethanol, THF, AcN and DMSO

	Energy/Compound	**4-PY**	**4-HP**	**5-PY**	**5-HP**	**6-PY**	**6-HP**
Gas	E_{HOMO}	-6.42	-6.65	-6.50	-6.74	-6.49	-6.75
	E_{LUMO}	-2.53	-2.28	-2.67	-2.42	-2.66	-2.41
	E_{gap}	3.89	4.37	3.83	4.32	3.83	4.34
Ethanol	E_{HOMO}	-6.45	-6.61	-6.45	-6.62	-6.44	-6.62
	E_{LUMO}	-2.45	-2.28	-2.50	-2.34	-2.50	-2.32
	E_{gap}	4.00	4.33	3.95	4.28	3.94	4.30
THF	E_{HOMO}	-6.45	-6.61	-6.47	-6.64	-6.46	-6.64
	E_{LUMO}	-2.46	-2.28	-2.54	-2.35	-2.52	-2.34
	E_{gap}	3.99	4.33	3.93	4.29	3.94	4.30
AcN	E_{HOMO}	-6.45	-6.61	-6.45	-6.62	-6.44	-6.61
	E_{LUMO}	-2.45	-2.28	-2.49	-2.34	-2.49	-2.32
	E_{gap}	4.00	4.33	3.96	4.28	3.95	4.29
DMSO	E_{HOMO}	-6.45	-6.61	-6.46	-6.62	-6.44	-6.62
	E_{LUMO}	-2.45	-2.28	-2.50	-2.34	-2.49	-2.33
	E_{gap}	4.00	4.33	3.96	4.28	3.95	4.29

Table 4.2.17 Calculated energies of the HOMO and LUMO orbitals and energy gap for compounds **7**, **8** and **9** in gas phase, ethanol, THF, AcN and DMSO

	Energy/Compounds	**7-PY**	**7-HP**	**8-PY**	**8-HP**	**9-PY**	**9-HP**
Gas	E_{HOMO}	-6.48	-6.71	-6.65	-6.87	-6.70	-6.92
	E_{LUMO}	-2.88	-2.77	-2.90	-2.85	-3.11	-3.00
	E_{gap}	3.60	3.94	3.75	4.02	3.59	3.92
Ethanol	E_{HOMO}	-6.49	-6.64	-6.49	-6.66	-6.50	-6.66
	E_{LUMO}	-2.87	-2.81	-2.85	-2.85	-3.03	-2.97
	E_{gap}	3.62	3.83	3.64	3.81	3.47	3.69
THF	E_{HOMO}	-6.50	-6.65	-6.53	-6.69	-6.53	-6.70
	E_{LUMO}	-2.88	-2.80	-2.87	-2.86	-3.04	-2.98
	E_{gap}	3.62	3.85	3.66	3.83	3.49	3.72
AcN	E_{HOMO}	-6.49	-6.64	-6.49	-6.64	-6.49	-6.66
	E_{LUMO}	-2.87	-2.81	-2.85	-2.85	-3.03	-2.97
	E_{gap}	3.62	3.83	3.64	3.79	3.46	3.69
DMSO	E_{HOMO}	-6.50	-6.65	-6.49	-6.66	-6.49	-6.66
	E_{LUMO}	-2.88	-2.82	-2.85	-2.86	-3.03	-2.97
	E_{gap}	3.62	3.83	3.64	3.80	3.46	3.69

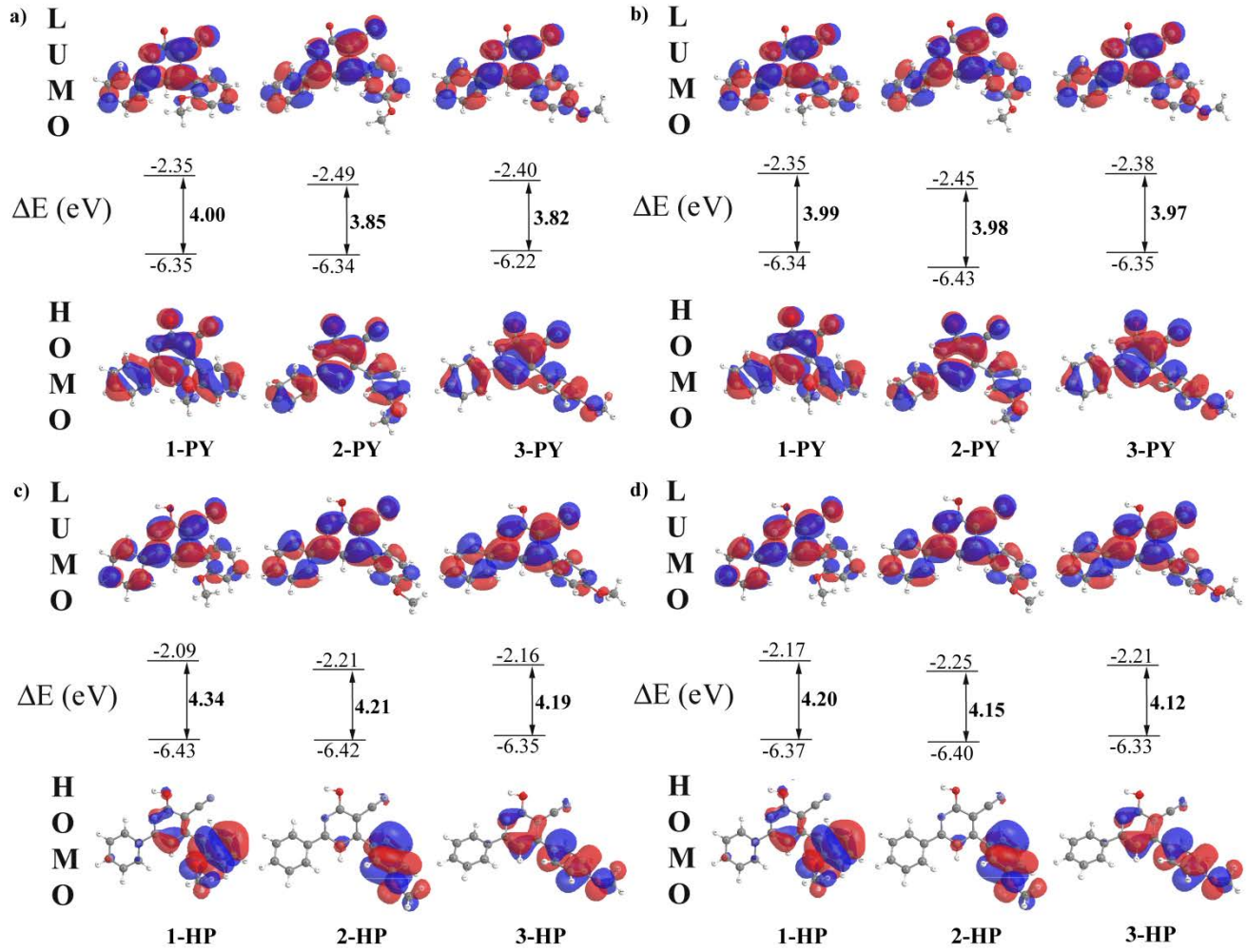

Fig. 4.2.11 The molecular orbitals and energy gaps between HOMO and LUMO orbitals of compounds **1 - 3** in the **PY** form in a gas phase a) and THF b), and the **HP** form in gas phase c) and THF d)

Generally, a lower E_{gap} values were observed for all compounds in the **PY** form, and lowest values were found for nitro substituted compounds in both **PY** and **HP** forms. Small influences of *ortho*-substitution on increased E_{gap} could be observed for compounds **1-6** in the **HP** form (Tables 4.2.15 and 4.2.16). Low effect on E_{gap} changes, in both forms of compounds **1 - 6** (Tables 4.2.15 and 4.2.16), was observed by inclusion of implicit solvent model. For compounds **4-6** (Table 4.2.16), the substituent effects influence on E_{gap} changes showed similar trend as for comps. **1-3** (Table 4.2.15). Higher values of E_{gap} was found for compounds **7-9** in **HP** form, and highest values for compounds **7** and **8** were noticed (Table 4.2.17)**.**

In order to obtain data on electronic density distribution, the Bader`s analysis was performed. Difference of atomic charges in the excited and in the ground state (Δ_{charge}) for appropriate atoms, as well as calculated changes in overall electron density of molecules are given in Tables 4.2.18-4.2.21, and Figs 4.2.12-4.2.14. Atom and ring numbering used in Bader's analysis is given in Fig. 4.2.10.

Table 4.2.18 Difference in atomic charges between (Δ_{Charge}) excited and ground state of appropriate atom in both **PY** and **HP** forms of compounds **1 - 3**

Atom Number*	Δ_{Charge}					
	1-PY	**1-HP**	**2-PY**	**2-HP**	**3-PY**	**3-HP**
1	0.0209	0.0095	0.0174	0.0173	0.0346	0.0099
2	0.0413	0.0486	0.0481	0.0554	0.0522	0.0561
3	-0.0029	-0.0033	0.0006	-0.0053	-0.0002	-0.0072
4	0.0509	0.0665	0.0671	0.0717	0.0774	0.0803
5	0.0051	-0.0038	-0.0001	-0.0011	0.004	-0.0022
6	0.0293	0.0478	0.0461	0.0483	0.045	0.0507
7	-0.0001	0.0006	-0.0003	-0.001	0	-0.0009
8	0.0001	-0.0003	0.0002	0.0002	0.0003	0.0003
9	0.0025	-0.0012	0.0007	-0.0011	-0.002	-0.0015
10	0.0001	-0.0001	0.0003	0	-0.0002	0.0002
11	-0.0002	-0.0002	-0.0005	-0.0002	0.0002	-0.0002
12	0.1393	0.2042	0.2208	0.2213	0.1906	0.2297
13	-0.182	-0.0716	-0.004	-0.0222	-0.0533	-0.1356
14	0.2153	0.2038	0.2043	0.1813	0.1549	0.2163
15	0.0616	0.1398	0.1182	0.1466	-0.0461	0.1309
16	0.013	-0.0093	0.03	-0.0035	0.0074	0.0029
17	-0.0107	0.0766	0.0662	0.0747	0.0447	0.0366
18	0.0011	0.0023	-0.0008	0	0.0001	0.001
19	0.0203	0.0296	0.0127	0.0274	0.0343	0.0347
20	0.0307	0.0745	0.0577	0.0723	-0.0289	0.0696
21	-0.1315	-0.0058	-0.0038	-0.0002	-0.1527	-0.004
22	0.0007	0	0.0003	0	-0.0003	0.0003
23	-0.0549	-0.1661	-0.0136	-0.0065	-0.1388	-0.2606
24	-0.0705	0.0397	-0.0972	-0.2719	0.0157	-0.025
25	-0.0323	-0.2312	-0.182	-0.0485	-0.0597	-0.0666
26	0.0072	-0.0326	-0.0681	-0.0729	-0.0613	-0.1508
27	-0.0991	-0.066	-0.0495	-0.1796	-0.0375	-0.1185
28	0.036	-0.1542	-0.2655	-0.1045	-0.0007	0.011
29	-0.0004	-0.0007	0.0009	0.0065	-0.0006	0.0009
30	0.0006	0.005	0.0044	0.0011	0.0007	0.0015
31	0.0016	-0.0002	0	0.0037	0.0002	0.0006
32	-0.0014	0.0011	0.0003	0.0017	0.0004	0.0006
33	-0.0815	-0.1808	-0.1873	-0.1876	-0.0709	-0.1419
34	0.0054	0.0103	0.0095	0.0126	0.0035	0.0109
35	-0.0073	-0.0169	0.0002	-0.0175	-0.0073	-0.013
36	0.0004	-0.0153	-0.0167	-0.0182	0	0.0006
37	-0.0085	0.0002	-0.0166	0.0001	-0.0059	-0.0175

Table 4.2.19 Difference in atomic charges (Δ_{Charge}) between excited and ground state of appropriate atom in both **PY** and **HP** forms of compounds **4 - 6**

Atom number*	Δ_{Charge}					
	4-PY	**4-HP**	**5-PY**	**5-HP**	**6-PY**	**6-HP**
1	0.0169	-0.0832	0.0165	-0.0896	0.0138	-0.0802
2	0.0367	0.0105	0.0325	0.0027	0.0345	0.008
3	-0.0036	-0.0183	-0.0006	-0.0181	-0.0017	-0.0166
4	0.0483	-0.045	0.043	-0.0581	0.0452	-0.0474
5	0.0046	-0.0042	0.0031	0.044	0.0009	-0.0023
6	0.0271	-0.0113	0.0259	-0.0707	0.0255	-0.0155
7	0.0008	0.0002	0.0005	0.0006	0.0002	0.001
8	0.0003	0.0001	0.0003	0.0001	0	0
9	-0.0001	0.0005	0	0.0005	0	0.0008
10	0.0002	0.0002	0	-0.0001	-0.0001	0.0003
11	-0.0003	0.0007	0.0004	0.0004	0	0.0013
12	0.1351	0.149	0.1247	0.1372	0.1188	0.1414
13	-0.2519	-0.2425	-0.2368	-0.2473	-0.2324	-0.2539
14	0.2044	0.2093	0.1926	0.202	0.1906	0.2011
15	-0.0475	-0.0098	-0.0666	-0.02	-0.071	0.0105
16	0.0173	-0.0608	0.0192	-0.0576	0.0159	-0.0535
17	-0.0296	0.0954	-0.0238	0.0992	-0.0176	0.089
18	0.002	0.0049	0.0023	0.0042	0.0033	0.0033
19	0.0307	0.0337	0.0319	0.0322	0.0287	0.0283
20	-0.0185	-0.0038	-0.0324	-0.0111	-0.0297	0.0049
21	-0.2374	-0.0741	-0.2405	-0.0687	-0.2402	-0.0669
22	0.0012	0.0018	0.0005	0.0006	0.0004	0.0009
23	0.0025	-0.0084	0.0081	0.0098	-0.0013	-0.0142
24	0.0139	0.0213	0.0296	0.0247	0.0406	0.0273
25	0.0044	-0.0003	0.0027	0.0042	-0.001	-0.0034
26	0.0183	0.024	0.0367	0.0452	0.0415	0.0271
27	0.0005	0.0006	0.0012	-0.0057	-0.0004	-0.0082
28	0.0234	0.0213	0.0294	0.0421	0.0311	0.029
29	-0.0002	-0.0005	-0.0002	-0.0003	0.0002	-0.0001
30	0.0005	0.0008	0	0.0003	0.0001	0.0002
31	0.0004	0.0002	-0.0004	-0.0003	-0.0001	0.0001
32	0	0	0.0001	0.0003	0.0005	0.0002
33	-0.0004	-0.0122	0.0004	-0.0025	0.004	-0.0123

Table 4.2.20 Difference in atomic charges (Δ_{Charge}) between excited and ground state of appropriate atom in both **PY** and **HP** forms of compounds **7 - 9**

Atom number*	Δ_{Charge}					
	7-PY	**7-HP**	**8-PY**	**8-HP**	**9-PY**	**9-HP**
1	-0.0079	-0.0922	-0.0067	-0.109	-0.0106	-0.1089
2	-0.0185	-0.0451	-0.0075	-0.047	-0.0043	-0.0439
3	-0.0014	-0.0109	-0.0015	-0.0115	-0.0029	-0.0111
4	-0.0287	-0.1115	-0.0141	-0.1315	-0.0127	-0.1235
5	-0.0006	-0.0061	-0.0005	-0.0092	-0.0004	-0.0107
6	-0.0203	-0.0547	-0.0113	-0.056	-0.0096	-0.0526
7	0	0.0008	0.0005	0.0003	0	0.0013
8	-0.0001	-0.0002	-0.0001	0	0.0001	0
9	0.001	0.0013	0.0005	0.0035	0.0001	0.0026
10	-0.0002	0.0002	0	-0.0004	0	0
11	-0.0006	0.001	0.0005	0.0004	0.0008	0.0023
12	-0.0989	-0.0765	-0.0419	-0.0619	-0.0162	-0.0198
13	-0.2433	-0.2117	-0.2265	-0.1921	-0.2424	-0.1875
14	0.0241	0.0223	0.051	0.0253	0.0884	0.069
15	-0.2276	-0.1949	-0.1976	-0.1935	-0.1426	-0.1423
16	-0.0052	-0.0737	0.0046	-0.0657	0.0095	-0.058
17	-0.0536	0.0179	-0.0416	0.0167	-0.0346	0.0467
18	0.0029	0.003	0.0046	0.0028	0.0027	0.0029
19	0.0194	0.0122	0.0189	0.0129	0.0193	0.0172
20	-0.0997	-0.0942	-0.0937	-0.0967	-0.0761	-0.0798
21	-0.1839	-0.0608	-0.2016	-0.0532	-0.2044	-0.0581
22	0.0001	0.001	0.0008	0.001	0.0004	0.0005
23	0.0965	0.0991	0.0116	0.003	0.0996	0.124
24	-0.0088	-0.01	0.1621	0.1608	0.026	0.0232
25	0.1122	0.119	-0.0058	-0.004	0.0471	0.0633
26	0.0112	0.0097	0.1186	0.1084	0.0691	0.0712
27	0.0655	0.067	0.0504	0.0548	0.0508	0.0606
28	0.0455	0.0445	0.0282	0.0664	0.029	0.0179
29	0.0001	0.0001	-0.0012	-0.0015	-0.0004	-0.0004
30	0.0002	0.0004	-0.0005	0.0001	-0.0001	0.0011
31	-0.0006	-0.0006	-0.0003	0.0003	-0.001	-0.0003
32	0.0001	-0.0001	0.001	0.0003	0.0009	0.0012
33	0.2533	0.2731	0.1597	0.2404	0.1248	0.1533
34	0.1839	0.1814	0.1149	0.166	0.0943	0.1199
35	0.1842	0.1889	0.1245	0.1699	0.0959	0.1186

Table 4.2.21 Difference in charges of R_1, R_2 and R_3 rings (Fig. 4.2.10) between excited and ground state in both **PY** and **HP** forms of compounds **1 - 9**

Compound	Charge		
	R_1	R_2	R_3
1-PY	+0.15	+0.16	-0.31
1-HP	+0.16	+0.65	-0.81
2-PY	+0.18	+0.70	-0.88
2-HP	+0.18	+0.70	-0.88
3-PY	+0.21	+0.15	-0.36
3-HP	+0.19	+0.58	-0.77
4-PY	+0.13	-0.19	+0.06
4-HP	-0.15	+0.10	+0.05
5-PY	+0.12	-0.23	+0.11
5-HP	-0.19	+0.07	+0.12
6-PY	+0.12	-0.23	+0.11
6-HP	-0.15	+0.10	+0.05
7-PY	-0.08	-0.87	+0.95
7-HP	-0.32	-0.65	+0.97
8-PY	-0.04	-0.72	+0.76
8-HP	-0.36	-0.60	+0.96
9-PY	-0.04	-0.60	+0.64
9-HP	-0.34	-0.41	+0.75

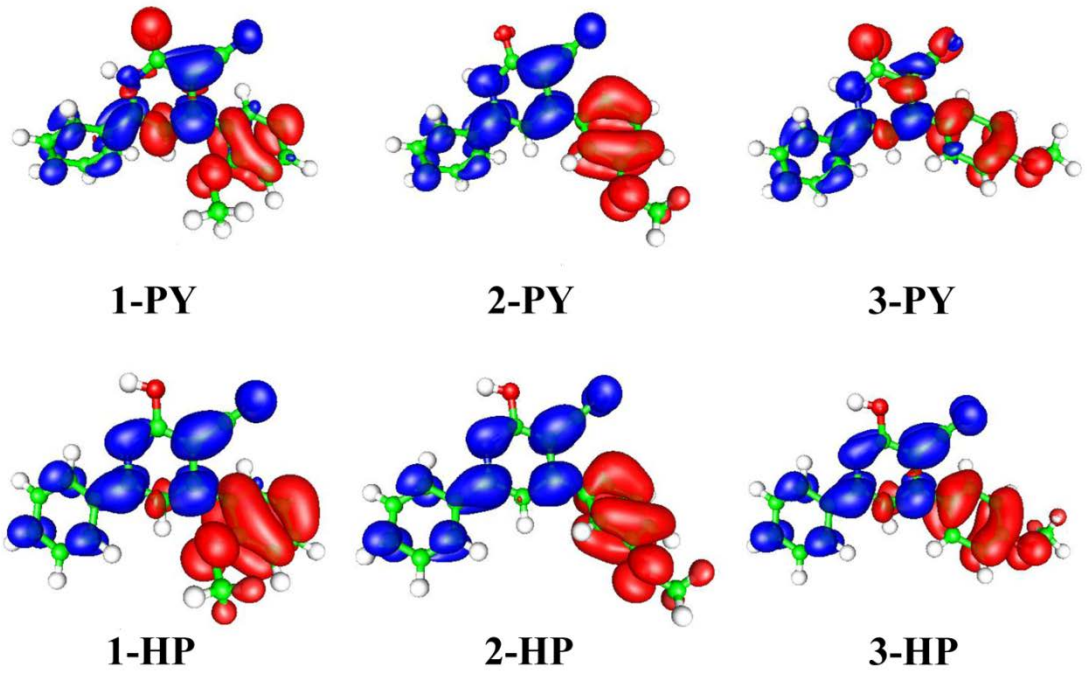

Fig. 4.2.12 ICT processes, *i.e.* charge transfer of electron density from ground state (red) to excited state (blue) in both **PY** and **PH** forms of compounds **1 - 3**

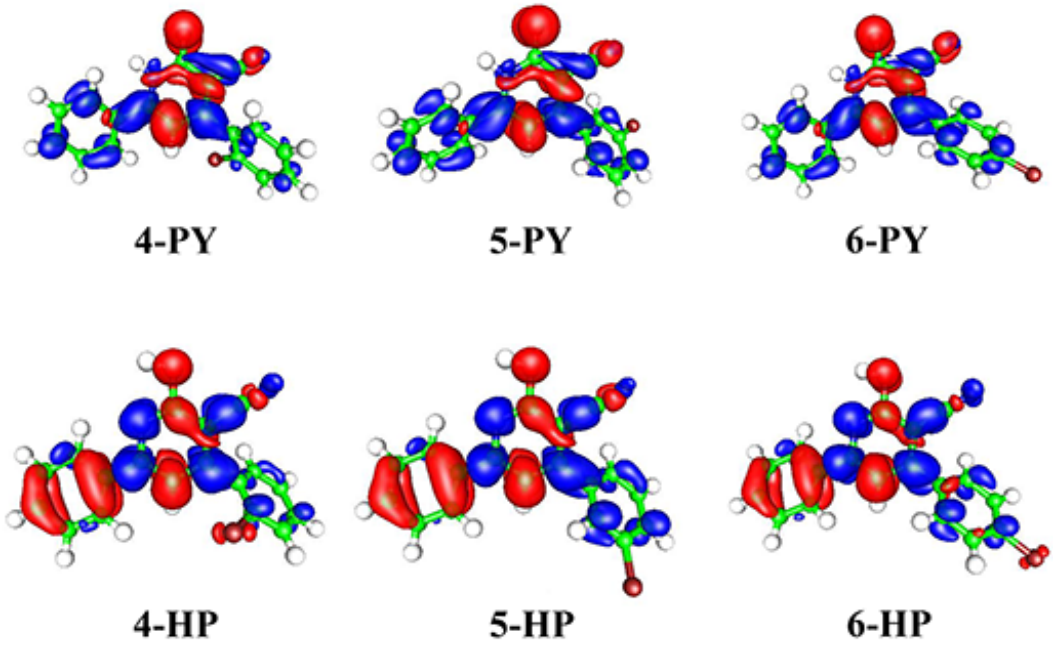

Fig. 4.2.13 ICT processes from ground state (red) to excited state (blue) in both forms of compounds **4 - 6**

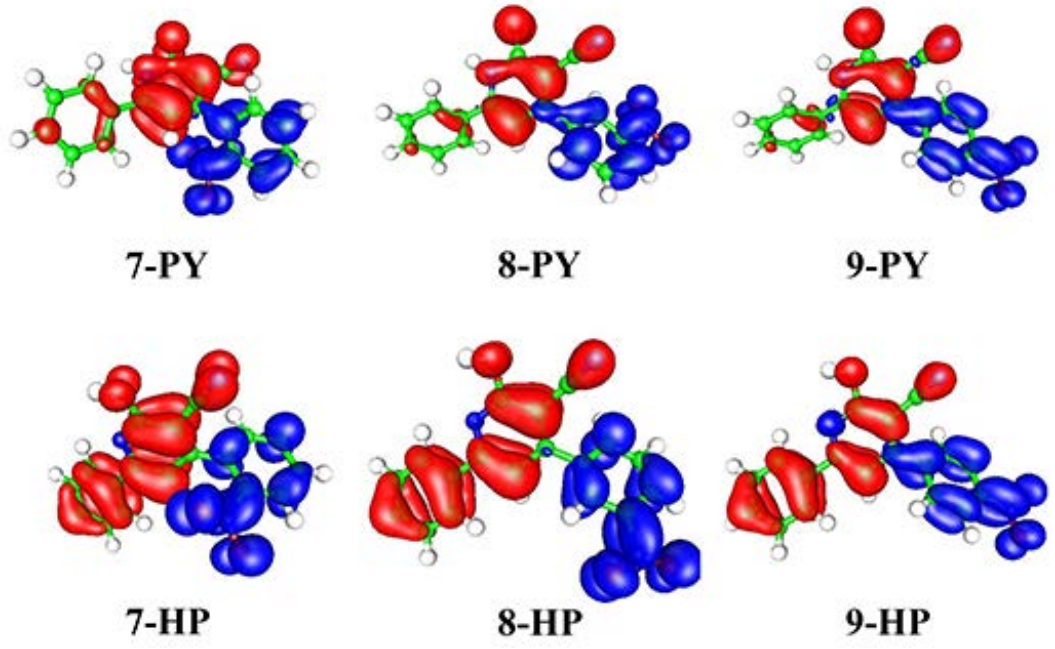

Fig. 4.2.14 ICT processes from ground state (red) to excited state (blue) in both forms of compounds **7 - 9**

According to the results shown in Tables 4.2.18-4.2.21 and Figs. 4.2.12-4.2.14, it could be observed that in both **HP** and **PY** forms of the methoxy- and nitro-substituted compounds (**1-3** and **7-9**, respectively) ICT processes can be clearly observed. In methoxy-substituted compounds electron density was transferred from the substituted phenyl to pyridine and unsubstituted phenyl moieties (Fig. 4.2.12). According to the character of the ICT processes molecules can be divided in two groups:

The first group includes **HP** forms (**1-HP**, **2-HP** and **3-HP**) along with **2-PY** compound. In these molecules significant ICT process can be observed; substituted rings lose from –0.77 to –0.88 electrons. The largest part of the charge is transferred to the pyridine ring (Δ_{charge} for the pyridine ring vary from 0.58 to 0.70), *i.e*. mostly to the ring carbon atoms (C12, C14 and C15).

In the second group, which includes compounds **1-PY** and **3-PY**, ICT process is less pronounced. The calculation showed that substituted phenyl moiety of **1-PY** and **3-PY** compounds loses –0.31 and –0.36 electrons, while pyridine ring receives 0.16 and 0.15 electrons, respectively. Along with this, O21 atom of the pyridone ring loses a significant amount of charge (Δ_{charge}): –0.1315 for **1-PY** and –0.1527 for **3-PY**). In the first group of compounds charge difference of this atom appeared negligible. Observed charge transfer can be compared with resonance effect for compounds **1-PY** and **3-PY**, bearing *ortho* and *para* MeO-substituent. It should be noted that in all *methox*y-substituted compounds charge difference between ground and excited state on unsubstituted phenyl ring are roughly similar (from 0.15 to 0.21).

Compounds with the chloro substituent (**4 - 6**) showed negligible ICT between the substituted ring and the other two ones. Charge density change for substituted ring varies from 0.05 to 0.12 (Table 4.2.21), with low changes of charge densities at the chloro atom (Table 4.2.19). It means that the position of the chlorine does not affect the excited state. Also, the values of Δ_{charge} of unsubsituted ring, in all **PY** forms, are similar (0.13, 0.12 and 0.12) as well as for the pyridone ring (–0.19, –0.23 and –0.23) (Table 4.2.21). The similar values and opposite sign of charge densities (Δ_{charge}) were obtained for **HP** forms: –0.15, –0.19 and –0.15 for unsubsituted rings, and 0.10, 0.07 and 0.10 for pyridine ring (Table 4.2.21). The main differences between **HP** and **PY** forms were noticed in following: in the **PY** form the unsubsituted ring gains, while the pyridine ring loses electron density. The opposite is true for the **HP** form, with notification that

magnitude of electronic density change at the unsubsituted ring atoms is negligible. The noticeable differences are found for the pyridone/pyridine ring, where C12 and C14 atoms of the both rings showed slightly larger positive Δ_{charge} value (from 0.1188 to 0.1490 and from 0.1906 to 0.2093 for both forms), and for C13 somewhat larger negative Δ_{charge} values (from –0.2539 to –0.2324). Perhaps the most important difference between the **HP** and the **PY** form was found for Δ_{charge} values for the oxygen atom (O21). In all compounds in the **PY** form larger negative Δ_{charge} values of –0.2374, –0.2405 and –0.2402 were found, while for the **HP** form significantly lower negative Δ_{charge} values: –0.0741, –0.0687 and –0.0669 were noticed (Table S18). Also, for the same compounds, pyridone nitrogen (N17) of **PY** form, has a negative Δ_{charge} value (–0.0296, –0.0238 and –0.0176) and opposite was found for **HP** form (0.0954, 0.0992 and 0.089) (Table 4.2.19).

The both forms of nitro substituted compounds (**7 - 9)** (Table 4.2.20), showed opposite behavior comparing to compounds **1 - 3**. *S*ubstituted ring was largely populated with electrons in the course of transition to the excited state (Δ_{charge} for the substituted ring varies from +0.64 to +0.97; Table 4.2.21). Most of the electron density (from 50 % to 66 %) was situated on the nitro group (atoms No. 33, 34 and 35 have a positive value of Δ_{charge}). Also, analysis of the ICT processes of these compounds indicated two kinds of electron transfer: in **HP** forms both the pyridine and the unsubstituted phenyl rings lose a significant amount of electron density: –0.65, –0.60 and -0.41 for the pyridine ring, and –0.32, –0.36 and –0.34 for the unsubsituted ring (Table S20?). Extent of ICT between the two unsubstituted rings and the substituted one decreases in the order **7-HP** > **8-HP** > **9-HP** (Δ_{charge} is +0.97, +0.96 and +0.75, respectively), and it seems that this order indeed reflect magnitude of inductive effect of the nitro group. Interestingly, the unsubsituted phenyl ring has similar Δ_{charge} values (Table 4.2.21) for all compounds, while Δ_{charge} of the pyridine ring decreases from *ortho*- to *para*-substituted ones.

The second group are the compounds in **PY** forms, in which the decrease of the extent of ICT processes with the increased distance between the substituent and pyridone ring (Δ_{charge} of substituted ring is 0.95, 0.76 and 0.64 for the *ortho*-, *meta*- and *para*-position of nitro group; Δ_{charge} for the pyridine ring is -0.87, -0.72 and -0.60) was observed. This is also an indication of the decreasing contribution of the substituent polar (inductive/field) effect. Lower extent of ICT

processes in **PY** form, in comparison to **HP** form, from unsubstituted ring to the rest of the molecule (Δ_{charge} values for unsubsituted ring is around -0.08, -0.04 and -0.04, which is negligible change) was also observed. This behavior can be explained by comparing geometries of both forms: torsional angles between substituted phenyl and pyridone rings are significantly higher in all **PY** forms (Tables 4.2.10-4.2.12). In the **PY** structures, the plane angle of two rings significantly deviated from planarity. This do not allow significant extent of the π-orbitals overlap; so it is reasonable that low ICT between these two rings exist. The **HP** forms, due to more planar conformation, showed larger extent of ICT processes (Fig. 4.2.14). This did not hold for *methoxy*-substituted compounds, where small differences in Δ_{charge} between the unsubstituted ring of both **HP** and **PY** forms were observed. Also, in these structures nitrogen (N17) in the pyridone ring of **PY** form has a negative Δ_{charge} value, and opposite was found for the **HP** form. This means that the low change of electron density at this nitrogen exist (in all structures Δ_{charge} for this nitrogen have a low negative values), while in all **HP** forms Δ_{charge} for the same atom are positive (Table 4.2.20).

4.3 Solvent and structural effects in tautomeric 6(2)-hydroxy-4-methyl-2(6)-oxo-1-(substituted phenyl)-1,2(1,6)-dihydropyridine-3-carbonitriles: UV, NMR and quantum chemical study

4.3.1 Resolution of UV spectra and solvent effects on 2-PY/6-PY equilibria

Pyridones exists in a solution as the equilibrium of dynamic processes of inter-conversion of tautomeric forms and eventually presence of dimer forms [228,229]. This phenomenon has significant influences on physico-chemical properties of studied pyridone. Tendency of 2-pyridone to aggregate was evaluated from NMR and FTIR spectral data [228]. State of tautomeric equilibrium depends on the stability of tautomeric, and equilibria sensitively depends on solvent properties like polarity, stabilization of the charges in the solvation sphere and from alteration of a solute's electronic structure in the ground and excited states due to both short- and long-range interactions with surrounding solvent molecules [230]. Additionally, geometries and substituent effects could be of appropriate significance.

Various spectroscopic techniques was applied for studying state of tautomeric equilibria, mechanism of proton-transfer (tautomer transformation) and solvent–solute interactions. Rate of prototropic exchange depends on energetic phenomena, *i.e*. transformation barrier, and the system parameters and environment. Slow proton exchange allowed observation of distinct signals in ^{1}H NMR spectra and quantitative determination of the tautomeric form [231,232,233]. Oppositely, only one, average, signal in the NMR spectrum was observed under fast proton exchange in tautomeric mixture. UV/Vis technique is a useful method for study of tautomeric equilibrium which could be based on following advantageous: different spectral properties of tautomeric forms, tautomeric equilibria is sensitive to environment (solvent), substituent effect, acidity, temperature, *etc*. Accordingly, state of the tautomeric equilibria, influences of substituent effect and geometry of investigated compounds **1-16** was performed by analyzing UV/Vis spectra. Absorption spectra of the investigated compounds, recorded in seventeen solvents, showed that spectra consisted of two overlapped bands in the region 300-500 nm (Fig. 4.3.1). Band structure depends on both substituent effects and solvent properties.

Due to presence of mobile proton at either 2 or 6 position of pyridone core, contrary to 2(1*H*)-pyridone, it contributes to multiple intermolecular interactions mainly lateral π,π-stacking interactions. Dimerization process was not observed at concentration lower than 1×10^{-5} mol dm^{-3}, indicating no monomer content rising upon dilution. Therefore, all UV/Vis spectra were recorded at concentration of 1×10^{-5} mol dm^{-3}.

The characteristic absorption spectra of investigated compounds in ethanol and THF are shown in Fig. 4.3.1.

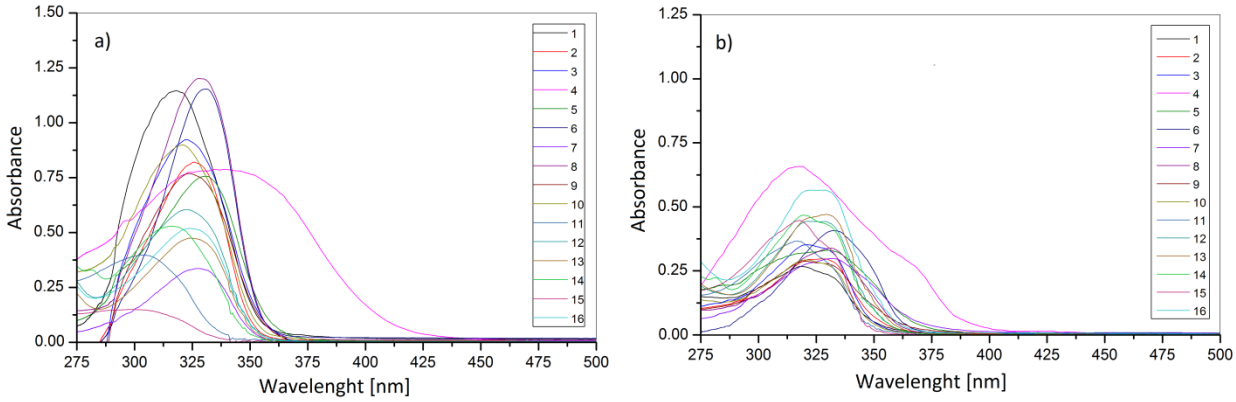

Fig. 4.3.1 Absorption spectra of compounds **1** - **16** in a) ethanol and b) THF

Due to impossibility of the determination of molar absorptivities of pure tautomeric forms a semi quantitative approach was applied for analysis of the state of tautomeric equilibria. The spectra were analysed by a stepwise procedure, whereby an estimation of both tautomerization constants, individiual spectra of the tautomers and absorption bands number were obtained from experimental data and DFT calculation. Second and fourth derivative spectroscopy was a useful methodology in determining the number and approximate position of the absorption bands [193]. In the second step, the initial approximation of the band intensities and band widths, and assignment to the appropriate tautomeric form was performed. The final refinement is performed by simultaneous resolution of the whole set of spectra according to literature procedures described in references [193,223,224]. Results of applied methodology are exemplified in Fig. 4.3.2., and absorption maxima of both 2-**PY** (higher wavelength energy band) and **6-PY** forms (lower one) obtained in the set of selected solvents are summarized in Tables 4.3.1 and 4.3.2, respectively. Such methodology provides differentiation without loss of the terminal spectral points [ref?].

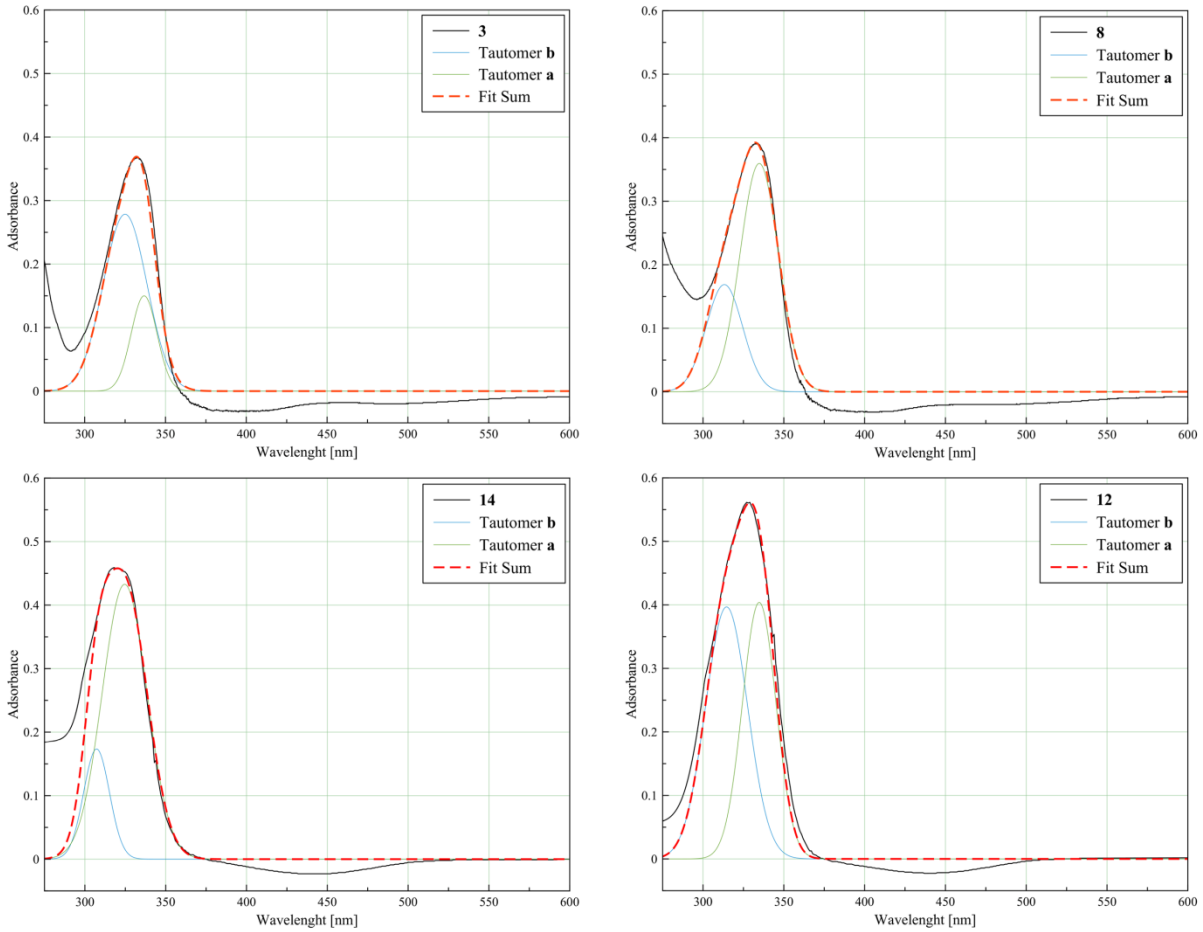

Fig. 4.3.2 Resolved overlapping bands of compounds **3**, **8**, **14** and **12** in DMSO

Table 4.3.1 Absorption frequencies of tautomer **a (2-PY)** in selected solvents

Solvent/ Compound	$\nu_{max} \times 10^{-3}$ (cm^{-1})															
	1	**2**	**3**	**4**	**5**	**6**	**7**	**8**	**9**	**10**	**11**	**12**	**13**	**14**	**15**	**16**
Ethanol	31.25	30.67	30.96	29.85	31.26	30.21	30.49	30.49	30.96	31.15	32.34	30.41	30.19	30.72	31.55	30.19
Methanol	31.55	30.86	31.25	29.85	31.63	30.49	30.49	30.86	31.25	31.25	32.26	30.34	30.56	30.87	31.62	30.11
2-Propanol	31.95	30.49	31.06	28.82	31.24	30.12	30.30	30.39	30.86	31.06	31.43	30.17	29.96	31.11	31.51	29.96
1-Propanol	31.35	30.67	30.77	28.40	30.98	30.39	30.30	30.30	30.49	31.06	32.09	30.11	30.11	30.72	31.43	30.41
1-Butanol	31.45	30.58	31.06	28.57	31.50	30.30	30.30	30.30	30.77	31.15	31.27	30.04	29.96	30.72	31.75	30.34
2-Butanol	31.35	30.39	30.96	28.41	31.23	30.21	30.21	30.30	30.77	30.96	31.72	29.97	30.10	30.71	31.35	30.10
DMSO	29.95	29.74	29.72	27.24	29.99	29.52	29.66	29.65	29.74	30.03	-*	29.87	29.73	30.73	30.71	29.86
THF	31.45	30.39	31.15	31.15	31.43	30.03	30.21	30.21	30.93	31.25	30.85	29.77	30.17	30.64	30.99	30.03
AcN	31.25	30.39	30.77	31.54	31.00	29.94	30.39	30.30	30.92	30.86	30.57	30.10	29.90	30.37	31.30	29.97
Anisole	31.06	30.96	31.06	31.35	31.20	30.58	30.77	30.67	30.96	31.06	30.22	30.04	28.85	30.04	30.28	30.01
DMAc	30.58	30.03	30.39	30.58	30.54	29.59	29.76	29.76	30.30	30.39	31.15	30.16	29.81	30.16	31.08	30.04
DMF	30.03	29.59	30.03	26.88	30.22	29.67	29.41	29.50	29.50	29.76	29.23	29.04	29.16	29.83	30.58	29.01
EtAc	31.35	30.39	31.15	31.75	31.42	30.03	30.21	30.49	30.49	31.25	30.40	29.75	29.69	30.43	30.53	29.97
Chl	31.68	30.95	31.00	32.00	31.21	30.45	30.98	30.85	31.36	31.35	32.24	30.31	30.60	30.81	31.45	30.06
Dioxane	31.40	30.54	31.25	31.21	31.45	30.05	30.15	30.66	30.89	31.31	32.03	29.70	29.50	30.31	30.41	30.21
Diethyl ether (DEE)	31.50	30.74	31.36	31.00	31.56	30.14	30.06	30.51	30.95	31.42	31.56	29.58	29.31	30.15	30.14	30.15

* tautomer **b** predominate

Table 4.3.2 Absorption frequencies of tautomer **b** in selected solvents

Solvent/ Comp.	$\nu_{max} \times 10^{-3}$ (cm^{-1})															
	1	**2**	**3**	**4**	**5**	**6**	**7**	**8**	**9**	**10**	**11**	**12**	**13**	**14**	**15**	**16**
Ethanol	32.95	32.46	32.43	32.31	31.87	31.51	31.94	31.56	32.99	32.51	29.45	32.43	31.56	32.78	36.15	31.21
Methanol	33.5	32.41	32.78	32.75	31.55	31.94	31.96	31.32	32.66	32.94	28.10	32.26	31.89	32.95	37.51	31.33
2-Propanol	32.97	31.97	32.45	32.68	31.71	31.12	32.14	31.67	32.51	32.46	30.06	32.43	31.25	32.95	35.54	31.05
1-Propanol	33.00	32.24	32.53	32.61	31.79	31.46	32.10	31.86	32.96	32.43	29.68	32.09	31.43	32.60	35.96	31.11
1-Butanol	32.86	32.21	32.50	31.46	32.05	31.56	32.01	31.77	32.65	32.35	29.89	32.09	31.54	32.60	35.87	31.16
2-Butanol	32.71	31.67	32.35	32.65	31.63	31.13	31.98	31.56	32.63	32.21	30.45	32.09	31.23	32.71	35.12	31.01
DMSO	32.22	31.45	31.51	30.56	31.00	-*	31.31	31.41	32.41	31.72	30.21	31.84	31.14	32.70	34.12	31.00
THF	31.84	31.41	31.59	31.66	33.38	30.86	31.21	32.42	31.66	31.54	31.89	31.57	31.11	31.97	33.84	31.21
AcN	32.00	31.75	31.62	31.47	31.58	30.56	31.13	31.67	31.84	31.74	31.45	31.94	31.45	32.17	33.98	31.51
Anisole	31.52	31.84	31.34	31.40	31.79	31.54	31.21	31.95	31.46	31.19	30.67	31.73	31.52	31.60	34.24	31.26
DMAc	32.20	31.34	31.65	31.63	31.73	-	31.82	31.79	31.95	31.73	30.70	32.96	31.03	32.47	33.94	31.00
DMF	32.11	31.35	31.66	30.50	32.06	-	31.11	31.48	31.68	31.72	30.74	30.63	31.11	32.29	33.82	31.10
EtAc	31.82	31.33	31.74	31.84	32.86	30.56	31.24	32.31	31.74	31.54	31.99	31.65	31.15	31.97	33.78	31.23
Chl	31.30	32.10	31.12	32.12	31.45	31.26	31.65	31.31	32.65	31.10	30.93	31.95	31.45	32.07	33.98	31.45
Dioxane	31.39	31.45	31.46	31.52	32.67	30.86	31.25	32.11	31.45	31.19	31.94	31.15	31.21	31.90	33.79	31.40
DEE	31.74	31.33	31.88	31.21	32.00	30.42	31.03	32.03	31.21	31.33	32.45	30.75	31.11	31.50	33.64	31.42

* tautomer **a** predominate

The absorption band maxima could be assumed to be π–π* transition involving the π-electronic system throughout the whole molecule including intramolecular charge transfer (ICT). The considerable ICT nature of this band is obvious from its broadness, the sensitivity of its λ_{max} to the substituent effects and the solvent properties. The data from Table 4.3.1 confirm that the positions of the UV/vis absorption frequencies depend on the nature of the present substituent on the benzene ring. The introduction of both electron-donating and electron-withdrawing substituents contributes to positive solvatochromism in all solvents. It was observed that, although slightly positive solvatochromism is evident comparing to the unsubstituted compound, except compounds **5**, **11** and **15**, the absorption spectra showed relatively low dependence with respect to both solvent and substituent effects for tautomer **a** (Table 4.3.1), and somewhat higher influences was observed for tautomer **b** (Table 4.3.2). Solvent dependent spectral shifts are influenced by non-specific (dipolarity/polarizability) and specific (HBA/HBD) solvent–solute interactions. Generally, tautomeric equilibrium is shifted to more dipolar form with increasing solvent polarity [233]. The solvent hydrogen-bonding ability plays a specific role in the stabilization of appropriate tautomeric forms, but their contribution is of minor differences due to low structural diversity. Both electron-donor and electron-acceptor substituents cause batochromic shifts.

LSER analysis of UV data

The contributions of specific and nonspecific solvent–solute interactions were qualitatively/quantitatively evaluated by the use of LSER Eqs. (x) and (x). The LSER concept developed by Kamlet and Taft and more appropriate define by Catalán are ones of the most used and successful quantitative treatments of solvation effects. This treatment assumes attractive/repulsive solvent/solute interactions and enables an estimation of the ability of the solvated compounds to form hydrogen bonds. Correlation results obtained by the use Kamlet-Taft (Eq. x) and Catalán (Eq. x) are given in Tables 4.3.3 and 4.3.4 for **2-PY** form, and 4.3.5 and 4.3.6 for **6-PY** form, respectively. The contribution percentages of the nonspecific (P_π) and the specific solvent/solute interactions (P_β and P_α) are given in Tables 4.3.7 and 4.3.8.

Table 4.3.3 Results of the correlation analysis for tautomer **a** according to Kamlet–Taft equation

Comp.	$\nu_0 \times 10^{-3}$ (cm^{-1})	$s \times 10^{-3}$ (cm^{-1})	$b \times 10^{-3}$ (cm^{-1})	$a \times 10^{-3}$ (cm^{-1})	R^a	Sd^b	F^c	Solvent excluded from correlation
1	32.69 ±0.25	–1.83 ±0.34	–0.97 ±0.26	0.46 ±0.19	0.93	0.22	23.45	2-Propanol
2	31.33 ±0.17	–1.00 ±0.23	–0.81 ±0.18	0.55 ±0.13	0.94	0.15	26.48	Anisole
3	32.53 ±0.22	–1.79 ±0.30	–1.05 ±0.22	0.28 ±0.16	0.93	0.19	27.11	-
4	36.10 ±1.01	–3.29 ±1.24	–7.51 ±1.40	0.78 ±0.40	0.91	0.77	16.59	DMAc, Chl
5	32.81 ±0.27	-1.75 ±0.34	-1.23 ±0.37	0.46 ±0.22	0.92	0.22	20.37	Chl
6	30.59 ±0.09	–0.66 ±0.13	–0.52 ±0.10	0.56 ±0.07	0.97	0.08	54.71	Anisole
7	30.81 ±0.17	–0.36 ±0.23	–1.10 ±0.18	0.77 ±0.13	0.93	0.15	25.28	Anisole
8	31.32 ±0.20	–0.95 ±0.27	–1.02 ±0.20	0.53 ±0.15	0.92	0.17	21.42	Anisole
9	31.94 ±0.29	–1.17 ±0.39	–1.46 ±0.29	0.84 ±0.22	0.91	0.24	16.36	THF, Anisole
10	32.55 ±0.22	–1.79 ±0.30	–1.03 ±0.26	-[d]	0.92	0.21	23.14	-
11	33.06 ±0.49	–2.96 ±0.67	–1.74 ±0.14	2.12 ±0.31	0.95	0.34	27.78	DMAc, Dioxane
12	29.49 ±0.14	0.81 ±0.19	–0.33 ±0.14	0.69 ±0.10	0.91	0.12	17.09	DMF
13	29.56 ±0.23	0.70 ±0.30	–0.87 ±0.23	1.19 ±0.17	0.91	0.19	16.43	THF, Anisole
14	29.70 ±0.21	0.40 ±0.25	0.82 ±0.29	0.31 ±0.17	0.91	0.15	13.73	THF, DMF, Chl, DMAc
15	30.30 ±0.28	0.48 ±0.20	-	1.41 ±0.21	0.93	0.24	20.16	AcN, Chl
16	32.47 ±0.39	–2.95 ±0.49	–1.21 ±0.34	0.30 ±0.20	0.94	0.16	16.59	DMAc, DMSO, Chl, 2-Butanol, DEE

[a] Correlation coefficient; [b] Standard deviation; [c] Fisher test of significance; [d] Negligible values with high standard errors

The positive value of the coefficient *a* obtained for both **2-PY** and **6-PY** forms, except for compounds **5, 8** and **11** in **6-PY** form, indicate better stabilization of the molecule in the ground state (Table 4.3.3). It means that proton-accepting capabilities of both pyridone nitrogen and keto/hydroxyl group contribute in moderate extent to the solute stabilization in ground state. Highest values of coefficient *a* was found for compound **11** in both **2-PY** and **6-PY** forms.

A negative sign of the coefficients *s* and *b*, obtained in correlations for the **2-PY** form (Table 4.3.3), except for comps. **12-15** in **2-PY** form, indicate a batochromic shift of the absorption maxima with the increasing contribution of solvent dipolarity/polarizability and hydrogen-

accepting capability. The largest value of coefficients *s* and *b* of the **2-PY** form was found in comp. **4** for coefficients *s* and *b* (Table 4.3.3). It means that the most effective transmission of the substituent effect, *i.e.* electron-accepting ability of the nitro group (comp. **4**), from *para*-position to the amide NH group increase contribution of the effect of solvent dipolarity/polarizability and hydrogen-bonding capability, *i.e.* higher value of coefficients *s* and *b* was obtained. In the case of the compounds in the **2-PY** form, non-specific solvent and HBA solvent effects are the main contributing factor influencing batochromic shift, while specific solvent effects showed a higher influence on solvatochromism of the investigated compounds (Table 4.3.3).

A negative sign of the coefficients *s* and *b*, obtained in correlations for the **2-PY** form (Table 4.3.3), except for comps. **12-15** in **2-PY** form, indicate a batochromic shift of the absorption maxima with the increasing contribution of solvent dipolarity/polarizability and hydrogen-accepting capability. The largest value of coefficients *s* and *b* of the **2-PY** form was found in comp. **4** for coefficients *s* and *b* (Table 4.3.3). It means that the most effective transmission of the substituent effect, *i.e.* electron-accepting ability of the nitro group (comp. **4**), from *para*-position to the amide NH group increase contribution of the effect of solvent dipolarity/polarizability and hydrogen-bonding capability, *i.e.* higher value of coefficients *s* and *b* was obtained. In the case of the compounds in the **2-PY** form, non-specific solvent and HBA solvent effects are the main contributing factor influencing batochromic shift, while specific solvent effects showed a higher influence on solvatochromism of the investigated compounds (Table 4.3.3).

Table 4.3.4 Results of the correlation analysis for tautomer **a** according to Catalán equation

Comp.	$v_0 \times 10^{-3}$ (cm^{-1})	$c \times 10^{-3}$ (cm^{-1})	$d \times 10^{-3}$ (cm^{-1})	$b \times 10^{-3}$ (cm^{-1})	$a \times 10^{-3}$ (cm^{-1})	R^a	Sd^b	F^c	Solvent excluded from correlation
1	35.12 ±0.93	-3.65 ±1.24	-1.39 ±0.37	–0.94 ±0.39	0.87 ±0.49	0.90	0.28	10.41	2-Propanol
2	32.23 ±0.59	-0.82 ±0.78	–1.17 ±0.23	–0.99 ±0.24	1.43 ±0.31	0.92	0.18	15.72	-
3	34.40 ±0.64	-3.15 ±0.85	–1.47 ±0.25	–0.60 ±0.26	0.57 ±0.34	0.93	0.19	18.23	-
4	43.13 ±2.56	-10.62 ±3.34	–3.27 ±1.06	–5.99 ±1.04	–0.84 ±1.37	0.93	0.75	15.52	DMAc
5	34.70 ±0.68	-3.27 ±0.91	-1.49 ±0.27	–0.58 ±0.28	0.79 ±0.36	0.93	0.21	17.45	-
6	30.89 ±0.41	-[d]	–1.19 ±0.18	–0.60 ±0.17	1.43 ±0.22	0.95	0.12	21.85	Dioxane
7	31.74 ±0.69	-	–0.89 ±0.32	–1.53 ±0.31	1.98 ±0.47	0.91	0.20	11.11	Methanol, Dioxane
8	32.59 ±0.46	-1.37 ±0.61	–1.15 ±0.18	–1.15 ±0.19	1.27 ±0.24	0.95	0.14	28.29	-
9	33.74 ±0.92	-2.36 ±1.23	–1.00 ±0.37	–1.66 ±0.411	1.48 ± 0.51	0.90	0.28	9.61	THF, 2-Butanol
10	34.37 ±0.72	-2.78 ±0.96	–1.59 ±0.29	–0.77 ±0.29	0.83 ± 0.38	0.92	0.22	15.76	-
11	29.08 ±1.37	-	–0.96 ±0.50	1.21 ±0.55	2.56 ± 0.60	0.94	0.32	15.76	Chl, DMF
12	28.73 ±0.49	1.27 ±0.60	0.67 ±0.18	–0.34 ±0.17	0.94 ± 0.21	0.92	0.11	13.42	DMF, DMSO
13	30.54 ±0.77	-2.90 ±1.06	1.03 ±0.37	0.44 ±0.39	0.98 ± 0.43	0.91	0.23	10.04	THF, Chl, Dioxane
14	29.67 ±0.55	-	0.62 ±0.25	0.90 ±0.27	-	0.90	0.16	9.07	DMF, DMAc, Chl
15	32.69 ±0.65	–2.34 ±0.93	–0.95 ±0.26	–0.64 ±0.25	1.22 ± 0.34	0.92	0.18	14.50	Anisole
16	28.75 ±1.13	2.30 ±1.47	–1.84 ±0.44	0.89 ±0.51	1.89 ± 0.56	0.90	0.21	6.03	DMAc, THF, EtAc, AcN,Chl

[a] Correlation coefficient; [b] Standard deviation; [c] Fisher test of significance; [d] Negligible values with high standard errors

Table 4.3.5 Results of the correlation analysis for tautomer **b** according to Kamlet–Taft equation

Comp.	$v_0\times10^{-3}$ (cm^{-1})	$s\times10^{-3}$ (cm^{-1})	$b\times10^{-3}$ (cm^{-1})	$a\times10^{-3}$ (cm^{-1})	R^a	Sd^b	F^c	Solvent excluded from correlation
1	30.81 ±0.25	0.51 ±0.34	1.24 ±0.26	1.15 ±0.19	0.95	0.22	39.43	-
2	31.40 ±0.18	0.47 ±0.24	-0.54 ±0.18	1.21 ±0.13	0.94	0.16	30.95	-
3	31.45 ±0.21	–0.56 ±0.29	0.95 ±0.21	0.70 ±0.16	0.94	0.19	33.12	-
4	32.32 ±0.36	–1.35 ±0.49	0.41 ±0.27	1.58 ±0.27	0.93	0.31	22.39	DMAc, 1-Butanol
5	34.87 ±0.46	–4.39 ±0.66	1.03 ±0.37	–1.81 ±0.30	0.92	0.29	16.62	DEE, 2-Butanol, 2-Propanol
6	29.71 ±0.38	2.19 ±0.58	-[d]	0.93 ±0.20	0.92	0.20	15.56	AcN
7	30.98 ±0.15	-	0.51 ±0.20	0.84 ±0.12	0.97	0.11	61.40	DMAc, Chl
8	32.26 ±0.24	–2.21 ±0.33	0.54 ±0.18	–1.11 ±0.15	0.92	0.15	19.58	2-Butanol, DEE
9	30.72 ±0.25	0.85 ±0.32	0.74 ±0.35	1.24 ±0.20	0.95	0.20	35.09	Chl
10	30.70 ±0.23	0.44 ±0.31	0.89 ±0.23	1.05 ±0.17	0.95	0.20	33.71	-
11	33.86 ±0.48	–3.32 ±0.65	-	-2.91 ±0.36	0.94	0.42	31.66	-
12	30.62 ±0.26	1.35 ±0.36	-	1.12 ±0.18	0.92	0.21	18.18	DMF, DMAc
13	31.35 ±0.11	0.47 ±0.14	-0.95 ±0.15	0.83 ±0.09	0.94	0.09	29.95	Chl
14	30.93 ±0.18	1.10 ±0.25	0.69 ±0.19	0.92 ±0.14	0.95	0.16	36.26	-
15	32.99 ±0.54	0.83 ±0.43	-	2.80 ±0.41	0.93	0.48	25.48	-
16	31.75 ±0.09	-	-0.81 ±0.13	0.17 ±0.08	0.90	0.08	16.36	Chl

[a] Correlation coefficient; [b] Standard deviation; [c] Fisher test of significance; [d] Negligible values with high standard errors

Oppositely, positive sign of the coefficients *s* and *a*, obtained for the **6-PY** form (Table 4.3.5; except for comps. **3-5**, **8** and **9** - coefficient ***s*****;** and compounds **2, 13** and **16** - coefficient *b*), indicate hypsochromic shift in relation to increased contribution of the non-specific and HBD solvent effects. Complex influences of solvent effects on ν_{max} change were observed for both forms. Non-specific solvent effect is of highest value for compound **4** in **2-PY** form (-3.29; Table 4.3.3), although HBD effect is even higher value (-7.51) for this compound. The complex influences of both solvent and substituent effect on UV/Vis absorption maxima of the compounds in **6-PY** form is observed as inconsistent alteration of correlation coefficients (Tables 4.3.3 and 4.3.5).

Table 4.3.6 Results of the correlation analysis for tautomer **b** according to Catalán equation

Comp.	$\nu_0\times10^{-3}$ (cm^{-1})	$c\times10^{-3}$ (cm^{-1})	$d\times10^{-3}$ (cm^{-1})	$b\times10^{-3}$ (cm^{-1})	$a\times10^{-3}$ (cm^{-1})	R^a	Sd^b	F^c	Solvent excluded from correlation
1	31.63 ±0.09	-1.28 ±0.12	0.83 ±0.04	0.99 ±0.04	2.19 ±0.05	0.99	0.03	2036.37	-
2	31.63 ±0.59	-[d]	-	-0.68 ±0.24	2.35 ±0.31	0.93	0.18	17.74	-
3	32.74 ±0.14	-2.20 ±0.19	-	0.84 ±0.06	1.54 ±0.08	0.99	0.04	523.75	-
4	35.43 ±1.38	-5.06 ±1.78	–1.17 ±0.51	0.95 ±0.61	1.59 ±0.71	0.93	0.35	11.78	1-Butanol, Chl, DEE
5	35.74 ±1.06	-3.97 ±1.34	–1.72 ±0.40	1.13 ±0.47	–2.51 ±0.74	0.90	0.27	7.84	DEE, 2-Butanol, THF, Methanol
6	27.66 ±0.27	4.50 ±0.31	-	-	2.67 ±0.10	0.99	0.05	258.84	-
7	30.43 ±0.68	-[d]	-	1.14 ±0.34	1.39 ±0.37	0.92	0.20	13.00	Chl
8	34.26 ±0.77	-2.97 ±1.05	–0.83 ±0.28	0.85 ±0.28	–1.63 ±0.38	0.90	0.19	8.87	2-Butanol, DEE, Anisole
9	30.24 ±0.85	-	0.60 ±0.30	1.23 ±0.42	2.03 ± 0.46	0.93	0.25	16.38	Chl
10	31.75 ±0.16	-1.55 ±0.21	0.72 ±0.06	0.65 ±0.06	1.87 ± 0.08	0.99	0.05	502.35	-
11	36.27 ±0.37	-5.38 ±0.49	-1.26 ±0.15	-	-6.21 ± 0.20	0.99	0.11	375.14	-
12	30.64 ±0.88	-	1.15 ±0.38	-	2.27 ± 0.62	0.91	0.24	9.30	DMAc, DMF, Methanol
13	31.52 ±0.23	-	-	-0.67 ±0.09	1.33 ± 0.12	0.97	0.07	40.14	-
14	30.53 ±0.70	-	1.04 ±0.29	0.69 ±0.28	1.27 ± 0.38	0.93	0.21	15.94	DMF
15	33.77 ±0.22	-	-	-	6.19 ± 0.12	0.99	0.07	1119.12	-
16	32.62 ±0.18	-1.23 ±0.24	-	-0.72 ±0.07	-	0.96	0.05	32.34	-

[a] Correlation coefficient; [b] Standard deviation; [c] Fisher test of significance; [d] Negligible values with high standard errors

Quantitative separation of the non-specific solvent effect (coefficient *s*; Tables 4.3.3 and 4.3.5) on polarizability and dipolarity term (coefficients *c* and *d*, Tables 4.3.4 and 4.3.6), showed high significance of the solvent polarizability on stabilization of the excited state in both forms, and HBD effect in **6-PY** form (Table 4.3.6). Exception are compounds **6**, **7** and **11** (**2-PY** form) with highest values of coefficient *b*. Similar values of coefficients *a* and *b* for **2-PY** and significantly higher values of coefficient *b* for **6-PY** indicates different site dependent hydrogen bonding capabilities of hydroxyl group. Negative values of the coefficient *b* indicate higher stabilization

of the excited state in **2-PY** form, while opposite is true for HBA solvent effect in **6-PY** form (Table 4.3.4).

High values of coefficient *c* and lower values of coefficient *d*, obtained for all compounds in the **2-PY** form (Table 4.3.4), indicate pronounced influence of solvent polarizability and less dipolarity effects on ν_{max} change. Highest value of coefficient *c* was found for compound **4** what means that strong electron-withdrawing character of the nitro group causes high extent of π-electron delocalization which contributes to larger π-electron polarizability of the **2-PY** form. This could not be applied for compounds in the **6-PY** form where the pronounced non-specific solvent effect was noticed for compounds **4**, **6** and **11**, showing that both strong electron-donor and electron-acceptor substituents contribute to high electron polarizability.

Solvent hydrogen-bonding interactions have moderate contribution on the absorption maxima shift, except comp. **4** in 2-PY form (Table 4.3.4), and preferentially acts through hydrogen-bonding with the hydroxyl and the pyridine aza groups. Significant number of compound show negligible values and complex influence of specific solvent effects on solvatochromism of the investigated compounds (Table 4.3.6).

The comparison of the correlation results obtained for unsubstituted compound in the **PY** form indicate moderate contribution of non-specific solvent effect (Tables 4.3.3 and 4.3.5), and similar results were obtained according to Catalán equation (Tables 4.3.4 and 4.3.6). Solvent polarizability and dipolarity are dominant effects contributing to higher stabilization of excited state of unsubstituted compound in the **2-PY** form (Tables 4.3.4). Larger polarizability and HBD effect in the **6-PY** form is a mainly consequence of appropriate molecular geometry which enable larger extent of π-electron conjugative transfer. Introduction of electron-donating substituents cause also increases of π-electron mobility and HBD ability.

Table 4.3.7 Percentage contribution of solvatochromic parameters calculated from correlation results given in Table 3 for tautomer **a** according to Kamlet–Taft equation

Compound	P_s (%)	P_b (%)	P_a (%)
1	56.13	29.76	14.11
2	42.37	34.32	23.31
3	57.37	33.66	8.97
4	28.41	64.85	6.74
5	50.87	35.76	13.37
6	37.93	29.89	32.18
7	16.14	49.33	34.53
8	38.00	40.80	21.20
9	33.72	42.07	24.21
10	63.48	36.52	-
11	43.40	25.51	31.09
12	44.26	18.04	37.70
13	25.36	31.52	43.12
14	26.15	53.59	20.26
15	25.40	-	74.60
16	66.14	27.13	6.73

Table 4.3.8 Percentage contribution of solvatochromic parameters calculated from correlation results given in Table S3 for tautomer **b** according to Kamlet–Taft equation

Compound	P_s (%)	P_b (%)	P_a (%)
1	17.59	42.76	39.65
2	21.17	24.33	54.50
3	25.34	42.99	31.67
4	40.42	12.28	47.30
5	60.72	14.25	25.03
6	70.19	-	29.81
7	-	37.78	62.22
8	57.25	13.99	28.76
9	30.03	26.15	43.82
10	18.49	37.39	44.12
11	53.29	-	46.71
12	54.66	-	45.34
13	20.89	42.22	36.89
14	40.59	25.46	33.95
15	22.86	-	77.14
16	-	82.65	17.35

The success of the quantification and interpretation of solvent effects on the position of the absorption maxima of the investigated molecules was evaluated by plotting the calculated frequency (ν_{calc}), obtained by Catalán parameter set, *versus* the measured frequency (ν_{exp}) (R=0.97, Sd=0.29, F=7100) (Fig. 4.3.3).

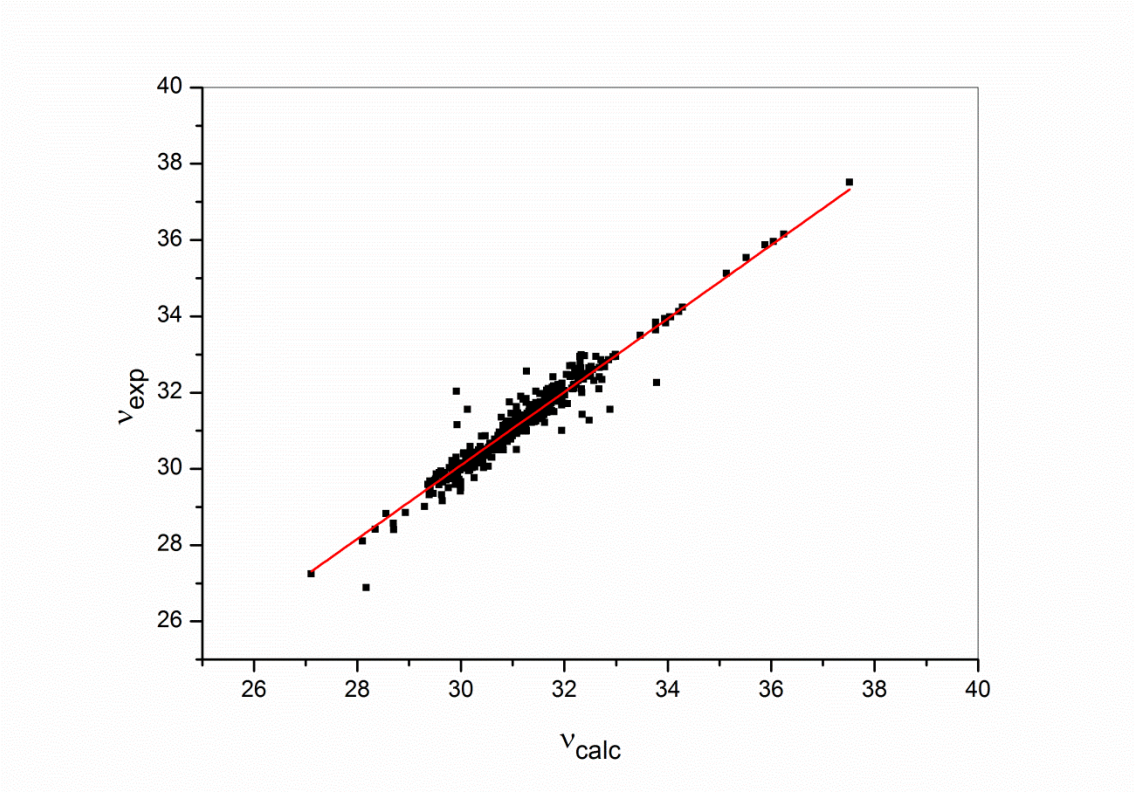

Fig. 4.3.3 Intercorrelation of ν_{exp} *vs* ν_{calc}

Applying described methodology, K_T values (K_T =[**b**]/[**a**]) of the investigated compounds were determined, and the results are presented in Table 4.3.9.

Table 4.3.9 Equilibrum constants K_T of investigated pyridones in selected solvents

Solvent/ Comp.	$\nu_{max}\times10^{-3}$ (cm^{-1})															
	1	**2**	**3**	**4**	**5**	**6**	**7**	**8**	**9**	**10**	**11**	**12**	**13**	**14**	**15**	**16**
Ethanol	0.32	1.99	0.13	0.83	2.01	1.33	1.53	1.87	0.33	2.47	22.1	1.04	1.50	1.07	1.18	1.68
Methanol	0.19	0.76	0.72	0.28	3.95	1.84	1.02	0.75	0.72	0.51	34.4	1.78	1.70	1.43	0.83	1.26
2-Propanol	3.53	1.63	2.39	2.54	2.97	1.17	1.39	1.49	2.65	3.87	21.2	1.17	0.39	1.12	0.58	0.86
1-Propanol	2.36	0.61	1.49	0.42	0.42	1.27	0.93	0.59	0.51	1.54	11.1	1.11	0.82			1.14
1-Butanol	1.25	1.24	3.01	1.47	3.17	0.99	1.16	1.60	2.35	3.73	8.2	1.52	1.62	1.78	1.65	0.83
2-Butanol	0.18	1.67	0.46	0.24	1.67	0.82	1.33	2.05	0.46	2.65	9.6	1.27	0.72	1.32	1.63	0.87
DMSO	1.41	0.42	3.42	2.38	0.35	-*	0.34	0.46	0.62	1.23	546	1.23	1.13	0.40	2.77	1.44
THF	3.63	3.12	3.02	2.06	0.50	1.21	1.27	0.85	1.23	3.91	18.7	2.08	0.57	1.04	1.70	1.71
AcN	1.24	0.67	0.55	5.72	0.87	2.75	2.23	1.29	1.57	1.00	26.5	0.95	0.80	0.39	2.11	1.08
Anisole	1.45	1.51	3.18	1.51	1.00	0.95	2.01	1.72	1.43	1.20	48.6	0.92	3.01	3.03	2.83	1.00
DMAc	0.57	1.43	1.66	0.74	1.23	-	1.56	0.89	1.19	0.68	328.1	1.09	0.71	1.08	2.06	0.85
DMF	2.71	1.13	0.47	1.23	1.32	-	0.78	0.37	0.63	0.80	420.3	1.86	0.69	0.92	1.06	5.27
EtAc	1.81	0.61	1.98	4.42	1.50	1.05	1.02	0.96	1.18	1.01	12.6	3.17	2.13	1.05	1.64	1.31
Chl	1.12	0.62	0.52	4.88	0.77	2.34	2.04	1.11	1.24	0.88	32.1	0.87	0.77	0.32	2.01	0.99
Dioxane	4.22	2.98	3.21	2.44	0.44	1.32	1.33	0.77	1.30	3.63	15.2	2.11	0.46	0.92	1.44	1.38
DEE	2.21	1.42	2.38	2.06	0.54	1.22	1.06	0.65	1.12	2.45	6.2	1.28	0.56	1.08	1.77	1.85

* tautomer **2-PY** exist in solution ($K_T \approx 0$)

Good agreement of the presented results (Table 4.3.9) with ones calculated from NMR data [193] in DMSO was obtained. The changes in the K_t values (Table 4.3.9) are consequence of the balanced contribution of both solvent and substituent effects. Balanced contribution of protic solvent effects on K_T (increased contribution of HBD effect) cause shift of the tautomeric equilibria to the **PY** form (higher K_t values); opposite is true for aprotic solvents, *i.e*. solvent with increased dipolarity/polarizability and proton-accepting capability (lower K_t values). It could be postulated that such behavior is a consequence in the differences in conjugational ability of the π-electron densities through localized or delocalized π-electronic systems of the appropriate tautomeric forms.

4.3.2 LFER analysis of UV data

A comprehensive analysis of substituent effects on absorption spectra of the investigated molecules, by using LFER principles in the form of the Hammett equation (Eq. x), was performed. The correlation results for **2-PY** and **6-PY** forms are given in Tables 4.3.10 and 4.3.11, respectively.

Table 4.3.10 Regression fits according to Eq. (x) for the **a** form

Solvent/ Compound	ν_0 x 10^{-3} (cm^{-1})	ρ x 10^{-3} (cm^{-1})	*R*	*Sd*	*F*	ν_0 x 10^{-3} (cm^{-1})	ρ x 10^{-3} (cm^{-1})	*R*	*Sd*	*F*	ν_0 x 10^{-3} (cm^{-1})	ρ x 10^{-3} (cm^{-1})	*R*	*Sd*	*F*
	2, 3, 15					**1, 7, 10, 14**					**9, 12, 13, 16**				
Methanol	30.07 ± 0.06	-4.45 ± 0.32	0.99	0.04	196.39	31.57 ± 0.02	-5.93 ± 0.23	0.99	0.03	660.08	32.58 ± 0.69	-5.89 ± 1.99	0.90	0.26	8.79
Ethanol	30.50 ± 0.15	-1.55 ± 0.78	0.90	0.11	3.95	31.31 ± 0.08	-4.52 ± 0.71	0.98	0.09	40.20	32.05 ± 0.24	-4.72 ± 0.68	0.98	0.09	43.38
	1, 4, 7, 8, 9, 12, 13, 14					**2, 3, 15**					**6, 10, 14**				
1-Propanol	31.25 ± 0.15	-3.38 ± 0.41	0.95	0.26	68.89	30.37 ± 0.06	-1.55 ± 0.32	0.98	0.04	23.83	30.89 ± 0.03	2.08 ± 0.14	0.99	0.05	1.77
2-Propanol	31.49 ± 0.18	-3.67 ± 0.49	0.94	0.31	56.07	30.24 ± 0.33	-2.65 ± 1.76	0.83	0.25	2.26	30.80 ± 0.22	1.27 ± 0.95	0.80	0.36	217.90
1-Butanol	31.27 ± 0.14	-3.35 ± 0.39	0.95	0.25	73.12	28.88 ± 0.41	-8.55 ± 2.16	0.97	0.31	15.59	30.79 ± 0.17	1.00 ± 0.75	0.80	0.28	1.78
2-Butanol	31.25 ± 0.14	-3.47 ± 0.38	0.96	0.24	81.76	29.79 ± 0.17	-4.15 ± 0.89	0.98	0.13	21.50	30.71 ± 0.14	1.29 ± 0.62	0.90	0.23	4.37
	2, 5, 6, 9, 14					**4, 7, 8, 11**					**12, 13, 16**				
AcN	30.45 ± 0.09	1.18 ± 0.29	0.92	0.20	16.93	29.67 ± 0.11	2.43 ± 0.34	0.97	0.22	50.10	33.79 ± 0.66	-10.00 ± 1.73	0.98	0.02	33.33
THF	30.59 ± 0.04	1.54 ± 0.14	0.99	0.09	122.12	29.97 ± 0.09	1.59 ± 0.22	0.97	0.14	49.96	22.39 ± 1.32	20.00 ± 3.46	0.98	0.05	33.33
	2, 5, 6, 9					**4, 7, 8, 11, 15**					**12, 13, 16**				
Chl	30.95 ± 0.13	0.87 ± 0.37	0.85	0.25	5.46	30.66 ± 0.11	1.64 ± 0.25	0.98	0.16	41.22	24.81 ± 8.67	14.7 ± 8.8	0.54	0.32	0.64
Anisol	30.90 ± 0.07	0.58 ± 0.21	0.89	0.14	7.45	30.27 ± 0.25	1.15 ± 0.60	0.74	0.38	3.66	52.24 ± 12.40	-59.5 ± 32.62	0.88	0.46	3.33
	2, 3, 7, 12, 13, 14, 15					**1, 8, 9, 10, 16**					**4, 5, 6**				
EtAc	30.44 ± 0.08	-1.76 ± 0.34	0.92	0.22	26.58	31.40 ± 0.04	-3.81 ± 0.20	0.99	0.06	358.16	30.61 ± 0.05	1.52 ± 0.08	0.99	0.07	343.95
Dioxane	30.42 ± 0.08	-2.10 ± 0.33	0.94	0.21	41.26	31.46 ± 0.08	-3.15 ± 0.37	0.98	0.11	73.15	30.55 ± 0.28	1.15 ± 0.48	0.92	0.41	5.70
DEE	30.46 ± 0.06	-2.66 ± 0.23	0.98	0.14	133.25	31.57 ± 0.14	-3.67 ± 0.62	0.96	0.19	34.69	30.61 ± 0.41	0.96 ± 0.71	0.80	0.60	1.82
	5, 7, 8, 9, 12, 13, 16					**3, 6, 14, 15**					**1, 2, 10**				
DMSO	29.47 ± 0.08	-0.95 ± 0.23	0.88	0.06	16.66	30.39 ± 0.04	2.45 ± 0.15	0.99	0.06	248.92	29.95 ± 0.01	1.25 ± 0.02	0.99	0.01	3830.6
	1, 2, 3, 5, 10, 11, 15, 16					**4, 7, 8, 16**					**3, 6, 9**				
DMAc	30.48 ± 0.08	1.76 ± 0.27	0.94	0.22	42.62	29.50 ± 0.04	1.35 ± 0.09	0.99	0.04	221.06	30.02 ± 0.01	1.18 ± 0.02	0.99	0.01	4973.75
	1, 2, 9, 11, 13, 14					**7, 10, 12, 16**					**2, 4, 6**				
DMF	30.06 ± 0.04	-2.16 ± 0.16	0.99	0.07	182.97	29.87 ± 0.04	-2.27 ± 0.15	0.99	0.09	219.24	29.44 ± 1.41	-1.70 ± 2.46	0.57	2.08	0.48

Table 4.3.11 Regression fits according to Eq. (x) for the **b** form

Solvent/ Compound	ν_0 x 10^{-3} (cm^{-1})	ρ x 10^{-3} (cm^{-1})	*R*	*Sd*	*F*	ν_0 x 10^{-3} (cm^{-1})	ρ x 10^{-3} (cm^{-1})	*R*	*Sd*	*F*	ν_0 x 10^{-3} (cm^{-1})	ρ x 10^{-3} (cm^{-1})	*R*	*Sd*	*F*
	1, 5, 9, 10, 12, 13, 14, 16					**7, 8, 11**					**3, 2, 6**				
Methanol	33.38 ± 0.19	-3.90 ± 0.62	0.93	0.30	39.32	34.84 ± 0.16	-15.63 ± 0.54	0.99	0.10	824.27	32.90 ± 0.45	2.35 ± 1.59	0.83	0.22	2.19
	1, 7, 8, 10, 11, 13, 16					**5, 9, 12, 14**					**3, 6, 15**				
Ethanol	32.95 ± 0.43	-5.68 ± 0.52	0.86	0.63	13.94	33.32 ± 0.32	-2.63 ± 0.96	0.89	0.27	7.52	36.62 ± 0.75	13.37 ± 2.80	0.98	0.60	22.87
1-Propanol	33.14 ± 0.36	-5.68 ±1.25	0.90	0.52	20.50	33.17 ± 0.40	-2.66 ± 1.20	0.84	0.34	4.91	33.77 ± 0.36	5.44 ± 1.34	0.97	0.29	16.59
2-Propanol	32.96 ± 0.23	-5.48 ± 0.81	0.95	0.34	45.28	33.30 ± 0.23	-2.95 ± 0.67	0.95	0.19	19.18	36.56 ± 0.06	14.78 ± 0.23	0.99	0.05	3952.69
1-Butanol	32.85 ± 0.33	-5.00 ± 1.16	0.89	0.48	18.51	32.88 ± 0.20	-1.76 ± 0.59	0.90	0.17	8.88	36.77 ± 0.64	14.83 ± 2.40	0.99	0.52	38.17
2-Butanol	32.64 ± 0.15	-4.39 ± 0.53	0.97	0.21	69.53	33.17 ± 0.15	-2.98 ± 0.46	0.98	0.13	42.26	35.89 ± 0.94	13.98 ± 3.53	0.97	0.76	15.72
DMSO	32.08 ± 0.20	-3.32 ± 0.71	0.90	0.30	21.65	33.34 ± 0.19	-4.45 ± 0.58	0.98	0.16	59.68					
	1, 7, 8, 10, 11, 13, 16,					**9, 12, 14**									
DMAc	31.19 ± 0.15	-3.05 ± 0.52	0.93	0.22	34.28	31.93 ± 0.88	2.19 ± 3.38	0.54	0.60	0.42					
DMF	31.93 ± 0.15	-2.46 ± 0.53	0.90	0.22	21.70	33.14 ± 0.14	-6.68 ± 0.55	0.99	0.10	145.61					
	1, 2, 5, 6, 8, 14					**9, 10, 11**					**13, 7, 16**				
THF	31.77 ± 0.09	2.80 ± 0.33	0.97	0.23	71.75	31.47 ± 0.04	0.95 ± 0.13	0.99	0.03	56.10	31.26 ± 0.13	-0.26 ± 0.41	0.54	0.07	0.40
EtAc	31.68 ± 0.05	2.58 ± 0.19	0.99	0.13	181.23	31.46 ± 0.01	1.22 ± 0.02	0.99	0.01	3346.68	31.29 ± 0.11	-0.26 ± 0.33	0.62	0.05	0.62
	1, 2, 8, 11					**5, 7, 9,**					**6, 10, 14**				
DEE	31.67 ± 0.04	1.79 ± 0.15	0.99	0.07	147.73	30.50 ± 0.03	3.00 ± 0.09	0.99	0.02	1142.25	31.22 ± 0.02	2.17 ± 0.07	0.99	0.03	843.64
	1, 2, 5, 6, 8, 14					**7, 9, 11**					**4, 12, 13**				
Dioxane	31.62 ± 0.06	2.03 ± 0.21	0.98	0.15	88.78	30.80 ± 008	2.67 ± 0.26	0.99	0.05	109.16	30.85 ± 0.05	0.85 ± 0.09	0.99	0.03	84.47
	6, 3, 9, 14					**1, 7, 12**					**4, 8, 10, 13, 16**				
ChL	32.01 ± 0.09	2.10 ± 0.35	0.97	0.18	30.18	31.31 ± 0.02	1.75 ± 0.10	0.99	0.03	277.25	30.96 ± 0.05	1.42 ± 0.12	0.99	0.06	134.35
	1, 2, 14					**7, 11, 13, 16**					**9, 10, 12**				
AcN	32.00 ± 0.01	1.45 ± 0.01	0.99	0.01	9397.8	30.88 ± 0.12	1.46 ± 0.35	0.95	0.07	17.47	31.70 ± 0.01	0.64 ± 0.04	0.99	0.01	320.33
	1, 5, 12, 16					**4, 7, 10, 16**					**2, 6, 15**				

Anisol	31.53 ± 0.01	0.54 ± 0.02	0.99	0.01	525.07	31.16 ± 0.01	0.30 ± 0.02	0.99	0.01	135.73	34.15 ± 1.33	7.93 ± 5.57	0.82	1.2	2.03

To explain the effects of substituent effects on electronic absorption spectra of investigated pyridones, the ν_{max} of the unsubstituted compound (**1**) in used solvents were taken as the reference. The complex influences of both solvent and substituent effect on UV/Vis absorption maxima of both forms was noticed (Tables 4.3.10 and 4.3.12). The correlation results (Table 4.3.10), classified in the eight sets of solvents and three groups (columns) of substituent-dependent correlation results, reflect the complex and balanced interplay of solvent and substituent effects on absorption maxima shifts. Similar results were found for **6-PY** form (Table 4.3.12). These results indicate that solvent effects: dipolarity/polarizability, HBD and HBA abilities cause appropriate sensitivity of the position of absorption maxima (ν_{max}) to substituent effect.

In the two sets of protic solvent and three of aprotic ones (first column; Table 4.3.10), except DMAc, a negative correlation slopes were obtained. Somewhat higher sensitivity of ν_{max} to substituent effect was found for protic solvents. In the third and fourth set of solvents (AcN, THF, Chl and Anisole), positive solvatochromism with respect to substitutent effects was noticed. Somewhat higher values and similar trend of correlation slope was found for second column, except DMSO, indicate utmost significance of the solvent dipolarity/polarizabilty and proton-accepting capabilities to higher stabilization of excited state of these compounds. Results presented in third column indicate that in second set of protic solvents contribution of aliphatic alcohol residue play a significant role in stabilization of ground state of compounds **6**, **10** and **1**4. Exceptionally high susceptibility of the ν_{max} shifts to the electronic substituent effects was generally found for aprotic solvents (AcN, THF, Chl and Anisole) in third column.

Results of LFER study of the compounds in 6-**PY** form clearly show more regular behavior: correlation results obtained for first two set of compounds show better stabilization of excited state of investigated compounds, and opposite is true for other solvents. Similar behavior of first and second columns could be noticed, except in DMAc and DMF. Correlation results presented in third column shows high sensitivity of ν_{max} to substituent effect in protic solvents and lower for aprotic ones causing higher stabilization of solute in ground state.

Generally speaking results of LFER study show better stabilization of both forms in the excited state in protic solvents. Lower sensitivities of their absorption frequencies to substituent effects

in aprotic solvents might be explained by the effect of high relative permittivity of surrounding medium which contribute that the energy necessary to bring about charge separation in the ground and excited state is relatively similar, which gives rise to a lower susceptibility to electronic substituent effects. Dipolar aprotic solvents behave as poor anion solvators, while they usually better stabilize larger and more dispersible positive charges. The electronic systems of the investigated pyridones, considering their *non*-planarity, could be more susceptible to the substituent influence. Study of the transmission of substituent electronic effects through defined π-resonance units (Fig. 1b?) showed that they behave either as isolated or conjugated fragments, and depend on substitution pattern under consideration.

4.3.4 LFER analysis of NMR data

A comprehensive analysis of the ^{13}C NMR chemical shifts has been performed to get a better insight into transmission mode of substituent effect. The experimental and calculated ^{13}C NMR chemical shifts of the corresponding carbon atoms are given in Tables 4.1.3 and 4.1.4. The differentiation in ^{13}C NMR chemical shifts is less than 8 ppm.

The general conclusion derived from the data in Tables 4.3.12 and 4.3.13 indicate that all substituents from the *N*(1)-phenyl ring influence *SCS* values of the carbon atoms of interest ($C_{1'}$, C_2-C_6) *via* their electronic effects. Effective transmission of substituent effects, *i.e*. differences in *SCS* values, is affected by the conformational (geometry) change of the investigated molecules which stems from an out-of-plane rotation of the *N*(1)-phenyl ring, *i.e.* defined by the torsion angle θ values (Scheme 1?). Optimized geometries was calculated by the use of B3LYP functional with 6-311G(d,p) basis set (Tables 4.1.7 and 4.1.8) [193].

Analysis of the substituent effect on the *SCS* of the carbon atoms of interest, performed by the use of LFER's Eq. (x?) (*i.e.* SSP) with σ or σ^+ substituent constants have been applied, and the correlation results obtained for $C_{1'}$, C_2 - C_6 carbons are presented in Tables 4.3.12 and 4.3.13.

Table 4.3.12 Correlation results of the *SCS* values of tautomer **a** with σ_p/σ_m and σ_p^+/σ_m^+ substituent constants using Hammett Eq. (x)

		ρ	h	R	F	sd	n	
C_1,	σ	13.76±1.59	–2.20±0.53	0.923	75	1.83	15	all
	σ^+	9.45±0.92	–0.53±0.41	0.943	105	1.58	15	all
	σ^-	10.05±1.43	–2.08±0.52	0.925	77	1.80	15	all
	σ	15.32±1.58	–2.41±0.56	0.960	94	1.66	10	4-substituted[a]
	σ^+	10.30±0.98	–0.22±0.49	0.966	111	1.53	10	4-substituted
	σ	16.62±0.87	–3.26±0.34	0.992	368	0.86	8	4-(H i Me excluded)
	σ^+	8.91±0.41	0.70±0.24	0.992	476	0.76	8	4-(H i Me excluded), σ_p^- (NO_2)
	σ	3.70±1.00	0.20±0.27	0.880	14	0.46	6	3-substituted[b]
	σ^+	3.36±1.00	0.28±0.28	0.860	11	0.50	6	3-substituted
	σ	4.58±0.46	0.20±0.11	0.985	99	1.93	5	3-(COMe excluded)
	σ^+	3.73±0.81	0.44±0.24	0.956	21	0.34	5	3-(COMe excluded)
C_2	σ	-1.70±0.17	0.02±0.04	0.985	96	0.06	5	H, OH, OMe, Me, F
	σ^+	-0.37±0.05	0.26±0.03	0.967	58	0.06	6	OH, OMe, Me, Cl, Br, COMe
	σ	1.13±0.21	0.03±0.06	0.936	28	0.10	6	3-substituted
	σ	0.95±0.09	0.02±0.02	0.988	28	0.04	5	H, 3-Br, 3-OMe, 3-Me, 3-COMe
C_3	σ	-1.94±0.16	0.18±0.04	0.975	156	0.13	10	H, OH, OMe, Me, Cl, Br, I, COMe, 3-Br, 3-Me
	σ^+	-1.17±0.12	-0.04±0.05	0.954	104	0.16	10	H, OH, OMe, Me, Cl, Br, I, COMe, 3-Br, 3-Me
C_4	σ	-0.64±0.12	0.10±0.03	0.912	30	0.08	8	H, OH, OMe, Me, F, I, COMe, 3-Me
	σ	-0.80±0.15	0.51±0.06	0.938	29	0.08	6	NO_2, Cl, Br, 3-Cl, 3-Br, 3-OMe
C_5	σ^+	0.55±0.05	0.38±0.03	0.965	109	0.08	10	OH, OMe, Me, F, Cl, Br, COMe, 3-Br, 3-Cl, 3-COMe
C_6	σ	(1.31±0.31) σ^2	(-0.65±0.18) σ	0.926	9	0.08	6	H, OH, F, I, COMe, NO_2
	σ	(4.79±0.72) σ^2	(-0.89±0.17) σ	0.958	22	0.08	7	Me, OMe, 3-Cl, 3-Br, 3-OMe, 3-Me, 3-COMe

[a] all 4-substituted compounds; [b] all 3-substituted compounds

Table 4.3.13 Correlation results of the SCS values with the Hammett substituent constants σ_p/σ_m and σ_p^+/σ_m^+ for tautomer **b** according to Eq. (x)

Atom		ρ	h	R	F	sd	n	
$C_{1'}$	σ	11.73±1.88	–2.13±0.64	0.866	39	1.94	15	all
	σ^+	8.59±1.28	–0.94±0.51	0.880	45	1.85	15	all
	σ^-	8.68±1.09	–1.88±0.50	0.911	63	1.61	15	all
	σ	14.04±2.08	–2.48±0.73	0.931	46	1.90	9	4-substituted[a]
	σ^+	10.23±1.42	–0.68±0.60	0.939	52	1.79	9	4-substituted
	σ^-	9.36±1.15	–2.53±0.62	0.951	67	1.61	9	4-substituted
	σ	16.58±1.20	–3.82±0.47	0.987	191	0.97	7	4-sub. (H i Me excluded)
	σ^-	10.50±0.66	-3.57±0.40	0.990	257	0.84	7	4-sub. (H i Me excluded)
	σ	2.57±1.02	0.24±0.31	0.747	6	0.52	7	3-substituted[b]
	σ^+	2.05±0.97	0.55±0.52	0.687	4	0.57	7	3-substituted
	σ^+	1.72±0.23	-0.01±0.07	0.985	58	0.11	4	H, 3-Me, 3-COMe, 3-CF_3
	σ^+	1.55±0.21	1.02±0.07	0.991	57	0.06	3	3-OMe, 3-Br, 3-Cl
C_2	σ	1.39±0.15	0.02±0.04	0.973	96	0.08	7	H, 3-CF_3, 3-Cl, 3-Br, 3-OMe, 3-Me, 3-COMe
	σ^+	1.22±0.09	0.05±0.03	0.986	171	0.06	7	H, 3-CF_3, 3-Cl, 3-Br, 3-OMe, 3-Me, 3-COMe
	σ	2.05±0.45	-0.03±0.08	0.934	20	0.09	5	H, F, Cl, Br, I
C_4	σ	-1.19±0.15	0.25±0.05	0.911	64	0.20	15	all σ^+(Me, OMe), σ^-(NO_2, I)
	σ	-1.33±0.21	0.24±0.07	0.922	40	0.19	9	4-substituted
	σ^+	-0.78±0.14	0.14±0.06	0.840	31	0.20	15	all
C_5	σ	1.44±0.26	-0.01±0.08	0.941	31	0.12	6	3-substituted
C_6	σ	(0.51±0.09) σ^2	(-0.65±0.01) σ	1.000	11078	0.00	4	H, I, COMe, NO_2
	σ	(6.32±1.12) σ^2	(-1.18±0.28) σ	0.930	16	0.14	8	Me, OMe, F, 3-Cl, 3-Br, 3-OMe, 3-Me, 3-COMe

[a] all 4-substituted compounds; [b] all 3-substituted compounds

The observed ρ values indicate different susceptibilities of the *SCS* to substituent effects. It can be noticed from Tables 4.3.16 and 4.3.17 that correlations are of good to high quality which means that the *SCS* values reflect electronic substituent effects. It is apparent that chemical shifts of $C_{1'}$ show an increased susceptibility and normal substituent effect. Reverse substituent effect was observed at C_2 for *para*-substituents, as well as for C_3 and C_4 atoms. The negative sign of reaction constant, ρ, means reverse behavior, *i.e.* the value of *SCS* decreases although the

electron–withdrawing ability of the substituents, measured by σ, increases. The reverse substituent effect at C_2 (for *para*-substituents), C_3 and C_4 atoms can be attributed to localized π-polarization, which predominates over the extended π-polarization (Table 4.3.16) in the compounds in **2-PY** form. Correlations for $C_{1'}$ carbon is slightly improved when electrophilic substituent constants σ^+ is used, which indicates that contribution of extended resonance interaction, *i.e*. more intensive interaction of electron-donating substituent with electrophilic $C_{1'}$ carbon. The *SCS* of C_6 showed nonlinear (parabolic) dependence with respect to substituent effect. Similar results were found for compounds in **6-PY** form (Table 4.3.17), except normal substituent effect found for C_2 carbon.

To measure separate contributions of the polar (inductive/field) and resonance effects of substituent, the regression analysis according to DSP Eq. (x) with σ_I and σ_R constants has been performed, and the results are given in Tables 4.3.14 and 4.3.15.

Table 4.3.14 Correlation results of the *SCS* values of tautomer **a** with σ_I and σ_R substituent constants using Eq. (x)

Atom		ρ_I	ρ_R	h	R	λ^a	F	Sd	n	
$C_{1'}$	σ	8.47±1.92	17.13±1.59	0.13±0.78	0.956	2.02	63	1.45	15	all
	σ	9.66±1.98	18.25±1.57	0.17±0.85	0.979	1.89	82	1.28	10	4-substituted[b]
	σ	9.75±5.43	18.26±2.38	0.14±2.70	0.982	1.87	58	1.51	8	4-sub. (H i Me excluded)
	σ	3.84±0.78	0.22±2.00	-0.05±0.25	0.947	0.06	13	0.36	6	3-substituted[c]
	σ	4.48±0.23	2.64±0.65	0.07±0.07	0.998	0.59	208	0.10	5	3-sub. (COMe excluded)
C_2	σ	-1.31±0.34	-1.30±0.26	0.08±0.09	0.963	0.99	13	0.12	5	H, OH, OMe, Me, F
	σ	1.12±0.25	1.22±0.63	0.03±0.08	0.936	1.09	11	0.11	6	3-substituted
	σ	0.94±0.09	1.12±0.21	0.04±0.03	0.992	1.19	59	0.04	5	H, 3-Br, 3-OMe, 3-Me, 3-COMe
C_3	σ	1.56±0.31	-2.06±0.26	0.02±0.10	0.957	1.32	38	0.19	10	H, OH, OMe, Me, Cl, Br, I, COMe, 3-Br, 3-Me
	σ	-0.55±0.24	-0.62±0.18	0.08±0.06	0.850	1.13	7	0.12	8	H, OH, OMe, Me, F, I, COMe, 3-Me
C_4	σ	-0.15±0.74	-1.22±0.51	0.18±0.39	0.945	8.13	12	0.08	6	NO_2, Cl, Br, 3-Cl, 3-Br, 3-OMe
	σ	2.42±0.76	1.92±0.67	0.02±0.31	0.779	0.79	9	0.57	15	all
	σ	2.65±1.02	2.04±0.81	0.10±0.44	0.813	0.77	7	0.66	10	4-substituted
C_5	σ	0.97±0.24	0.83±0.18	0.17±0.09	0.898	0.86	17	0.13	11	H, OH, OMe, Me, Cl, Br, I, COMe, 3-Br, 3-Me, 3-OMe
	σ	1.80±0.44	4.16±1.04	0.16±0.17	0.965	2.31	14	0.17	5	3-substituted

[a] $\lambda = \rho_R/\rho_I$; [b] all 4-substituted compounds; [c] all 3-substituted compounds

Table 4.3.15 Correlation results of the *SCS* values with the Hammett DSP equation for tautomer **b**

Atom		ρ_I	ρ_R	h	R	λ^a	F	Sd	n	Compounds included
$C_{1'}$	σ	8.28±2,61	13.23±2,39	–0.77±1.03	0.870	1.60	19	2.00	15	all
	σ	7.93±2.34	12.96±2.34	0.32±1.00	0.963	1.58	39	1.51	9	4-substituted[b]
	σ	6.00±6.61	18.44±3.15	1.32±3.28	0.963	3.07	26	1.82	7	4- (H i Me excluded)
	σ	3.68±0.93	1.34±0.87	-0.19±0.33	0.917	0.36	8	0.35	6	3-substituted[c]
C_2	σ	1.09±0.48	-0.14±0.41	0.02±0.15	0.855	0.13	5	0.19	7	H, 3-CF_3, 3-Cl, 3-Br, 3-OMe, 3-Me, 3-COMe
	σ	2.31±0.68	2.95±1.09	-0.02±0.12	0.927	1.28	6	0.12	5	H, F, Cl, Br, I
C_4	σ	-0.85±0.27	-1.20±0.24	0.15±0.11	0.851	1.41	16	0.20	15	all
	σ	-0.96±0.29	-1.56±0.27	0.07±0.12	0.938	1.63	22	0.19	9	4-substituted
C_5	σ	0.93±0.61	-0.59±0.58	-0.03±0.22	0.810	0.63	3	0.23	6	3-substituted

[a] $\lambda = \rho_R/\rho_I$; [b]all 4-substituted compounds; [c] all 3-substituted compounds

The DSP equation does not provide significant improvement in fits when compared to the results of SSP Eq. (x). The positive ρ_I and ρ_R values have been obtained for the $C_{1'}$, C_2 (3-sub. comps.), C_3 and C_5 atoms, while the negative values have been found for C_2 (comps. **1**, **2**, **3**, **6** and **10**) and C_4 confirming that reverse substituent effect is operative at this carbon. All the λ values are higher than 1, except C_5 for *para*-substituted compounds, which means that resonance substituent effect predominates over field effect, and the most pronounced is at C_4. The resonance interaction significantly depends on spatial arrangement of the molecules, *i.e.* the values of torsional angle θ, and thus, the resonance substituent effect is most effectively transmitted to $C_{1'}$ and C_4 carbons, *i.e.* C_4 is para-position of the carbon of pyridone ring with respect to *N*-substituted phenyl ring.

Comparative analysis of the structural effect of the substituent at C_6 position: OH group in compounds in **6-PY** form and methyl group in a series of *N*(1)-(4-substituted phenyl)-3-cyano-4,6-dimethyl-2-pyridones [225] could gives some additional information on structural effect on the mode and extent of transmission of substituent effect.

On the basis of the sign of the constants ρ (Table 4.3.18) and from literature data for N(1)-(4-substituted phenyl)-3-cyano-4,6-dimethyl-2-pyridones [236] could be noticed similar behavior. Effects of substituent have the same direction at all carbon atoms, except at C2 for para-substituted compounds (line 6; Table 4.3.18).

Substituent show the highest influences at C1’ carbon with somewhat higher values in *N*(1)-(4-substituted phenyl)-3-cyano-4,6-dimethyl-2-pyridones. Oppositely higher values of correlation coefficients for C3 and C5 carbons indicates significance of electron-donating capabilities of hydroxyl group at C6 carbon, in comparison to low hyperconjugative character of methyl group.

4.3.5 DFT, TD-DFT and Bader's analysis. Evaluation of electronic transition and charge density change

An additional analysis of solvent and substituent effects on absorption frequencies, tautomeric equilibria and conformational changes of the studied compounds necessitated quantum-chemical calculations, *i.e.* geometry optimization and charge density analysis. Geometry optimization of the investigated molecules was performed by the use of B3LYP functional with 6-311G(d,p) basis set. The most stable conformations of compounds **1-16** in **2-PY** and **6-PY** forms are presented in Figs. 4.3.4 and 4.3.5, respectively. Elements of optimized geometries of compounds **1-16** are given in Tables 4.1.7 and 4.1.8.

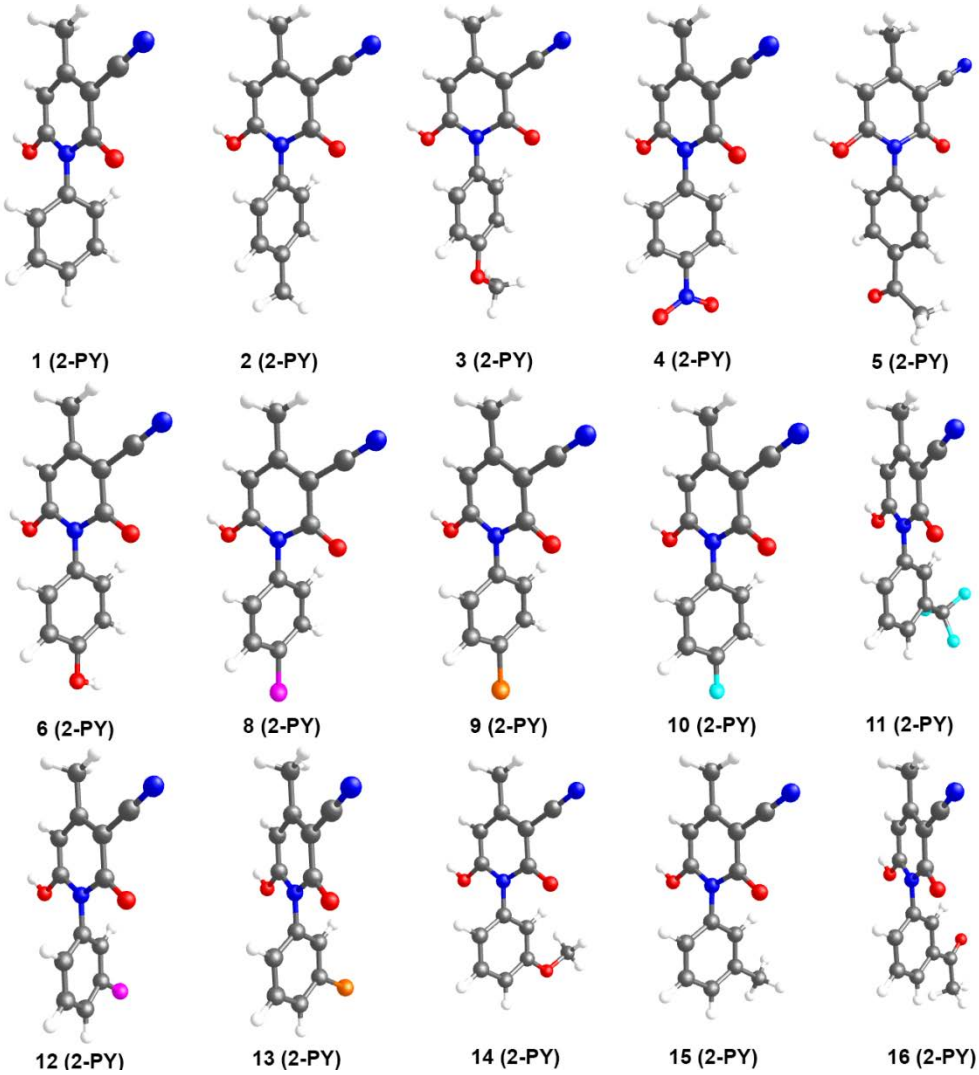

Fig. 4.3.4 Optimal geometries of compounds **1 - 16** in **2-PY** forms

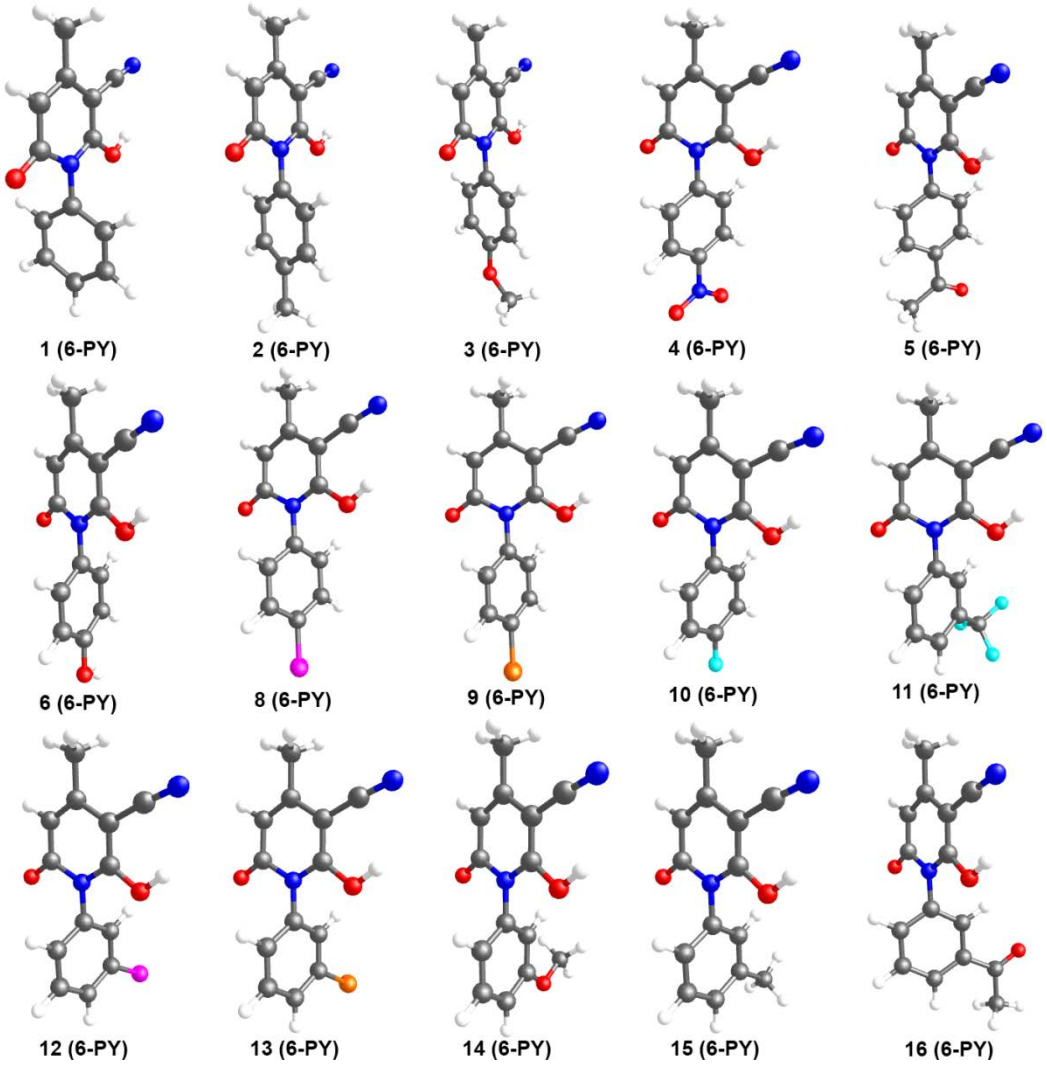

Fig. 4.3.5 Optimal geometries of compounds **1** - **16** in **6-PY** form

The element of geometry feature of the greatest interest for understanding of the transmission of substituent effects is the values of torsion angle θ_1 (Scheme S1?). Higher planarity of molecule, *i.e*. lower torsional angle, induces red shift in the absorption spectra [193]. In the investigated molecules, these values are fairly similar and mostly depend on substituent presents. Somewhat larger differences of θ was noticed for electron-donor substituted compounds (Tables 4.1.7 and 4.1.8: 80.18 for compound **2** in 2-PY form and 82.77 for compound 14 in **6-PY** form), indicating significance of extended resonance interaction in electron-donor substituted compounds. Oppositely, in electron-acceptor substituted compounds appropriate contribution of n,π-conjugation (nitrogen lone pair participation) to overall electronic interaction with π-electronic system of pyridone unit causing perturbation of π–electron density.

The results shown in Tables 4.1.7 and 4.1.8 indicate that bond lengths of the **2-PY** and **6-PY** forms are obviously different and similar alteration of the values with respect to form under consideration. Appropriate values of bond distances are in the frame of statistical errors and thus they are not suitable for evaluation purpose. Generally, low influences of electronic substituent effect could be noticed.

Mechanism of electronic excitations and the electron density distribution in ground and excited states were studied by calculation of HOMO/LUMO energies (E_{HOMO}/ E_{LUMO}) and E_{gap} values (Tables 4.3.16 and 4.3.17, and Fig. 4.3.6-4.3.9). Generally, a lower E_{gap} values were observed for all compounds in the **2-PY** form, and lowest values were found for nitro substituted compound. Small influences of electron-donor substituents on changes E_{gap} could be observed. For compounds **1-16** in **6-PY** form (Table 4.3.16), the substituent effects influence on E_{gap} changes showed similar trend as for compounds in **2-PY** form.

Table 4.3.16 Calculated energies of the HOMO and LUMO orbitals and energy gap for compounds **1 - 16** in gas phase

Compound	Tautomer	Orbitals energy (eV)		
		Gas phase		
		E_{HOMO}	E_{LUMO}	E_{gap}
1	**2-PY**	-6.02	-1.49	4.53
	6-PY	-6.12	-1.18	4.94
2	**2-PY**	-5.98	-1.45	4.53
	6-PY	-6.07	-1.13	4.94
3	**2-PY**	-5.94	-1.44	4.50
	6-PY	-6.03	-1.1	4.92
4	**2-PY**	-6.40	-2.70	3.70
	6-PY	-6.49	-2.72	3.77
5	**2-PY**	-6.18	-1.93	4.25
	6-PY	-6.27	-1.90	4.37
6	**2-PY**	-5.98	-1.47	4.51
	6-PY	-6.07	-1.15	4.92
8	**2-PY**	-6.17	-1.67	4.50
	6-PY	-6.26	-1.38	4.88
9	**2-PY**	-6.16	-1.67	4.49
	6-PY	-6.25	-1.38	4.87
10	**2-PY**	-6.11	-1.59	4.52
	6-PY	-6.21	-1.28	4.93
11	**2-PY**	-6.22	-1.74	4.48
	6-PY	-6.31	-1.47	4.84
12	**2-PY**	-6.17	-1.67	4.50
	6-PY	-6.26	-1.38	4.88
13	**2-PY**	-6.16	-1.67	4.49
	6-PY	-6.25	-1.37	4.88
14	**2-PY**	-6.01	-1.50	4.51
	6-PY	-6.10	-1.14	4.96
15	**2-PY**	-5.99	-1.47	4.52
	6-PY	-6.08	-1.12	4.96
16	**2-PY**	-6.11	-1.81	4.30
	6-PY	-6.20	-1.80	4.40

Table 4.3.17 Calculated energies of the HOMO and LUMO orbitals and energy gap for compounds **1 - 16** in DMSO, EtOH and THF

Compound	Tautomer	Orbitals energy (eV)								
		DMSO			Ethanol			THF		
		E_{HOMO}	E_{LUMO}	E_{gap}	E_{HOMO}	E_{LUMO}	E_{gap}	E_{HOMO}	E_{LUMO}	E_{gap}
1	**2-PY**	-6.07	-1.46	4.62	-6.07	-1.46	4.61	-6.07	-1.47	4.60
	6-PY	-6.15	-1.13	5.02	-6.15	-1.13	5.02	-6.15	-1.14	5.01
2	**2-PY**	-6.06	-1.45	4.61	-6.06	-1.45	4.61	-6.05	-1.46	4.60
	6-PY	-6.14	-1.12	5.02	-6.13	-1.12	5.02	-6.13	-1.12	5.01
3	**2-PY**	-6.03	-1.45	4.58	-6.03	-1.45	4.58	-6.02	-1.46	4.57
	6-PY	-6.09	-1.12	4.97	-6.09	-1.11	4.97	-6.09	-1.12	4.96
4	**2-PY**	-6.18	-2.71	3.47	-6.18	-2.71	3.48	-6.23	-2.70	3.52
	6-PY	-6.26	-2.73	3.53	-6.26	-2.72	3.53	-6.30	-2.72	3.58
5	**2-PY**	-6.12	-1.86	4.26	-6.13	-1.86	4.27	-6.15	-1.87	4.28
	6-PY	-6.20	-1.85	4.35	-6.20	-1.85	4.35	-6.23	-1.85	4.37
6	**2-PY**	-6.01	-1.45	4.57	-6.01	-1.44	4.57	-6.01	-1.45	4.56
	6-PY	-6.08	-1.11	4.96	-6.07	-1.11	4.96	-6.08	-1.12	4.96
8	**2-PY**	-6.12	-1.53	4.59	-6.11	-1.53	4.58	-6.13	-1.56	4.57
	6-PY	-6.19	-1.23	4.96	-6.19	-1.23	4.96	-6.21	-1.26	4.95
9	**2-PY**	-6.11	-1.53	4.58	-6.11	-1.53	4.58	-6.13	-1.56	4.57
	6-PY	-6.19	-1.24	4.95	-6.19	-1.24	4.95	-6.21	-1.26	4.95
10	**2-PY**	-6.09	-1.49	4.60	-6.09	-1.49	4.60	-6.10	-1.51	4.59
	6-PY	-6.17	-1.16	5.00	-6.17	-1.16	5.00	-6.18	-1.19	5.00
11	**2-PY**	-6.13	-1.56	4.56	-6.13	-1.57	4.56	-6.15	-1.60	4.55
	6-PY	-6.20	-1.28	4.92	-6.20	-1.28	4.92	-6.23	-1.31	4.92
12	**2-PY**	-6.12	-1.54	4.58	-6.12	-1.54	4.58	-6.14	-1.57	4.57
	6-PY	-6.20	-1.23	4.97	-6.20	-1.23	4.96	-6.22	-1.26	4.96
13	**2-PY**	-6.12	-1.54	4.58	-6.12	-1.54	4.58	-6.13	-1.57	4.57
	6-PY	-6.20	-1.23	4.97	-6.20	-1.23	4.97	-6.21	-1.25	4.96
14	**2-PY**	-6.07	-1.47	4.59	-6.07	-1.48	4.59	-6.07	-1.49	4.58
	6-PY	-6.14	-1.12	5.03	-6.14	-1.12	5.03	-6.15	-1.13	5.02
15	**2-PY**	-6.06	-1.45	4.60	-6.06	-1.46	4.60	-6.05	-1.46	4.59
	6-PY	-6.14	-1.11	5.03	-6.14	-1.11	5.03	-6.14	-1.11	5.02
16	**2-PY**	-6.11	-1.74	4.37	-6.11	-1.74	4.37	-6.12	-1.75	4.37
	6-PY	-6.19	-1.75	4.43	-6.18	-1.75	4.43	-6.20	-1.75	4.44

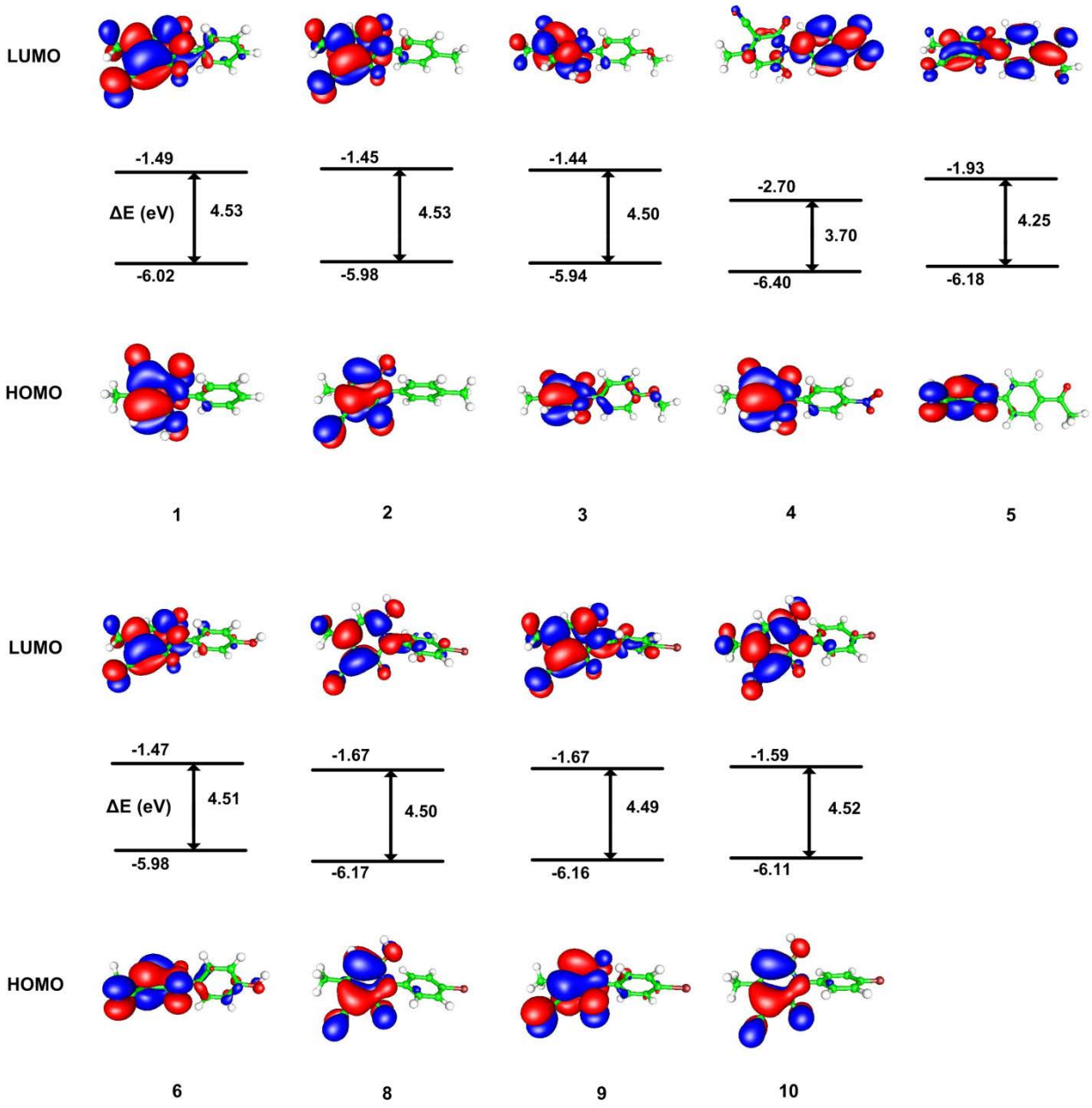

Fig. 4.3.6 The molecular orbitals and energy gaps between HOMO and LUMO orbitals of compounds **1** - **10** in the 2-**PY** form in a gas phase

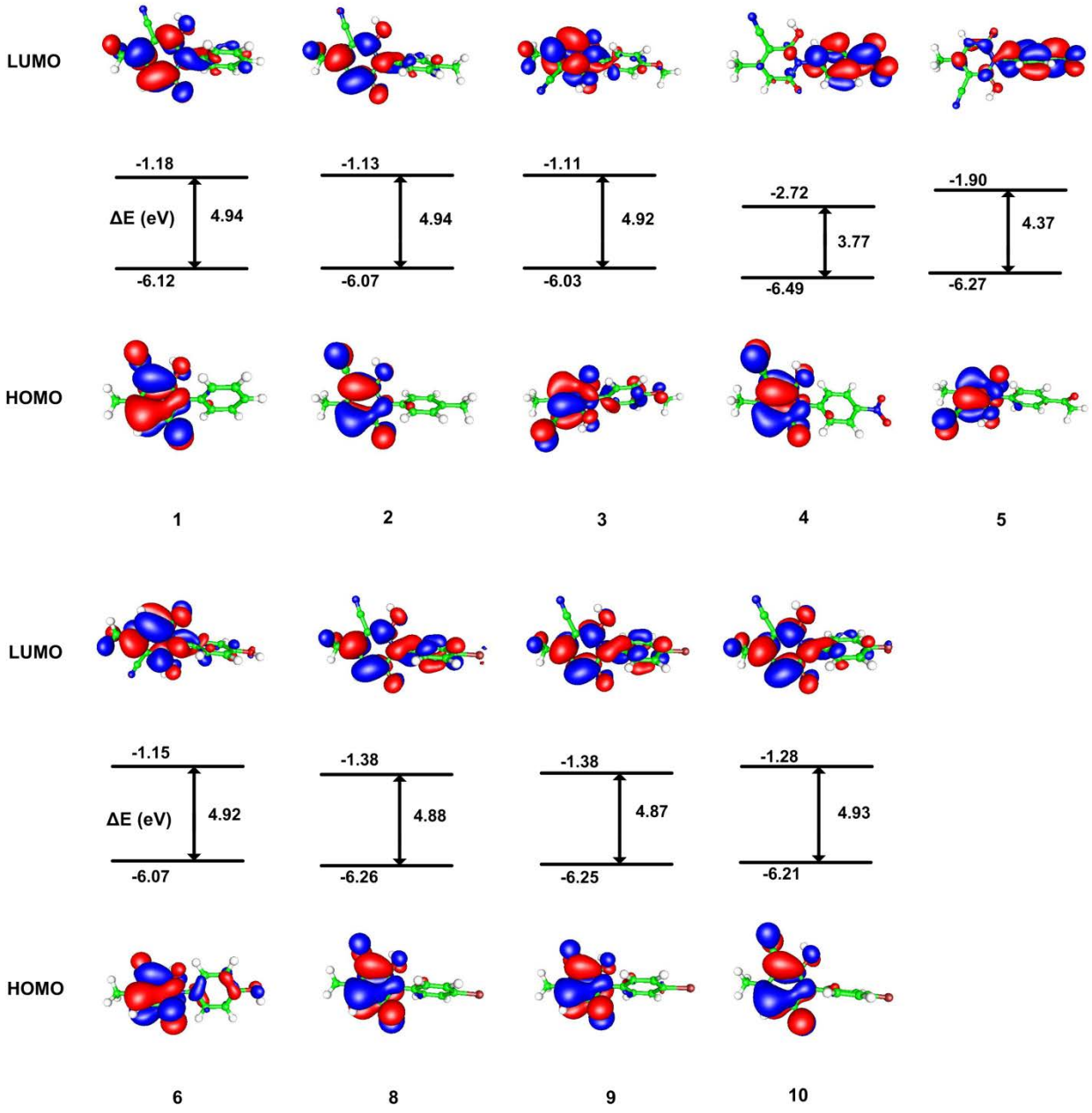

Fig. 4.3.7 The molecular orbitals and energy gaps between HOMO and LUMO orbitals of compounds **1** - **10** in the **6-PY** form in a gas phase

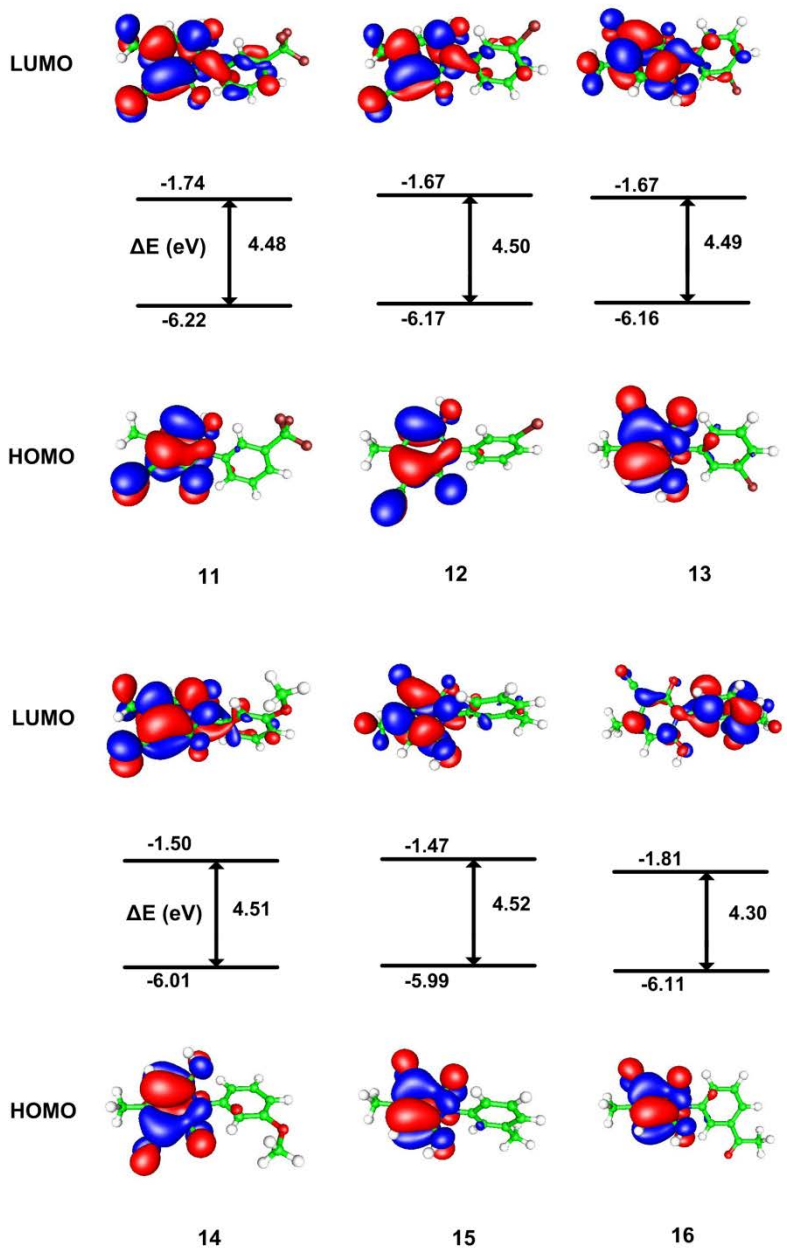

Fig. 4.3.8 The molecular orbitals and energy gaps between HOMO and LUMO orbitals of compounds **11 - 16** in the **2-PY** form in a gas phase

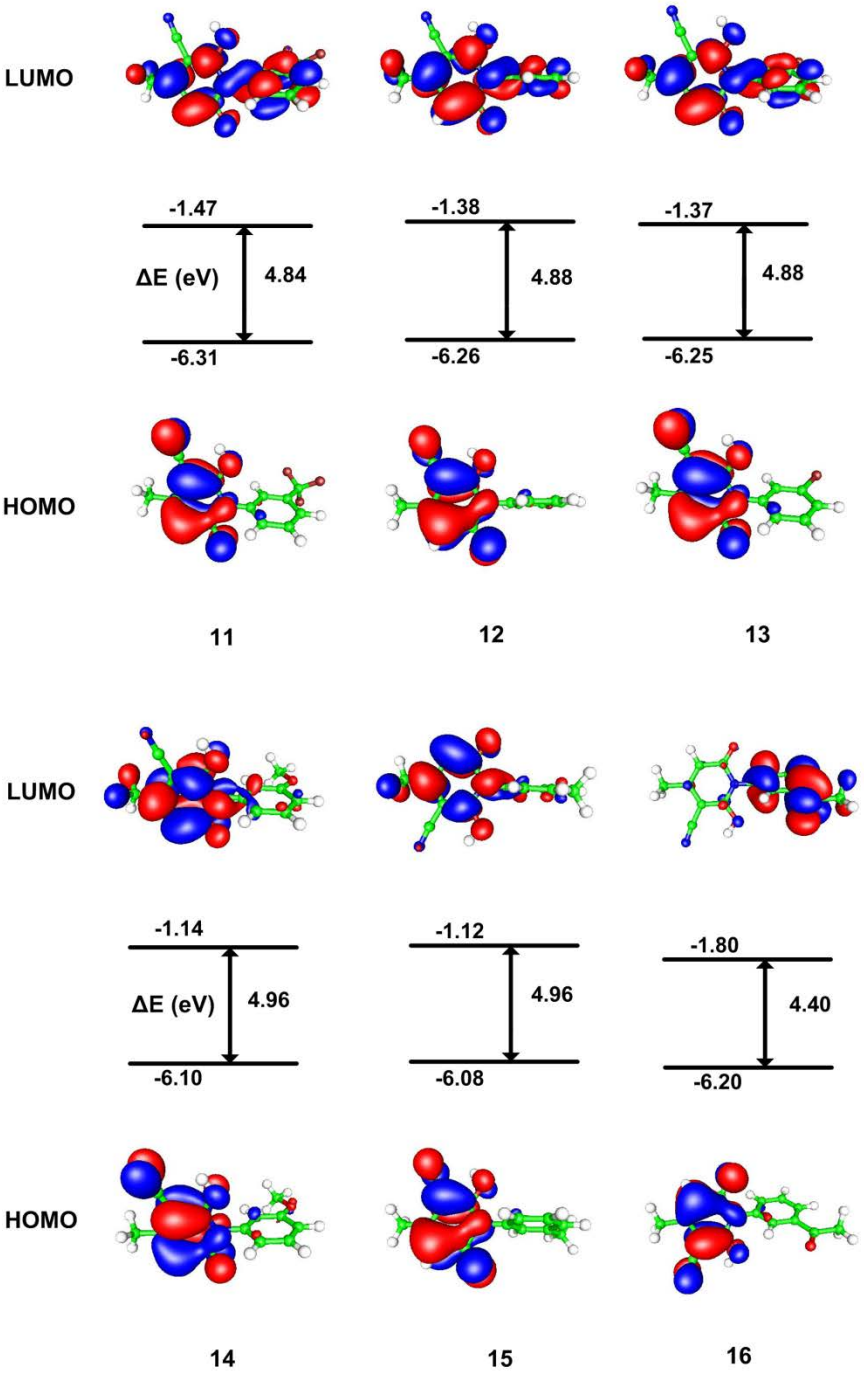

Fig. 4.3.9 The molecular orbitals and energy gaps between HOMO and LUMO orbitals of compounds **11 - 16** in the **2-PY** form in a gas phase

In order to obtain data on electronic density distribution, the Bader`s charge analysis was performed. Bader's theory of atoms in molecules is useful to define the charge enclosed within

the Bader volume as an good approximation of the total electronic charge of an atom. Atom and ring numbering used in Bader's analysis is given in Fig. 4.3.10. Difference of atomic charges in the excited and in the ground state (Δ_{charge}) for appropriate atoms, as well as calculated changes in overall electron density of molecules are given in Tables 4.3.18-4.3.22, and Figs 4.3.11 and 4.3.12.

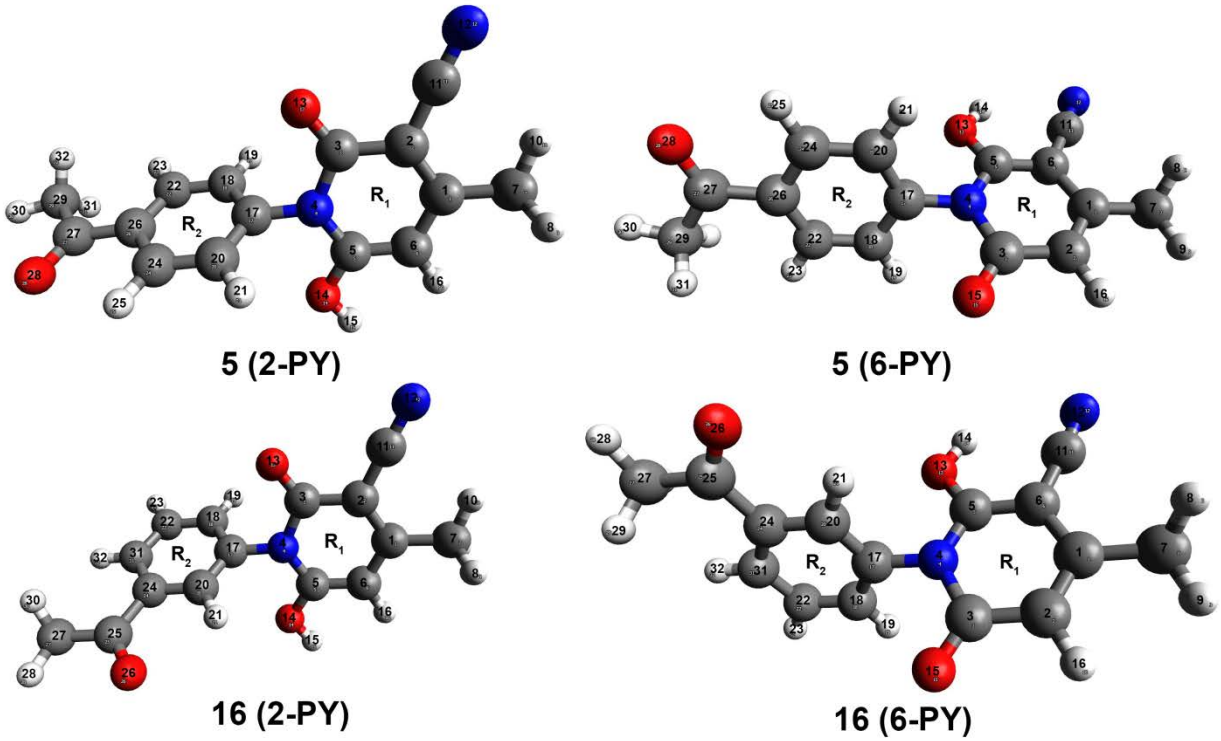

Fig. 4.3.10 Numbering of the atoms used in Bader's analysis for all investigated compounds (examples given for 5 (2-PY), 5 (6-PY), 16 (2-PY) and 16 (6-PY) compounds)

Table 4.3.18 Difference in atomic charges (Δ_{Charge}) between excited and ground state of appropriate atom in **2-PY** form of *para* substituted compounds

Atom number* /Compound	Δ_{Charge}								
	1	**2**	**3**	**4**	**5**	**6**	**8**	**9**	**10**
1	0.3529	0.3623	0.3512	0.0214	0.0093	0.345	0.3296	0.33	0.3497
2	-0.1151	-0.1122	-0.0435	-0.2623	-0.0068	-0.0626	-0.1207	-0.1168	-0.1121
3	0.0391	0.0435	0.0263	0.0099	0.0092	0.0283	0.0421	0.0384	0.0402
4	-0.0213	-0.0241	-1E-04	-0.0616	-0.0081	-0.0099	-0.0261	-0.0264	-0.0183
5	0.2102	0.2128	0.242	-0.0599	0.0112	0.2127	0.194	0.1934	0.214
6	-0.2941	-0.3023	-0.2301	-0.2617	-0.0116	-0.2261	-0.291	-0.2907	-0.2976
7	-0.0208	-0.0183	-0.0186	-0.0004	-0.0004	-0.0233	-0.0161	-0.024	-0.0188
8	0.0261	0.0243	0.0186	-0.0002	0.0005	0.022	0.0212	0.0179	0.022
9	0.0218	0.0197	0.0269	-1E-04	0.0006	0.0287	0.0209	0.0283	0.0212
10	1E-04	0.0003	0.001	0.0001	0	0.001	-1E-04	0.0006	0.0002
11	0.0475	0.0449	0.0397	0.0184	0.0009	0.0407	0.0374	0.0431	0.0423
12	-0.0409	-0.0342	-0.0036	-0.12	-0.0026	-0.0144	-0.039	-0.0474	-0.0391
13	-0.2202	-0.2219	-0.1703	-0.1917	-0.0069	-0.1855	-0.2122	-0.2108	-0.216
14	-0.0081	-0.0051	0.0032	-0.031	0.0003	0.0025	-0.0065	-0.0052	-0.01
15	0.0004	0.0004	-0.0008	0.0008	0.0003	0.0005	0.0005	0.0002	0.0003
16	0.002	0.0043	0.002	0.0037	0.0004	0.0021	0.0035	0.0077	0.0021
17	0.0022	-0.0039	-0.0854	0.1569	0.1307	-0.0616	0.0176	0.0169	-0.0022
18	0.0032	0.0025	0.0048	0.0048	-0.0029	0.0002	0.0059	0.028	0.0037
19	0	-0.0004	0.0003	-0.0003	-0.001	0.0006	-0.0004	-0.0002	0
20	0.0069	0.0053	-0.0092	0.0074	0.0018	-0.0025	0.0183	0.0193	0.0132
21	0.0005	0	0.0006	1E-04	-0.0024	0.0003	1E-04	0.0003	-1E-04
22	0.0014	0.0013	-0.0448	0.0864	0.0837	-0.0301	0.003	-0.0192	-0.0005
23	0.0002	-1E-04	0.0009	-0.0008	-0.0023	0.0007	-0.0004	-0.0002	0.0008
24	0.0003	0.0005	-0.015	0.0814	0.0865	-0.0101	-0.0011	-0.0008	1E-04
25	1E-04	0	-0.0005	-0.0008	0.0002	0.0006	-1E-04	-0.0002	0
26	0.0053	0.0002	-0.0437	0.0649	-0.0551	-0.0339	0.0209	0.0223	0.0055
27	0.0001	0	-0.046	0.216	0.4388	-0.0269	-0.0015	-0.0048	-0.0007
28		0	0.0017	0.1594	-0.554	0.0005			
29		0	0	0.1594	-0.1911				
30		1E-04	-0.0036		0.0019				
31			-0.0039		0.0577				
32					0.0111				

Table 4.3.19 Difference in atomic charges (Δ_{Charge}) between excited and ground state of appropriate atom in **2-PY** form of *meta* substituted compounds

Atom number* /Compound	Δ_{Charge}					
	11	**12**	**13**	**14**	**15**	**16**
1	0.2966	0.3253	0.32	0.3448	0.3464	0.0253
2	-0.1445	-0.1234	-0.121	-0.1164	-0.1148	-0.1271
3	0.0434	0.0411	0.0388	0.0393	0.0384	0.0024
4	-0.0344	-0.0278	-0.0258	-0.0214	-0.0242	-0.0334
5	0.1668	0.1905	0.1934	0.2027	0.2147	-0.0148
6	-0.285	-0.2879	-0.2862	-0.2925	-0.2964	-0.1413
7	-0.0157	-0.0176	-0.0261	-0.0163	-0.0213	-0.0019
8	0.022	0.0242	0.0324	0.0243	0.0183	0.0014
9	0.0163	0.0192	0.0179	0.0189	0.0286	0.0012
10	0.0002	0.0003	-0.0002	0.0003	0.0013	1E-04
11	0.0413	0.0411	0.043	0.0429	0.0458	0.0117
12	-0.0597	-0.0469	-0.049	-0.0386	-0.038	-0.0552
13	-0.2117	-0.211	-0.2097	-0.2162	-0.2202	-0.1068
14	-0.0089	-0.0073	-0.0068	-0.0053	-0.0056	-0.0117
15	0.0007	0.0002	0.0004	0.0004	0.0007	0.0008
16	0.0017	0.0037	0.0056	0.0037	0.0049	0.0025
17	0.0425	0.0225	0.0211	-0.0184	0.0009	0.0111
18	0.0484	0.0144	0.0142	0.0249	0.0036	0.1742
19	0.001	-0.0003	1E-04	0	0	0.0006
20	0.002	0.0108	0.01	0.0117	0.0089	0.0607
21	1E-04	1E-04	-1E-04	-0.0004	0	-0.0002
22	-0.0018	0.0008	0.0018	0.0021	0.001	-0.0015
23	-0.0004	-1E-04	-0.0002	1E-04	-0.0002	-0.003
24	0.0181	0.0032	0.0031	-0.0004	-0.0008	0.0336
25	0.003	-0.0007	-0.001	-0.0005	0	0.3305
26	0.0008	0.0256	0.0232	1E-04	1E-04	-0.2165
27	0.001	-1E-04	0.001	0.0001	0.0001	-0.0811
28	0.0004			0.0002	0	0
29	0.0565			0	0.0077	0.0128
30	-0.0009			0.0101	0	0.0149
31				-0.0003		0.1097
32						0.0008

Table 4.3.20 Difference in atomic charges (Δ_{Charge}) between excited and ground state of appropriate atom in **6-PY** form of *para* substituted compounds

Atom number* /Compound	Δ_{Charge}								
	1	**2**	**3**	**4**	**5**	**6**	**8**	**9**	**10**
1	-0.2946	0.2691	0.2657	0.0125	0.0036	-0.2512	0.2213	0.2139	0.2616
2	0.2142	-0.0751	-0.076	-0.2591	-0.0001	0.249	-0.1212	-0.1144	-0.0868
3	0.2565	0.0867	0.0851	0.0058	0.0097	0.2699	0.0855	0.0701	0.0797
4	0.0011	-0.0097	-0.0099	-0.0619	-0.0094	0.0145	-0.0617	-0.023	0.0006
5	-0.0844	0.2205	0.2254	-0.0141	0.0106	-0.0263	0.2134	0.1896	0.2129
6	0.0802	-0.289	-0.2909	-0.3059	-0.0004	0.0746	-0.2794	-0.2852	-0.2908
7	0.0248	-0.0111	-0.0215	0.0005	-0.0003	-0.0514	-0.012	-0.0134	-0.0167
8	0.0062	0.0162	0.0181	-0.0011	0.0003	-0.0004	0.015	0.0149	0.0179
9	0.033	-0.0003	0	1E-04	0	0.015	0.0002	1E-04	1E-04
10	0.0112	0.0154	0.0236	-0.0013	0.0002	-0.0216	0.0124	0.0158	0.0174
11	-0.0011	0.0231	0.0232	0.0189	0.0007	-0.0076	0.0249	0.0248	0.0283
12	0.0299	-0.1181	-0.1173	-0.1168	1E-04	-0.0241	-0.1169	-0.1145	-0.1236
13	-0.1908	-0.0079	-0.0088	-0.0296	0.0008	-0.1641	-0.0119	-0.0113	-0.008
14	-0.0104	0.001	0.0004	0.0009	0.0002	0.0021	0.0007	-1E-04	0.0004
15	0.0246	-0.1868	-0.186	-0.1924	-0.0003	0.019	-0.1922	-0.1886	-0.188
16	-0.1211	0.0033	0.0028	0.0051	0.0011	-0.0996	0.0042	0.0031	0.0036
17	-0.0115	0.0092	0.0375	0.1581	0.1342	-0.0145	0.0585	0.0614	0.0147
18	0.0031	0.0205	0.0273	0.005	-0.0079	0.0027	0.0532	0.0218	0.0396
19	1E-04	0.0003	0.0003	0	-0.0014	0.0003	-0.0018	0.0008	0.0002
20	-0.003	0.0091	-0.0261	0.0057	0.0025	0.0011	0.0158	0.0151	0.0013
21	0.0004	-0.0003	-0.0002	0.0001	-0.0027	0.0004	0	1E-04	-1E-04
22	0	0.0007	0.0003	0.0822	0.0873	0.0002	-0.0006	0.0292	-0.0019
23	0.0003	0	0	0.0002	-0.0031	-0.0249	-1E-04	-0.0002	0
24	0.0007	0.0037	0.0092	0.0842	0.0852	1E-04	0.022	0.0205	0.0123
25	0.0152	0.0002	-0.0007	1E-04	0	0.018	0.0003	0	0.0003
26	1E-04	0.0187	0.0173	0.0646	-0.0501	1E-04	0.068	0.0691	0.0249
27	0.0151	-0.0023	-0.0001	0.2164	0.4395	0.0179	0.0021	0.0004	1E-04
28		0	0.0012	0.1597	-0.5768	0.0009			
29		0.002	0.0004	0.1618	-0.151				
30		0.0013	0		0.0012				
31			1E-04		0.015				
32					0.0112				

Table 4.3.21 Difference in atomic charges (Δ_{Charge}) between excited and ground state of appropriate atom in **6-PY** form of *meta* substituted compounds

Atom number* /Compound	Δ_{Charge}					
	11	**12**	**13**	**14**	**15**	**16**
1	0.1654	0.2152	0.2168	0.2795	0.2763	0.0022
2	-0.1552	-0.1181	-0.1171	-0.0573	-0.0783	-0.0169
3	0.0715	0.0759	0.0724	0.0831	0.0803	0.0004
4	-0.0402	-0.018	-0.062	0.0137	0.0022	-0.0093
5	0.1252	0.1752	0.2194	0.2227	0.2277	-0.0003
6	-0.284	-0.2845	-0.2844	-0.2759	-0.2967	-0.0213
7	-0.0103	-0.0099	-0.0126	-0.0384	-0.0144	-0.0002
8	0.0103	0.0149	0.0136	0.0176	0.0177	0
9	0	-1E-04	-0.0002	0.0003	0.0003	0
10	0.0097	0.0112	0.0144	0.0417	0.0168	0.0004
11	0.026	0.0215	0.026	0.0193	0.0235	0.0009
12	-0.1167	-0.1175	-0.1164	-0.1094	-0.1192	-0.0078
13	-0.0141	-0.0136	-0.0137	-0.0133	-0.0136	-0.0003
14	0.0011	0.0014	0.0014	0.0008	0.0006	0.0003
15	-0.1992	-0.1918	-0.1871	-0.1754	-0.1897	-0.0156
16	0.0045	0.0037	0.0039	0.0028	0.0045	0.0002
17	0.102	0.07	0.0672	0.0093	0.013	0.0014
18	0.118	0.0401	0.0442	-0.0132	0.0196	0.1436
19	0.0005	0.0049	-1E-04	0.0007	-0.0003	-1E-04
20	-0.0064	0.0226	0.0171	0.0045	0.0045	0.0758
21	0	-0.0003	0.0004	0.0004	-0.0002	0.0004
22	-0.0098	0.0017	0.0006	0.0065	-0.0017	-0.0105
23	-0.0006	-1E-04	-0.0003	1E-04	0.0002	-0.0031
24	0.0608	0.0182	0.0193	-0.0163	0.0072	-0.0022
25	0.0073	0.0014	0.0019	-0.0152	-0.0001	0.4659
26	0.001	0.0744	0.0741	0.0006	0	-0.523
27	0.0029	0.0017	0.0009	1E-04	0	-0.1592
28	0.0007			-0.0012	0.0022	0.0003
29	0.1295			-0.0012	0.017	0.0133
30	0			0.0138	0.0006	0.0133
31				-0.0003		0.0518
32						-0.0004

Table 4.3.22 Difference in charges of R_1 and R_2 rings between excited and ground state in both **2-PY** and **6-PY** forms

Compound	Δ_{Charge}			
	2-PY		**6-PY**	
	R_1	R_2	R_1	R_2
1	-0.0204	0.0202	-0.0207	0.0205
2	-0.0056	0.0055	-0.0627	0.0631
3	0.2439	-0.2438	-0.0661	0.0665
4	-0.9346	0.9348	-0.9384	0.9381
5	-0.0037	0.0036	0.0168	-0.0169
6	0.1617	-0.1622	-0.0022	0.0023
8	-0.0625	0.0623	-0.2177	0.2174
9	-0.0617	0.0614	-0.2182	0.2182
10	-0.0199	0.0198	-0.0914	0.0914
11	-0.1709	0.1707	-0.406	0.4059
12	-0.0763	0.0762	-0.2345	0.2346
13	-0.0733	0.0732	-0.2256	0.2253
14	-0.0294	0.0293	0.0118	-0.0114
15	-0.0214	0.0213	-0.062	0.062
16	-0.4468	0.4466	-0.0673	0.0673

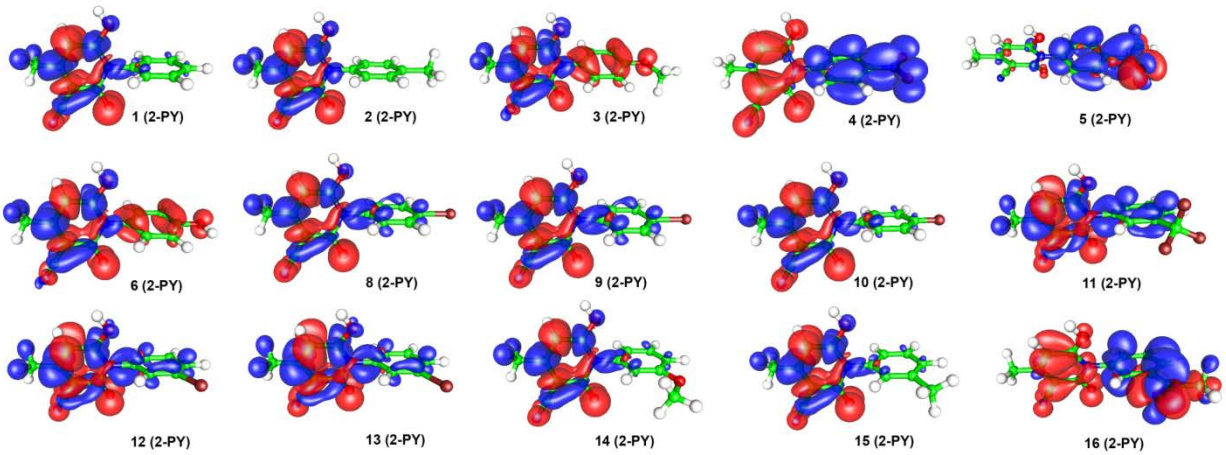

Fig. 4.3.11 ICT processes from ground state (red) to excited state (blue) of compounds **1 - 16** in **2-PY** form

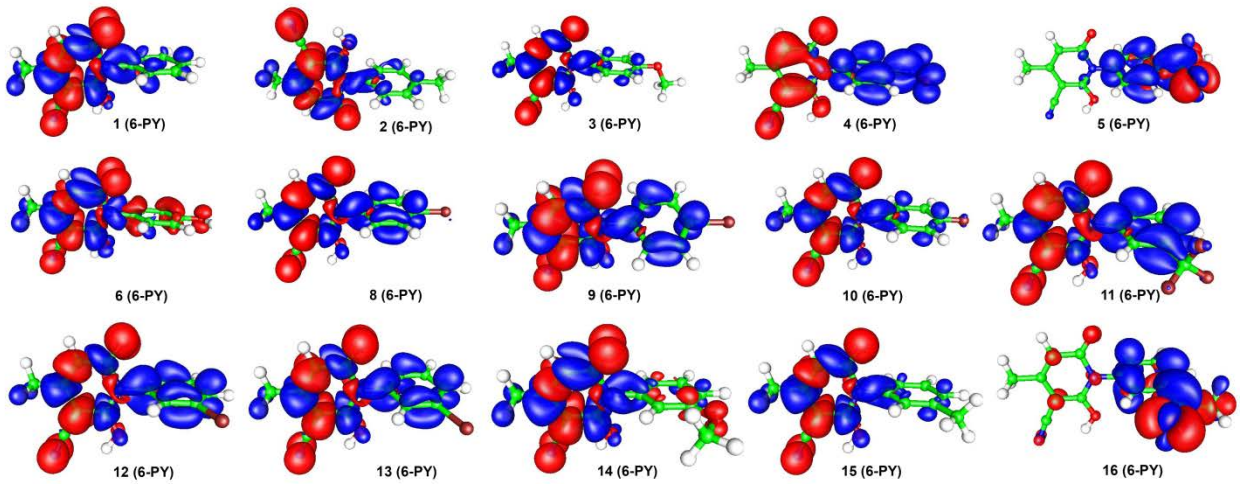

Fig. 4.3.12 ICT processes from ground state (red) to excited state (blue) of compounds **1 - 16** in **6-PY** form

According to the results shown in Tables 4.3.18-4.3.22 and Figs. 4.3.11 and 4.3.12, it could be observed that in both **2-PY** and **6-PY** forms nitro-substituted compounds **4** shows distinct ICT processes. Electron density was transferred from the pyridone ring to substituted phenyl. According to the character of the ICT processes molecules can be divided in three groups:

The first group includes compounds **1, 2, 8-10, 14, 15** in **2-PY** form (Fig. 4.3.11) along with **1-3**, **6**, **14** and **15** in **6-PY** compound (Fig. 4.3.12). In these molecules no observable ICT process can be observed, and electron density was concentrated on pyridone moieties in both ground and excited states: moderate Δ_{charge} for the pyridone ring vary from -0.0056 to -0.0625 in **2-PY** form and from -0.0022 to -0.0661 in **6-PY** form. Along with this, carbonyl O13 atom of the pyridone ring loses a significant amount of charge (Δ_{charge}): from –0.039 to -0.2219 for compounds in **2-PY** form, while in 6-PY form non-consistent alteration at carbonyl O15 atom was found. Exception is compound **5** in **2-PY** form and compounds **5** and **16** in **6-PY** form where low extent of ICT is operative with mostly observable Δ_{charge} at substituted phenyl ring.

In the second group, which includes compounds **4** and **16** in **2-PY** and compounds **4** (strong), while **8**, **9** and compounds **11-13** in **6-PY,** ICT process is less pronounced. The calculation showed that pyridone moiety of compounds **4** and **16** loses –0.9346 and -0.4468 electrons, while nitro and acetyl substituted phenyl ring receives 0.9438 and 0.4466 electrons, respectively.

Along with this, O13 carbonyl oxygen of the pyridone ring loses low amount of charge (Δ_{charge}): –0.1917 for comp. **4** and –0.1068 for comp. **16**). Similar result was found for compound **4** in **6-PY** form: Δ_{charge} shows loses from pyridone is -0.9384 and nitro substituted phenyl ring receives 0.9381 electron.

4.4 Hydrazone-azo tautomerism and solvatochromic properties of 5-arylazo-6(2)-hydroxy-4-methyl-3-cyano-*N*(1)-phenyl-2(6)-oxo-pyridine-3-carbonitrile dyes

4.4.1 Spectral characteristics and tautomerism

Synthesis of pyridone tautomeric mixture precursor for aryl azopyridone dyes is given in with an example of diazotization of compound **1** (Figure 4.1.7) producing azo derivatives which are easily rearranged to more stable hydrazone form. In the same manner was performed synthesis of aryl azopyridone dyes based on 6(2)-hydroxy-4-methyl-2(6)-oxo-1-(phenyl)-1,2(1,6)-dihydro-pyridine-3-carbonitrile.

Theoretical calculations showed that **Hydrazo** form is for 15 kcal/mol more stable than **Azo/b** form mainly because of the formation of intramolecular hydrogen bond. DFT calculation showed that higher reactivity of tautomer **a** in all compounds, which is also consequence of coplanaraity of hydroxyl group at C6 and pyridone ring thus exerting higher extent of overlapping (n,π-conjugation) of oxygen lone pairs (p-orbitals) and π–electrons of the pyridone ring contributing to an increased electron density at C5 carbon. Such results are in agreement with data obtained from FTIR and NMR analysis. The arylazo pyridone dyes could exist in two tautomeric forms (Figure 4.1.7). The infrared spectra of all synthesized dyes showed two intense carbonyl bands at about 1642 and 1699 cm^{-1}, which were assigned to the diketohydrazone form. The spectra exhibited broad bands in the region 3137–3225 cm^{-1} and 3421–3438 cm^{-1} which were assigned to the N–H group from pyridone ring and hydrazone form, respectively. The ^{1}H NMR spectra of the dyes exhibit a broad signal near 14.34–14.69 ppm. This signal corresponds to imine NH proton resonance of the hydrazone form (Figure 4.1.7, Structure B). In our previous publication [208], spectroscopical investigation of ten 5-arylazo-6-hydroxy-4-methyl-3-cyano-2-pyridone dyes showed that these dyes exist in the hydrazone tautomeric form in the solid state and in the solvent DMSO-d_6, with N–H peaks in the range 14.35–14.87 ppm. The 1H NMR spectra of some azo pyridone dyes in $CF_3COOD/CDCl_3$ have been reported [197] and showed that these dyes exist in the hydrazone form with NH peaks in the range of 15.1–15.6 ppm. The

^{13}C NMR studies of some N-alkyl derivatives of azo pyridones in solutions in $CDCl_3$ and DMSO-d_6 led to the conclusion that pyridone azo dyes exist in the hydrazone form [226,227].

4.4.2 Solvent effects on the UV–vis absorption spectra

The electronic absorption spectra of 5-arylazo-6-hydroxy-4-(4-methoxyphenyl)-3-cyano-2-pyridone dyes (1–11) were measured at room temperature in seventeen solvents in the range 300–600 nm and the characteristic spectra in representative solvents are shown in Fig. 4.4.1. The UV–vis spectra of some dyes showed a weak band at about 330–360 nm and for all a strong band at 420–480 nm which were assigned to azo and hydrazone tautomeric forms, respectively. The absorption maxima, which correspond to a transition in which electron density is transferred from the hydrazone –NH group to the pyridone carbonyl group (lower energy band), are presented in Tables 4.4.1 and 4.4.2, and were studied in this paper.

The data from Table 4.4.1 indicate that values of absorption frequencies of investigated compounds depend on the electronic effect of the substituent present on phenylazo group at C(5) position of pyridone core. The introduction of *methoxy*, *nitro*, *bromo* and *iodo* substituents contributes to the positive solvatochromism, comparing to the unsubstituted compound, while the other compounds show shift to lower wavelength. The absorption spectra showed relatively low dependence on both solvent and substituent effects.

Applying described methodology [193], K_T values (K_T = [**Hydrazo**]/[**Azo**]) of the investigated compounds were determined in DMF, DMAc and NMF, and the results are presented in Table 4.4.3. The changes in the K_T values are consequence of the balanced contribution of both solvent and substituent effects. The NMF solvent effect on K_T change (contribution of both dipolarity/polarizability effect and hydrogen bonding ability) causes shift of the tautomeric equilibria to **Hydrazo** form (higher K_T values). The highest value of K_T was found for halogen substituted azo dyes. The opposite is true for aprotic solvents DMF and DMAc, *i.e.* solvent with increased dipolarity/polarizability causes an complex influence on K_T values change. It could be postulated that such behavior is a consequence of differences in conjugational ability of the π-electron densities through localized or delocalized π-electronic systems of the appropriate tautomeric forms.

Table 4.4.1 Absorption frequencies of the hydrazo (**Hydrazo**) form of investigated compounds in selected solvents

Solvent/Compound	ν_{max} x 10^{-3} (cm^{-1})										
	1	**2**	**3**	**4**	**5**	**6**	**7**	**8**	**9**	**10**	**11**
Methanol	23.33	23.26	22.09	23.17	23.81	22.46	22.75	23.64	23.84	23.53	23.95
Ethanol	23.08	22.36	21.51	23.02	23.08	21.83	21.98	22.92	23.69	23.41	23.41
1-Propanol	23.01	22.24	21.39	22.96	23.01	21.62	21.51	22.84	23.39	23.34	23.24
2-Propanol	23.03	22.21	21.35	22.73	23.00	21.41	21.53	22.86	23.37	23.28	23.18
1-Butanol	22.94	22.19	21.28	22.86	22.97	21.36	21.46	22.81	23.31	23.24	23.06
2-Butanol	22.93	22.21	21.31	22.79	22.92	21.35	21.51	21.76	23.26	23.20	23.05
1,4-Dioxane (dioxane)	22.78	22.59	20.71	23.45	23.09	22.72	22.58	22.67	23.39	23.12	22.49
Ethyl acetate (EtAc)	23.31	22.86	21.91	23.21	23.51	22.35	22.46	23.72	23.46	23.54	23.61
Tetrahydrofuran (THF)	23.22	22.78	21.81	23.24	23.25	22.84	22.79	23.13	23.73	23.48	23.24
Acetonitrile (AcN)	24.03	24.21	23.15	23.91	24.19	23.65	23.89	23.17	23.84	24.03	23.58
Acetone	23.29	22.71	22.54	23.51	23.26	22.76	22.81	23.12	23.81	23.43	23.87
Dimethyl sulfoxide (DMSO)	24.82	24.89	24.83	22.45	24.91	24.37	24.36	24.75	24.25	24.26	24.31
N,*N*-Dimethylformamide (DMF)	24.74	24.85	24.76	22.54	24.81	24.18	24.20	24.31	24.19	24.18	24.17
N,*N*-Dimethylacetamide (DMAc)	24.91	24.34	24.86	22.43	24.53	24.03	24.01	24.52	24.26	24.23	24.23
N-Methylformamide (NMF)	25.41	25.41	25.40	22.85	25.34	24.78	24.86	25.24	24.9	24.95	24.75
Dichloromethane (DCM)	25.19	25.23	25.39	24.87	25.23	24.98	24.99	25.35	25.39	25.01	25.31
Chloroform (Chl)	24.43	23.95	24.12	24.98	24.23	24.31	24.23	24.21	24.76	24.36	24.45

Table 4.4.2 Absorption frequencies in selected solvents of **Azo/a** form

Solvent/ Compound	ν_{max} x 10^{-3} (cm^{-1})										
	1	**2**	**3**	**4**	**5**	**6**	**7**	**8**	**9**	**10**	**11**
Methanol	-										
Ethanol											
1-Propanol											
2-Propanol											
1-Butanol											
2-Butanol											
Dioxane											
EtAc											
THF				22.31							
AcN				22.55				22.17			22.43
Acetone											
DMSO				19.31							
DMF	22.79	22.82	21.97	19.99	22.61	22.13	22.18	22.44			20.37
DMAc	22.83	22.67	22.21	19.93	22.58	22.07	22.23	22.47			20.41
NMF	22.48	21.86	22.4	20.14	23.31	22.02	22.15	22.25			21.04
DCM											
Chl											

Table 4.4.3 Equilibrum constants K_T of the investigated pyridones in selected solvents

Solvent/Compound	K_T = **Hydrazo**/**Azo**										
	1	**2**	**3**	**4**	**5**	**6**	**7**	**8**	**9**	**10**	**11**
THF	–	–	–	2.22	–	–	–	–	–	–	–
AcN	–	–	–	2.05	–	–	–	0.55	–	–	0.47
Acetone	–	–	–	–	–	–	–	–	–	–	–
DMSO	–	–	–	0.73	–	–	–	–	–	–	–
DMF	1.11	1.05	0.87	0.19	1.20	1.96	2.13	1.60	1.26	1.35	1.42
DMAc	1.34	1.02	0.91	0.52	1.35	2.15	1.98	1.73	1.26	1.43	1.40
NMF	1.69	1.39	1.18	1.04	1.56	2.02	2.15	2.02	1.33	1.53	1.44

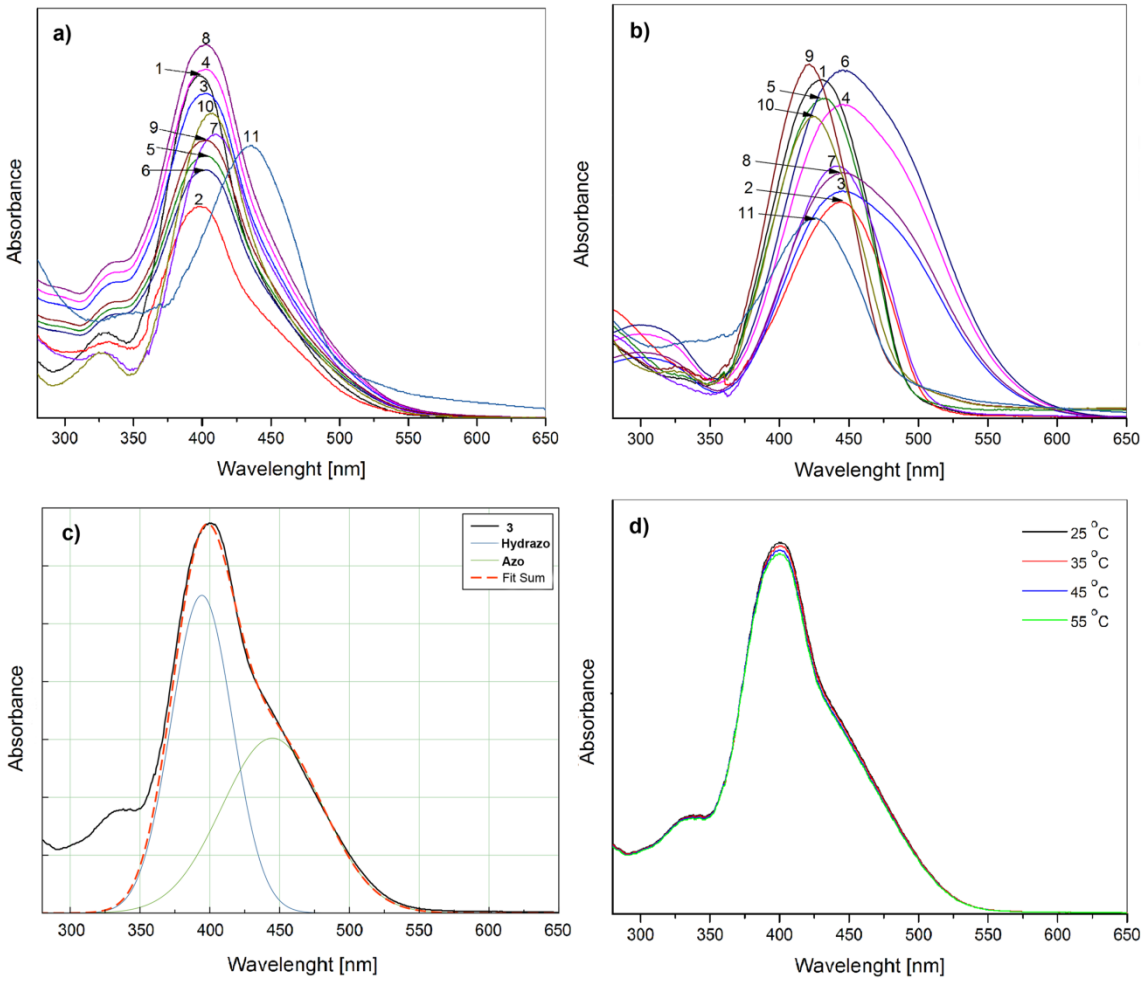

Fig. 4.4.1 Absorption spectra of compounds **1**–**10** in a) NMF and b) DMF

4.4.3 Correlation with multiparameter solvent polarity scales

The effect of solvent dipolarity/polarizability and hydrogen bonding on the absorption spectra is interpreted by means of linear solvation energy relationship (LSER) using a Kamlet–Taft solvatochromic Eq. (x) [190]. The correlations of the absorption frequencies ν_{max} for hydrazone tautomer were carried out by means of multiple linear regression analysis. The results are presented in Table 4.4.4, and coefficients v_0, *s*, *b* and *a* fit at the 95% confidence level.

As it can see from Table 4.4.4 the non-specific solvent effect is the main factor that influences on the spectral shifts of all investigated compounds.

Table 4.4.4 The results of the correlation analysis for the **Hydrazo** form according to Kamlet–Taft equation

Comp.	$\nu_0 \times 10^{-3}$ (cm^{-1})	$s \times 10^{-3}$ (cm^{-1})	$a \times 10^{-3}$ (cm^{-1})	$b \times 10^{-3}$ (cm^{-1})	R^a	Sd^b	F^c	P_π [d]	P_α	P_β
1	20.66 ±0.52	5.08 ±0.64	0.72 ±0.34	–0.83 ±0.37	0.92	0.39	24.73	76.62	10.86	12.52
2	19.53 ±0.52	6.52 ±0.65	0.93 ±0.34	–1.32 ±0.37	0.95	0.39	42.79	74.34	10.60	15.06
3	17.22 ±0.89	9.22 ±1.10	1.21 ±0.58	–1.56 ±0.64	0.93	0.67	28.77	76.90	10.09	13.01
4	24.69 ±0.22	-[e]	0.68 ±0.14	–2.75 ±0.16	0.98	0.16	105.02	-	19.83	80.17
5	20.87 ±0.41	4.89 ±0.50	0.74 ±0.27	–0.93 ±0.29	0.95	0.31	37.37	74.54	11.28	14.18
6	20.01 ±0.51	6.10 ±0.63	-	–2.00 ±0.36	0.96	0.38	53.42	72.02	4.37	23.61
7	19.94 ±0.47	6.18 ±0.58	0.54 ±0.31	–1.98 ±0.34	0.97	0.35	60.93	71.03	6.21	22.76
8[f]	20.54 ±0.54	5.46 ±0.67	0.84 ±0.35	–1.35 ±0.40	0.93	0.41	27.52	71.37	10.98	17.65
9	22.36 ±0.36	3.06 ±0.44	0.84 ±0.23	–1.31 ±0.26	0.92	0.27	23.59	58.73	16.13	25.14
10	21.96 ±0.36	3.23 ±0.44	0.71 ±0.24	–0.95 ±0.26	0.91	0.27	21.87	66.05	14.52	19.43
11	21.56 ±0.46	3.81 ±0.57	1.04 ±0.30	–1.20 ±0.33	0.90	0.35	18.25	62.98	17.19	19.83

[a] Correlation coefficient; [b] Standard deviation; [c] Fisher test of significance; [d] The percentage contribution of solvatochromic parameters obtianed by the use of Kamlet-Taft equation (%); [e] Negligible values with high standard errors; [f] AcN excluded from correlation;

From the analysis of absorption frequencies according to Kamlet–Taft equation it was found that the negative sign of *b* coefficient for all arylazo dyes (Table 4.4.4) indicates a hypsochromic shifts with both increasing solvent hydrogen-bond basicity. This suggests stabilization of the electronic excited state relative to the ground state. The positive sign of *s* and *a* coefficients for all investigated dyes indicates a bathochromic shifts with an increasing solvent dipolarity/polarizability and hydrogen-bond donor acidity which suggests stabilization of the ground state relative to the electronic excited state. The

percentage contribution of solvatochromic parameters (Table 4.4.4) for all azo dyes, showed that the most of the solvatochromism is due to solvent dipolarity/polarizability rather than on the hydrogen-bond acidity or basicity.

All the results obtained using Kamlet–Taft model indicate that the solvent effects on azo-hydrazone equilibrium and UV–vis absorption spectra of the investigated azo pyridone dyes are very complex. This also indicated that the electronic behavior of the nitrogen atoms of hydrazone group is somewhat different between derivatives with electron-donating and electron-accepting substituents. The non-specific solvent effect is a factor of the highest contribution to UV-Vis spectral shifts of all investigated compounds (**Table 4.4.4**). According to the correlation analysis obtained by the use of Kamlet–Taft equation it was found that the negative sign of *b* coefficient, for all arylazo dyes (**Table 4.4.4**), indicates a batochromic shift with increasing solvent hydrogen-bond accepting capability. This suggests better stabilization of the electronic excited state relative to the ground state, *i.e.* better hydrogen-bond proton donating capability of the investigated compounds in excited state. The positive sign of *s* and *a* coefficients for all investigated dyes indicates a hypsochromic shifts with increasing solvent dipolarity/polarizability and hydrogen-bond donor capability. This suggests better stabilization of the ground state relative to the electronic excited state with increasing solvent polarity, *i.e.* higher dipolar properties of molecule in the ground state. The percentage contribution of solvatochromic parameters (**Table 4.4.4**) for all azo dyes, showed that the most of the solvatochromism is due to solvent dipolarity/polarizability rather than the solvent hydrogen-bonding ability. Presented results, obtained by the use Kamlet–Taft model, indicate that the solvent effects on azo-hydrazo tautomeric equilibrium and UV–Vis absorption spectra of the investigated azo pyridone dyes are very complex due to diversity of the contribution of both solvent and substituent effect in studied azo dyes. This also indicated that the electronic behavior of the nitrogen atoms of hydrazo group is somewhat different between derivatives with electron-donating and electron-accepting substituents.

In order to investigate the influence of the substituent electronic effects to the state of tautomeric equilibria, log K_T values were correlated with combination of substituent constants, σ_p/σ_m and σ_p^+/σ_m^+ (Table S2), and the results obtained for DMF, DMAc and NMF are presented in **Table 4.4.5**.

Table 4.4.5 Correlation results of the log K_T values with σ_p/σ_m and σ_p^+/σ_m^+ substituent constants

Solvent		ρ	h	R^a	Sd^b	F^c	ρ	h	R	Sd	F
		4-H, 4-Me, 4-OMe, 4-F, 4-Cl					4-Br, 4-I, 3-Cl, 3-Br, 3-CF_3, 4-NO_2				
DMF	σ_p/σ_m	0.47 ± 0.08	0.07 ± 0.01	0.965	0.03	40	-1.78 ± 0.22	0.75 ± 0.10	0.972	0.10	67
	σ_p^+/σ_m^+	0.23 ± 0.08	0.11 ± 0.03	0.864	0.06	9	-1.43 ± 0.35	0.62 ± 0.16	0.900	0.19	17
DMAc	σ_p/σ_m	0.56 ± 0.03	0.11 ± 0.01	0.995	0.02	286	-1.03 ± 0.07	0.53 ± 0.03	0.999	0.03	197
	σ_p^+/σ_m^+	0.29 ± 0.07	0.15 ± 0.03	0.920	0.16	16	-0.87 ± 0.12	0.47 ± 0.06	0.963	0.07	51
NMF	σ_p/σ_m	0.43 ± 0.07	0.20 ± 0.01	0.962	0.03	38	-0.53 ± 0.09	0.40 ± 0.04	0.949	0.04	36
	σ_p^+/σ_m^+	0.23 ± 0.05	0.24 ±0.02	0.943	0.03	24	-0.47 ± 0.04	0.38 ± 0.02	0.989	0.02	176

[a] Correlation coefficient; [b] Standard deviation; [c] Fisher test of significance

The correlation analysis of the substituent effect on tautomeric equilibria pointed out that there are two different trends involving two groups of substituents (**Table 4.4.6**). The first group, that includes electron-donating substituents and *chloro* substituent, exhibits similar sensitivity of log K_T to substituent effect, irrespectively to solvent used. Similar correlation coefficients and lower ρ values were obtained by using electrophilic substituent constants. These results indicate low contribution of extended resonance interaction through overall molecule. In that way, stable intramolecular hydrogen bonding bridge N-H--O=C6 is established, causing stabilization of pseudo six-membered heterocyclic ring, and consequently, higher planarization of whole molecule. Due to overall planarization, transmission of electronic substituent effects exhibit low sensitivity to external factors such as solvent effects. The second group of substituents contains compounds with electron-accepting substituents and *halogen* substituted ones. The negative sign of proportionality constant, ρ, for second series means reverse behavior, *i.e.* it indicates equilibrium shift to **Azo** form with increasing electron-accepting character of the substituent. The most pronounced sensitivity to solvent effects, in second series, was found for DMF, lower for DMAc (it displays lower proton-accepting capability), and lowest for NMF solvent due to

obvious proton-donating effect of N-H hydrogen. Higher sensitivities of log K_T to substituent effects in solvent with higher relative permittivity can be explained by the fact that, in dipolar surrounding medium, energies necessary to bring about charge separation in the ground and excited state are relatively similar inducing higher susceptibility of log K_T to electronic substituent effects. Tautomeric equilibrium shift to **Azo**/**a** form is a consequence of electronic density shift in electron-acceptor substitued **Hydrazo** form favoring hydrogen transfer to C6 carbonyl oxygen.

4.4.4 Substituents effects on the UV–vis and NMR absorption spectra

The absorption spectra of the dyes with electron-accepting substituents were generally shifted hypsochromically in all used solvents. It is well known that the absorption maxima of the hydrazone tautomeric form of an azo dye shift to higher wavelengths when substituents with electron-donating characteristics are introduced. In contrast, electron-accepting substituents generally produce hypsochromic shift. The results presented in Table 4.4.1 are in agreement with this conclusion. The observed relationship between the substituent constants and the absorption maxima strongly suggests that the absorption maxima of the lower energy band of investigated azo dyes originate from hydrazone tautomeric form. The LFER concept was applied to the ν_{max} of arylazo pyridone dyes with the aim to get an insight into factors determining the absorption maxima shifts. The transmission of electronic substituent effects was studied using the Hammett Equation, [142]. Linear Hammett correlation was obtained in protic and non-dipolar aprotic solvents (Table 4.4.7). The existence of these correlations was interpreted as an evidence of significant effect of substituent on azo-hydrazone tautomerism. The azo group (–N=N–) is an electron-acceptor group and the imino group (–NH–) is an electron-donor, so that azo group is stabilized by the more electron-donating substituents, while an electron-accepting group stabilizes the hydrazone form.

The LFER results indicate complex influences of both solvent and substituent effect on UV-Vis absorption maxima of **Hydrazo** form (Table 4.4.7). These results indicate that solvent effects: dipolarity/polarizability, HBD and HBA abilities cause appropriate sensitivity of the position of absorption maxima (ν_{max}) to substituent effect.

Table 4.4.6 Correlation results of the absorption maxima of compounds **1 - 11** in **Hydrazo** form with σ_p/σ_m and σ_p^+/σ_m^+ substituent constants

Solvent	ν_0x10^{-3} (cm^{-1})	ρx10^{-3} (cm^{-1})	*R*	*Sd*	*F*	ν_0x10^{-3} (cm^{-1})	ρx10^{-3} (cm^{-1})	*R*	*Sd*	*F*	*Substituents*
	σ					σ^+					
Methanol	23.38 ± 0.10	1.31 ± 0.27	0.890	0.29	23	23.38 ± 0.11	1.24 ± 0.28	0.875	0.31	20	NO_2, Br, I excluded
Ethanol	22.62 ± 0.13	2.37 ± 0.46	0.901	0.32	26	21.88 ± 0.06	1.56 ± 0.16	0.971	0.18	97	
1-Propanol	22.52 ± 0.14	2.25 ± 0.49	0.882	0.34	21	22.75 ± 0.08	1.49 ± 0.19	0.955	0.22	63	
2-Propanol	22.50 ± 0.14	2.23 ± 0.51	0.871	0.36	19	22.73 ± 0.08	1.49 ± 0.20	0.948	0.23	53	
1-Butanol	22.44 ± 0.15	2.20 ± 0.52	0.865	0.37	18	22.67 ± 0.09	1.47 ± 0.21	0.943	0.24	48	
2-Butanol	22.45 ± 0.16	2.14 ± 0.55	0.867	0.38	15	22.66 ± 0.10	1.42 ± 0.22	0.945	0.25	42	NO_2, Br, I, Cl excluded
Dioxane	21.86 ± 0.20	2.66 ± 0.50	0.909	0.39	29	22.25 ± 0.11	1.77 ± 0.22	0.956	0.27	64	H, Me, F excluded
EtAc	23.16 ± 0.14	3.40 ± 0.78	0.930	0.31	19	23.48 ± 0.07	2.00 ± 0.20	0.986	0.14	103	H, Me, OMe, F, Cl
	23.91 ± 0.05	-0.92 ± 0.10	0.981	0.04	78	23.85 ± 0.05	-0.76 ± 0.10	0.973	0.05	52	Cl, 3-CF_3, 3-Br, 3-Cl, NO_2
THF	22.84 ± 0.14	1.83 ± 0.48	0.840	0.34	14	23.03 ± 0.08	1.25 ± 0.19	0.934	0.22	41	NO_2, Br, I excluded
Acetone	23.05 ± 0.09	1.59 ± 0.31	0.902	0.22	26	23.22 ± 0.07	1.00 ± 0.17	0.927	0.19	37	
DMSO	24.83 ± 0.07	-1.22 ± 0.25	0.907	0.14	23	24.74 ± 0.05	-0.96 ± 0.15	0.945	0.11	41	NO_2, Br, I, OMe excluded
DMF	24.71 ± 0.05	-1.33 ± 0.19	0.954	0.10	51	24.61 ± 0.06	-0.97 ± 0.18	0.925	0.13	30	
DMAc	24.62 ± 0.04	-0.90 ± 0.11	0.970	0.07	64	24.49 ± 0.03	-0.50 ± 0.06	0.975	0.06	76	OMe, F, Cl, 3-CF_3, 3-Br, 3-Cl
	24.43 ± 0.22	-2.36 ± 0.58	0.921	0.42	17	24.25 ± 0.25	-2.01 ± 0.64	0.877	0.51	10	H, Me, Br, I, NO_2
NMF	25.35 ± 0.04	-0.92 ± 0.16	0.941	0.09	31	25.29 ± 0.04	-0.69 ± 0.12	0.946	0.08	34	H, Me, OMe, F, Br, I
	25.32 ± 0.09	-1.68 ± 0.21	0.939	0.26	67						all (NO_2 (σ^-))
DCM	25.18 ± 0.03	-0.48 ± 0.09	0.909	0.08	29	25.13 ± 0.02	-0.35 ± 0.06	0.932	0.07	40	Cl, 3-CF_3, 3-Cl excluded
Chl	24.08 ± 0.06	1.10 ± 0.16	0.936	0.12	49	24.18 ± 0.05	0.89 ± 0.12	0.942	0.11	55	Cl, 3-CF_3, 3-Cl excluded

Generally, the correlation results could be divided in two sets: the first set includes protic solvents (alcohols), THF, acetone, Chl and EtAc with positive correlation coefficients. In these solvents, it was found higher susceptibility of the ν_{max} shifts to the electronic substituent effects, and the highest influence was found for solvent EtAc. For alcohol, the hydrogen-bonding ability is the factor of primary significance which contributes to better stabilization of the ground state of molecules. Somewhat lower negative values of correlation coefficients were found for other solvents (second set), indicating the significance of solvent dipolarity/polarizabilty to better stabilization of excited state. The lower sensitivities of absorption frequencies to substituent effects in aprotic solvents could be explained from the aspect of exceptional dipolarity of surrounding media. Dipolar aprotic solvents behave as poor anion solvators, while they usually better stabilize larger and more dispersible positive charges. Lower contribution of substituent effects in solvent with higher relative permittivity can be explained by the fact that highly dipolar surrounding medium suppresses electron density shift inducing lower susceptibility of absorption maxima shift to electronic substituent effects. The transmission of substituent electronic effects through π-resonance units of investigated compounds takes place by contribution of both defined π-electronic unit and overall conjugated system. Ratio of their contribution depends on substitution pattern, as well as solvent under consideration. It was found that extended resonance interaction is effectively transmitted to C5 carbon showing normal substituent effect (Table 4.4.8), which confirms that pseudo-cyclic hydrogen bridge plays significant role in transmission of substituent effects. This fact implies that electron density change is of local phenomena, mainly concentrated at phenylazo group, in electron-acceptor substituted compounds. The consequence is lower substituent effect in a solvent with high hydrogen bond accepting ability.

The LFER concept was applied to the ν_{max} and *SCS* values of arylazo pyridone dyes with the aim to get an insight into electronic effect of substituent to the absorption maxima shifts and NMR chemical shifts. An analysis of substituent effects on absorption spectra and *SCS* of the investigated molecules, by using LFER principles in the form of the

Hammett equation was performed [142]. The correlation results for **Hydrazo** form are given in Tables 4.4.8 and 9.

Table 4.4.7 Correlation results of the *SCS* values with σ_p/σ_m and σ_p^+/σ_m^+ substituent constants using Hammett (SSP) equation

Atom	ρ	h	R	F	sd	n	Substituents included
C2	-1.27 ±0.20	–0.08 ±0.03	0.964	39	0.06	5	H, Me, F, Cl (σ^+), Br
	-1.21 ±0.22	0.81 ±0.10	0.951	29	0.17	5	MeO, I (σ^+), 3-Br, 3-CF_3, NO_2
C3	-0.63 ±0.08	0.05 ±0.03	0.951	67	0.07	9	H, OMe, Me (σ^+), F, Cl, I (σ^+), 3-Cl, 3-Br, NO_2
C4	-1.27 ±0.14	0.00 ±0.04	0.976	79	0.07	6	H, Me, Cl, Br, 3-Br, 3-CF_3
C5	3.52 ±0.24	-0.25 ±0.08	0.984	220	0.20	9	H, OMe, F, Cl, Br, I, 3-Cl, 3-Br, NO_2
C6	-0.61 ±0.08	0.01 ±0.03	0.946	52	0.06	8	H, Me, Cl, Br, 3-Br, 3-Cl, 3-CF_3, NO_2

The observed ρ values indicate different susceptibilities of the *SCS* to substituent effects. It can be noticed from Table 4.4.8 that correlations are of good to high quality which means that the *SCS* values reflect electronic substituent effects. It is apparent that chemical shifts of C_5 show an increased susceptibility and normal substituent effect. Reverse substituent effect was observed at C_2, C_3, C_4 i C_6 carbons.

To measure separate contributions of the polar (inductive/field) and resonance effects of substituent, the regression analysis according to DSP equation with σ_I and σ_R constants has been performed, and the results are given in Table 4.4.9.

The existence of these correlations was interpreted as an evidence of appropriate substituent effect on the state of azo-hydrazo tautomerism. The azo group (–N=N–) is an electron-accepting group, while the imino group (–NH–) present in **Hydrazo** form is an electron-donating group. According to that, it is expected that electron-accepting group stabilizes the **Hydrazo** form. Presented results indicate that both substituent, electron-donating and electron-accepting, have significant influence on stabilization of **Hydrazo** tautomeric form. These results are in accordance with results presented in Table 6, which

leads to conclusion that introduction of both strong electron-acceptor and electron-donor substituent causes appropriate equilibrium shift to **Hydrazo** tautomeric form.

Table 4.4.8 Correlation results of the *SCS* values with σ_I and σ_R substituent constants using DSP equation

Atom	ρ_I	ρ_R	h	R	F	sd	λ^*	n	Substituents included in correlation
C2	-0.69 ±0.25	-0.30 ±0.50	0.01 ±0.08	0.874	5	0.11	0.43	6	H, Me, F, Cl, Br
	-2.38 ±1.48	-0.49 ±0.60	1.42 ±0.70	0.932	7	0.25	0.21	5	MeO, I, 3-Br, 3-CF_3, NO_2
C3	-0.67 ±0.16	-0.51 ±0.16	0.10 ±0.07	0.912	15	0.11	0.76	9	H, OMe, Me, F, Cl, I, 3-Cl, 3-Br, NO_2
C4	-1.12 ±0.24	-0.98 ±0.42	0.02 ±0.09	0.947	13	0.12	0.88	6	H, Me, Cl, Br, 3-Br, 3-CF_3
C5	2.71 ±0.46	3.53 ±0.36	0.06 ±0.22	0.981	77	0.23	1.30	9	H, OMe, F, Cl, Br, I, 3-Cl, 3-Br, NO_2
C6	-0.67 ±0.08	-0.39 ±0.14	0.06 ±0.03	0.975	48	0.05	0.58	8	H, Me, Cl, Br, 3-Br, 3-Cl, 3-CF_3, NO_2

$^*\lambda = \rho_R/\rho_I$

The effective transmission of substituent effects, *i.e*. differences in *SCS* values, is affected, among other factors, by the conformational (geometry) change of the investigated molecules which stems from an out-of-plane rotation of the *N*(1)-phenyl ring, *i.e.* defined by the torsion angle θ_1 and θ_2 values (Fig. 4.4.1; Table 4.4.10). The results obtained by the use of DSP equation do not provide significant improvement in fits when compared to the results of SSP eq. (3). However, on the other hand, DSP results are useful for the estimation of contribution of appropriate substituent effects on *SCS* change of the atom of interest. It is obvious that chemical shifts of C5 show an increased susceptibility and normal substituent effect. Reverse substituent effect was observed at C2, C3, C4 and C6 carbons (Table 4.4.8). The negative sign of reaction constant, ρ, indicates reverse behavior, *i.e*. the value of *SCS* decreases although the electron–withdrawing ability of the substituents, measured by σ, increases. The reverse substituent effect at observed carbons could be attributed to localized

π-polarization, which predominates over the extended π-polarization. Resonance interaction in extended conjugated system of aryl azo dyes has an opposite effect to the polarization caused by electron-acceptor substituent. The net result is that the electron-acceptor substituents increase the electron density on C2, C3, C4 and C6 carbons. Correlations for C5 carbon gives λ value of 1.3 which means that contribution of resonance interaction, *i.e.* more intensive interaction of substituent with this electron density at this carbon is operative within arylazo group. The resonance interaction significantly depends on spatial arrangement of the molecules, and thus, the resonance substituent effect is effectively transmitted to C5 carbon. All the other λ values are lower than 1, which means that polar (inductive/filed) substituent effect predominates over resonance effect. The alternation of polar substituent effects have been manifested as variation of the values of ρ_I coefficients (Table 4.4.8) which reflect distance/angle dependence of field effect as well as path-length dependence of the inductive substituent effect.

Table 4.4.9 Elements of the optimized geometries of investigated compounds obtained by the use of DFT method

Comp.	Interatomic distance (Å)						Torsion angle	
	H--O	N2-H	N1-N2H	C5-N1	C6=O	C2=O	θ_1	θ_2
1	1.0248	1.8066	1.2984	1.3246	1.2307	1.2094	89.766	0.026
2	1.0250	1.8049	1.2975	1.3258	1.2312	1.2096	89.685	0.026
3	1.0257	1.7960	1.2960	1.3258	1.2323	1.2101	90.020	-0.026
4	1.0283	1.7729	1.3067	1.3188	1.2303	1.2080	90.083	0.026
5	1.0252	1.7997	1.2988	1.3246	1.2311	1.2092	90.126	0.026
6	1.0250	1.7988	1.3006	1.3233	1.2307	1.2090	90.034	-0.026
7	-*	-	-	-	-	-	-	-
8	1.0249	1.8003	1.3007	1.3231	1.2307	1.2089	90.103	0.026
9	1.0248	1.8040	1.3022	1.3211	1.2299	1.2086	90.056	0.026
10	1.0247	1.8047	1.3013	1.3219	1.2301	1.2088	90.123	0.026
11	1.0248	1.8005	1.3012	1.3221	1.2302	1.2088	89.941	0.026

* basis set for iodo substituted compound is not available

4.4.5 Evaluation of electronic transition and charge density change. Nature of the frontier molecular orbitals

The optimized molecular geometries, highest occupied molecular orbitals (HOMOs) and lowest unoccupied molecular orbitals (LUMOs) are shown in Fig. 4.4.2 and 4.4.3. Energies of frontier orbitals and E_{gap} are shown in Table 4.4.11. Qualitatively, HOMO of the neutral compounds is delocalized over the entire molecule, while LUMO is shifted towards the central pyridine and phenylazo rings. The introduction of the weakly electron-donating methoxy groups in compounds **2** and **3** does not produce any appreciable change in the position of HOMO and LUMO orbitals with respect to compound **1**. The energy gap of these compounds resembles that of compound **1**, although the involvement of the oxygen atoms in HOMO slightly lowers E_{gap}. On the other hand, the introduction of the strong electron-withdrawing nitro group in compound **4** causes a shift of the electron density of LUMO at N(1)-phenyl ring towards the phenylazo ring. In addition, the introduction of the nitro group leads to a stronger stabilization of both HOMO and LUMO orbitals, and the energy gap for this compound is the lowest, when compared with other neutral compounds. In the halogen substituted compounds also does not produce any appreciable change in the position of HOMO and LUMO orbitals with respect to compound **1**, except noticeable shift from phenylaxo ring to central pyridone unit in compound **7**. In compounds with *meta*-substituent **9** - **11**, which is symmetrical as the other compounds, both HOMO and LUMO orbitals are delocalized over N(1)-phenyl and mostly substituted pheylazo rings, respectively in unsymmetrical fashion, and energies of both HOMO and LUMO are lowered with respect to compound **2**.

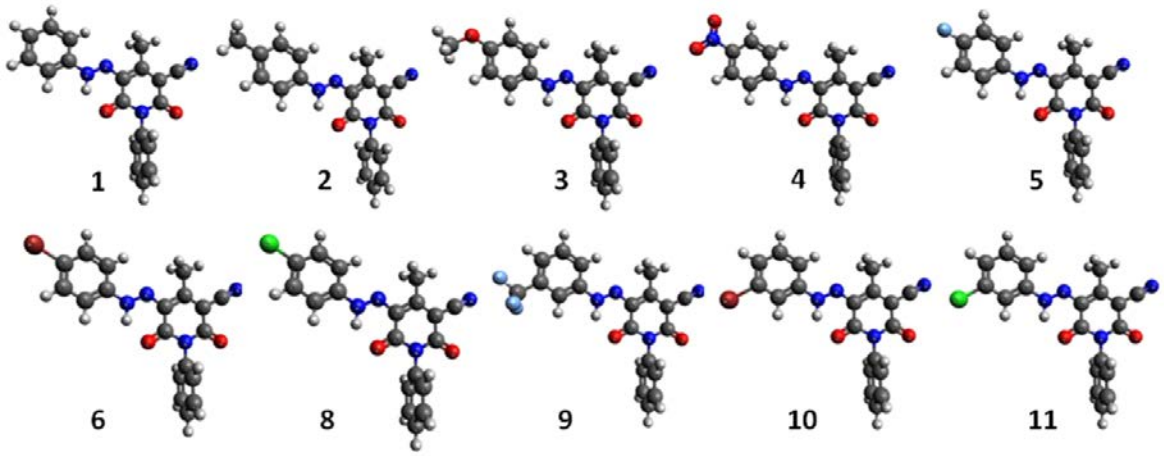

Fig. 4.4.2 Optimal geometries of compounds **1** - **11** in **Hydrazo** form

The geometries of the investigated molecules were fully optimized by the use of *ab initio* B3LYP/6-311G(d,p) method. The highest stability of the **Hydrazo** tautomer was obtained, and results of the elements of geometry of arylazo dyes are presented in Table 4.4.11. It can be seen that the elements of geometries of substituted derivatives are similar to those for the unsubstituted one. Similar conclusion stands for the results of analysis of absorption bands of investigated compounds, where appropriate relationship between structure and the main absorption band could be observed. The main absorption bands of both electron-donor and electron-acceptor substituted derivatives appear at similar wavelengths (in the range 10–20 nm) compared to those of **1**. The introduction of both electron-donor and electron-accepting substituent causes decrease of N2-H bond length. An electron-donor substituent supports an electron density shift from the phenylazo group to the pyridone moiety causing whole molecule planarization. An increase of the C5-N1 and decrease of N1-N2H bond lengths, which are a part of the hydrazo group, contribute to a greater extent of the π,π-delocalization with π-electronic system of pyridone ring. As a consequence, the length of carbonyl groups are slightly longer in the electron-donor substituted derivatives. This result is an additional support for the extended conjugation, *i.e.*, the π-electron density shifts towards C6=O carbonyl group increasing both carbonyl bond lengths and supporting more intensive hydrogen bonding between C6=O---HN atom

(Fig. 4.1.7, **Hydrazo** form). The results of geometry optimization are slightly different for the electron acceptor substituted compounds. The low deviation from the planarity and an increase of the N1-N2H bond length and decrease of C5-N1 and N2–H bond lengths indicate that two opposite electron accepting effects operate in investigated compounds: electron-accepting phenylazo group and pyridone core cause appropriate geometrical adjustment as a response to electronic demand of the electron deficient environment. The normal carbonyl groups polarization is suppressed and that causes a slight bond length decrease of carbonyl groups. Nevertheless, the shift to higher λ_{max} are obtained in comparison to compound **1**.

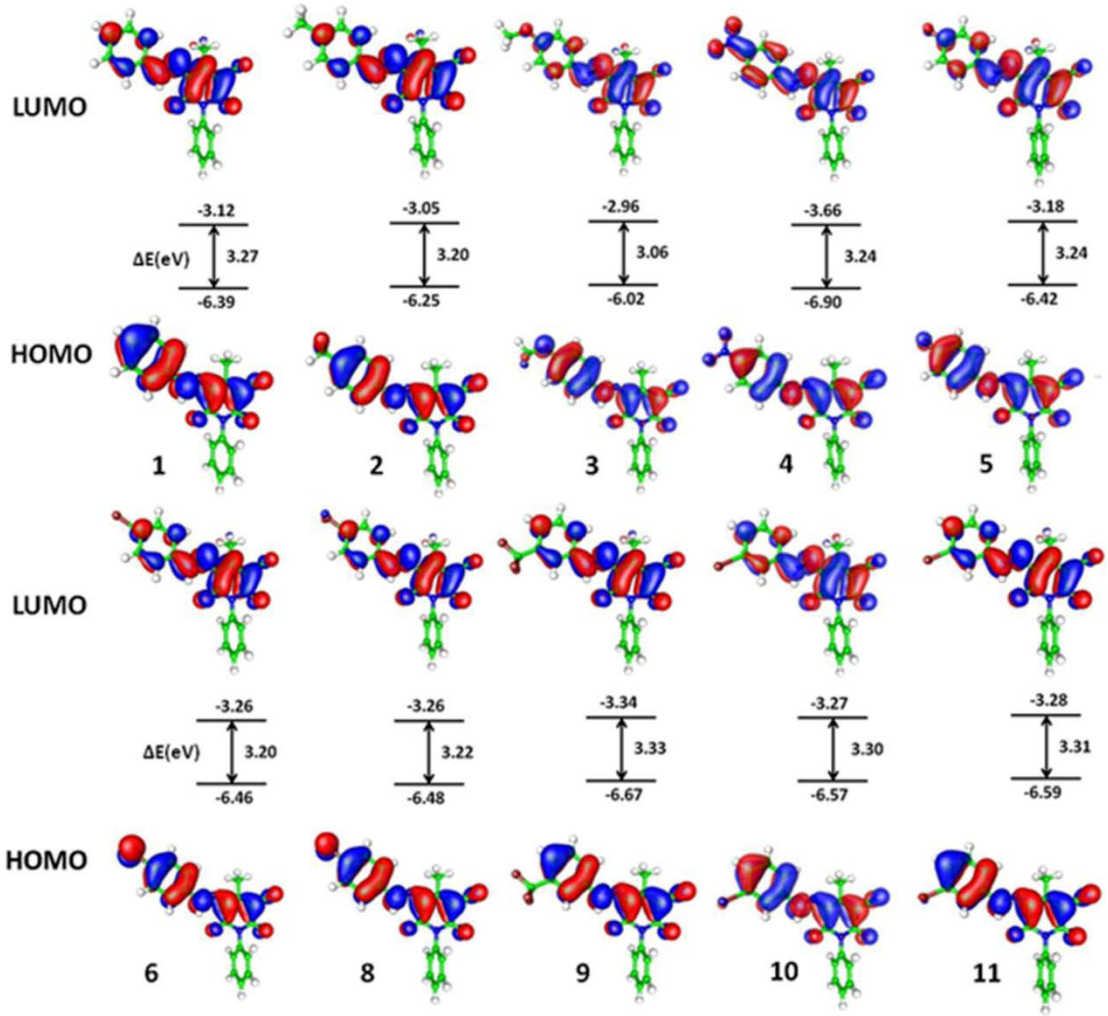

Fig. 4.4.3 The molecular orbitals and energy gaps between HOMO and LUMO orbitals of compounds **1 - 11** in the **Hydrazo** form in a gas phase

Table 4.4.10 Calculated energies of the HOMO and LUMO orbitals and energy gap for compounds **1 - 11** in gas phase (**Hydrazo** form)

Compound*	E_{HOMO} (eV)	E_{LUMO} (eV)	E_{gap} (eV)
1	-6.39	-3.12	3.27
2	-6.25	-3.05	3.20
3	-6.02	-2.96	3.06
4	-6.90	-3.66	3.24
5	-6.42	-3.18	3.24
6	-6.46	-3.26	3.20
8	-6.48	-3.26	3.22
9	-6.67	-3.34	3.33
10	-6.57	-3.27	3.30
11	-6.59	-3.28	3.31

* basis set for iodo substituted compound is not available

Qualitatively, HOMO of the neutral compounds is delocalized over the entire molecule, while LUMO is shifted towards the central pyridine and phenylazo rings. Similar E_{gap} values were obtained for all compounds, and the lowest E_{gap} was found for compound **3**. Furthermore, the ICT character could not be clearly observed during the orbital transition process from the HOMO to LUMO. The introduction of weak and moderate electron-donating *methyl* and *methoxy* group, respectively, in compounds **2** and **3,** produce appropriate change in the position of HOMO and LUMO orbital with respect to compound **1**. The energy gap of these compounds are lower than that for compound **1**, and the lowest value found for compound **3** because of the involvement of the electron-donating oxygen atom, causes increasing of n,π-resonance interactions, which brings about lower energy values of both HOMO and LUMO orbital. Due to more significant stabilization of LUMO orbital, slightly lower E_{gap} value was found for compound **3**. On the other hand, the introduction of the strong electron-withdrawing *nitro* group in compound **4** causes similar increase of energy for both HOMO and LUMO orbital which gives similar E_{gap} value as found for compound **1**. In addition, the introduction of the *nitro* group leads to a higher stabilization of both HOMO and LUMO orbitals. Halogen substituted compounds also does not produce any appreciable change of the position of HOMO and LUMO orbitals with

respect to compound **1**. In compounds with *meta*-substituent **9 - 11**, both HOMO and LUMO orbitals are better stabilized than in other compounds (except for comp. **4)**, and E_{gap} values are higher than in other compounds due to significantly better stabilization of HOMO orbital (Table 4.4.11).

The variation of substituent patterns clearly indicates that contributions of both conformational arrangement and donor–accepting character are involved in the ICT mechanism of the investigated molecules.

4.4.6 MEP (molecular electrostatic potential) analysis

MEP (molecular electrostatic potential) analysis was used to evaluate and visualize charge distribution over investigated compounds and illustrates the three dimensional charge distributions overall investigated molecules. MEP potential at a point in space around a molecule gives information about the net electrostatic effect produced at that point by total charge distribution (electron + proton) of the molecule and correlates with dipole moments, electro-negativity, partial charges and chemical reactivity of the molecules. It provides a visual method to understand the relative polarity of the molecule [234,235]. An electron density isosurface mapped with electrostatic potential surface depicts the size, shape, charge density and site of chemical reactivity of the molecules. MEP shown in Fig. 4 illustrates the three dimensional charge distributions overall investigated molecules. As it can be seen from the Fig. 4, the different values of the electrostatic potential at the surface are represented by different colors; red represents regions of most electronegative electrostatic potential, it indicates the region of high electron density, *i.e.* sites favorable for electrophilic attack; blue represents regions of the most positive electrostatic potential, *i.e.* region of low electron density favorable for nucleophilic attack, and green represents regions of zero potential. Potential increases in the order red < orange < yellow < green < blue. The blue color indicates the strong attractive potential, region favorable for HBA solvent interaction, while red color indicates the repulsive potential, and includes sites favorable for HBD solvent interactions. As can be seen from the MEP map of the molecules, negative regions are mainly localized over the cyano and carbonyl groups attached at the pyridone rings and over the *nitro* substituent in the compound **4**. The

positive region is localized on the phenyl and pyridone rings. The negative potential of oxygen atoms oriented symmetrically in 2,6-positions of **Hydrazo** form, with respect to the central pyridone unit, is clearly visible on the Fig. 4.4.4. Most of HBA capabilities of aryl azo dyes could be assumed to be from 2,6-dioxo groups which are strong attractive electron-acceptor groups and cause increase of electron densities at these two sites creating favorable interaction with proton-donating solvents. HBD capabilities of solute molecule is mostly concentrated at azo pyridone moiety. As can be seen from the MEP map of the compounds, the regions having the negative potential are over the electronegative atoms, the regions having the positive potential are over the phenylazo and pyridone rings and the remaining species are surrounded by zero potential.

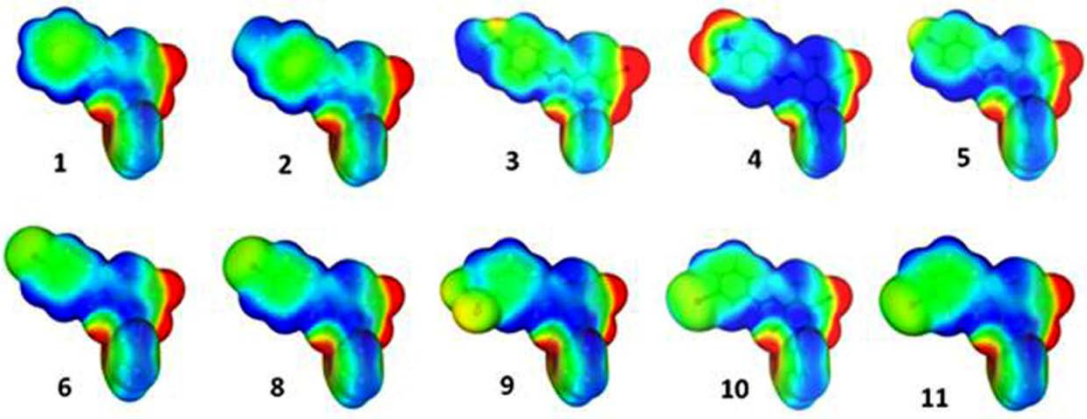

Fig. 4.4.4 MEP map of compounds **1-11** calculated by B3LYP/6-311G(d,p) method in ground state

DFT study of arylazo dyes showed the most interesting feature in NMF. Calculated energies of **Azo**/**a**, **Azo**/**b** and **Hydrazo** tautomers for compounds with NO_2 and OCH_3 substituent in NMF are presented in Table 12. All structures are optimized by B3LYP method and 6-311(d,p) basis basis set in NMF solvent simulated by PCM method. ΔG_{solv} is calculated with the same basis set applying SMD methodonPCM optimized structures (Table 4.4.12).

Table 4.4.11 Calculated energies of the **Azo**/**a**, **Azo**/**b** and **Hydrazo** tautomers for compounds **3** and **4** in NMF

Compound			**4**			**3**
Tautomer	**Azo**/**a**	**Azo**/**b**	**Hydrazo**	**Azo**/**a**	**Azo**/**b**	**Hydraz**
Energy in a gas phase (kcal/mol)	26.36	26.56	0	26.77	26.41	0
ΔG_{solv} (kcal/mol)	21.61	19.93	19.34	22.32	20.87	19.57
Energy in NMF solvent (kcal/mol)	24.10	25.98	0	24.02	25.11	0

As it can be seen from the results presented in Table 4.4.12, **Hydrazo** tautomer is the most stable for both compounds. Interestingly, in NMF solvent, due to high value of dielectric constant and hydrogen bonding ability, the optimization of molecular structure of tautomer **Azo**/**a** was successful. Otherwise, in other solvents, as well as in gas phase, calculations have shown that **Azo**/**a** tautomer is not a minimum on potential energy surface. All B3LYP/6-311(d,p) optimizations, which started from **Azo**/**a** geometry, are optimized to much more stable geometry of **Hydrazo** form. Theoretical calculations and NMR results clearly indicated that, if both tautomers (**Azo**/**a** and **Azo**/**b**) are obtained by pyridone **1** diazotization, subsequent hydrogen rearrangements drive the equilibrium to more stable **Hydrazo** form [193]. Free energy of solvation has the highest value for **Azo**/**a** and the lowest for **Hydrazo** tautomer, with small differences in ΔG_{solv} (about 2 kcal/mol) indicating small contribution of solvation effect on stabilization of the solute molecule. It is an additional evidence that **Hydrazo** form is the most stable molecular structure both in the gas phase and in solvated state. The optimized structure of **Azo**/**a**, **Azo**/**b** and **Hydrazo** form of compound **3** and **4** in NMF are given in Figs. 4.4.5. The molecular orbitals and energy gaps between HOMO and LUMO orbitals, and MEP map of compound **3** a) and **4** b) for all tautomers are given in Figs. 4.4.5 and 4.4.6, respectively.

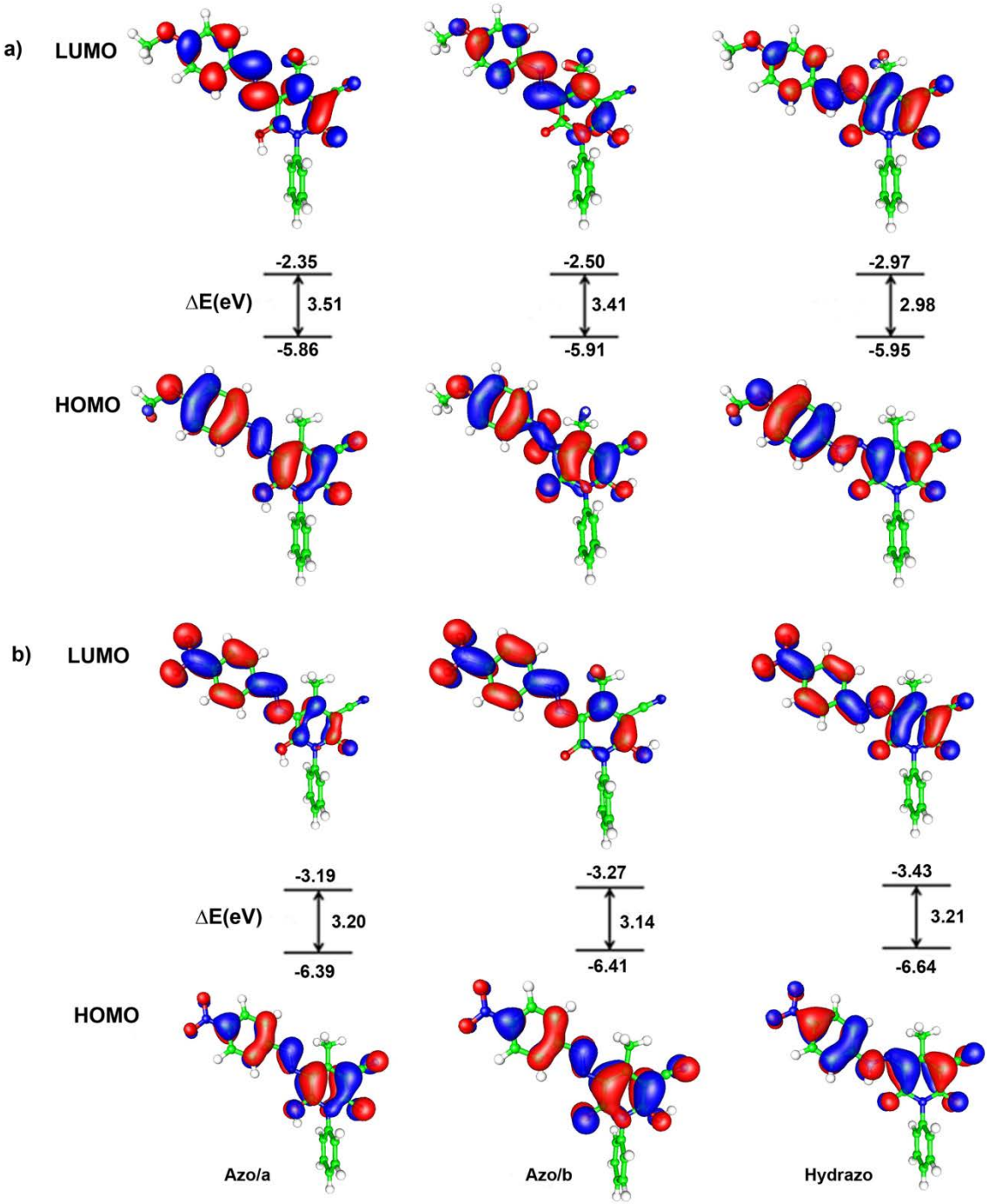

Fig. 4.4.5 The molecular orbitals and energy gaps between HOMO and LUMO orbitals of compound **3** a) and **4** b) in the **Azo**/**a**, **Azo**/**b** and **Hydrazo** form in NMF

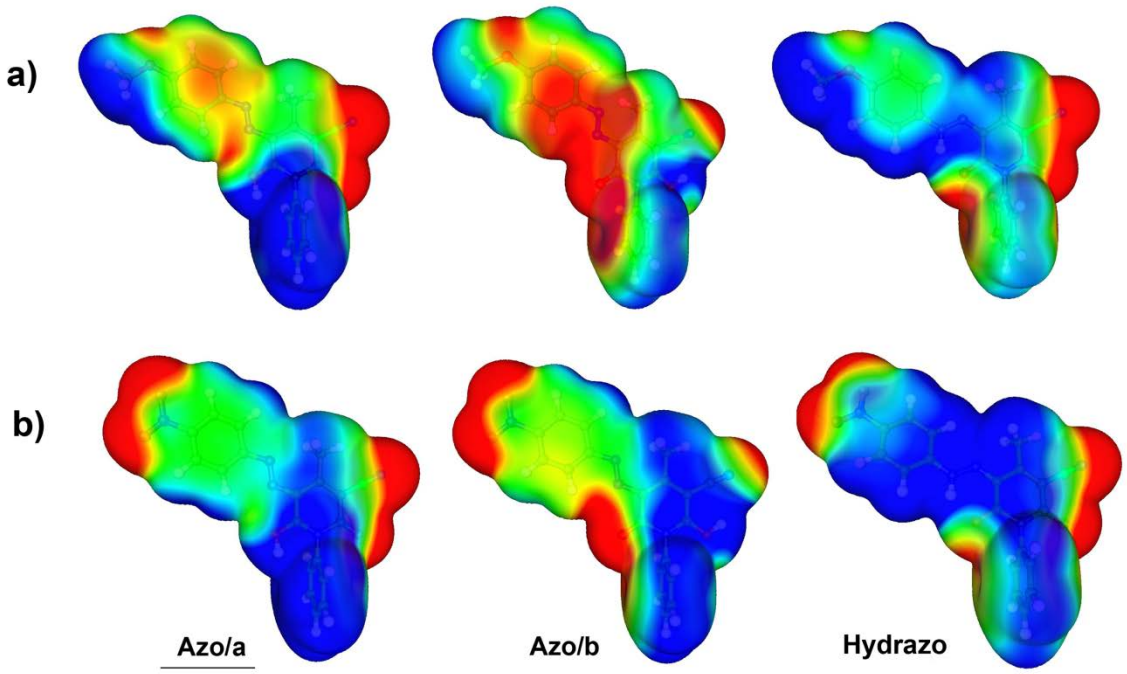

Fig. 4.4.6 MEP map of compound **3** a) and **4** b) in the **Azo**/**a**, **Azo**/**b** and **Hydrazo** form, respectively, in NMF

Obviously, the ICT process is more feasible in NMF solvent. For compound **3**, the reason is higher planarity, while, in compound **4**, higher rotation around the bond connecting the two electron-accepting groups can decouple the orbitals of these two groups providing means for significant charge transfer. The highly polarizable ground and excited states of compounds **3** and **4** can be, under appropriate solvation conditions, preferentially stabilized by dipolar interactions. Due to this, the excited and ground states of compound **3** in **Hydrazo** form are closer and more rapid internal conversion is permitted.

The planar structure of investigated compounds supports conclusion that contribution of strong directional electronic transfer within two electronic structures: phenylazo and semi-aromatic pyridone ring is of high significance for electronic density transfer through overall compounds investigated. Structural diversity of studied compounds in different solvents depends on the contribution of the appropriate tautomeric form. Two oxygen atoms, present in **Hydrazo** form, show strong electron-accepting character of two keto groups (1,3-dicarbonyl structure in pyridone moiety). Electron-attracting power of two carbonyl groups in investigated molecules shifts more significantly electron densities from

outer part of molecule. Compounds which distinguish from others are *meta*-substituted compounds which exert non-directional transmission of substituent effect that contributes even more that 1,3-diketo structure displaying larger electron-accepting character. In this way, *N*(1)-phenyl ring, due to lower n,π-resonance interaction, showed larger deviation from planarity providing higher accessibility of two keto groups to the stabilization by solvent hydrogen bond interaction.

5 CONCLUSIONS

A simple and convenient synthesis of tautomeric (6 or 2)-hydroxy-4-methyl-(2 or 6)-oxo-1-(substituted phenyl)-(1,2 or 1,6)-dihydro- pyridine-3-carbonitriles from ethyl acetoacetate and 2-cyano-*N*-(substituted phenyl)-ethanamides using microwave assisted chemistry is presented. The structure of the obtained product was confirmed by the use of FTIR, NMR, UV and MS techniques. Presence of tautomeric forms, 6-hydroxy-4-methyl-2-oxo-1-(substituted phenyl)-1,2-dihydropyridine-3-carbonitriles and 2-hydroxy-4-methyl -6-oxo-1-(substituted phenyl)-1,6-dihydropyridine-3-carbonitriles, and state of equilibrium in DMSO-d_6 of the obtained product was studied by ^{1}H and ^{13}C NMR spectroscopy, as well as B3LYP/6-311++G(d,p) and GIAO/WP04/aug-cc-pVDZ theoretical calculations.

Tautomeric equilibria of title compounds were quantitatively analyzed by UV/Vis spectroscopy and theoretical approaches. The results were obtained by stepwise procedure with conclusion that state of equilibrium is determined by a balanced contribution of solvent and structural effect. From the results of the Kamlet-Taft and Catalán correlation analysis, positive value of coefficient *a* indicates better stabilization of the ground of the **PY** form, and the excited state of the **HP** form, while solvent dipolarity and polarizability are dominant factor influencing the batochromic shift. The contribution of HBD specific solvent effect on the state of tautomeric equilibrium of the investigated compounds was confirmed in the mixture of THF/NMF. Adjustments of HBD/HBA properties in solvent mixture could control shift of tautomeric equilibrium. The LFER correlation results showed significant influence of the solvent effects on the transmission mode of substituent effects. The positive solvatochromism for both electron-donor and electron-acceptor substituted compounds in all solvents, except for compounds **1**, **4**, **5**, **7**, **8** in DMSO, DMF and DMAc, was found. Quantum chemical calculations of the optimal geometries of both tautomeric forms were performed by the use of B3LYP functional with 6-311G(d,p) basis set. The inclusion of solvent effects and the TD–DFT calculations demonstrated that substituents, depending on their position on molecules, significantly change the conjugation, and further affect the ICT character of the investigated 2(1*H*)-pyridones. Generally, the most important conclusions derived from Bader's analysis could be defined in following: *methoxy* substituent induces ICT, in the excited state, from substituted ring to the other two rings;

nitro substituent exert an opposite effect, *i.e*. induces ICT from the other two rings to substituted one, while the chloro substituent induces negligible ICT process.

Tautomeric equilibria of 6(2)-hydroxy-4-methyl-2(6)-oxo-1-(substituted phenyl)-1,2(1,6)-dihydropyridine-3-carbonitriles were quallitatively/quantitatively analyzed by UV/Vis spectroscopy and quantum chemical calculations. Results of LSER analysis, obtained by the use of Kamlet-Taft and Catalán equations, imply that the positive value of the coefficient *a* obtained for both **2-PY** and **6-PY** forms, except for compounds **5, 8** and **11** in **6-PY** form, indicate better stabilization of the molecule in the ground state. Highest values of coefficient *a* was found for compound **11** in both **2-PY** and **6-PY** forms. A negative sign of the coefficients *s* and *b*, obtained in correlations for the **2-PY** form, except for compounds **12-15**, indicate a batochromic shift of the absorption maxima with the increasing contribution of solvent dipolarity/polarizability and hydrogen-accepting capability. The largest value of coefficients *s* and *b* of the **2-PY** form was found in compound **4**. Interestingly, highest value of coefficients *s* and *b* were found for compounds **5** and **1**, respectively, indicating complex structure-properties relationship of investigated compounds in **6-PY** form. Moreover, LSER analysis by using Catalán equation showed highest contribution of solvent polarizability in **2-PY** form, while HBD effect is somewhat higher in comp. **15** than polarizability effect in compound **11**.

The LFER correlation results showed significant influence of the solvent effects on the transmission mode of substituent effects. The positive solvatochromism for both electron-donor and electron-acceptor substituted compounds in all solvents, except for compounds **1**, **4**, **5**, **7**, **8** in DMSO, DMF and DMAc, was found. Quantum chemical calculations of the optimal geometries of both tautomeric forms were performed by the use of B3LYP functional with 6-311G(d,p) basis set. The inclusion of solvent effects and the TD–DFT calculations demonstrated that substituents, depending on their position on molecules, significantly change the conjugation, and further affect the ICT character of the investigated 2(1*H*)-pyridones.

Theoretical calculations and experimental results gave insight into the influence of the molecular conformation on the transmission of substituent effects, as well as on contribution

of different solvent–solute interactions. Bader's analysis showed that similar processes of electronic excitation are operative in both **2-PY** and **6-PY** forms. In *nitro*-substituted compounds a distinct ICT was noticed, as well as moderate process in halogen substituted compounds in **6-PY** form.

In this work, eleven new 5-arylazo-6(2)-hydroxy-4-methyl-3-cyano-*N*(1)-phenyl-2(6)-oxo-pyridine-3-carbonitrile dyes were synthesized. Characterization and the absorption ability of the dyes were studied. All the synthesized dyes exist in the hydrazone tautomeric form in the solid state and the dyes were predominantly as hydrazones in all the employed solvents. The results showed that the solvent effect on the absorption maxima of the investigated arylazo pyridone dyes is very complex and strongly depends on the nature of the substituent on the arylazo component. The introduction of electron-donating substituents into the arylazo ring results in strong bathochromic shifts in all solvents. These solvatochromic properties are evident for the hydrazone tautomeric form. The effect of electron-accepting substituents is different and produces slight bathochromic or hypsochromic shifts of the absorption maxima. The solvatochromism of the arylazo pyridone dyes was analyzed with ENT, er and n solvent parameters and by multilinear regressions with Catalan and Kamlet–Taft solvents scales. Catalan solvent scales are more appropriate than the Kamlet–Taft scales for describing the solvatochromism of the azo dyes. The obtained results show that the solvent polarizability is the main factor which influences the shift of absorption maxima, whereas the solvent dipolarity, acidity and basicity are less important.

6 REFERENCES

1. S.Shima, E.L., M.Sordel-Klippert, M.Kauss, J.Kahnt, R.Thauer, K.Steinbach, X.Xie, L.Verdier, C.Griesinger, Angew Chem, 2004. 43: p. 2547.
2. Studies on pyridines, available at .ac.in:8080/jspui/bitstream/10603/3514/8/08_chapter%201.pdf, h.s.I.
3. G.Hammes, P.L., J Am Chem Soc, 1970. 92: p. 7578.
4. L.Forlani, G.C., C.Boga, P.Todesco, E.Del Vecchio, S.Selva, M.Monari, Arkivoc, 2002. 11: p. 198.
5. H.Yang, B.C., Acta Crystallogr, 1998. 54: p. 912.
6. V.Rybakov, A.B., E.Babaev, L.Aslanov, Acta Crystallogr E, 2004. 6: p. 160.
7. C.Fischer, H.S., D.Stephenson, H.Zipse, J Phys Org Chem, 2005. 18: p. 901.
8. V.Litvinov, S.K., V.Dyachenko, Chem Heterocyclic Comp, 1999. 35: p. 509.
9. Hunger, K., Industrial Dyes: Chemistry, Properties, Applications2007 John Wiley & Sons.
10. S.Portnoy, J Org Chem, 1965. 30: p. 3377.
11. D.Mijin, G.U., N.Valentić J Serb Chem Soc 2001. 66: p. 507.
12. N.Aqui, R.V., Cancer Biol Ther, 2008. 7: p. 1888.
13. A.Abd-el-Rahman, E.K., J Heterocycl Chem, 1981. 18: p. 371.
14. R.Blackwood, G.H., C.Larrabee, F.Pilgrim, J Am Chem Soc, 1958. 80: p. 6244.
15. P.Fanta, R.S., J Am Chem Soc, 1955. 77: p. 1045.
16. N.Hamdy, A.G.-E., Eur J Med Chem, 2009. 44: p. 4547.
17. L.Perez-Medina, R.M., S.McElvain, J Am Chem Soc, 1947. 69: p. 2574.
18. S.Sonar, B.S., An Indian Journal, 2007. 3: p. 1.
19. U.Schmidt, Ann Chem, 1962. 657: p. 156.
20. G.Walker, B.W., J Org Chem, 1961. 26: p. 4441.
21. M.Miles, T.H., C.Hauser, J Org Chem, 1965. 30: p. 1007.
22. T. Harris, S.B., C. Hauser, J Amer Chem Soc, 1963. 85: p. 3273.
23. T. Rotopopova, A.S., J Gen Chem USSR, 1957. 27: p. 1360.
24. B.Chase, J.W., J Chem Soc, 1953: p. 3548.

25. T.Kametani, K.O., A.Kozuka, Yakugaku Zasshi, 1967. 87: p. 168.
26. A.Sakurai, H.M., Bull Chem Soc Japan, 1968. 41: p. 165.
27. M.Abdalla, A.E., A.Deeb, Pak J Sci Ind Res, 1977. 20: p. 139.
28. T.Kametani, A.K., S.Tanaka, Yakugaku Zasshi, 1970. 90: p. 1574.
29. G.Kaupp, M.N.-J., J.Schmeyers, Tetrahedron, 2003. 59: p. 3753.
30. M.Shamma, R.L., P.Miller, E.Walker, Tetrahedron, 1965. 21: p. 3255.
31. J.Powers, I.P., J Amer Chem Soc, 1968. 90: p. 7102.
32. P.Mortimer, Aust J Chem, 1968. 21: p. 467.
33. E.Ziegler, K.B., G.Brus, Monatsh Chem, 1967. 98: p. 555.
34. C.Kappe, T.K., Monatsh Chem, 1989. 120: p. 1095.
35. J.Debenham, C.M.-D., T.Walsh, J.Wang, X.Tong, G.Doss, J.Lao, T.Fong, M.Schaeffer, J.Xiao, C.Huang, C.Shen, Y.Feng, D.Marsh, D.Stribling, L.Shearman, A.Strack, D.MacIntyre, L.Van der Ploeg, M.Goulet, Med Chem Lett, 2006. 16: p. 681.
36. A.Al-Najjar, M.A., A.Al-Enezi, M.Elnagdi, Molecules, 2009. 14: p. 68.
37. I.Collins, C.M., W.Davey, M.Rowley, F.Bromidge, K.Quirk, J.Atack, R.McKernan, S.Thompson, K.Wafford, G.Dawson, A.Pike, B.Sohal, N.Tsou, R.Bull, J.Castro, J Med Chem, 2002. 45: p. 1887.
38. S.Ghozlan, A.H., Tetrahedron, 2002. 58: p. 9423.
39. Y.Yamaguchi, I.K., K.Funabiki, M.Matsui, K.Shibata, J Heterocycl Chem, 1998. 35: p. 805.
40. D.Tyndall, T.A.N., M.Meegan, Tetrahedron Lett, 1988. 29: p. 2703.
41. M.Al-Arab, J Heterocycl Chem, 1989. 26: p. 1665.
42. G.Elgemeie, H.Z., S.Sherif, Phosph Sulfur and Silicon, 1990. 54: p. 215.
43. M.Radwan, E.A., Monatsh Chem, 2009. 140: p. 229.
44. S.Kajihara, Nippon Kagaku Zasshi, 1965. 86: p. 893.
45. P.Tomasik, E.P., Rosz Chem, 1965. 39: p. 1911.
46. E.Behrman, B.P., J Amer Chem Soc, 1958. 80: p. 3717.
47. A.Porter, P.S., J Chem Soc D, 1970: p. 1103.
48. W.Ried, F.B., Ann Chem, 1969. 230: p. 725.
49. Zollinger, H., Colour Chemistry1987, Weinheim: VCH.

50. N. Seto, Y.K., T. Fujimori, Colored curable compositions containing phthalocyanine and pyridone azo dyes and manufacture of color filters using them with excellent light and heat resistance, L. Fuji Photo Film Co., Editor 2006.

51. Oberholzer, M., Concentrated storage-stable aqueous dye solution without any solubilizer content, C.I. Ltd., Editor 2005.

52. G. Elhemeie, M.H., H. El-Sayed, Recent trends in synthesis and application of nitrogen heterocyclic azo dyes. Pigm. Resin Technol., 2001. 30: p. 210-228

53. M. Yen, I.W., A facile syntheses and absorption characteristics of some monoazo dyes in bis-heterocyclic aromatic systems. Part I. Synthesis of polysubstituted 5-(2-pyrido-5-yl and 5-pyrazolo-4-yl)azo-thiophene derivatives. Dyes Pigm., 2004. 62: p. 1-9.

54. D. Mijin, G.U., N. Valentić, A. Marinković, Sinteza arilazo piridonskih boja. Hem. Ind. , 2011. 65: p. 517-532.

55. D. Mijin, M.M.-V., Investigation of the reaction conditions for the synthesis of 4,6-disubstituted-3-cyano-2-pyridones and 4-methyl-6-hydroxy-2-pyridone. J. Serb. Chem. Soc., 1994. 59: p. 969-975.

56. M. Mišić-Vuković, D.M., M. Radojković-Veličković, N. Valentić, V. Krstić, Condensation of 1,3-diketones with cyanoacetamide: 4,6-disubstituted-3-cyano-2-pyridones. J. Serb. Chem. Soc. , 63. 63: p. 585-599.

57. D. Mijin, G.U., N. Perišić-Janjić, I. Trkulja, M. Radetić, P. Jovančić, Synthesis, propreties and colour assessment of some new 5-(3- and 4- substituted phenylazo)-4,6-dimethyl-3-cyano-2-pyridones. J. Serb. Chem. Soc. , 2006. 71: p. 2006.

58. J. Dostanić, N.V., G. Ušćumlić, D. Mijin, Synthesis of 5-(substituted phenylazo)-6-hydroxy-4-methyl-3-cyano-2-pyridones from ethyl 3-oxo-2-(substituted phenyl-diazenyl)butanoates. J. Serb. Chem. Soc. , 2011. 76: p. 499-504.

59. D. Mijin, M.B., C. Reidlinger, C. Kappe, The microvawe-assisted synthesis of 5-arylazo-4,6-disubstituted-3-cyano-2-pyridone azo dyes. Dyes Pigm. , 2010. 85: p. 73-78.

60. D. Mijin, A.M., Synthesis of N-substituted 4,6-dimethyl-3-cyano-2-pyridones under microvawe irradiation. Synth. Commun., 2006. 36: p. 193-198.

61. Johnson, S., Synthesis of azo dyas derived from pyridine as coupling components and their application on nylon and polyester fabrics, 2011, Ahmadu Bello University: Zaria.

62. L. Abd-Alredha, R.A.-R., R. Jameel Mhessn E J Chem, 2012. 9: p. 465-470.

63. S. Ravichandran, E.K., Microwave Synthesis-A Potential Tool for Green Chemistry. Int. J. ChemTech. Res., 2011. 3: p. 466-470.

64 D. Stuerga, M.D., Microwaves in Organic Synthesis, ed. A. Loupy2002, Weinheim: Wiley-VCH.

65 Mingos, M., Microwave-Assisted Organic Synthesis, ed. J.P.T. P. LidstrUm2004, Oxford: Blackwell.

66 D. Baghurst, D.M., Chem. Soc. Rev., 1991. 20: p. 1– 47.

67 C. Gabriel, S.G., E. Grant, B. Halstead, D. Mingos, Chem. Soc. Rev. , 1998. 27: p. 213–223.

68 D. Stass, J.W., C. Timmel, P. Hore, K. McLauchlan, Chem. Phys. Lett. , 2000. 329: p. 15– 22.

69 Kappe, C., Angew Chem Int Edn, 2004. 43: p. 6256.

70 M. Kidwai, P.S., Synthesis, 2001. 10: p. 1509.

71 M. Csiba, J.C., A. Loupy, J. Malthete, S. Gero, Tetrahedron Lett., 1993. 34: p. Tetrahedron Lett.

72 R. Varma, R.S., R. Dahiya, Tetrahedron Lett., 1997. 38: p. 7823.

73 M. Kidwai, P.S., Org. Prep. Proced. Int. , 2001. 33: p. 381.

74 M. Kidwai, R.G., K. Bhushan, J. Chem. Res., 2000: p. 586.

75 D. Artman, R.W., J.Amer. Chem. Soc., 2007. 129: p. 6336.

76 S. Ravichandran, K.S., R. Arun Kumar, Int. J.Chem.Sci., 2008. 6: p. 1800.

77 C. Zhang, L.L., S. Gong, Green Chemistry, 2007. 9: p. 303.

78 M. Tsuji, M.H., Y. Nishizawa, M. Kubokawa, T. Tsuji, Chemistry–A European Journal, 2005. 11: p. 440.

79 S. Sinwell, H.R., Aus. J. Chem., 2007. 60: p. 729.

80 J. Collins, N.L., Organic and Biomolecular Chemistry, 2007. 5: p. 1141.

81 R. Trotzki, M.N., B. Ondruschka, Green Chem., Green Chem. 5: p. 285–290.

82 R. Gedye, F.S., K. Westaway, H. Ali, L. Baldisera, L. Laberge, J. Rousell, Tetrahedron Lett. , 1986. 27: p. 279.

83 R. Giguere, T.B., S. Duncan, G. Majetich, Tetrahedron Lett., 1986. 27: p. 4945.

84 A. Loupy, A.P., J. Hamelin, F. Texier-Boullet, P. Jacquault, D. Mathk, Synthesis, 1998. 34: p. 1213.

85 Varma, R., Green Chem. , 1999: p. 43.

86 A. Bose, M.M., S. Ganguly, A. Sharma, B. Banik, Synthesis 2002: p. 1578.

87 Strauss, C., Microwaves in Organic Synthesis, ed. A. Loupy2002, Weinheim: Wiley-VCH.

88 Adam, D., Nature, 2003. 421: p. 571.

89 Mingos, D., Chem. Ind., 1994: p. 596-599.

90 A. Hoz de la, A.D., A. Moreno, Chem. Soc. Rev., 2005. 34: p. 164-178.

91 M. Nuchter, B.O., W. Lautenschlager, Synth. Commun., 2001. 37: p. 1277-1283.

92 Li, C., Chem. Rev., 1993. 93: p. 2023-2035.

93 C. Kappe, D.D., Nat. Rev. Drug Discovery, 2006. 5: p. 51-63.

94 V. Polshettiwar, R.V., Acc. Chem. Res, 2008. 41: p. 629-639.

95 V. Polshettiwar, R.V., Chem. Soc. Rev., 2008 37 p. 1546-1557.

96 Klingsberg, E., Pyridine and its Derivitives1960, New York: Interescience.

97 N. Gorobets, B.Y., F. Belaj, C. Kappe, Rapid microwave-assisted solution phase synthesis of substituted 2-pyridone libraries. Tetrahedron, 2004. 60: p. 8633-8644.

98 Schmid, H., Process for the preparation of pyridone compounds, S. AG, Editor 1994.

99 D. Mijin, G.U., N. Valentić, Synthesis and investigation of solvent effects on the ultraviolet absorption spectra of 5-substituted-4-methyl-3-cyano-6-hydroxy-2-pyridones. J. Serb. Chem. Soc. , 2001. 66: p. 507-516.

100 J. Bobbit, D.S., Synthesis of Isoquinoline Alkaloids. II. The Synthesis and Reactions of 4-Methyl-3-pyridinecarboxaldehyde and Other 4-Methyl-3-substituted Pyridines. J. Org. Chem., 1960. 25: p. 560- 564.

101 J. Dostanić, D.L., P. Banković, O. Cvetković, D. Jovanović, D. Mijin, Influence of process parameters on the photodegradation of synthesized azo pyridone dye in TiO2 water suspension under simulated sunligh. J. Environ. Sci. Health, Part A: Toxic/Hazard. Subst. Environ. Eng., 2011. 46: p. 70-79.

102 C. Dave, G.C., D. Shah, Y. Agrawal A simple and convient synthesis of 4,6-disubstituted 3-cyanopyridin-2(1H)-ones under solvent-free microwave conditions. Indian J. Chem., Sect. B: Org. Chem. Incl. Med. Chem., 2004. 43B: p. 885-887.

103 S. Al-Neyadi, A.H., I. Abdou, Microwave-assisted synthesis of 2(1h)-pyridones and their glucosides as cell proliferation inhibitors Nucleos. Nucleot. Nucl., 2011. 30: p. 120-134.

104 A. Abadi, O.A.-D., A. Al-Afify, H. El-Kashef, Synthesis of 4-alkyl (aryl)-6-aryl-3-cyano-2(1H)-pyridinones and their 2-imino isosteres as nonsteroidal cardiotonic agents Il Farmaco 1999. 54: p. 195-201.

105 R. Jia, S.T., Y. Zhang, B. Jiang, J. Zhang, C. Yao, F. Shi, An efficient and greener approach to the synthesis of 3,5-dicyanopyridin-2(1H)-one derivatives in aqueous media under microwave irradiation conditions. J. Heterocyclic Chem., 2007. 44: p. 1177-1180.

106 H. Rodriguez, M.S., R. Perez, A. Petit, A. Loupy Solvent-free synthesis of 4-aryl substituted 5-alkoxycarbonyl-6-methyl-3,4-dihydropyridones under microwave irradiation. Tetrahedron Lett. , 2003. 44: p. 3709-3712.

107 Y. Xiang, W.-J.Z., One-pot synthesis of pyridones and related compounds under microwave irradiation in water. Jiamusi Daxue Xuebao, 2010. 28: p. 753-755.

108 S. Tu, C.M., F. Fang, Y. Feng, T.Li, Q. Zhuang, X. Zhang, S. Zhu, D. Shi, New potential calcium channel modulators: design and synthesis of compounds containing two pyridine, pyrimidine, pyridone, quinoline and acridine units under microwave irradiation. Bioorg. Med. Chem. Lett. , 2004. 14 p. 1533-1536.

109 Merino, E., Synthesis of azobenzenes: the coloured pieces of molecular materialsw. Chem. Soc. Rev., 2011. 40: p. 3835-3853.

110 Mihailović, M., Osnovi teorijske organske hemije i stereo hemij1972, Beograd: Građevinska knjiga.

111 E.Nir, M.M., L.Grace, M.De Vries, Chem Phys Lett, 2002. 355: p. 59.

112 F.Dong, R.M., Science, 2002. 298: p. 1227.

113 K.Choi, J.L., S.Kim, J Am Chem Soc, 2005. 127: p. 15674.

114 J.Lopez, M.P., S.Eugenia, J.Alonso, J Chem Phys Lett, 2007. 126: p. 191103.

115 S.Brunken, M.M., P.Thaddeus, P.Godfrey, R.Brown, Astron Astrophys, 2006. 459: p. 317.

116 V.Vaquero, M.S., J.Lopez, J.Alonso, J Phys Chem A, 2007. 111: p. 3443.

117 H.Schleger, P.G., E.Fluder, J Am Chem Soc, 1982. 104: p. 5347.

118 J.Rawson, R.W., Coordin Chem Rev, 1995. 139: p. 313.

119 D.De Kowalewski, R.C., E.Diez, A.Esteban Mol Phys, 2004. 102: p. 2607.

120 S.Millefiori, A.M., Bull Chem Soc Jpn, 1990. 63: p. 2981.

121 C.Reichardt, Solvent Effects on Tautomeric Equilibria2003, Weinheim: Wiley.

122 A.Michelson, A.P., J.Lee, J Org Chem, 2012. 77: p. 1623.

123 P.Chou, C.W., J Phys Chem B, 1997. 101: p. 9119.

124 Ł.Szyc, J.G., M.Yang, J.Dreyer, P.Tolstoy, E.Nibbering, B.Czarnik-Matusewicz, T.Elsaesser, H.Limbach, J Phys Chem A, 2010. 114: p. 7749.

125 Y.Yukawa, Y.T., M.Sawada, Bull Chem Soc Jpn, 1966. 39: p. 2274.

126 T. Hihara, Y.O., Z. Morita, Azo-hydrazone tautomerism of phenylazonaphthol sulfonates and their analysis using semiempirical molecular PM5 method. Dyes Pigm., 2003. 59: p. 25-4.

127 P. Wang, I.W., Photofading of azo pyridone dyes in solution. Part II: Substituent effects on the UV absorption spectra and photostability of 3-(mono- and di-substituted arylazo)-2-hydroxy-4-methyl-5-cyano-6-pyridone in N,N-dimethylformamide. Text. Res. J., 1990. 60: p. 519-524.

128 A. Hassanzadeh, A.Z.-I., M. Habibi, M. Poor Heravi, M. Abdollahi-Alibeik 1H, 13C, N-H, H-H, C-H COSY, H-H NOESY NMR and UV-vis studies of Solophenyl red 3BL dye azo-hydrazone tautomerism in various solvents. Spectrochim. Acta A, 2006 63 p. 247-254.

129 Adegoke, O., Relative predominance of azo and hydrazone tautomers of 4-carboxyl-2,6-dinitrophenylazohydroxynaphthalenes in binary solvent. Spectrochim. Acta A, 2011. 83: p. 504-510.

130 M. Dakiky, K.K., M. Khamis, Aggregation of o,o'-dihyroxyazo dyes. II. Interaction of 2-hydroxy-4-nitrophenylazoresorcionol in DMSO and DMF. Dyes Pigm. , 1999. 41: p. 199-209.

131 Lyčka, A., 15N, 13C and 1H NMR spectra and azo-hydrazone tautomerism of some dyes prepared by coupling of 1-naphthalenediazonium salt. Dyes Pigm., 1999. 43: p. 27-32.

132 P. Ball, C.N., Azo-hydrazon tautomerism of hydroxyazo- a review. Dyes Pigm. , 1982. 3: p. 5-26.

133 D. Mijin, G.U., N. Perišić-Janjić, N. Valentić, Substituent and solvent effects on UV/vis absorption spectra of 5-(3- and 4-substituted arylazo)-4,6-dimethyl-3-cyano-2-pyridones. Chem. Phys. Lett. , 2006. 418: p. 223-229.

134 A.Alimmari, A.M., D.Mijin, N.Valentić, N.Todorović, G.Uščumlić, J Serb Chem Soc 2010. 75: p. 1019.

135 L. Cheng, X.C., K. Gao, J. Hu, J. Griffiths, Colour and constitution of azo dyes derived from 2-thioalkyl-4,6-diaminopyrimidines and 3-cyano-6-hydroxy-2-pyridone as coupling components. Dyes Pigm. , 1986. 7: p. 373-388.

136 E. Anslyn, D.D., Modern Physical Organic Chemistry2006, USA.

137 E. M. Arnett, D.M., J. Am. Chem. Soc., 1965. 87: p. 1393.

138 M. Abraham, R.A., J. Chem. Soc. Perkin II, 1974: p. 74.

139 Isaacs, N., Physical Organic Chemistry. 2nd Edition ed1995: Longman Scientific & Technical.

140 Jones, R., Physical and Mechanistic Organic Chemistry1st published 1979: Cambridge University Press

141 Hammett, L., Chem. Rev., 1935. 17: p. 125.

142 Hammett, L., J. Am. Chem. Soc., 1937. 59 p. 96.

143 G. Burkhardt, W.F., E. Singleton, J. Chem. Soc. D, 1936: p. 17.

144 Hammett, L., Physical Organic Chemistry1940, New York: McGraw-Hill.

145 Jaffe, H., Chem. Rev., 1953. 53: p. 191.

146 D. McDaniel, H.C.B., J. Org. Chem. 1958. 23: p. 420.

147 Shorter, J., Correlation Analysis of Organic Reactivity1982, England: Research Studies Press.

148 T. Krygowski, B.S., Chem. Rev., 2005. 105: p. 3482.

149 Shorter, J., Correlation Analysis in Organic Chemistry, Oxford: Clarendon Press.

150 H. Neuvonen, K.N., A. Koch, E. Kleinpeter, Journal of Molecular Structure: THEOCHEM, 2007. 815: p. 95-104.

151 H. Neuvonen, K.N., F. Fülöp The Journal of organic chemistry, 2006. 71: p. 3141-8.

152 H. Neuvonen, F.F., K. Neuvonen, A. Koch, E. Kleinpeter, Journal of Physical Organic Chemistry, 2008. 21: p. 173-184.

153 Y. Yukawa, Y.T., Bull. Chem. Soc. Japan, 1959 32: p. 971.

154 A. Humffary, J.R., J. Chem. Soc. B, 1969: p. 1138.

155 J. Bromilow, R.B., D. Brownlee, S. Craik, R. Taft J. Org. Chem., 1980 45: p. 2429.

156 S. Bhattacharyya, A.D., A. Chakravarty, J. Brunskill, D. Ewing, J. Chem. Soc., Perkin Trans. II, 1985: p. 473.

157 E. Amis, J.H., Solvent Effects on Chemical Phenomena1973, New York: Academic Press.

158 Kosower, E., An Introduction to Physical Organic Chemistry1968, New York: Wiley.

159 Kakabadse, J., Solvent Problems in Industry 1984, London: Elsevier Applied Science Publishers.

160 Marcus, Y., Ion Solvation1985, Chichester: Wiley.

161 Connors, K., Chemical Kinetics-The Study ofReaction Rates in Solution1990, Weinheim: VCH Publishers.

162 J. Fabian, H.H., Journal of Molecular Structure 1975. 27: p. 67-78.

163 S. Dähne, F.M., Progress in Physical Organic Chemistry, 1985. 15: p. 1-130.

164 R. Radeglia, S.D., Journal of Molecular Structure: THEOCHEM, 1970. 5: p. 399-411.

165 Reichardt, C., Chemical Reviews 1994. 94: p. 2319-2358.

166 M. Berthelot, L.P.d.S.-G., Ann Chin. Et. Phys., 1862 65: p. 385.

167 Menschutkin, N., Z. Phys. Chem. , 1900. 34: p. 157.

168 Claisen, L., Liebigs Ann. Chem. , 1896. 291: p. 25.

169 Stobbe, H., Libigs Ann. Chem. , 1903. 326: p. 347.

170 Dimroth, O., Liebigs Ann. Chem., 1910. 377: p. 27.

171 Meyer, K., Liebigs Ann. Chem. , 1911. 380 p. 212.

172 F. Carey, R.S., Advanced Organic Chemistry, Part A, Structure and Mechanism. 3rd edition ed1990, New York: Plenum Press.

173 Epley, T., Journal of American Chemical Society, 1967. 89: p. 5770-5773.

174 V. Mayer, V.G., W. Gerget, Monatshefte fuer Chemie, 1975. 106: p. 1235-1257.

175 Drago, R., Applications of Electrostatic-Covalent Models in Chemistry1994, Gainesville, Florida: Scientific Publishers.

176 I. Koppel, V.P., Advances in Linear Free Energy Relationships1972, London: Plenum Press. 204-280.

177 E.M. Arnett, D.M., J Am Chem Soc 1967. 87: p. 1393

178 E. Arnett, L.J., E. Mitchell, T. Murty, T. Gorrie, P. Schleyer, Journal of American Chemical Society, 1970. 92: p. 2365-2377.

179 P. Maria, J.G., Journal of Physical Chemistry, 1985. 89: p. 1296-1304.

180 M. Kamlet, R.T., Journal of American Chemical Society, 1976. 98: p. 377-383.

181 R. Taft, M.K., Journal of American Chemical Society, 1976. 98: p. 2886-2894.

182 J. Catalán, C.D., P. Perez, G. De Paz, J. Rodriguez, Liebigs Annalen der Chemie, 1996: p. 1785-1794.

183 Kirkwood, J., Journal of Chemical Physics, 1934. 2: p. 351-361.

184 Onsager, L., Journal of American Chemical Society, 1936. 58: p. 1486-1493.

185 Kosower, E., Journal of American Chemical Society, 1958. 80: p. 3253-3260.

186 L. Brooker, A.C., D. Heseltine, P. Jenkins, L. Lincoln, Journal of American Chemical Society, 1965. 87: p. 2443-2450.

187 D. Dong, M.W., Canadian Journal of Chemistry, 1984. 64: p. 2560-2565.

188 M. Kamlet, J.A., R. Taft, Journal of American Chemical Society, 1977. 99: p. 6027-6038.

189 Drago, R., Journal of Chemical Society, Perkin Transactions, 1992. 2: p. 1827-1838.

190 M. Kamlet, J.A., R. Taft, Prog. Phys. Org. Chem, 1981. 13 p. 485.

191 J.Catalan, J Phys Chem B, 2009. 113: p. 5951.

192 A.Marinković , B.J., N.Todorović , I.Juranić J Mol Struct 2009. 920: p. 90.

193 I. Ajaj, D.M., V. Maslak, D. Brkovic, M. Milcic, N. Todorovic, A. Marinkovic, Monatshefte fuer Chemie, 2013. 144: p. 665-675.

194 Acin doktorat

195 A.Habashi, Ann Chem, 1986. 9: p. 1632.

196 H.Mustroph, R.B., Reinhard, T.Seele 1990.

197 N.Ertan , P.Gurkan, Dyes Pigments, 1997. 33: p. 137.

198 M.Frisch , G.T., H.Schlegel , G.Scuseria , M.Robb , J.Cheeseman , J.Montgomery , T.Vreven , K.Kudin , J.Burant , J.Millam , S.SIyengar , J.Tomasi , V.Barone , B.Mennucci ,

M.Cossi , G.Scalmani , N.Rega , G.Petersson , H.Nakatsuji , M.Hada , M.Ehara , K.Toyota, R.Fukuda , J.Hasegawa, M.Ishida , T.Nakajima , Y.Honda , O.Kitao , H.Nakai , M.Klene , X.Li , J.Knox , H.Hratchian , JB.Cross , V.Bakken, C.Adamo , J.Jaramillo , R.Gomperts , R.Stratmann , O.Yazyev , A.Austin , R.Cammi , C.Pomelli , J.Ochterski , P.Ayala , K.Morokuma , GAVoth , PSalvador, JJDannenberg , VGZakrzewski , SDapprich , ADDaniels , MCStrain , OFarkas , DKMalick , ADRabuck , KRaghavachari , JBForesman , JVOrtiz , QCui , AGBaboul , SClifford , JCioslowski, BBStefanov, GLiu , ALiashenko , PPiskorz , IKomaromi , R.Martin , D.Fox , T.Keith , M.Al-Laham, C.Peng , A.Nanayakkara , M.Challacombe , P.Gill , B.Johnson , W.Chen , M.Wong , C.Gonzalez , J.Pople Gaussian 03, Revision C.02, Gaussian, Inc. 2004: Wallingford CT.

199 W.Tang , E.S., G.Henkelman J Phys Condens Matter, 2009. 21: p. 084204.

200 L.Laaksonen, J Mol Graph, 1992. 10: p. 33.

201 Exner, O., The Hammett Equation - the Present Position, Advances in Linear Free Energy Relationship1972, London: Plenum Press.

202 Kamlet MJ, A.J., Abraham MH, Taft RW, J Org Chem, 1983. 48: p. 2877-2887.

203 T.Glasnov, C.K., Macromol Rapid Comm, 2007. 28: p. 395.

204 N.Tsuchida , S.Y., J Phys Chem A, 2005. 109: p. 1974.

205 E.Kolehmainen , B.O., T.Krygowski , R.Kauppinen , M.Nissinen , R.Gawinecki, J Chem Soc Perkin Trans, 2000. 2: p. 1259.

206 E.Kolehmainen , B.O., M.Nissinen , R.Kauppinen , R.Gawinecki, J Chem Soc Perkin Trans, 2000. 2: p. 2185.

207 C.Hansch , A.L., D.Hoekman, Exploring QSAR Hydrophobic, Electronic and Steric Constants1995, Washington DC: American Chemical Society.

208. G.Ušćumlić , D.M., N.Valentić , V.Vals , B.Sušić, Chem Phzs Lett, 2004. 397: p. 148.

209 B.Khalili, T.T., M.Hashemi, Tetrahedron, 2009. 65: p. 6882.

210 E.Raczyńska , W.K., B.Ośmialowski , R.Gawinecki, Chem Rev, 2005. 1055: p. 3561.

211 H.Limbach, F.M., CDetering, G.Denisov, Chem Phys Lett, 2005. 319: p. 69.

212 J.Baldwin, K.G., J Am Chem Soc, 1976. 98: p. 8283.

213 S.Angelova, M.S., V.Deneva, M.Rogojerov, L.Antonov Chem Phys Chem, 2011. 12: p. 1747.

214 V.Barone , A.P., Chem Soc Rev, 2007. 36: p. 1724.

215 P.Wiggins , J.W., D.Tozer J Chem Phys Lett, 2009. 131: p. 091101.

216 T.Iijima , E.J., L.Antonov , S.Stoyanov , T.Stoyanova Dyes and Pigments, 1998. 37: p. 81.

217 L.Antonov, W.F., D.Nedeltcheva, F.Kamounah J Chem Soc Perkin Trans, 2000. 2: p. 1173.

218 L.Antonov, D.N., Anal Lett, 1996. 29: p. 2055.

219 H.Tavakol, Struct Chem, 2011. 22: p. 1165.

220 V.Petrov, L.A., H.Ehara, N.Harada Comput Chem, 2000. 24: p. 561.

221 L.Antonov, S.K., M.Satoh, J.Komiyama Dyes Pigments, 1999. 40: p. 163.

222 Y.Marcus, Chem Soc Rev, 1993. 22: p. 409.

223 Y. Tsuno, Y.K., M. Sawada, T. Fuji, Y. Yukawa, Bull. Chem. Soc. Jpn., 1975. 48: p. 3337-3346.

224 Antonov L, S.S., Anal Chim Acta, 1995. 314: p. 225-232.

225 Marinković Aleksandar D., V.N.V., Mijin Dušan Ž., Uščumlić Gordana G., Jovanović Bratislav Ž. , J. Serb. Chem. Soc., 2008. 73: p. 513-524.

226 A. Lučka, V.M., Dyes Pigments, 1986. 7: p. 171-185.

227 A. Cee, B.H., A. Lyčka, Dyes Pigments, 1988. 9: p. 357-369.

228 L. Laaksonen, *J. Mol. Graphics* 10 (1992) 33-34.

229 Ł. Szyc, J. Guo, M. Yang, J. Dreyer, P.M. Tolstoy, E.T.J. Nibbering, B. Czarnik-Matusewicz, T. Elsaesser, H.H. Limbach, *J. . Chem. A* 114 (2010) 7749–7760.

230 E. Kolehmainen, B. Ośmialowski, T.M. Krygowski, R. Kauppinen, M. Nissinen, R. Gawinecki, *J. Chem. Soc., Perkin Trans. 2* (2000) 1259-1266.

231 Y. Manolova, V. Deneva, L. Antonov, E. Drakalska, D. Mornekova, N. Lambov, *Spectrochim. Acta A 132 (*2014), 815-820.

232 S. Ortiz, M.C. Alvarez-Ros, M. Alcolea Palafox, V.K. Rastogi, V. Balachandran, S.K. Rathor, *Spectrochim. Acta A 130 (*2014), 653-668.

233 Antonov, L., Tautomerism: Methods and Theories 2013. Wiley-VCH, Weinheim.

234 Chidangil S., Shukla, M.K., Mishra, P.C., J. Mol. Model. 1998. 4, 250–258.

235 Luque, F.J., Lopez, J.M., Orozco, M., Theor. Chem. Acc. 2000. 103, 343–345.

BIOGRAPHY

Ismail Abdalrhman Ajaj je rođen 10.07.1979. godine u Zliten-u, Libija, gde je završio osnovno obrazovanje. Osnovne studije na Fakultetu za nauku, Univerzitet 7. Oktobar, upisao je 1996/1997 i uspešno završio sa prosečnom ocenom 67.52%. Diplomski rad pod nazivom „Study of the effect of time polymerization on Low Density Polyethylene properties“ odbranio je 1999/2000 godine na Katedri za Hemiju. Magistarske studije je upisao na Fakultetu za Umetnost i nauku, Almergheb Univerzitet, Zliten, Libija, školske 2001/2002 godine. Položio je sve ispite sa prosečnom ocenom 82,77%. Magistarsku tezu pod naslovom "Synthesis and Spectral Characterization of Nickel, Copper, Cobalt and Mercury Complexes of Substituted Thiourea 1,3-Bis-(Pyridine-2-yl)-2-Thiourea" odbranio je 2005 godine. Školske 2010/11. započeo je izradu doktorske disertacije na Tehnološko–metalurškom fakultetu, Univerziteta u Beogradu, naučna oblast Hemija i hemijska tehnologija.

Stečeno naučnoistraživačko iskustvo

Ismail Ajaj je koautor 3 rada objavljena u časopisima međunarodnog značaja (M22 – 2 rada, M23 – 1 rad). Iz oblasti istraživanja kojoj pripada predložena tema doktorske disertacije, kandidat je koautor 2 rada M22 kategorije.

Spisak objavljenih radova i saopštenja

Rad u istaknutom međunarodnom časopisu (M22)

1. Ismail Ajaj, Dušan Mijin, Veselin Maslak, Danijela Brković, Miloš Milčić, Nina Todorović Fathi H. Assaleh, Aleksandar D. Marinković, “A simple and convenient synthesis of tautomeric (6 or 2)-hydroxy-4-methyl-(2 or 6)-oxo-1-(substituted phenyl)-(1,2 or 1,6)-dihydropyridine-3-carbonitriles” *Monatsh. Chem.* 144 (2013) 665-675. ISSN 0026-9247; *DOI:*10.1007/s00706-012-0911-5.

2. Ismail Ajaj, Jasmina Markovski, Jelena Marković, Maja Jovanović, Miloš Milčić, Fathi Assaleh, Aleksandar Marinković, "Solvent and structural effects in tautomeric 3-cyano-4-(substituted phenyl)-6-phenyl-2(1*H*)-pyridones: experimental and quantum chemical study", *Struct. Chem.*, Accepted manuscript, (2014); DOI: 10.1007/s11224-014-0401-y; ISSN: 1040-0400 (print version); ISSN: 1572-9001 (electronic version)

Rad u međunarodnom časopisu – M23

3. Milica P. Rančić, Nemanja P. Trišović, Miloš K. Milčić, Ismail A. Ajaj, Aleksandar D. Marinković, " Experimental and theoretical study of substituent effect on ^{13}C NMR chemical shifts of 5-arylidene-2,4-thiazolidinediones", *J. Mol. Struct.*, 1049 (2013) 59-68. ISSN 0022-2860; *DOI:* 10.1016/j.molstruc.2013.06.027

Прилог 1.

Изјава о ауторству

Потписана Исмаил Ајај

број индекса -

Изјављујем

да је докторска дисертација под насловом

Synthesis, structure and properties of 2(6)-hydroxy-6(2)-oxo-*N*(1),4-disubstituted-1,2(1,6)-dihydropyridine-3-carbonitriles and their azo derivatives

- резултат сопственог истраживачког рада,
- да предложена дисертација у целини ни у деловима није била предложена за добијање било које дипломе према студијским програмима других високошколских установа,
- да су резултати коректно наведени и
- да нисам кршио/ла ауторска права и користио интелектуалну својину других лица.

Потпис докторанда

У Београду, 30.03.2015. године

_____

Прилог 2.

Изјава о истоветности штампане и електронске верзије докторског рада

Име и презиме аутора Исмаил Ајај

Број индекса -

Студијски програм Органска хемија

Наслов рада Synthesis, structure and properties of 2(6)-hydroxy-6(2)-oxo-*N*(1),4-disubstituted-1,2(1,6)-dihydropyridine-3-carbonitriles and their azo derivatives

Ментор др Александар Маринковић, доцент

Потписани Исмаил Ајај

Изјављујем да је штампана верзија мог докторског рада истоветна електронској верзији коју сам предао/ла за објављивање на порталу **Дигиталног репозиторијума Универзитета у Београду.**

Дозвољавам да се објаве моји лични подаци везани за добијање академског звања доктора наука, као што су име и презиме, година и место рођења и датум одбране рада.

Ови лични подаци могу се објавити на мрежним страницама дигиталне библиотеке, у електронском каталогу и у публикацијама Универзитета у Београду.

Потпис докторанда

У Београду, 30.03.2015. године

_____

Прилог 3.

Изјава о коришћењу

Овлашћујем Универзитетску библиотеку „Светозар Марковић“ да у Дигитални репозиторијум Универзитета у Београду унесе моју докторску дисертацију под насловом:

Synthesis, structure and properties of 2(6)-hydroxy-6(2)-oxo-*N*(1),4-disubstituted-1,2(1,6)-dihydropyridine-3-carbonitriles and their azo derivatives

која је моје ауторско дело.

Дисертацију са свим прилозима предао/ла сам у електронском формату погодном за трајно архивирање.

Моју докторску дисертацију похрањену у Дигитални репозиторијум Универзитета у Београду могу да користе сви који поштују одредбе садржане у одабраном типу лиценце Креативне заједнице (Creative Commons) за коју сам се одлучио/ла.

1. Ауторство

2. Ауторство - некомерцијално

3. Ауторство – некомерцијално – без прераде

4. Ауторство – некомерцијално – делити под истим условима

5. Ауторство – без прераде

6. Ауторство – делити под истим условима

(Молимо да заокружите само једну од шест понуђених лиценци, кратак опис лиценци дат је на полеђини листа).

Потпис докторанда

У Београду, 30.03.2015. године

_____

1. Ауторство - Дозвољавате умножавање, дистрибуцију и јавно саопштавање дела, и прераде, ако се наведе име аутора на начин одређен од стране аутора или даваоца лиценце, чак и у комерцијалне сврхе. Ово је најслободнија од свих лиценци.

2. Ауторство – некомерцијално. Дозвољавате умножавање, дистрибуцију и јавно саопштавање дела, и прераде, ако се наведе име аутора на начин одређен од стране аутора или даваоца лиценце. Ова лиценца не дозвољава комерцијалну употребу дела.

3. Ауторство - некомерцијално – без прераде. Дозвољавате умножавање, дистрибуцију и јавно саопштавање дела, без промена, преобликовања или употребе дела у свом делу, ако се наведе име аутора на начин одређен од стране аутора или даваоца лиценце. Ова лиценца не дозвољава комерцијалну употребу дела. У односу на све остале лиценце, овом лиценцом се ограничава највећи обим права коришћења дела.

4. Ауторство - некомерцијално – делити под истим условима. Дозвољавате умножавање, дистрибуцију и јавно саопштавање дела, и прераде, ако се наведе име аутора на начин одређен од стране аутора или даваоца лиценце и ако се прерада дистрибуира под истом или сличном лиценцом. Ова лиценца не дозвољава комерцијалну употребу дела и прерада.

5. Ауторство – без прераде. Дозвољавате умножавање, дистрибуцију и јавно саопштавање дела, без промена, преобликовања или употребе дела у свом делу, ако се наведе име аутора на начин одређен од стране аутора или даваоца лиценце. Ова лиценца дозвољава комерцијалну употребу дела.

6. Ауторство - делити под истим условима. Дозвољавате умножавање, дистрибуцију и јавно саопштавање дела, и прераде, ако се наведе име аутора на начин одређен од стране аутора или даваоца лиценце и ако се прерада дистрибуира под истом или сличном лиценцом. Ова лиценца дозвољава комерцијалну употребу дела и прерада. Слична је софтверским лиценцама, односно лиценцама отвореног кода.